STRUCTURE-PROPERTY BEHAVIOR of

POLYIMIDE HOMOPOLYMERS, COPOLYMERS, and BLENDS

by

Cynthia A. Arnold

Dissertation submitted to the Faculty of the

Virginia Polytechnic Institute and State University

in partial fulfillment of the requirements for the degree of

Doctor of Philosophy

in

Materials Engineering Science

APPROVED:

James E. McGrath, Chairman

G. L. Wilkes

T. C. Ward

N. S. Eiss

D. A. Dillard

October, 1989

Blacksburg, Virginia

STRUCTURE-PROPERTY BEHAVIOR of

POLYIMIDE HOMOPOLYMERS, COPOLYMERS, and BLENDS

by

Cynthia A. Arnold

James E. McGrath, Committee Chairperson

Department of Chemistry

(ABSTRACT)

Fully imidized, high molecular weight polyimide homopolymers and random segmented poly(siloxane imide) and poly(aryl ether imide) copolymers were prepared for use as environmentally stable, tough structural matrix resins, structural adhesives, and dielectric materials. Although polyimides are well suited for such high performance engineering applications due to their excellent thermal and mechanical properties, their typical intractability in the fully imidized state has been a serious limitiation. Therefore, this research has specifically focused upon several methods by which the processability of polyimide systems may be improved. One method involved the utilization of a solution imidization technique in converting the poly(amic acid) intermediate to the fully cyclized polyimide. Another important method was the incorporation of a monofunctional reagents to obtain controlled endgroups and molecular weights.

Structural modifications achieved by either copolymerization with polydimethylsiloxane or polyaryl ether sulfones or ketones, or variation of the dianhydrides or diamines resulted in major strides in obtaining enhanced processability, particularly when coupled with controlled molecular weight and the solution imidization technique. Significant reductions in the dielectric constant and water sorption, and improvements in processability were obtained by incorporating relatively nonpolar reactants, such as fluorinated dianhydrides, hydrophobic aromatic diamines, and polydimethylsiloxane oligomers.

The poly(aryl ether imide) segmented copolymers displayed high glass transition values, excellent toughness, and remarkable solution processability. In some cases, a two phase morphology was obtained, dependent upon the polarity of the imide component.

The thermal behavior of the poly(siloxane imide) segmented copolymers was dependent upon the siloxane oligomer molecular weight, the level of siloxane incorporation, and the nature of the imide component. Microphase separation was achieved at a relatively low molecular weight for a copolymer system based upon benzophenone tetracarboxylic dianhydride (BTDA) and 3, 3'-diaminodiphenylsulfone (m-DDS). Decreasing the polarity of the imide component, however, resulted in a more phase mixed morphology, as determined by thermal analysis. The BTDA and m-DDS based copolymer systems, with a siloxane oligomer <Mn> of 950 g/mole, behaved essentially as modified polyimides at low siloxane levels. At higher siloxane concentrations, the copolymers were analogous to thermopolastic elastomers. The incorporation of polydimethylsiloxane imparted a number of additional benefits, including enhanced solubility, reduced water sorption, good thermal and ultraviolet stability, resistance to degradation in aggressive oxygen environments, flammability resistance, improved impact resistance, and modified surface properties.

Another approach to capitalize on the benefits of siloxane incorporation was to utilize poly(siloxane imide) segmented copolymers as blend components with other high performance engineering polymers, such as polybenzimidazole (PBI) and poly(ether ether ketone) (PEEK). Miscibility was obtained for most PBI and PEEK blend systems which were investigated. Blends of PEEK with polyimides based on BTDA and m-DDS were not miscible. Likewise, blends of PBI with polyimides based upon 6F dianhydride and m- or p-DDS were immiscible as well. Poly(siloxane imide) segmented copolymers and blends of these copolymers with PBI displayed excellent stability to high energy, high flux atomic oxygen, due to a conversion of the siloxane component to a stable silicate-like structure.

ACKNOWLEDGEMENTS----------

For good reason, not a disseration or thesis has passed without first acknowledging Dr. James E. McGrath for his personal and professional contributions to the experience of graduate education. Working for Dr. McGrath has been a great pleasure and outstanding opportunity, for which I am very grateful. Appreciation is also extended to my committee members, Drs. Thomas C. Ward, Garth L. Wilkes, Norman S. Eiss, David A. Dillard, and Herve Marand, for their involvement and support of this research. I am also indebted to Eastman Kodak for support of my graduate research that has extended beyond only financial contributions.

Part of the benefit of working in Dr. McGrath's research group has been the numerous interactions with many talented colleagues. In this regard, I would like to particularly thank Dr. John Summers for an introduction to polyimide chemistry; Maria Spinu and Ann Hellstern, for friendship and NMRs; Martin Rogers, for talented, helpful, hardworking synthetic support; Drs. David and Diana Chen, for their major contributions to the PBI-polyimide blend program; Jeff Hedrick, for the PEEK-polyimide blend research; Tae Ho Yoon, for adhesive data; Greg York and Steve McCartney, for XPS and microscopy; Dr. J. P. Puglia of Polygen Corporation for the molecular models of polyimide repeat units, and Bonnie Johnson, for keeping it all together.

For inspiration, encouragement, friendship, and faith, I owe my deepest appreciation to my parents, Ted and Nancy Skrocki, my companion Herb, and my sisters Tracey and Maria. Finally, but very importantly, I am indebted to Mr. John Turko for direction and first opportunities. (Oh, you young people!)

dedicated with love to my mother and Herb

to my mother,

for teaching by example the excitement and joy of life and learning

to Herb,

for friendship and love,

sharing the good times,

and helping me (us) through the not-so-good times

TABLE OF CONTENTS----------

		PAGE
1.0	*CHAPTER 1: INTRODUCTION*	*1*
2.0	*CHAPTER 2: BACKGROUND AND PERSPECTIVE*	*4*
2.1	*Effect of synthetic procedure on polyimide properties*	*4*
2.1.1	*Bulk thermal imidization*	*4*
2.1.2	*Chemical imidization*	*7*
2.1.3	*Electromagnetic imidization*	*7*
2.1.4	*Solution imidization*	*9*
2.2	*Structural requirements for high performance applications*	*10*
2.2.1	*Polyimides containing flexible spacers*	*10*
2.2.2	*Introduction of bulky side groups*	*19*
2.2.3	*Introduction of asymmetry*	*25*
2.3	*Examples of commercial polyimides*	*25*
2.4	*Controlled molecular weight*	*29*
2.4.1	*The influence of molecular weight on linear polyimides*	*29*
2.4.2	*Addition imides*	*33*
2.5	*Structural modification by copolymerization*	*37*
2.5.1	*Poly(siloxane imide) copolymers*	*37*
2.5.2	*Poly(aryl ether imide) copolymers*	*41*
2.5.3	*Other copolyimides*	*46*
2.6	*Property modification by blending*	*54*
2.6.1	*Thermodynamic theory of homopolymer blend miscibility*	*54*
2.6.2	*High performance miscible polymer blends*	*58*
2.6.3	*Semi-interpenetrating polymer networks (IPNs)*	*67*

2.7 *Requirements for electronics packaging applications* 68

2.7.1 *Dielectric constant* 68

2.7.2 *Thermal coefficient of expansion (TCE)* 71

2.8 *Requirements of aerospace applications* 71

3.0 *CHAPTER 3: EXPERIMENTAL TECHNIQUES* 80

3.1 *Solvent Purification* 80

3.2 *Anhydrides* 83

3.2.1 *3, 4, 3', 4'-biphenyltetracarboxylic dianhydride (BPDA)* 83

3.2.2 *Pyromellitic dianhydride (PMDA)* 83

3.2.3 *Benzophenone tetracarboxylic dianhydride (BTDA)* 84

3.2.4 *4, 4'-oxydiphthalic anhydride (ODPA)* 84

3.2.5 *Sulfonyl bis(phthalic anhydride) (SDA)* 85

3.2.6 *5, 5'-[2, 2, 2-Trifluoro-1-(trifluoromethyl) ethylidene bis-1,3-isobenzofuranedione (6F)* 85

3.2.7 *Maleic anhydride (MA)* 86

3.2.8 *Phthalic anhydride (PA)* 86

3.3 *Diamines* 87

3.3.1 *Synthesis of 1, 4-(3-aminophenoxy) 2, 3, 5, 6-tetrafluoro-benzene (4F)* 87

3.3.2 *Synthesis of bis(3-aminophenoxy-4'-phenyl) phenyl phosphine oxide diamine (PO)* 88

3.3.3 *4, 4'-isopropylidene dianiline (Bis A)* 90

3.3.4 *4, 4'-[1, 4-phenylene-bis-(1-methyl ethylidene)] bisaniline (Bis P)* 90

3.3.5 *m-aminophenol (m-AP)* 90

3.3.6 *3, 3'-diaminodiphenyl sulfone (m-DDS)* 91

3.3.7 *4, 4'-diaminodiphenyl sulfone (p-DDS)* 91

3.4	*Other monomers*		*92*
	3.4.1	*Bis(4-fluoro or chlorophenyl) phenyl phosphine oxide (POX)*	*92*
	3.4.2	*4, 4'-dichlorodiphenyl sulfone (DCDPS)*	*92*
	3.4.3	*2, 2-bis (4-hydroxyphenyl) propane (Bisphenol A)*	*93*
	3.4.4	*4, 4'-difluorobenzophenone (DFBP)*	*93*
	3.4.5	*Bis (3-aminopropyl) tetramethyldisiloxane (DSX)*	*94*
	3.4.6	*Octamethylcyclotetrasiloxane (D_4)*	*94*
3.5	*Oligomer synthesis*		*95*
	3.5.1	*Polydimethylsiloxane (PSX)*	*95*
	3.5.2	*Poly(aryl ether)s: sulfones and ketones (PSF, PEK)*	*97*
	3.5.3	*Imide oligomers*	*98*
3.6	*Molecular weight and end group control of polyimides via the Carothers equation*		*99*
3.7	*Synthesis of poly(amic acid)s*		*101*
	3.7.1	*Synthesis of homopolymer (amic acid)s*	*101*
	3.7.2	*Determination of quantities of reactants for the synthesis of copolymer (amic acid)s*	*102*
	3.7.3	*Sample calculation for the determination of the quantities of reactants of a copolymer*	*104*
	3.7.4	*Synthesis of poly(siloxane amic acid)s*	*107*
	3.7.5	*Syntheis of poly(aryl ether amic acid)s*	*108*
3.8	*Imidization of poly(amic acid)s*		*108*
	3.8.1	*Bulk thermal imidization*	*108*
	3.8.2	*Solution imidization technique*	*109*
3.9	*Crosslinking of reactive maleimide end groups*		*111*
3.10	*Preparation of films of solution imidized polyimides*		*111*

3.11 *Preparation of polymer blends* 112

3.11.1 *Polybenzimidazole (PBI) blends* 112
3.11.2 *Poly(ether ether ketone) (PEEK) blends* 113
3.11.3 *Poly(ether ketone) (PEK) blends* 113

3.12 *Characterization of solvents, monomers, oligomers, polymers, and blends* 114

3.12.1 *Solvent water contents* 114
3.12.2 *Potentiometric end group titration* 114
3.12.3 *Determination of monomers' melt temperatures* 115
3.12.4 *Intrinsic viscosity [n]* 115
3.12.5 *Gel permeation chromatography (GPC)* 115
3.12.6 *Fourier transform infrared spectroscopy (FTIR)* 116
3.12.7 *Proton nuclear resonance spectroscopy (NMR)* 116
3.12.8 *Solubility* 117
3.12.9 *Thermal characterization: differential scanning calorimetry (DSC), thermal gravimetric analysis (TGA), thermal mechanical analysis (TMA)* 118
3.12.10 *Dynamical mechanical thermal analysis (DMTA)* 119
3.12.11 *Mechanical properties* 119
3.12.12 *Adhesive and durability properties* 119
3.12.13 *Dielectric properties* 120
3.12.14 *Oxygen plasma stability* 120
3.12.15 *Atomic oxygen stability* 121
3.12.16 *Water sorption studies* 122
3.12.17 *X-ray photoelectron spectroscopy (XPS)* 122
3.12.18 *Scanning electron microscopy (SEM)* 122
3.12.19 *Transmission electron microscopy (TEM)* 123
3.12.20 *Rheological properties* 123

3.13 *Suppliers* 124

4.0 CHAPTER 4: RESULTS AND DISCUSSION 125

4.1 Nomenclature 125

4.2 Synthesis of polyimide homopolymers and copolymers 126

4.3 Solubility 127

4.3.1 Solubilities of homopolyimides 129

4.3.2 Solubilities of poly(siloxane imide) and poly(aryl ether imide) segmented copolymers 131

4.3.3 Influence of molecular weight on adhesive and melt flow properties 134

4.3.4 Solubility and molecular weight control of addition imide oligomers 137

4.4 Thermal properties 139

4.4.1 Glass transitions and morphologies of homopolyimides and poly(siloxane imide) segmented copolymers 139

4.4.2 Glass transitions of poly(aryl ether imide) segmented copolymers 147

4.4.3 Initial investigation of the thermal properties of crosslinked addition imides 151

4.4.4 Dynamic thermogravimetric analysis of homopolyimides, poly(siloxane imide), and poly(aryl ether imide) segmented copolymers 151

4.5 Mechanical properties 155

4.5.1 Initial stress-strain analysis of poly(siloxane imide) segmented copolymers 155

4.5.2 Initial stress-strain analysis of homopolyimides 158

4.6 Surface analysis 158

4.6.1 Surface analysis of poly(siloxane imide) segmented copolymers 160

4.6.2 Surface analysis of poly(siloxane imide) segmented copolymers after exposure to atomic oxygen 160

4.7 *Resistance to aggressive oxygen species* 165

4.7.1 *Oxygen plasma stability of homopolyimides and poly(siloxane imide) copolymers* 165

4.7.2 *Atomic oxygen stability of homopolyimides, poly(siloxane imide) copolymers, and blends with polybenzimidazole* 171

4.8 *Dielectric behavior* 183

4.9 *Water sorption* 187

4.9.1 *Water sorption of homopolyimides* 187

4.9.2 *Water sorption of polybenzimidazole blends* 189

4.10 *Rheological properties* 189

4.10.1 *Influence of molecular weight and composition variations on viscosity and shear stress* 189

4.10.2 *Thermomechanical analysis* 195

4.11 *Blends of polyimides with polybenzimidazole* 199

4.12 *Blends of polyimides with poly(ether ether ketone)* 203

4.13 *Molecular modelling of imide repeat units* 208

5.0 *CHAPTER 5: CONCLUSIONS* 213

6.0 *CHAPTER 6: SUGGESTIONS FOR FUTURE RESEARCH* 216

7.0 *REFERENCES* 219

8.0 *APPENDIX: Surface analysis via x-ray photoelectron spectroscopy of polyimide homopolymers, poly(siloxane imide) copolymers, and blends with polybenzimidazole exposed to atomic oxygen* 236

9.0 *VITA* 240

LIST of FIGURES----------

FIGURE #		*PAGE*
1	Mechanism of chemical conversion of poly(amic acid) to polyimide, with the formation of isoimide	8
2	Thermomechanical analysis of polyimides with pendant alkyl groups	22
3	Representative structures of some commercially available polyimides	28
4	Influence of molecular weight: the influence of number average molecular weight on polymer properties and the influence of weight average molecular weight on melt flow and processability	31
5	Influence of end groups on thermal stability	32
6	Representative crosslinking reaction of bismaleimides	34
7	PMR-15 chemistry	36
8	Thermal stability for poly(amide)s, poly(imide)s, and poly(amide imide) copolymers	48
9	Synthesis of poly(heterocyclic imide)s	52
10	Free energy of mixing as a function of concentration in a binary liquid system	56
11	Glass transitions of blends of sulfonated PEEK and polyetherimide and poly(amide imide)	62
12	Glass transitions of miscible blends of polybenzimidazole with Ultem	66
13	Concept of semi-interpenetrating polyimide networks	69
14	Atmospheric composition as a function of altitude in the low earth orbit	73
15	Etching rate versus silicon content in poly(methyl methacrylate) resins	78
16	Apparatus used for solvent distillation	81
17	Solution imidization apparatus	110

18	Proton NMR spectra of BTDA-Bis P-PA (25,000) homopolyimide and BTDA-Bis P-38 PSX 3650-PA (25,000) poly(siloxane imide) segmented copolymer	128
19	Polyimide homopolymer based on 6F and m-DDS with phthalimide endgroups	135
20	Molecular weight distribution as determined by gel permeation chromatography with a viscosity detector for 6F-Bis A-MA addition imide oligomer with theoretical <Mn> = 10,200 g/mole	140
21	Dynamic mechanical thermal analysis of microphase separated BTDA-m-DDS-40 PSX 950 poly(siloxane imide) segmented copolymer, indicating imide (183°C) and siloxane (-106°C) phase transitions	145
22	Transmission electron micrographs of BTDA-m-DDS-10 PSX poly(siloxane imide) segmented copolymers with siloxane segment molecular weights of 2,000 and 10,000 g/mole	146
23	Differential scanning calorimetry of BTDA-Bis A-30 PSF 6050-PA (25,000), indicating two phase morphology	149
24	Differential scanning calorimetry of BTDA-m-DDS-30 PSF 6050-PA (25,000), indicating two phase morphology	149
25	Dynamic mechanical thermal analysis of BTDA-Bis A-30 PSF 6050-PA (25,000), indicating two phase morphology	150
26	Thermogravimetric analysis in an air atmosphere of polyimide homopolymers	152
27	Thermogravimetric analysis in an air atmosphere of phosphorous containing BTDA-PO bulk imidized homopolyimide	153
28	Thermogravimetric analysis in an air atmosphere of poly(siloxane imide) segmented copolymers; polysiloxane segment <Mn> = ~1000 g/mole	154
29	Thermogravimetric analysis of poly(sulfone imide) segmented copolymers as a function of polysulfone content; polysulfone segment <Mn> = 6050 g/mole	156
30	Initial stress-strain response of BTDA-m-DDS based poly(siloxane imide) segmented copolymers with constant siloxane molecular weight of ~1000 g/mole	157
31	Initial stress-strain response of bulk imidized homopolyimides	159

32	Wide scan spectra of BTDA-m-DDS-40 PSX 950 poly(siloxane imide) segmented copolymer before exposure to atomic oxygen (90° take-off angle)	162
33	Wide scan spectra of BTDA-m-DDS-40 PSX 950 poly(siloxane imide) segmented copolymer after exposure to atomic oxygen (90° take-off angle), depicting increase in oxygen atomic abundance	163
34	Curve fitting and deconvolution of silicon 2p peak of BTDA-m-DDS-40 PSX 950 poly(siloxane imide) segmented copolymer exposed to atomic oxygen, indicating presence of siloxane and silicate species (lower); upper spectra indicates silicon 2p peak before exposure to atomic oxygen	164
35	Scanning electron micrographs of BTDA-m-DDS homopolyimide after exposure to oxygen plasma at 1600 and 6400 magnifications	168
36	Scanning electron micrographs of BTDA-m-DDS-10 PSX 950 poly(siloxane imide) segmented copolymer after exposure to oxygen plasma at 1600 and 6400 magnifications	169
37	Scanning electron micrographs of BTDA-m-DDS-20 PSX 950 poly(siloxane imide) segmented copolymer after exposure to oxygen plasma at 1600 and 6400 magnifications	170
38	Scanning electron micrographs of BTDA-m-DDS-40 PSX 950 poly(siloxane imide) segmented copolymer *before* exposure to atomic oxygen at 6600 magnification	174
39	Scanning electron micrographs of polybenzimidazole after exposure to atomic oxygen at 1600 and 6600 magnifications	175
40	Scanning electron micrographs of Kapton after exposure to atomic oxygen at 1600 and 6600 magnifications	176
41	Scanning electron micrographs of BTDA-m-DDS polyimide homopolymer after exposure to atomic oxygen at 1600 and 6600 magnifications	177
42	Scanning electron micrographs of BTDA-m-DDS-10 PSX 950 poly(siloxane imide) segmented copolymer after exposure to atomic oxygen at 1600 and 6600 magnifications	178
43	Scanning electron micrographs of BTDA-m-DDS-40 PSX 950 poly(siloxane imide) segmented copolymer after exposure to atomic oxygen at 1600 and 6600 magnifications	179
44	Scanning electron micrographs of a blend of polybenzimidazole (40 weight %) and BTDA-m-DDS-10 PSX 950 poly(siloxane imide) segmented copolymer (60 weight %); 24 overall PSX content; after exposure to atomic oxygen at 1600 and 6600 magnifications	179

45	Scanning electron micrographs of a blend of polybenzimidazole (25 weight %) and BTDA-m-DDS-10 PSX 950 poly(siloxane imide) segmented copolymer (75 weight %); 30 overall PSX content; after exposure to atomic oxygen at 1600 and 6600 magnifications	180
46	Scanning electron micrograph of Kapton coated with ~1500 Å BTDA-mDDS-40 PSX 950 poly(siloxane imide) segmented copolymer after exposure to atomic oxygen at 1600 and 6600 magnifications	181
47	Dielectric constants as a function of frequency for polyimide homopolymers	185
48	Water sorption for a series of polyimide homopolymers	188
49	Complex viscosity as a function of temperature and angular frequency for 6F-m-DDS-PA (10,000) and 6F (50) BTDA (50)-m-DDS-PA (10,000), both solution imidized	192
50	Complex viscosity as a function of temperature and angular frequency for solution imidized 6F (50) BTDA (50)-m-DDS-PA (30,000)	194
51	Shear stress versus angular frequency as a function of molecular weight for 6F (50) BTDA (50)-m-DDS-PA at 340°C	196
52	Summary of initial rheological investigation of polyimides: variation of molecular weight and composition relative to commerically available Ultem	197
53	Thermal mechanical analysis of polyimide homopolymers and copolymers imidized in bulk or in solution, as indicated, with constant siloxane molecular weight of ~1000 g/mole	198
54	Dynamic mechanical thermal analysis of blends of polybenzimidazole with BTDA-m-DDS homopolyimide and BTDA-m-DDS-40 PSX 950 poly(siloxane imide) segmented copolymer	200
55	Dynamic mechanical thermal analysis of amorphous blend of 70 weight percent PEEK and 30 weight percent BTDA-Bis P-4 PSX 2500-PA (25,000) poly(siloxane imide) segmented copolymer	205
56	Differential scanning calorimetry of blend of 70 weight percent PEEK and 30 weight percent BTDA-Bis P-4 PSX 2500-PA (25,000) poly (siloxane imide) segmented copolymer	206
57	Low energy conformers of imide repeat units:	
	• BTDA-p-DDS and BTDA-m-DDS	209
	• 6F-p-DDS and 6F-m-DDS	210
	• ODPA-p-DDS and ODPA-p-DDS	211
	• BPDA-p-DDS	212

LIST of TABLES----------

TABLE #		*PAGE*
1	Methods of synthesizing linear, high molecular weight polyimides	5
2	Glass transitions of polyimides containing oxyethylene units	12
3	Thermal transitions of polyimides containing ether and carbonyl connecting groups	15
4	Influence of bridging group of the diamine portion on glass transition	16
5	Glass transitions of phenylsuccinimides	18
6	Mechanical properties of phenylsuccinimides	20
7	Glass transitions of polyimides based on hexafluoroisopropylidene dianhydride and various diamines	23
8	Glass transitions of polyimides from isomeric diamines and benzophenone tetracarboxylic dianhydride and pyromellitic dianhydride	26
9	Glass transitions of polyimides from isomeric diamines and oxydianhydride and hexafluoroisopropylidene dianhydride	27
10	Properties of polydimethylsiloxane	38
11	Mechanical properties of block copolyimides based upon benzophenone tetracarboxylic dianhydride and 4, 4'-oxydianiline as the imide component and poly(aryl ether ketone) oligomers	45
12	Properties of poly(amide imide)s	47
13	Structures and properties of liquid crystalline poly(ester imide)s	50
14	Glass and melting transitions of miscible blends of poly(aryl ether ketone) with polyetherimide	60
15	Glass transitions of amorphous blends of poly(ether ether ketone) and molecular weight controlled polyimide based upon benzophenone tetracarboxylic dianhydride and 4, 4'-[1, 4-phenylene-bis-(1-methyl ethylidene)] (Bis P)	64
16	Dielectric constants for polyimides	70

17	Thermal expansion coefficient for polyimides	72
18	Reaction efficiencies of selected materials with atomic oxygen in the low earth orbit	75
19	Common solvents for polyimide synthesis and solubility studies	82
20	Solubilities of solution imidized polyimide homopolymers	130
21	Solubilities of solution imidized poly(siloxane imide) segmented copolymers	132
22	Solubilities of solution imidized poly(aryl ether imide) segmented copolymers based on BTDA and Bis P, with molecular weight controlled to 25,000 g/mole by the addition of phthalic anhydride	133
23	Molecular weight and endgroup control of 6F-m-DDS homopolyimides by incorporation of phthalic anhydride	135
24	Single lap shear strengths for a series of molecular weight and endgroup controlled BTDA-Bis P-PA polyimides and a corresponding poly(siloxane imide) segmented copolymer with 30 weight percent siloxane of 2500 g/mole molecular weight	136
25	Solubilities of 6F-Bis A-MA imide oligomers	138
26	Molecular weight data for 6F-Bis A based addition imide oligomers	141
27	Upper glass transitions of polyimide homopolymers and poly(siloxane imide) segmented copolymers	142
28	Glass transitions of BTDA-Bis P-PA (25,000) based poly(aryl ether imide) segmented copolymers	148
29	X-ray photoelectron spectroscopy of poly(siloxane imide) segmented copolymers based on BTDA and m-DDS	161
30	Weight loss of BTDA-m-DDS and BTDA-p-ODA based poly(siloxane imide) segmented copolymers due to exposure to oxygen plasma	166
31	Weight loss incurred by homopolymers, poly(siloxane imide) segmented copolymers and blends with polybenzimidazole due to exposure to high energy, high flux atomic oxygen	172
32	Dielectric constants at 15 GHz for a series of polyimide homopolymers and poly(siloxane imide) segmented copolymers	184
33	Dielectric constants of 6F-Bis A-MA addition imide oligomers which were thermally crosslinked	186

34	Water sorption of blends of polybenzimidazole and BTDA-m-DDS homopolyimide	190
35	Water sorption of blends of polybenzimidazole and BTDA-m-DDS-40 PSX 950 poly(siloxane imide) segmented copolymer	191
36	Glass transitions of blends of polybenzimidazole and BTDA-m-DDS homopolyimide determined by DMTA	201
37	Glass transitions of blends of polybenzimidazole and BTDA-m-DDS-40 PSX 950 poly(siloxane imide) segmented copolymer determined by DMTA	202

CHAPTER 1

INTRODUCTION----------

During the late 1950's and early 1960's, a great amount of synthetic research generated many new polymers in response to the need within the aerospace industries for ablative systems, high temperature adhesives and coatings, and heat and flame resistant fibers. The stringent requirements for these high performance aerospace applications included excellent thermal oxidative stability, resistance to other nonoxidative types of degradation, high softening temperatures, stability to radiation and chemical reagents, and the ability to operate under static or cyclic loadings under harsh atmospheric conditions. Many aromatic polymers, including a number of heteroatomic systems, were produced which were capable of meeting these requirements. Unfortunately, those types of chemical structures which impart high heat resistance have tended to lead to insolubility and infusibility, therefore, relatively few of the very many polymers which were synthesized achieved commercialization. Much research effort hence has been spent on modifications of existing structures in order to facilitate processing and fabrication without a concomitant loss of thermal stability.

The aromatic polyimides are considered one of the first classes of high temperature polymers and are virtually alone among the other early developed polymer heterocycles in having attained commercial viability. Part of the reason for their success is undoubtedly due to the availability of relatively inexpensive starting materials, preparative routes that easily accomodated product changes, and support through the early stages of commercialization by the DuPont Company. A large part of their success may also be understood in terms of the compromise achieved between their ease of processing and

retention of performance. For instance, polyimides may be easily fabricated in their soluble, intermediate, high molecular weight, open chain amic acid form, and subsequently cyclized. The nature of the fabrication process, however, generally produces nonstructural materials such as films, fibers, coatings, and film adhesives. Therefore, careful molecular design was required to produce *high molecular weight, fully imidized,* processable polyimides for structural applications. Molecular modifications which have successfully been employed include copolymerization, or the introduction of bulky side groups, flexibilizing units (ether, sulfone, alkylene, ...) or backbone asymmetry (meta versus para catenation). In this regard, copolymers such as poly(ester imide)s, poly(amide imide)s, poly(ether imide)s, and poly(siloxane imide)s have been synthesized. Phenylation and fluorination have advanced processability without a substantial loss of attractive thermal properties. Processability has also been enhanced by molecular weight control and endgroup functionalization with unsaturated groups, such as maleimide, ethynyl, or norbornene, to yield reactive oligomers. These terminal groups cure by addition mechanisms either thermallly or by electromagnetic means, or by chain extension with suitable reactants. Such crosslinking reactions yield networks with improved thermal and high temperature dimensional stability. The relationships between polyimide structures and properties will be elaborated in Chapter 2.

The focus of this research was specifically the investigation of the structure-property behavior of polyimide homopolymers, copolymers and blends for applications as *processable* structural matrix resins, structural adhesives, coatings, and dielectric materials. Thus, a series of dianhydride and diamine monomers were systematically chosen for the synthesis of the homopolyimides and random, segmented copolymers. Phthalic anhydride was added to control molecular weight and endgroups of high molecular

weight systems, i.e, >15,000 g/mole, and maleic anhydride was incorporated to obtain imide oligomers which could be further reacted by thermal means or by microwave energy across the terminal unsaturation to obtain network structures. Incorporation of the polysiloxane component imparted a number of beneficial properties for the applications of interest, including enhanced solubility, reduced water sorption, good thermal and ultraviolet stability, resistance to degradation in aggressive oxygen environments, impact resistance and modified surface properties. The poly(aryl ether)s were investigated for potentially improving processability and toughness of the copolymer systems.

Solubility and processability, thermal and mechanical properties, morphology, surface composition anaylsis, water sorption, and dielectric behavior of the homopolymer and copolymer systems have been explored. Particularly for the poly(siloxane imide) segmented copolymers and blends of these copolymers with polybenzimidazole, stability in a simulated low earth orbit environment (LEO) was evaluated. The miscibility of blends of novel, structurally varied polyimides with poly(ether ether ketone) was also evaluated.

In the forthcoming Chapter 2 literature review, a detailed discussion of polyimide structure-property relationships will be presented. Atomic oxygen degradation and the theoretical aspects and practical applications of blend miscibility are also briefly overviewed. The variety of dianhydride and diamine monomers, the oligomers, and the synthetic and analytical procedures utilized in this work are outlined in Chapter 3. Chapter 4 details the experimental results, followed by conclusions and suggested future research.

CHAPTER 2

BACKGROUND AND PERSPECTIVE----------

2.1.0 Effect of synthetic procedure on polyimide properties

The most widespread method for the preparation of aromatic polyimides involves the reaction of an aromatic tetracarboxylic acid dianhydride with an aromatic diamine, although other synthetic routes are available (Table 1). This reaction is performed by both two- and one-step methods, with the two-step approach being the most common (1, 2). The first step involves the synthesis of a soluble, fabricable poly(amic acid) intermediate, which can be used for the preparation of films, fibers, and coatings, but not structural parts (3, 4, 5).

The second step, dehydration and cyclization of the poly(amic acid) to yield the aromatic polyimide, may be induced in a number of ways. The mechanism of the conversion is not well understood, although a great deal of research, particularly concerning the kinetics of this process, has been conducted (6-17). Additionally, the physical properties of the resultant polyimide may be somewhat affected by the method of conversion. Of major concern is the removal from the reacting poly(amic acid) system of the water eliminated upon cyclization. Presumably, the presence of sufficient quantities of water causes significant hydrolytic degradation of the uncyclized amic acid, yielding low molecular weights (5).

2.1.1 Bulk thermal imidization

By far the most common method of conversion of the poly(amic acid) to the fully cyclized polyimide is by a bulk thermal imidization of a solution cast film of the intermediate (5).

Table 1: Methods of synthesizing linear, high molecular weight polyimides

- Aromatic dianhydride and aromatic diamine [form poly(amic acid)] in solution and subsequently cyclodehydrate chemically or thermally
- Aromatic dianhydride and aromatic diisocyanate
- Aromatic dianhydride or tetracarboxylic acid and aromatic or aliphatic diamine in m-cresol (catalytic amount of organic base, v.g., quinoline) and subsequently heat to yield the polyimide
- Aromatic dianhydride and caprolactam followed by heating with an aromatic diamine to displace $HN_2(CH_2)_5CO_2H$
- Aromatic tetracarboxylic acid and aromatic diamine (solvents such as diglyme), evaporate solvent, heat
- Esters of aromatic tetracarboxylic acid with aromatic diamine
- Displacement of activated nitro group with phenoxide anion [v. g., bis(nitrophthalimides) and bisphenol salts]
- Transamidation of bisimides with aryl diamines

Thermal treatment is generally accomplished in an inert atmosphere or vacuum via staged heating to first remove residual solvent and then affect cyclodehydration (3, 4, 18, 19). Temperatures in excess of the ultimate glass transition are required to obtain adequate chain mobility for complete conversion. Due to the similarity of this temperature cycle to the network formation cycle employed for thermosets, the bulk thermal imidization is sometimes, although erroneously, referred to as "curing". This is not to be confused with the true curing of oligomeric addition polyimides which are terminated with unsaturated functionalities (e.g., maleimide, propargyl, ethynyl, norbornene, benzocyclobutene, ...). The topic of addition imides will be covered in more detail in section 2.4.2.

One factor which may partially account for the typical insolubility of polyimides is the potential for *intermolecular*, as opposed to *intramolecular* cyclization, occurring at the elevated temperatures of the bulk thermal process. Hermans and Streef proposed that intramolecular reactions between adjacent chains, or the reaction of chain ends in the same fashion, could result in branched and eventually crosslinked structures (20). Early work by Russian researchers concerned the physical properties of polyimides at various stages of the bulk thermal treatment; above 300°C, they believed that transimidization leading to crosslinking occurred (21). Evidence from hydrazinolysis of polyimides so treated provided support to this theory. Sacher proposed that steric and kinetic restrictions of a pyromellitic dianhydride-oxydianiline poly(amic acid) promoted cyclization via transimidization to yield a crosslinked network . At high temperatures, partial conversion of the transimide to cyclic imide occurred, however, some crosslinking still remained (22).

2.1.2 Chemical imidization

Poly(amic acid)s may also be cyclodehydrated in solution at room temperature by chemical means to obtain polyimides (23-26). Generally, dehydrating agents are used in combination with basic catalysts. Some of the basic catalysts which have been employed are pyridine, triethylamine, and isoquinoline. Dehydrating agents may be anhydrides, such as acetic anhydride, propionic anhydride, and n-butryic anhydride. The process of chemical conversion is illustrated in Figure 1. Some of the major disadvantages include incomplete conversion of the poly(amic acid) and isoimide formation (26-28). Open chain amic acid and isoimide along the backbone of the resultant polymer represent unstable linkages which depress thermal and mechanical properties. Nevertheless, polyimides obtained by chemical conversion have achieved some degree of commercial acceptance, probably due to the improved processability associated with the presence of the amic acid and isoimide moieties (29)

2.1.3 Electromagnetic imidization

Electromagnetic, or microwave, energy is currently being explored as an efficient, accelerated method for curing thermoset resins, most notably epoxies (30). An initial study demonstrated that this technique was also applicable to the imidization of poly(amic acid)s (31). Quantitative imidization was achieved at a 20 to 40 fold increase in the imidization rate over conventional thermal cycling. An interesting observation was that a low molecular weight, ethynyl terminated poly(amic acid) could be quantitatively imidized without crosslinking the terminal ethynyl groups. Thus, the electromagnetic energy could be directed to the more polar amic acid moieties, allowing for the facile, quantitative imidization of addition imide oligomers. The thermal properties of the electromagnetically

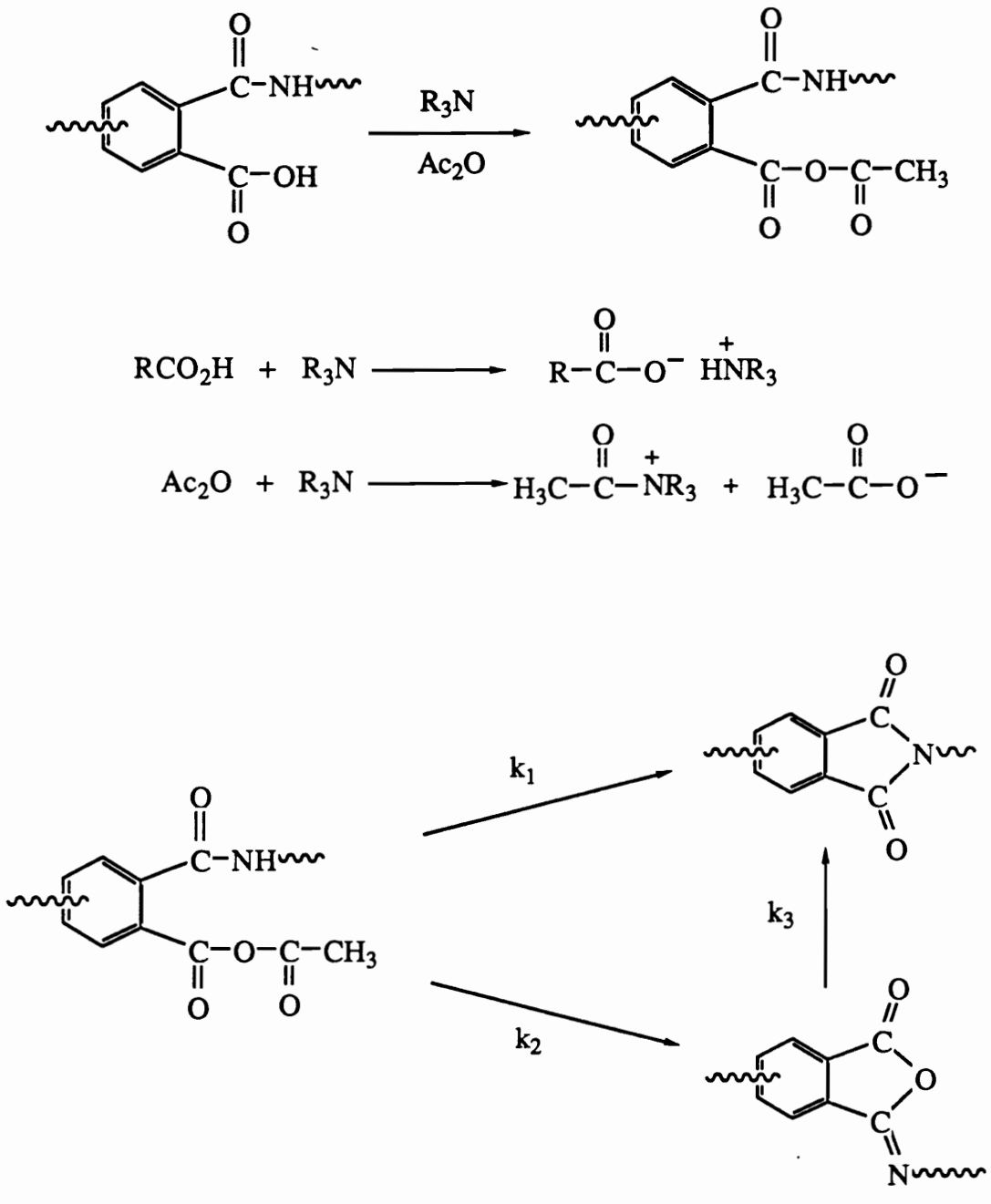

Figure 1: Mechanism of chemical conversion of poly(amic acid) to polyimide, with the formation of isoimide (27)

and thermally converted polyimides were similar, although other properties were not reported.

2.1.4 Solution imidization

Quantitative imidization has been reported at imidization temperatures less than the ultimate glass transition of the fully cyclized polyimide when the imidizing species has remained solubilized throughout the entire conversion (14, 32-34). Several high molecular weight polyetherimides were successfully synthesized at moderate temperatures of 160 to 180°C in solvents such as phenols and cresols, in combination with azeotroping quantities of toluene or chlorobenzene (34). Hydrolytic degradation of the poly(amic acid) to low molecular weights was avoided by the presence of the azeotroping solvents. Johnson (32) and Summers (14) employed a novel azeotroping agent, cyclohexylpyrollidinone (CHP), in a solution imidization technique performed at 150 to 170°C. N-methylpyrollidinone was also present as a cosolvent. Waldbauer successfully substituted o-dichlorobenzene as the azeotroping agent in a one-pot approach, eliminating the use of the costlier, higher boiling CHP (33). Polymers obtained by the solution technique demonstrated enhanced solubility and slightly depressed glass transitions, on the order of 2 to 7°C, relative to the bulk imidized analogues. Gel permeation chromatographs (GPCs) of the solution imidized polyimides were unimodal and symmetric, whereas GPCs of a bulk imidized analogue exhibited assymmetry, potentially indicative of deleterious side reactions occurring at the high temperatures of the bulk thermal imidization (14).

2.2.0 Structural requirements for high performance applications

The heat resistance of polymers is determined primarily by their chemical structure. Pure thermal stability is strongly influenced by the strength of chemical bonds, and combinations of atoms with weak bond strengths should not be used (35). Thus, most aromatic polymers, including heteroaromatic systems, exhibit excellent thermal oxidative stability, as well as superior mechanical properties. Other general ways of improving thermal stability include increasing crystallinity, crosslinking, promoting secondary bonding forces, molecular symmetry, and eliminating unstable moieties (35-40, 67). Unfortunately, those structures which impart thermal stability typically also result in intractability and infusibility. The development of high molecular weight, heat resistant, processable polymers is therefore all the more challenging, and an understanding of structure to property relationships is critical in their molecular design. The purpose of this section is to highlight those structural variations which result in enhanced processability, without significantly sacrificing the thermal and mechanical properties which make polyimides suitable for high performance applications. The focus will be upon polyimide applications for structural matrix resins, structural adhesives, specialty coatings, high modulus fibers, and as dielectric materials. Indeed, polyimides are suitable for an even wider variety of applications, such as reverse osmosis membranes and photoimageable resists. Because the current research is not involved in these areas, structure-property behavior relevant to these areas will not be emphasized.

2.2.1 Polyimides containing flexible spacers

One early approach to the fabrication problems of the highly rigid, fully imidized polyimides was to incorporate a flexible spacer (41-49). Harris utilized an aliphatic oxyethylene based diamine with a variety of dianhydrides (44-46). Increased chain lengths

resulted in lower glass transition temperatures (Table 2), and enhanced solubility and processability. However, the gain in flexibility was offset by decreased thermal oxidative stability, as expected, given the lower bond strengths of the aliphatic units. The thermal oxidative stability of a polyimide which contains only aromatic rings in its backbone, based upon 3, 6-diphenylpyromellitic dianhydride and m-phenylene diamine, however, was excellent, experiencing only a 5 percent weight loss at 585°C (50, 51). Likewise, greater aromaticity in pyromellitimides increased thermal oxidative stability in both air and nitrogen, according to the following order: tolan > stilbene > bibenzyl (52)

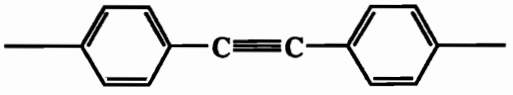

tolan-containing

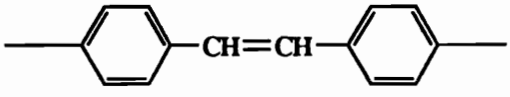

stilbene-containing

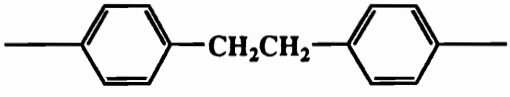

bibenzyl-containing

Incorporation of substituted oxyethylenes as well as oxyethylenes with napthalene subunits have also been reported (44). Complimentary work by Evans reports the influence of increasing the number of methylene units in the diamine, $H_2N(CH_2)_nNH_2$, reacted with pyromellitic dianhydride or monobrominated pyromellitic dianhydride (53). Glass transitions were lower for polyimides with bromide substitution. For instance, with 12 methylene units in the diamine, the glass transition was 238°C for the brominated pyromellitimide, versus 305°C for the nonbrominated version. Room temperature solubility, however, was poor in amide solvents.

Table 2: Glass transitions of polyimides containing oxyethylene units (44-46)

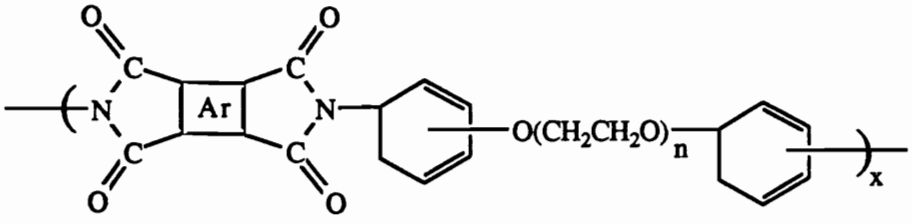

-Ar- DIANHYDRIDE	META or PARA	n	Tg	Tm	TGA
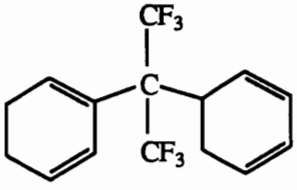	p	1	255	---	460
	p	2	180	---	425
	p	3	175	---	425
	p	4	140	---	385
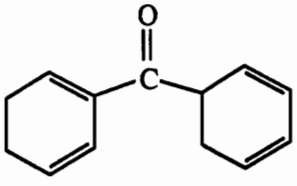	p	1	246	460	438
	p	2	235	410	425
	p	3	200	395	430
	m	1	192	290, 315	455
	m	2	154	243	430
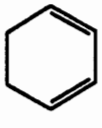	p	1	330	505	436
	p	2	320	465	444
	p	3	320	450	415
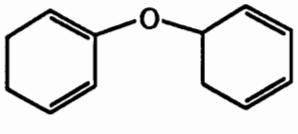	m	1	134	---	----
	m	2	128	---	----
	p	1	184	470	----
	p	2	164	370	----

Lower glass transitions and solubility and tractability were achieved by incorporating perfluoroalkylene [$(CF_2)_n$] and oxyperfluoroalkylene [$O(CF_2)_nO$] linked dianhydrides without significantly reducing thermal oxidative stability (54. 55). The glass transition of the polyimide utilizing the perfluoroalkylene dianhydride (n = 3) and p-oxydianiline (p-ODA) as the diamine component was 213°C. By incorporating the more rigid pyromellitic dianhydride (PMDA), the glass transitions were increased and specific heat changes were decreased accordingly. As an example, for equimolar amounts of pyromellitic and the perfluoroalkylene dianhydride with p-ODA, the glass transition was 251°C. The PMDA-p-ODA polyimide, commercially available as DuPont's Kapton™ polyimide, exhibits a weak transition near 380°C , indicated by torsional braid analysis, and in the fully imidized state is soluble only in sulfuric acid.

Many other bridging units in both the dianhydride and diamine component have been investigated, such as ether, sulfone, sulfide, carbonyl, phenyl phosphine oxide, dimethylsilyl, etc... Isomeric diamines with ether linked bipyridyl units reacted with benzophenone tetracarboxylic dianhydride displayed glass transitions between 230 and 310°C, and enhanced solubility (56, 57). Polypyromellitimides based on 4, 4'-[sulfonylbis (p-phenyleneoxy)] dianiline displayed high heat distortion temperatures, good solvent resistance, excellent mechanical properties, and high thermal oxidative stability. Thermoplasticity was exhibited by some molecular weight controlled compositions. Polyimides containing ether and carbonyl connecting groups, many of them semicrystalline, were recently investigated by Hergenrother (Table 3, 58-60). The semicrystalline polyimide based upon benzophenone tetracarboxylic dianhydride and 1, 3-bis (4-aminophenoxy-4'-benzoyl)benzene exhibited excellent tensile and adhesive properties, exceptional resistance to solvents and strong base, and high thermal oxidative

stability. The effect of variations of the bridging moiety in the diamine portion of a benzophenone tetracarboxylic dianhydride based polyimide is illustrated in Table 4. Resistance of a series of dianhydrides to thermal gravimetric weight loss has been reported as (43):

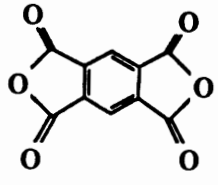

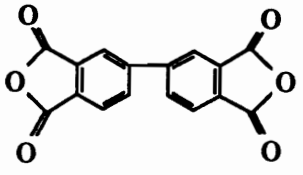

PMDA > BPDA >

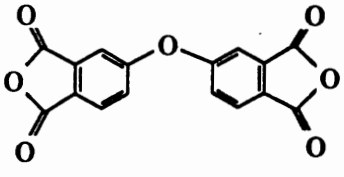

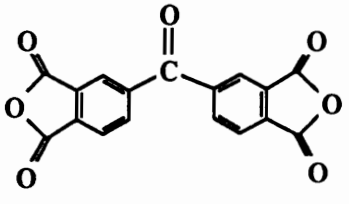

ODPA > BTDA >

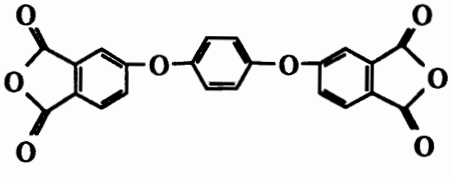

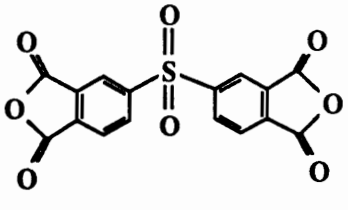

O-phenyl-O > SO_2

Table 3: Thermal transitions of polyimides containing ether and carbonyl connecting groups (58); ND: not detected

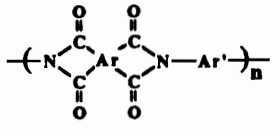

Ar	Ar'	Polyamide acid η_{inh} (dl/g)	Tg - Tm °C
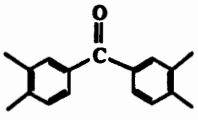	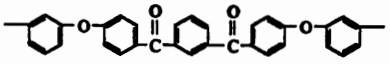	0.67	207 - ND
	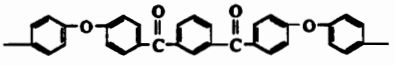	0.81	222 - 350
	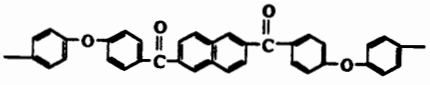	0.42	246 - 424
	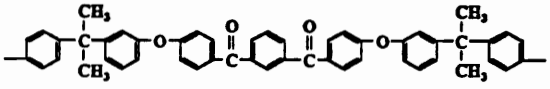	0.55	164 - ND
	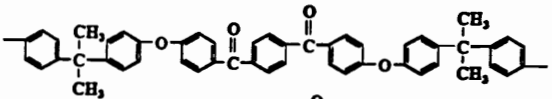	0.65	222 - ND
	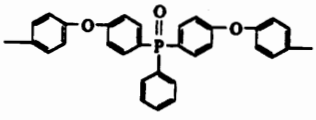	0.64	258 - ND
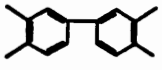	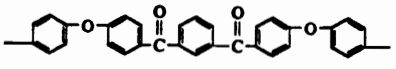	1.25	222 - ND
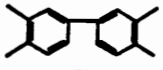	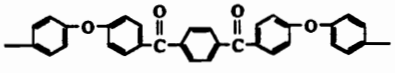	0.41	245 - 414
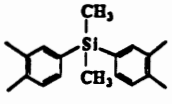	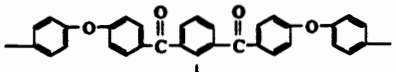	1.10	206 - ND
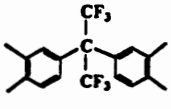		1.40	236 - ND
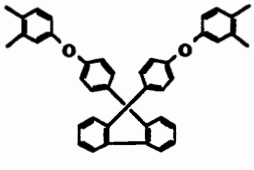		0.64	235 - ND
	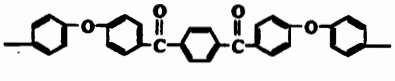	1.26	253 - ND

Table 4: Influence of bridging group of the diamine portion on the glass transition (43)

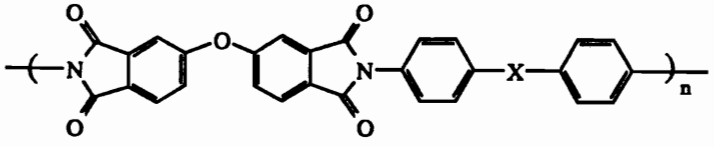

-X-	Glass Transition, °C
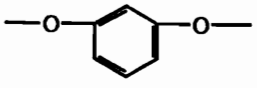	200
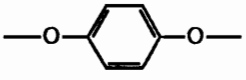	250
-S-	265
-O-	270
-CO-	280
$-SO_2-$	310

Woo introduced flexibility by replacing the fused ring structure of pyromellitic dianhydride with that of phenylsuccinic dianhydride (illustrated below, 61):

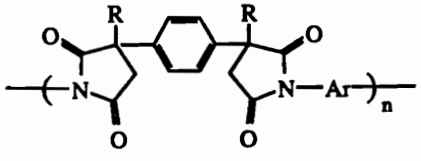

The thermal transitions, presented in Table 5, indicate high glass transitions of 250 to 315°C with aromatic diamines, and a lower glass transition (126°C) with the aliphatic hexamethylene diamine. The higher glass transition obtained for the polyimide based on the methylated phenylsuccinic dianhydride and p-oxydianiline cannot be readily explained on the basis of a rotational barrier height. A plausible explanation is that since the methyl groups are attached to sp^2 carbons, they are not coplanar with the imide or phenylene groups. In addition to increasing the rotational barrier, their presence also brings about greater chain separation due to the increased bulk, thus reducing interchain dipole-dipole interactions with an attendant depression of the glass transition. Of these two opposing effects, the latter was apparently more pronounced. The same theory is effective in explaining the lower glass transitions obtained with monobrominated pyromellitimides, than the nonbrominated analogues (53).

Thermal gravimetric analysis of the more aliphatic phenyl succinimide was comparable to other bis(phthalic anhydride) structures, such as benzophenone tetracarboxylic dianhydride, suggesting that the benzylic hydrogens are the reactive sites for oxidative degradation. The existence of a low temperature transition by thermal mechanical analysis suggested that phenylsuccinimides may possess outstanding toughness. Their mechanical

Table 5: Glass transitions of phenylsuccinimides; asterisk (*) indicates methylated phenylsuccinimide where R = CH_3 (61); ND: not detected

Diamine Component	Glass Transition, °C	Low Temp Transition, °C
4, 4'-oxydianiline (ODA)	275	- 95
4, 4'-methylene dianline	278	- 76
4, 4'-oxydianiline*	250	- 90
3, 3'-phenylene diamine	285	ND
2, 4-toluene diamine (TDA)	293	ND
2, 4 (75%) + 2,6 (25%)-TDA	315	ND
(Bis-4-aminocyclohexyl) methane	255	ND
Hexamethylene diamine (HMDA)	126	ND
ODA (75%) + HMDA (25%)	237	- 90
ODA (50%) + HMDA (50%)	194	- 85

properties (Table 6), and solvent insensitivity to trichloroethylene and chloroform, were also attractive features of this class of materials.

2.2.2 *Introduction of bulky side groups*

Soluble, but not necessarily fusible, polyimides have been synthesized from aromatic polyimides with large pendant groups on the repeat unit. These "cardo" polymers were developed primarily in the Soviet Union, and to a lesser extent in the United States (62-67). Their properties are governed primarily by the nature of the pendant groups and the imide portion of the chain. Their ability to enhance solubility has been attributed in part to a reduction in charge-transfer complexing between polyimide chains through steric hindrance (68). Thus, as a means of enhancing solubility without substantially decreasing the rigidity of the polyimide backbone, 3, 6-diphenylpyromellitic dianhydride was polymerized with various aromatic diamines in refluxing m-cresol containing isoquinoline by a one step procedure to yield phenylated pyromellitimides (51). Higher temperatures were required to overcome the steric hindrance which limited molecular weight buildup during chemical room temperature imidization. The polymers containing flexible ether or methylene linkages, meta-catenation, or bulky cardo linkages were soluble in m-cresol, N-methylpyrollidinone, and tetrachloroethane. The polymers from p-diaminodiphenylether, p-diaminodiphenylmethane, and m-phenylenediamine underwent extensive crystallization in concentrated m-cresol solutions. These polyimides displayed weak glass transitions between 310 and 320°C, and melting points of ~430°C. Interesting liquid crystalline behavior was exhibited in solutions of the polyimide based upon the fluorinated diamine:

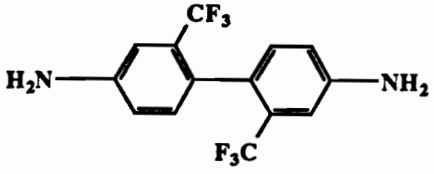

Table 6: Mechanical properties of phenylsuccinimides (61)

Properties	ODA*	MDA*	Polycarbonate
Glass Transition (°C)	275	278	150
Tensile Strength (psi)			
-Yield	9,200	8,900	9,075
-Break	12,100	9,000	7,900
Elongation (%)			
-Yield	9.0	5.5	5.7
-Break	27.0	65.5	45.3
Tensile Modulus (x 10^5 psi)	3.35	3.45	2.78
Izod Impact (ft lb per inch)	19.6	12.0	21.3

* ODA: 4, 4'-oxydianiline; MDA: 4, 4'-methylene dianiline

which is currently being investigated, and will be reported at an upcoming meeting (51, 69). Polyimides based upon phenylated diamines have also been prepared, although difficulties were encountered in maintaining solubility throughout the entire one-step polymerization. Glass transitions based on a tetraphenylated diamine with biphenyl, ether, and sulfone linked bis(phthalic anhydride)s were 376, 318, and 316 °C, respectively (70-73).

The effect on glass transition due to the incorporation of pendant alkyl groups is depicted in Figure 2. Pendant isobutyl, isopropyl, methyl, hydroxy, and methoxy groups on the diamine or dianhyride also convey solubility in conventional organic solvents to high molecular weight bis(phthalic anhydride)s and polypyromellitimides (43, 74).

Aromatic polyimides containing the relatively bulky, nonpolar hexafluoroisopropylidene [$C(CF_3)_2$] dianhydride (6F), originally investigated by Rogers (75), exhibited high glass transitions (~300°C) and marked solubility in common solvents. Gibbs (76, 77), in particular, developed the DuPont NR-150 polyimides based upon this "6F" dianhydride, in which the diamine component was selected from a range of nonfluorinated aromatics (Table 7). These systems possessed sufficient thermoplasticity to undergo melt flow when pressure was applied at temperatures greater than their glass transition. Other polyimides based upon the 6F moiety are currently being marketed by Hoechst Celanese [Sixef™ (78, 79)], Ethyl Corporation [Eymyd™ (80-83)], and Hysol Composites [addition imide PMR-II (84)].

Polyimides based upon thianthrene dianhydride (illustration follows) and aromatic diamines, such as 4, 4'-oxydianiline or 3, 3'-phenylene diamine, have recently appeared in

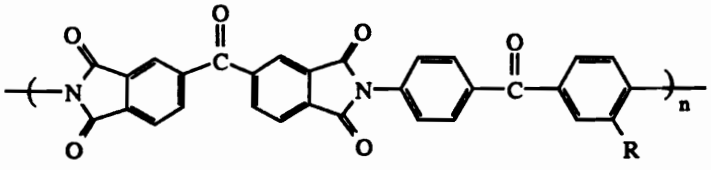

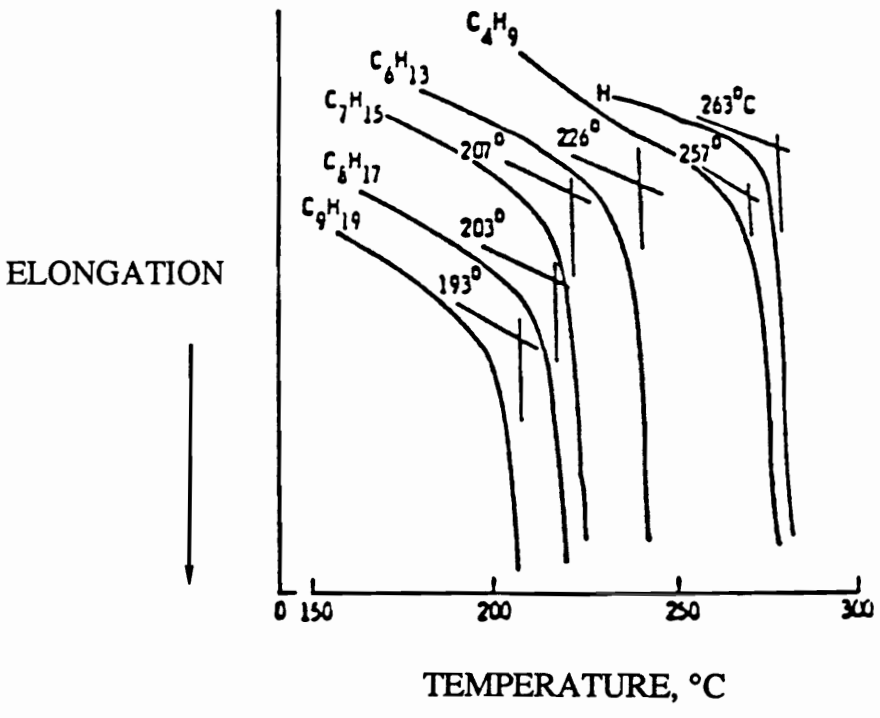

Figure 2 : Thermomechanical analysis of polyimides with pendant alkyl groups (43)

Table 7: Glass transitions of polyimides based on hexafluoroisopropylidene dianhydride and various diamines (77)

R	[η] inh (dl/g)	Tg (°C)
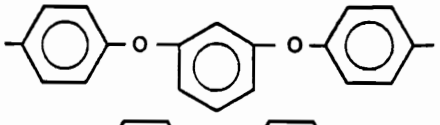	0.35	229
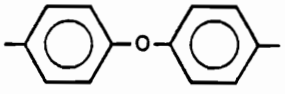	0.46	285
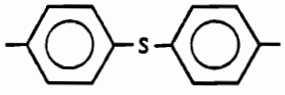	0.35	283
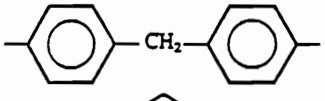	0.38	291
	0.41	297
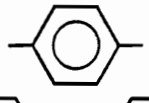	0.35	326
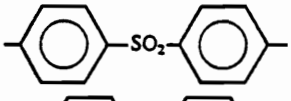	0.31	336
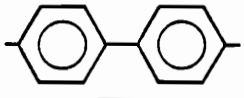	0.40	337
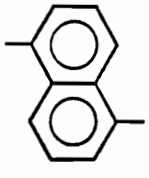	0.64	365

the patent literature (85). Their glass transitions were greater than 400°C. The pendant groups could be short chain alkyl, alkoxy or aryl substituents.

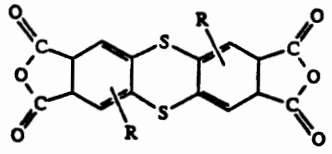

Thianthrene dianhydride

Polyimidines represent a new class of polymers which are structurally similar to polyimides but possess bulky, pendant groups on the backbone which greatly enhance solubility (below, 36, 86, 87). The thio monomers are more reactive than the oxo, and yield more thermally stable polymers. Thermal stabilities for one aromatic backbone were 560°C in air, as judged by 10 percent weight loss by thermal gravimetric analysis. The polymers were soluble in chloroform. One inherent drawback, however, has been the relative lack of reactivity of the starting materials, and therefore only low molecular weights have been obtained. As a means of circumventing this problem, copolymers of polyimidines and polyimides have been investigated (88). The copolymers were soluble in polar aprotic solvents and possessed sufficient molecular weights which allowed solution casting of tough films with moderate mechanical properties. Their thermal stabilities ranged from 410 to 475°C.

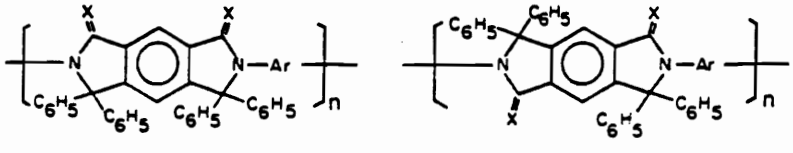

Polyimidines, X = O or S

2.2.3 Introduction of asymmetry

Another successful route to improved processability involves the introduction of asymmetry into the polyimide backbone (59, 89-95). Early reports by Bell and Gillham utilized isomeric bis(aniline)s (89-92). The results clearly indicated that a change from para to meta catenation led to a significant lowering of the glass transition (Table 8). In general, the decrease in the glass transition ranged from ~30°C for polyimides based upon benzophenone tetracarboxylic dianhydride, and ~100°C for pyromellitic dianhydride. The ortho orientation also reduced the glass transition, but to a lesser extent than the meta orientation. More recent research by St. Clair supports this trend for isomeric diamines reacted with 6F and oxydiphthalic dianhydrides (Table 9). Higher solubilities were associated with polyimides which contained ortho linkages, rather than either meta or para orientation (57, 95).

2.3.0 Examples of commerical polyimides

In order to highlight the importance of structure-property relationships in the design of commercially viable materials, the structures of some commercially available polyimides are illustrated in Figure 3. As has been emphasized, the rigid structure of the classic, fully imidized polyimides makes them insoluble in most solvents. This is illustrated by DuPont's Kapton™, which is processed from solution in the open chain, intermediate, poly(amic acid) stage (96). The poly(amic acid) is hydrolytically unstable, and therefore, possesses a limited shelf life. Further limitations of the solution technique, the high temperatures required for quantitative imidization, and elimination of water as the by-product, make processing from the poly(amic acid) stage amenable only to films, coatings, and film adhesives, not to structural parts.

Table 8: Glass transitions of polyimides from isomeric diamines of diaminobenzophenone (DABP), diamino biphenyl (DABiP), methylene dianiline (MDA), or oxydianiline (ODA) and benzophenone tetracarboxylic dianhydride (BTDA) or pyromellitic dianhydride (PMDA) (89)

Dianhydride	Diamine	Glass Transition, °C
BTDA	p, p-DABP	295
BTDA	m, p-DABP	283
BTDA	m, m-DABP	264
BTDA	o, p-DABP	289 (N, TBA)
BTDA	o, m-DABP	259
BTDA	o, o-DABP	289
PMDA	p, p-DABP	380
PMDA	m, p-DABP	339
PMDA	m, m-DABP	321
BTDA	m, p-MDA	259
BTDA	m, m-MDA	234
BTDA	o, p-MDA	289
BTDA	o, m-MDA	258
BTDA	o, o-MDA	285 (N, TBA)
BTDA	p, p-ODA	279
BTDA	o, p-ODA	278
PMDA	p, p-ODA	361 (A, TBA)
PMDA	o, p-ODA	386 (A, TBA)
BTDA	p, p-DABiP	382 (A)
BTDA	o, p-DABiP	305

Imidization environment: constant temperature of 300°C and vacuum, unless noted (N) for nitrogen or (A) for air; TBA: glass transition determined by torsional braid analysis

Table 9: Glass transitions of polyimides from isomeric diamines of oxydianiline (ODA) or aminophenoxybenzene (APB) and oxydianhydride (ODPA) or hexafluoroisopropylidene (6F) dianhydride (95)

Polymer	η_{inh} (dl/g)	Tg, oC	Refractive Index (n)
6F + 3,3'-ODA	1.00	244	1.60
6F + 2,4'-ODA	0.75	276	---
6F + 3,4'-ODA	0.79	280	1.60
6F + 4,4'-ODA	1.11	326	1.60
ODPA + 3,3'-ODA	1.09	186	1.69
ODPA + 2,4'-ODA	0.77	264	1.67
ODPA + 3,4'-ODA	0.61	245	1.69
ODPA + 4,4'-ODA	0.34	273	1.69
6F + 1,4(4)-APB	1.82	281	1.60
6F + 1,3(4)-APB	1.58	255	1.62
6F + 1,4(3)-APB	1.19	230	1.61
6F + 1,3(3)-APB	1.02	209	1.61
ODPA + 1,4(4)-APB	1.46	245	1.67
ODPA + 1,3(4)-APB	1.29	217	1.69
ODPA + 1,4(3)-APB	1.06	204	1.68
ODPA + 1,3(3)-APB	0.98	182	1.68

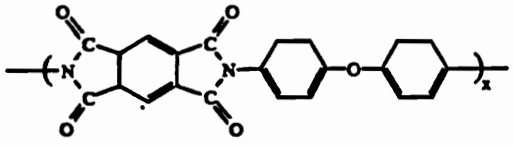

DuPont's Kapton: Tg by TBA ~380°C, rigid and intractable

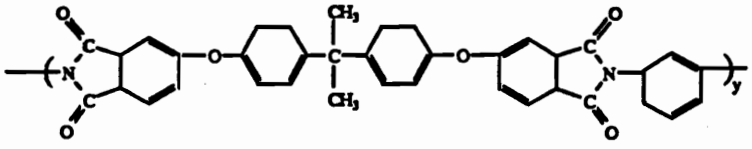

General Electric's Ultem polyetherimide: Tg ~220°C, flexible link and asymmetry

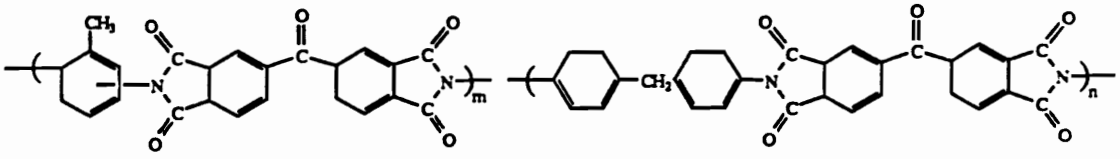

Upjohn's 2080: m ~ 80%, n ~ 20%, Tg ~310°C, asymmetry approach

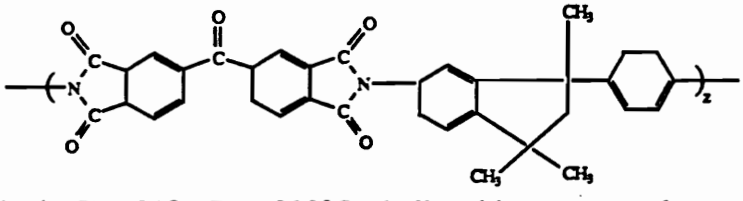

Ciba Geigy's XU 218: Tg ~320°C, bulky side groups and asymmetry

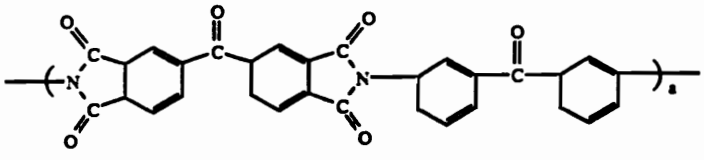

Mitusi Toatsu's and Rogers Corp. LARC-TPI: Tg ~ 260°C, asymmetry approach

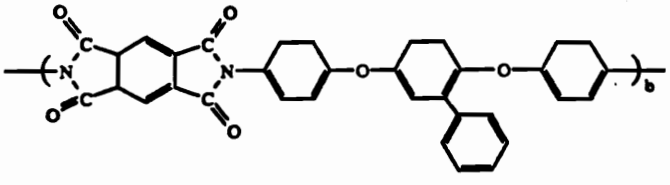

DuPont's Avimid K-III Proposed Structure: Tg ~ 294°C, bulky side group approach

Figure 3: Representative structures of some commerically available polyimides

Generally, the success of the thermoplastic polyimides is based upon molecular weight control, and the aforementioned structural modifications which promote processability: incorporation of flexible spacers, bulky side groups, and asymmetry. Examples of these commercially available thermoplastic polyimides include General Electric's Ultem™ polyetherimide (97-102), Ciba-Geigy's XU 218 (103), Upjohn's 2080 (104-105), DuPont's Avimid K-III (106-108), and Mitsui-Toatsu's or Rogers's LARC-TPI (109-114).

2.4.0 Controlled molecular weight

In addition to structural modifications, another effective, indeed critical, means of obtaining processable polyimides is by the control of molecular weight. Three scenarios are worthy of consideration:

- limiting the molecular weight of linear, thermoplastic polyimides (115),
- low molecular weight addition imide oligomers with reactive endgroups, which may be subsequently reacted to yield a network structure (section 2.4.2, 116), and
- blending high molecular weight polymer with low molecular weight oligomer terminated with reactive end groups, yielding a semi-interpenetrating polymer network (section 2.6.3).

The first approach is the focus of this research.

2.4.1 The influence of molecular weight on linear polyimides (117, 118)

In general, a minimum molecular weight, near the onset of entanglements, is required in order to attain good physical and mechanical properties for linear polymers. For many commercial step growth thermoplastic polymers, this value is approximately 20,000 to 30,000 grams per mole. A plateau is reached, however, where only a substantial increase

in molecular weight will continue to provide a noticeable improvement in properties. The relationship between *number average* molecular weight and physical properties, such as glass transition, tensile strength, density, and heat capacity, is depicted in Figure 4 (upper), and may be approximated as Polymer Property = Polymer Property at infinite molecular weight - $K\langle Mn\rangle^{-1}$.

The *weight average* molecular weight is the most important variable determining the rheological properties of polymers, therefore, molecular weight control is critical in promoting processability. The molecular weight dependence of the melt viscosity exhibits two distinct regions, depending on whether the chains are long enough to be significantly entangled (Figure 4, lower). Below a critical molecular weight for entanglements, the polymer exhibits inferior physical properties, and the melt viscosity is given by $n = K\langle Mw\rangle^{1.0}$. Above the critical molecular weight, the melt viscosity is given by $n = K'\langle Mw\rangle^{3.4}$. Furthermore, the existence of reactive end groups, particularly amines, decreases the thermal stability of polyimides markedly, as can be seen from the curves of Figure 5 (37), representing excess dianhydride (A), excess diamine (B), and equimolar stoichiometry (C). Amine end groups may potentially react under certain conditions, such as a subsequent processing step, to destabilize melt flow.

Molecular weight control may be achieved by the incorporation of a monofunctional reagent, such as phthalic anhydride or aniline, to obtain nonreactive phthalimide end groups. Alternatively, endcapping an oligomeric imide with maleic anhydride would introduce reactive endgroups which may be subsequently reacted to form a network structure. The latter approach is the basis of addition imide oligomers, an important area of

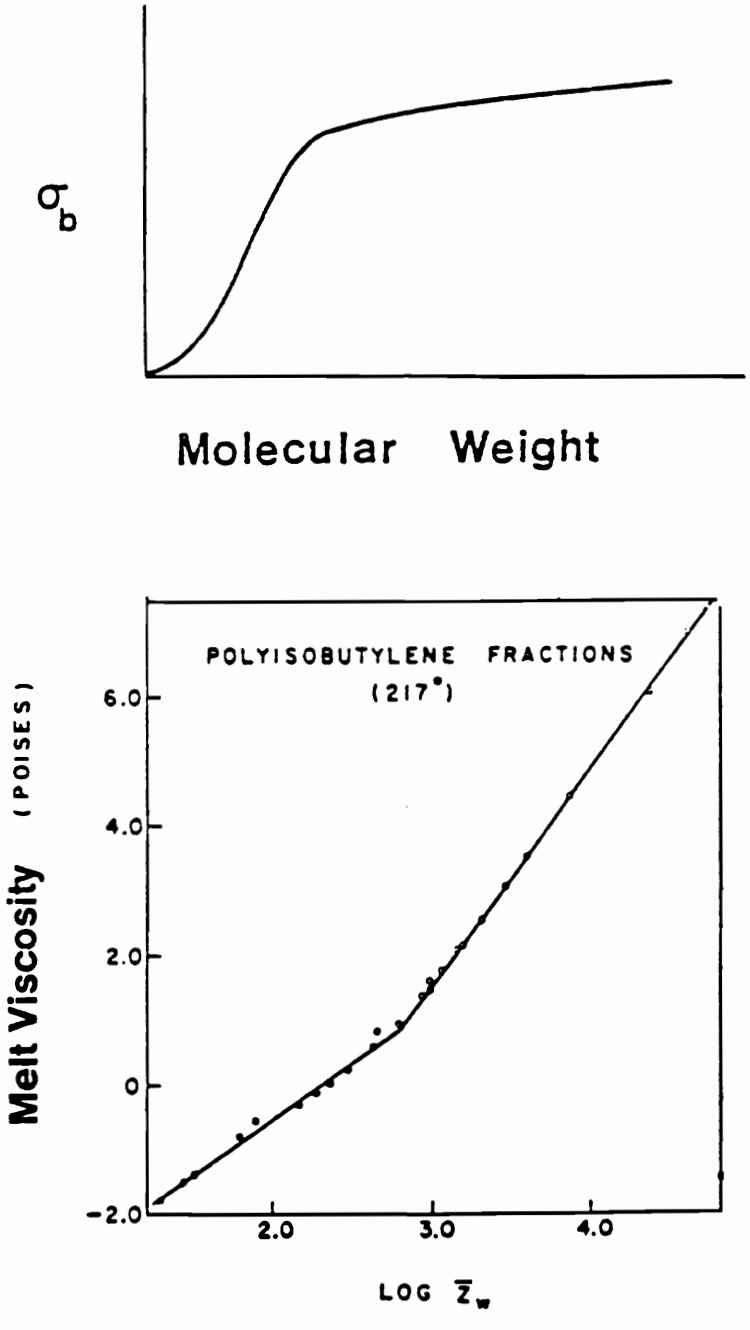

Figure 4: Influence of molecular weight: the influence of number average molecular weight on polymer properties (upper) and the influence of weight average molecular weight on melt flow and processability (lower) (117, 118)

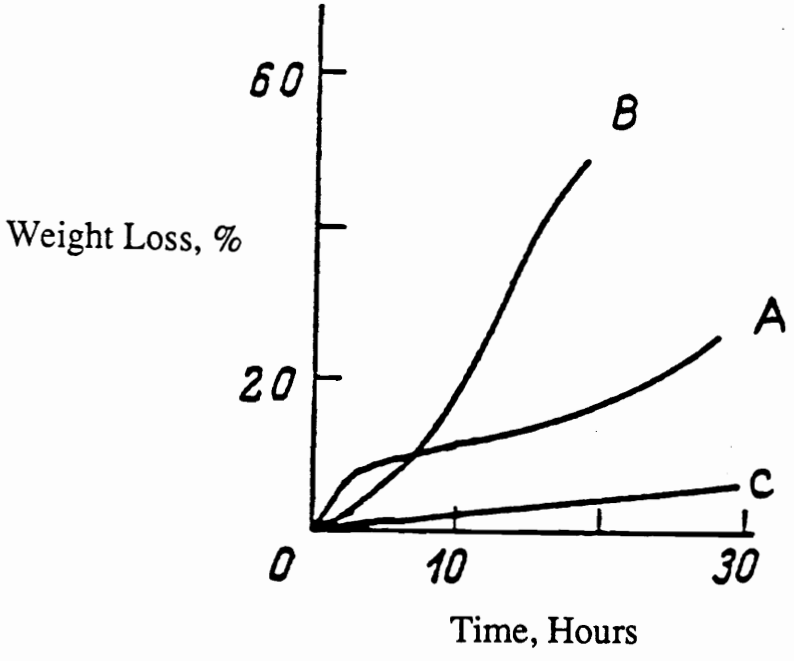

Figure 5: Influence of end groups on thermal stability: (A) anhydride, (B) amine, (C) equimolar stoichiometries employed (37)

polyimide chemistry, although not a major aspect of this research (116). An overview of addition imide oligomers is presented in the next section.

A more unique approach to enhancing processability involves the addition of diamic acid additives to the polyimide, thus broadening the molecular weight distribution. Although melt viscosities of the polyimides are decreased with the incorporation of the low molecular weight additives, mechanical properties may be compromised (119).

2.4.2 Addition imides

Addition polyimides are low molecular weight preformed imides flanked by terminal polyfunctional reactive groups. A variety of terminal groups have been used to obtain addition imides, the most common being maleimide. Other terminal groups include ethynyl, propargyl, norbornene, and benzocyclobutene. The bismaleimides are obtained by the condensation reaction of a diamine with maleic anhydride to yield the bismaleamic acid, followed by either thermal or chemical cyclodehydration. The thermally induced crosslinking reaction occurs via a free radical process across the terminal unsaturated double bonds, which can react with themselves or with other coreactants, such as vinyl, allyl, or amine functionalities. The most likely crosslinking reaction of bismaleimides is illustrated in Figure 6, however, very little fundamental information is available (120-122).

Addition imides offer the significant advantage of improved processability in the oligomeric state relative to their high molecular weight, linear polyimide analogues. Their most serious disadvantage is their extreme brittleness, and a number of techniques have been employed in order to enhance their toughness. These include increasing the chain length between the terminal endgroups (decreasing crosslink density), judicious choice of

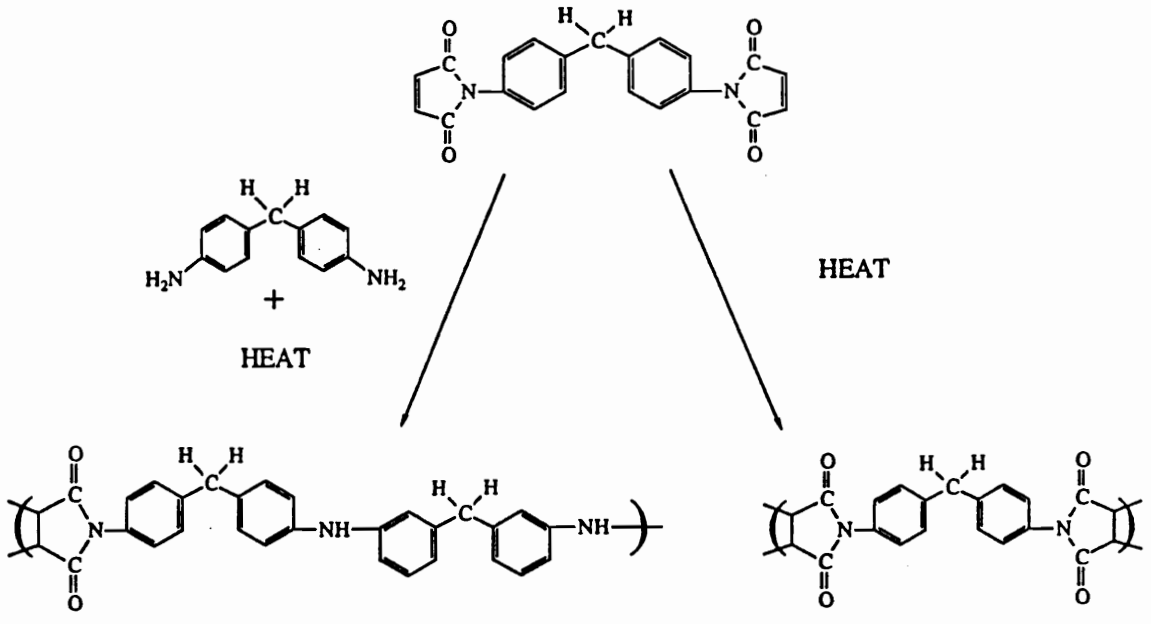

Figure 6: Representative crosslinking reactions of bismaleimides

coreactants, addition of a toughening phase, or Michael addition reactions with aromatic diamines. Several thermoplastics such as polysulfone, polyetherimide, and polyhydantoin have been successfully used to toughen bismaleimides (123). In addition, different molecular weight versions of a poly(aryl ether ketone) effectively toughen bismaleimides (124-126). A few toughened bismaleimide matrix resins are commercially available, such as Narmco's 5250 series (127).

Other addition types of polyimides, namely ethynyl and norbornene (nadic) terminated imide oligomers, are also commercially available. Ethynyl terminated imide oligomers were initially reported in 1974, and since then, these materials have received considerable attention (128, 129). Several forms of ethynyl terminated imide and isoimide oligomers are commercially available (130). The following oligomer is representative of this class of material.

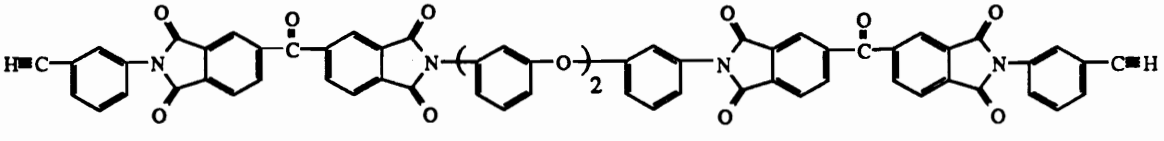

Nadic (norbornene) terminated imide oligomers were initially reported in 1970 and led to the development of PMR-15 polyimides (131, 132). The PMR chemistry, illustrated in Figure 7, involves the in-situ polymerization of monomeric reactants to yield an oligomer with a number average molecular weight of ~1500 grams per mole. Originally developed at NASA Lewis Research Center, PMR-15 is used primarily as a matrix resin in composites for use in hot environments. The crosslinking chemistry is rather complex and not fully understood (133).

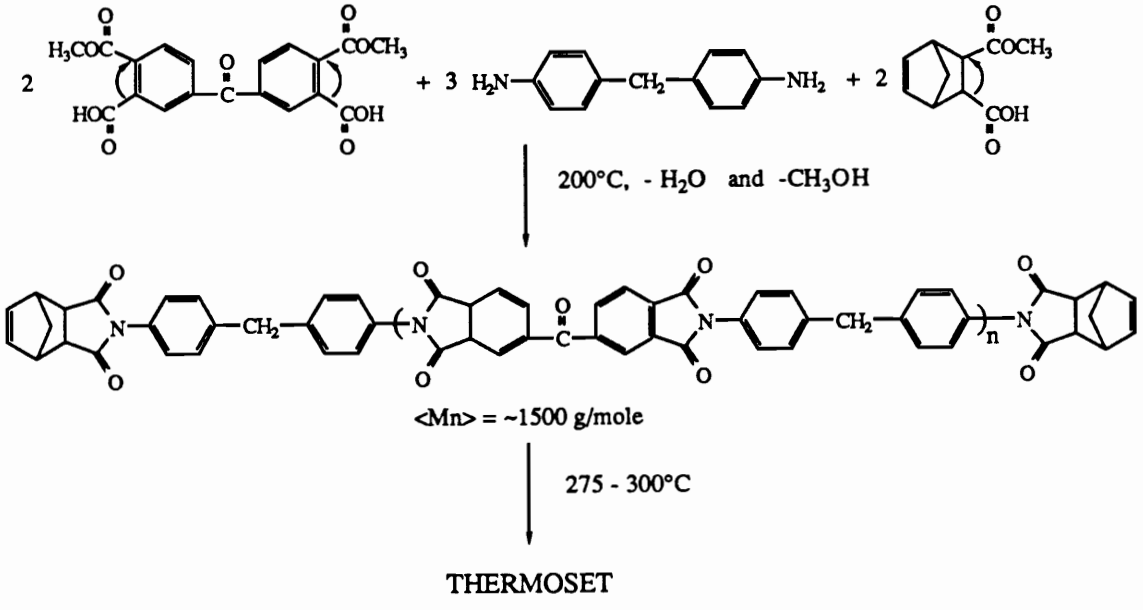

Figure 7: PMR-15 chemistry

2.5.0 Structural modification by copolymerization

A wide variety of copolyimides have been synthesized. Two particular copolyimides have been investigated in this research, poly(siloxane imide) and poly(aryl ether imide) segmented copolymers. These systems will be reviewed first, followed by an overview of other copolyimides and properties.

2.5.1 Poly(siloxane imide) copolymers

Polysiloxanes are a unique class of commercially important organic-inorganic polymers. The most commonly used siloxane is polydimethylsiloxane, although alkyl, haloalkyl, vinyl, and phenyl substituents are also possible. Various routes are available for the synthesis of polydimethylsiloxane oligomers and polymers. These include: hydrolytic reactions of organohalosilanes or organoalkoxysilanes, nonhydrolytic reactions of organohalosilanes with alcohols or bases, anionic polymerization of the cyclic tetramer using organolithium initiators (134), and equilibration reactions of cyclic monomers and low molecular weight dimers (135, 136). The equilibration process was utilized to synthesize the aminopropyl terminated polydimethylsiloxane oligomers employed in this research .

The unique properties of polydimethylsiloxane may be understood on the basis of the structure and bonding in the siloxane polymer (Table 10). The silicon-oxygen bond strength of 445 kJ per mole is stronger than the typical aliphatic carbon-carbon bond of 349 kJ per mole. This may be attributed to the ionic character of the silicon-oxygen bond, estimated at 40 to 50 percent, and to the possibility of backbonding between the filled p-orbitals of the oxygen atoms and the unfilled d-orbitals of the silicon atom (138). Thus, polysiloxanes exhibit excellent thermal stability, however, the lower bond strength of the

Table 10: Properties of polydimethylsiloxane (137)

- Low surface energy
- High compressibility
- Biological inertness
- Atomic oxygen resistance
- Low temperature flexiblity
- Low polarity (hydrophobicity)
- Thermal and oxidative stability
- Ultraviolet radiation resistance
- High permeability to small molecules
- Low viscosity for a given molecular weight
- Minimum change in viscosity with temperature
- Broad service temperature range due to low glass transition

silicon-carbon bond, at 328 kJ per mole, generally dictates that cleavage preferentially occurs at this site, with the elimination of the alkyl, or aryl, framing groups. Additionally, due to their high ionic character, siloxanes are susceptible to chemical attack by acids or bases.

The nonpolar nature of the siloxane molecule, arising from its helical conformation, results in weak intermolecular forces (138). Thus, the surface tensions of siloxanes tend to be low, in the range of 15 to 22 dynes per cm. This accounts for the surface active nature of the siloxane component of blends or multiphase block polymers. Their low energy barrier to rotation also contributes to their unique properties of low glass transitions, high gas permeability, compressibility, and hydrophobicity.

Although polysiloxanes and polyimides possess vastly different glass transitions, both exhibit excellent thermal stability attributed to the high bond strengths of their backbone units. It is not surprising, therefore, that poly(siloxane imide) copolymers have been extensively reported in the patent literature, as a means of improving the intractibility (14, 139-143) and fracture toughness (144) of polyimides, while reasonably maintaining their high use temperature. The first poly(siloxane imide)s were synthesized by Kuckertz (145), and were based upon various amine terminated siloxane dimers and pyromellitic dianhydride. Aliphatic amine terminated siloxane dimers have been extensively utilized to modify other linear polyimide systems since then (146-152). The copolyimides possess enhanced solubility and processability, however, the glass transitions and thermal oxidative stability decreased significantly, due to the aliphatic character of the siloxane end groups. The mechanical properties of copolyimides with high siloxane concentrations were similar to thermoplastic elastomers, while at low siloxane levels, more rigid behavior indicative of

a modified polyimide was exhibited (153). Siloxane dimers have also been used to modify addition polyimide systems (154-158). Monomeric siloxane containing dianhydrides have been used as well (143, 159, 160).

Microphase formation of the siloxane segment of poly(siloxane imide) segmented copolymers may arise due to the vast solubility parameter differences between the siloxane and imide components. The microphase separated structures and their corresponding interphase regions are responsible for thermal and mechanical properties that are unlike those of either homopolymer or those of a random copolymer of equal composition (14, 32, 161-163). Microphase separation favorably contributes to the thermodynamic driving force which results in an air or vacuum interface being dominated by the low surface energy siloxane component. Because of the low molecular weight and aliphatic nature of the siloxane dimer, however, microphase separation cannot occur and a single depressed glass transition results (164). Thus, incorporation of the siloxane dimer, rather than a siloxane oligomer, results in suboptimal thermal and mechanical properties. Despite these shortcomings, most of the reported research in the area of poly(siloxane imide) copolymers has involved the use of the siloxane dimer, perhaps because the incorporation of the dimer is more facile than oligomer incorporation. The patent for M & T Chemicals's poly(siloxane imide) segmented copolymer emphasizes these points, however, the high temperature stability of their segmented system is questionable due to the presence of unstable weak links along the polymer backbone (165).

Some of the applications of interest for poly(siloxane imide) copolymers include:

- toughened epoxy and bismaleimide networks (154-158),
- toughened linear polyimides (144),

- impermeable encapsulants and interlevel dielectrics for integrated circuits (166-169),
- photosensitive poly(siloxane imide)s (170-177),
- moisture and corrosion resistant adhesives (178-183),
- gas separation membranes (141, 184), and
- spacecraft coatings (185, 186).

Incorporation of silicon into polyimides may also be achieved via poly(silane imide) copolymers, which are being investigated as electrical insulators, coatings, and molded products (187). Polyimide-modified silicate hybrid networks are being explored as a means of modifying the typically brittle inorganic silicate glass, while maintaining excellent thermal stability (188, 189).

2.5.2 *Poly(aryl ether imide) copolymers*

Incorporation of the sulfone ether diamines into the polyimide backbone was motivated by several observations:

- the highest softening temperatures displayed by polyimides were those in which the heteroatoms were a sulfone type (v. g., ~500°C, for a polyimide based on sulfonyl bis(phthalic anhydride) and 4, 4'-diaminodiphenylsulfone (190), and

- to convey excellent mechanical properties, particularly toughness, and thermal stability in high temperature thermoplastics, v.g., Amoco's Udel™ polysulfone (illustrated next page) (191-194).

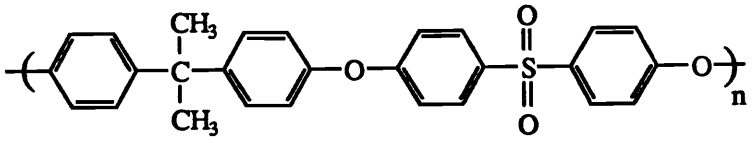

Amoco's Udel™ polysulfone

The research focused upon the incorporation of the diamine structure (below) into trimellitic anhydride acid chloride, and pyromellitic or benzophenone tetracarboxylic dianhydride (195). By enhancing solubility and tractability, the utility of the simple poly(sulfone imide) based upon pyromellitic dianhydride and 3, 3' or 4, 4'-diaminodiphenylsulfone, reported by Sroog (3, 196), was extended. In order to extend the molecular weight of the sulfone ether component, complementary sulfone ether oligomers were subsequently synthesized which were based on either bisphenol A or hydroquinone. The diamines were synthesized via a nucleophilic aromatic substitution reaction, as described by Johnson and Farnham (197).

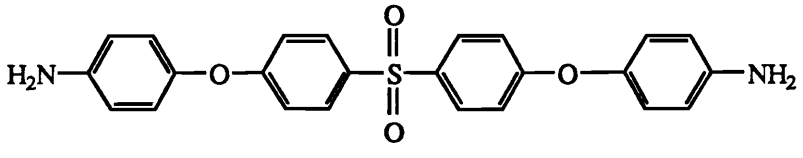

Sulfone ether diamine

The polyimides displayed good mechanical properties, high glass transitions, good thermal stability and toughness, and excellent environmental stress cracking resistance. Some properties are indicated below:

DIANHYDRIDE	TENSILE MODULUS	TENSILE STRENGTH	ELONGATION TO BREAK, %	Tg (°C)
Benzophenone	440,000 psi	14,000 psi	8	260
Pyromellitic	270,000 psi	9,600 psi	15	320

Johnson incorporated various concentrations of preimidized dihydroxy terminated imide monomers based on benzophenone tetracarboxylic dianhydride into poly(aryl ether sulfone)s (32, 198). The poly(aryl ether sulfone)s were based upon biphenol and dichlorodiphenylsulfone, and exhibited a glass transition of 229°C for the homopolymer. As the concentration of the imide component increased, thermal stability and glass transitions improved, solubility decreased, and mechanical strength increased although ultimate elongation decreased.

Considerable research has been successfully devoted to incorporating amine terminated, oligomeric poly(aryl ether sulfone)s into epoxy networks in order to improve their toughness (199-201). A similar concept has been employed by using high molecular weight poly(aryl ether ketone)s as toughness modifiers for bismaleimide resins, thus yielding a semi-interpenetrating polymer network (section 2.6.3). Amine functionalized poly(aryl ether ketone) oligomers (ATPAE, below) have been incorporated into high molecular weight polyimides to obtain block copolyimides (202). The poly(aryl ether ketone) molecular weights were ~3000 and ~6500 grams per mole. The polyimide component was based upon benzophenone tetracarboxylic dianhydride and 4, 4'-oxydianiline.

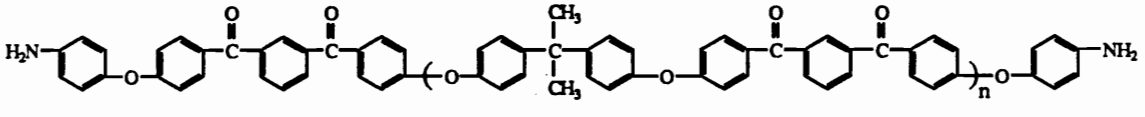

Amine functionalized poly(aryl ether ketone) oligomers (ATPAE)

Differential scanning calorimetry indicated two glass transitions for copolymers with the longer polyimide block lengths of 6500 grams per mole, whereas only one glass transition

was detected for copolymers with polyimide block lengths of 3000 grams per mole, independent of the ATPAE segment length. Mechanical properties, indicated in Table 11, followed the Fox equation "rule of mixtures" for copolymers with shorter block lengths. Copolymers with longer aryl ether segments yielded films with textured surfaces, presumably due to incompatibility, and inferior mechanical properties. The high temperature mechanical properties of the copolymer based on a segment molecular weight of 6500 grams per mole for both the aryl ether and imide components were excellent, however.

Simple poly(imide sulfone)s have been readiliy synthesized by the reaction of benzophenone tetracarboxylic dianhydride and 3, 3'-diaminodiphenylsulfone; they possess a glass transition of 270°C (203, 204). A novel approach to obtain aromatic poly(imide sulfone)s is by the oxidation of aromatic polyimide-polysulfides (below, I) or their precursor amic acids (below, II) with percarboxylic acids, where the pendant groups may be alkyl, alkoxy, acyl, or halo (205). This route offers the advantage of substituting the less reactive 4, 4'-diaminodiphenylsulfone (pKa = 2.03) with the more reactive 4, 4'-diaminodiphenyl sulfide (pKa = 4.03) to obtain high molecular weights which are not possible to achieve easily with the former diamine.

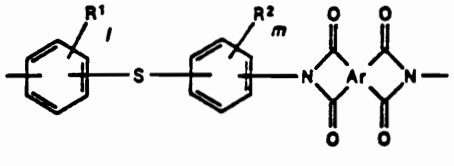

I: Polyimide-sulfide

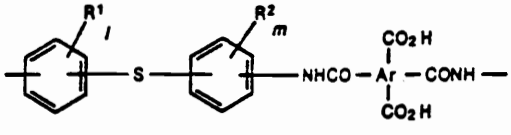

II: Polyamic acid-sulfide

Table 11: Thermal and mechanical properties of block copolyimides based upon benzophenone tetracarboxylic dianhydride and 4, 4'-oxydianiline as the imide component and poly(aryl ether ketone) oligomers (202)

		Tensile Strength, ksi			Tensile Modulus, ksi			Elongation,%		
Polymer	TGA[a]	RT	93°C	177°C	RT	93°C	177°C	RT	93°C	177°C
PAE 3110 BTDA	410	10.9	9.1	1.2	367	333	124	4.0	3.3	80
PAE 6545 BTDA	425	11.1	8.5	—	367	329	—	5.7	5.2	>100
PAE 3110 IMIDE 3110	420	14.1	11.7	3.8	415	400	158	4.9	4.9	10.3
PAE 3110 IMIDE 6545	445	16.2	13.0	6.2	431	389	50	5.7	5.3	19.1
PAE 6545[b] IMIDE 3110	440	5.8	4.2	—	321	268	—	1.9	1.9	----
PAE 6545[b] IMIDE 6545	420	11.2	9.4	3.9	324	299	60	4.6	4.6	17.7
PAE 6545+ ODA + BTDA (6545) (Random)	440	15.4	11.5	11.7	358	363	354	23.2	>50	>50
POLYIMIDE BTDA /ODA	490	19.5	15.7	9.6	526	393	290	14.6	24.4	18.2
POLY(ARYL ETHER)	475	12.7	7.6	----	381	340	—	136	124	----
POLYIMIDE/ POLY(ARYL ETHER) 1:1 BLEND	—	9.1	5.9	----	289	200	—	0.5	9.0	----

a: Thermal gravimetric analysis in air, 2.5°C per minute heating rate, temperature (°C) for 5 % weight loss

b: textured surface indicating incompatibility

2.5.3 Other copolyimides

In general, poly(amide imide)s exhibit improved solubility and processability relative to polyimide homopolymers, due to the incorporation of the amide linkage, while thermal stability is somewhat sacrificed (206-209). They are perhaps the best known copolyimides, due to the commercialization of Amoco's Torlon™, resulting from the condensation reaction between trimellitic anhydride and various diamines, including some fused heterocyclic sulfones (206). Torlon poly(amide imide)s have the highest strength of any commerical unreinforced plastic, with a tensile strength in excess of 25,000 psi and a heat distortion temperature of ~250°C at 264 psi. The poly(amide imide sulfone) is tractable with a glass transition of 270°C, tensile modulus of 370,000 psi, tensile strength of 12,500 psi, elongation of 15 percent, and impact of 171 ft-lb per cubic inch. Poly(amide imide)s have been applied in many high performance applications, such as within the space shuttle and on world class race car parts.

A series of aromatic polyimide-co-amides were synthesized by Wrasidlo (209), and illustrate the high performance properties available with this class of copolymers (Table 12). The improvement of the thermal stability of polyamides by incorporation of the imide rings is indicated in Figure 8. Another type of poly(amide imide) incorporates aliphatic and cycloaliphatic repeat units, which reduce thermal stability. However, due to the lower glass transitions for these systems (50 to 200°C), melt spun fibers and plastics with high impact strength and acceptable thermal stability up to 417 to 445°C may be obtained.

Poly(ester imide)s are commonly used as wire enamels which experience occasional temperatures in the 150 to 180°C range (210). The chemistry of the poly(ester imide) differs from that of the polyesters in that methylene dianline is one of the monomers.

Table 12: Properties of poly(amide imide)s (209)

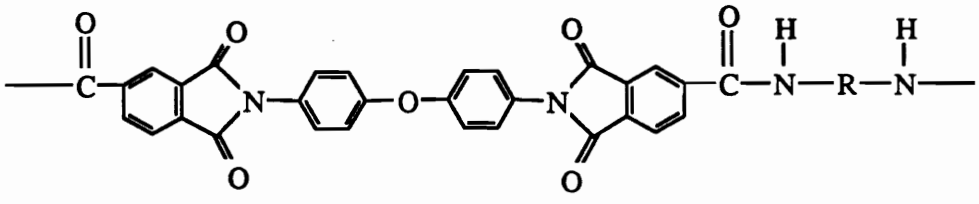

R-group	Solubility in DMAc	Intrinsic viscosity [η]	Glass transition temperature T_g, °C	Thermal decomposition PDT, °C	Isothermal weight loss at 325°C in air, %	
					After 120 hr	After 240 hr
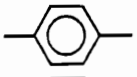	Ins	0.7	—	455	9.8	11.5
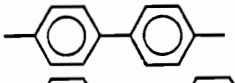	Ins	0.9	315	520	10.1	10.1
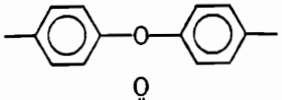	Sol	2.0	290	460	14.8	19.5
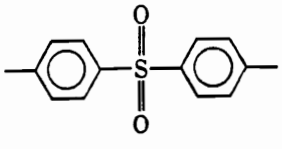	Sol	1.6	275	475	7.4	7.4

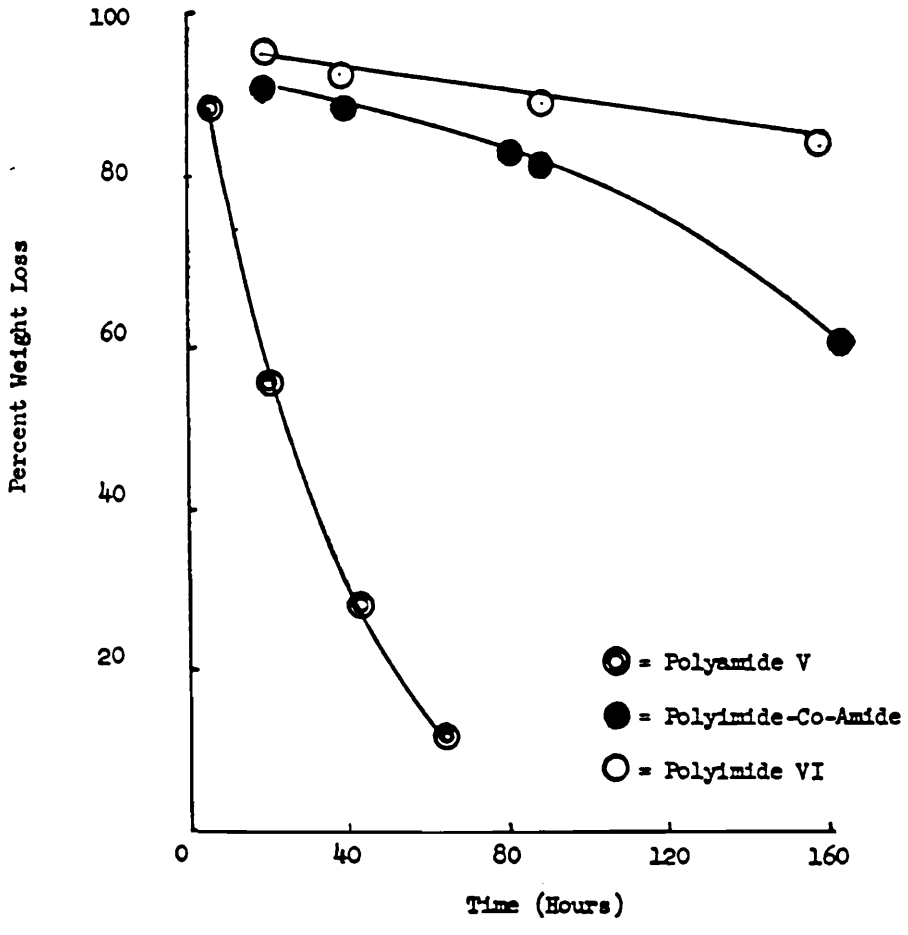

Figure 8: Thermal stability, as judged by thermal gravimetric analysis, for poly(amide)s, poly(imide)s, and poly(amide imide) copolymers (209)

Reaction with anhydrides such as trimellitic anhydride provides for the imide content, and the remaining acid groups of the trimellitic anhydride are available to form ester linkages. Although poly(ester imide)s are processable and possess a reasonable balance of mechanical and electrical properties, they exhibit inferior thermal stability to the aromatic polyimides.

A series of novel potentially liquid crystalline poly(ester imide)s have recently been synthesized by Kircheldorf (211, 212). Some polymers of this series were obtained by the condensation reaction of diacids based upon either pyromellitic or benzophenone tetracarboxylic dianhydride with methylene spacers, with the diacetates of hydroquinone, 2,6-dihydroxynapthalene, or biphenol. Some of the structures are indicated in Table 13. The high heat distortion temperatures of the poly(ester imide)s based upon the pyromellitimide unit were related to the melting points and not to the glass transitions, suggesting that the crystallites of these polymers formed the coherent matrix. In contrast to these polymers, the poly(ester imide)s based upon benzophenone tetracarboxylic dianhydride displayed amorphous fraction glass transitions which decreased from ~140°C to ~46°C with increasing length of the methylene spacer. Most of the poly(ester imide)s based upon hydroquinone and napthalene did not form a mesophase, except for the poly(ester imide) based upon hydroquinone with a 10 unit methylene spacer. This observation was attributed to a weak charge-transfer complex between the bisphenol and the benzophenone imide. Furthermore, it was noted that a 10 unit methylene spacer exactly fit with the length of a benzophenone imide unit. Thus, the molecular dimensions of these poly(ester imide)s favor a high degree of crystallinity. Formation of a mesophase was observed for poly(ester imide)s derived from pyromellitic dianhydride and hydroquinone, however, the pyromellitimide unit itself is a mesogenic group.

Table 13: Structures and properties of liquid crystalline poly(ester imide)s (212)

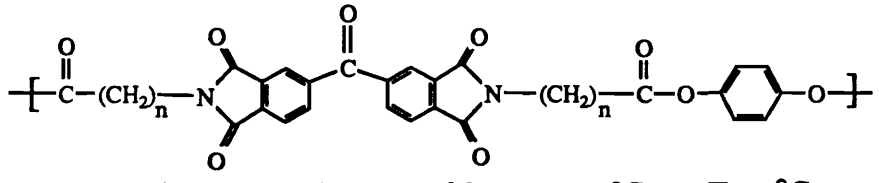

n	Yield, %	η_{inh}(dl/g)	Tg, °C	Tm_1, °C	Tm_2, °C	mesophase, °C
3	83	0.36	119			
4	92	0.21	109			
5	91	0.30	84			
6	84	0.40	79	133	147	
10	93	0.47	46	146	168	136-167
11	97	0.40	46	143		

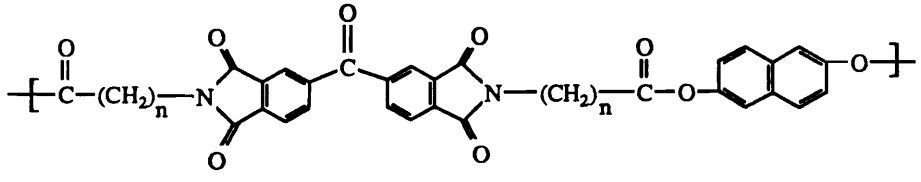

n	Yield, %	η_{inh}(dl/g)	Tg, °C	Tm_1, °C	Tm_2, °C	mesophase, °C
3	85	0.37	139			
4	83	0.32	116			
5	90	0.32	99			
6	84	0.60	92			
10	84	0.64	58	149	169	
11	88	0.57	57	163		

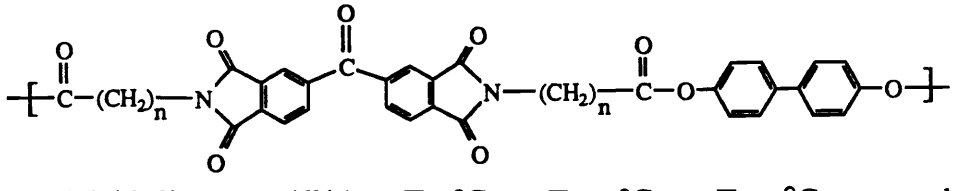

n	Yield, %	η_{inh}(dl/g)	Tg, °C	Tm_1, °C	Tm_2, °C	mesophase, °C
3	88	0.31	120	268	315	272-320
4	95	0.32	111	279	309	281-305
5	83	0.46	105	197	221	203-228
6	92	0.31	90	194	212	208-224
10	82	0.66	76	193	210	200-216
11	82	0.55	59	182		

A successful effort to simultaneously improve mechanical properties, thermal stability, and processability of polyimides involved the ordered introduction of heterocyclic units into the imide backbone (36, 213-219). A common approach has involved the preparation of dianhydrides containing preformed heterocyclic units which may be reacted with diamines and subsequently imidized (Figure 9). Diamine functional heterocycles have also been reacted with a variety of diamines, alhthough this route potentially introduces less order if an unsymmetrical diamine reacts in a fashion other than head-to-tail (214, 215). Some of the heterocyclics have included benzoxazole (216), benzoxazinone, benzothiazole (217), benzimidazole (218), and oxadiazole (218, 219). Thermal stabilities are comparable to analogous homopolyimides, in the order of oxazole (530°C), oxazinone (510°C), and thiazole (430°C), as determined by thermal gravimetric analysis in air (10 percent weight loss). Solution stabilities, however, are superior to the simple pyromellitimides (36).

In an effort to remove all hydrogen and thereby improve thermal oxidative stability, Hirsch has synthesized the following structure (220):

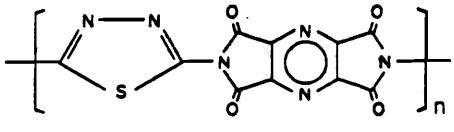

Film strength was adversely affected by limited conversions, due to a lack of solubility of the high molecular weight amic acid. Thermal stability was reported to be excellent, with higher stability obtained in air (10 percent weight loss at 450°C) than nitrogen (410°C). A 20 psi stress was applied to a strip of film and the sample was heated at 4°C per minute to demonstrate the zero strength temperature of 590°C, compared to the polypyromellitimide based on 4, 4'-oxydianiline, which chars at 320°C under these conditions.

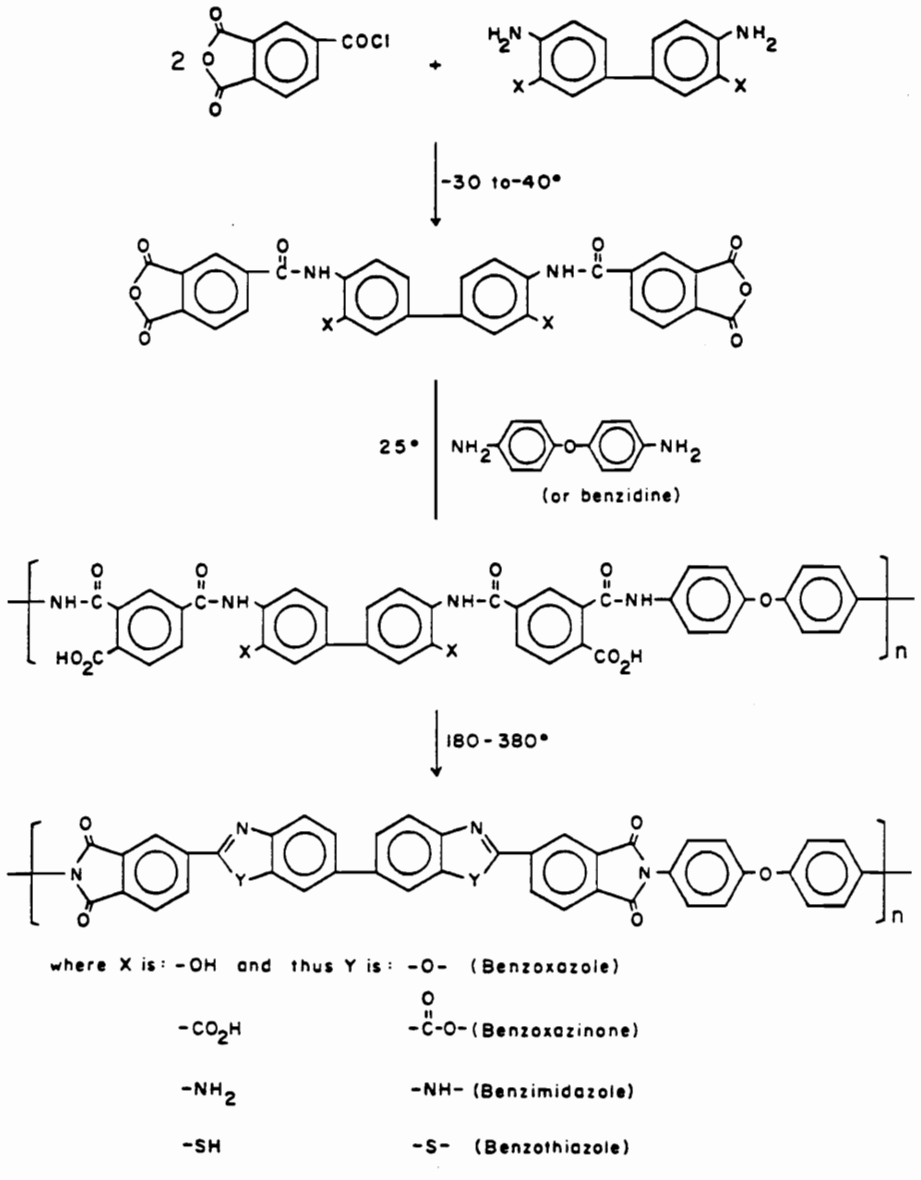

Figure 9: Synthesis of poly(heterocyclic imide)s (213)

An interesting approach to a heterocyclic imide involves the rearrangement upon heat treatment (1 hour at 200°C, 0.5 hour at 300°C) of a polyimide based upon various dianhydrides and the isobenzoxazole diamine illustrated below:

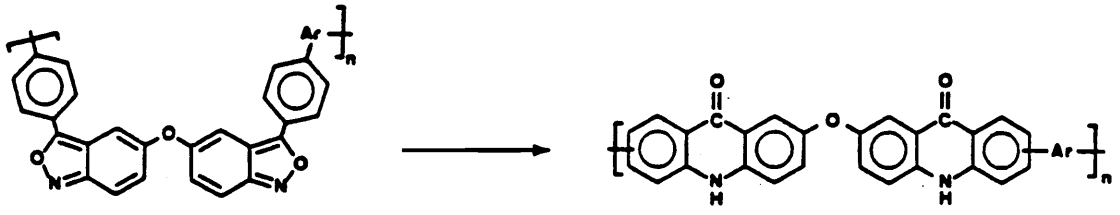

The conversion was accompanied by a significant increase in the glass transition from 194°C to 313°C when based upon the hexafluoroisopropylidene dianhydride. The rearrangement was monitored by fourier transform infrared spectroscopy (221).

An extreme approach to improving the processability of polyimides for fabrication of thick samples and adhesives has involved the incorporation of elastomeric blocks (222-226). Thus, an isocynate terminated polybutiadiene was reacted with an aromatic diamine, then condensed with a dianhydride (225, 226). The resulting A-B-A block polymer possessed a rigid imide center flanked by soft ends. The 1, 2-polybutadiene segments were also sites for post-peroxide cure. Thermal gravimetric analysis indicated a high degree of stability for the cured materials, with a 70 percent imide copolymer exhibiting 10 percent weight loss at 465°C.

Polyimides based upon benzophenone tetracarboxylic dianhydride and 4, 4'-oxidianiline were modified with aromatic amine terminated butadiene acrylonitrile elastomers (ATBN) of various acrylonitrile contents (226). As these modified polyimides were linear and noncrosslinked, thermal stability, tensile properties and density decreased with ATBN

incorporation. Variations in the acrylonitrile content in a 15 percent ATBN copolyimide could not be correlated with mechanical properties. Some films, however, exhibited enhanced tear resistance, although correlations with morphology were not obvious.

The condensation of dianhydride terminated imide oligomers with diamine terminated polyformal oligomers yielded poly(imide formal) block copolymers which generally exhibited two glass transitions, depending on the block lengths and oligomer compositions (227). Flexibility was qualitatively greater than for the hompolyimide. Most of the copolymers exhibited good thermal oxidative stability, particularly systems based upon bisphenol A and fluorenone formal oligomers.

2.6.0 Property modification by blending

2.6.1 Thermodynamic theory of homopolymer blend miscibility

The field of polymer science and technology has expanded rapidly over the last several decades primarily through the development and study of new homopolymers, followed by copolymerization for polymer modification, and finally, the more controlled syntheses of block and graft copolymers. The economics of expansion driven by the development of new polymers, however, have become increasingly prohibitive. Furthermore, new chemical structures are not always needed to meet current needs. As a result, the concept of polymer blending to obtain new products has been advanced, representing a more physical approach to property diversification than through chemical modifications (228-231).

The thermodynamics of polymer-polymer blends is one of the most important fundamental elements of blend technology, since it affects the molecular state of dispersion, the morphology of the mixture, the adhesion between the phases, and consequently influences most properties and applications (230). For a blend to exhibit thermodynamic stability, the Gibb's free energy of mixing must be negative, $\Delta G = \Delta H - T \Delta S < 0$. Such a statement, however, is only a degenerate form of the total Gibb's criteria, because it does not distinguish between unstable, metastable, or stable states, which is so important in phase separation phenomena. Therefore, a homogeneous, single phase blend with a negative free energy of mixing could possibly achieve an even lower free energy state by splitting into two phases via nucleation and growth or spontaneous spinodal decomposition, depending on the shape and location along its free energy curve. This point is illustrated in Figure 10 (232); the boundary between the stable one phase region and the metastable composition is called the binodal, and the boundary between metastable and unstable compositions is called the spinodal. Thermodynamic miscibility, in fact, is governed not only by a negative free energy of mixing, but also by the composition dependence of the Gibb's free energy of mixing, $\partial 2G/\partial V2 > 0$, where V is the volume fraction of the second polymer component. This criteria defines the spinodal stability limit. The binodal curve of the phase boundary is defined by the equality of the chemical potentials in the two equilibrium phases, $\Delta \mu_1 = \Delta \mu'_1$ and $\Delta \mu_2 = \Delta \mu'_2$.

Until recently, techniques for examining the thermodynamics of miscible polymer-polymer blends were limited. Neutron scattering experiments which are now beginning to appear are starting to fill this need. Miscibility, therefore, has frequently been defined on a practical, macroscopic scale, such that the blend in question exhibits properties analogous to those expected from a single phase material, intermediate of the components. In most

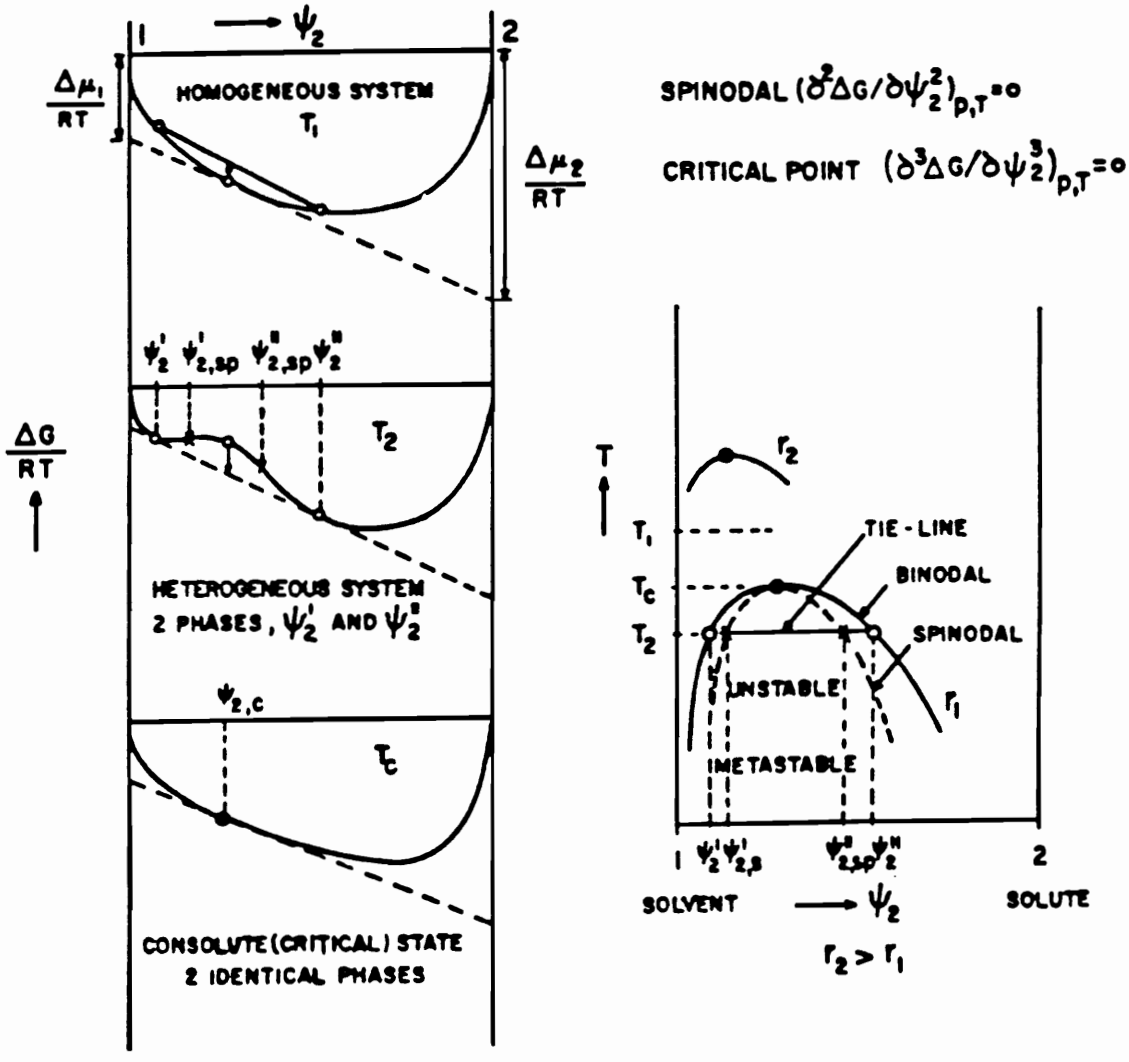

Figure 10: Free energy of mixing as a function of concentration in a binary liquid system showing partial miscibility (232)

instances, the critical property is a single glass transition. Miscibility is usually a rare occurrence among polymer blends, because the required negative Gibb's free energy of mixing is difficult to obtain for high molecular weight components. From a thermodynamic point of view, however, every polymer has some solubility in every other polymer. Therefore, the magnitude of miscibility has become the critical, property determining issue. For many purposes, miscibility in polymer blends is neither a requirement nor desired, however, adhesion between the components frequently is (228). Arising from this perspective is the term compatible, which has come to mean, in a technological sense, that a desired or beneficial result has been obtained when two materials are combined together, independent of whether the blend is miscible or not. The rubbery modification of glassy polymers illustrates a compatible, although not miscible system, and miscibility is not, in fact, desired. Also, numerous blends exhibit behavior which is neither truly single phase or indicative of two pure phases. For instance, the glass transition of a blend may be broadened over that usually observed for single phase systems, or a two phase blend may exhibit both glass transitions shifted from the pure component values. At the extreme, gross immiscibility in polymer blends is usually easily detected by opacity, delamination, double glass transitions, or a combination of these properties.

The miscibility of nonpolar polymers of substantial molecular weights is only a rare occurrence because the entropy of mixing will be very small, owing to the few moles of each polymer in the blend, and the enthalpy of mixing is generally positive. However, the enthalpy of mixing can be exothermic if specific interactions between polar moieties are involved. Olabisi proposed the concept of complementary dissimilarity, wherein a wide range of many-body interactions provides the driving force for miscibility (230, 233). These specific interactions may be nonpolar-polar, hydrogen bonding (234, 235), charge-

transfer, electronic, acid-base, or dipole-dipole (230). However, an endothermic contribution still exists from the dispersive interactions, or van der Waals forces, between the remaining parts of the structure which do not specifically interact. The specific interactions perhaps account for the many examples of miscibility or partial miscibility among halogenated polymers and those containing oxygen (ester groups) (228). In addition to having the proper types and concentration of interacting groups, they must also be properly arranged spatially to produce the desired interaction.

2.6.2 High performance miscible polymer blends

Despite the thermodynamic and practical restrictions, a great number of miscible polymer blends are known (228-231, 236). Very few, however, are considered high performance materials. The first amorphous engineering thermoplastic blend, introduced by General Electric in 1968, was the miscible blend of polyphenylene oxide and polystyrene, known as Noryl™ (237a). The Noryl GTX™ resins, on the other hand, are truly incompatible blends of polyphenylene oxide and polyamide (237b). In this case, morphology, rheology, and properties are mainly controlled through compatibilization and impact modification technology. The advantages of a high glass transition, ductile amorphous polymer, bisphenol A polycarbonate, and the semicrystalline, chemically resistant thermoplastic polybutylene terephthalate are displayed in General Electric's Xenoy™ blends (237b). These blends were mainly characterized by partial miscibility, with stabilization and impact modification being required to upgrade properties for certain applications.

Miscible blends of semicrystalline poly(aryl ether ketone)s (PAEKs) with other polymers have been mentioned in the patent literature (238, 239), and PAEK miscibility with General

Electric's amorphous polyetherimide (PEI) Ultem™ 1000 has been reported (240, 241). This combination offers an interesting balance of properties as it exhibits miscibility in the amorphous state. The semicrystalline PAEK component imparts excellent hydrolytic, thermal, acid, base, and chemical resistance, along with excellent mechanical properties and a very high upper use temperature. The PEI possesses a high glass transition of 220°C, but suffers from chemical sensitivity. The PAEK component of this study was of two types:

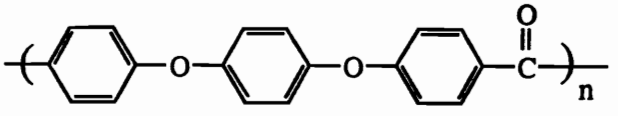

PAEK-I
(or PEEK™, ICI)

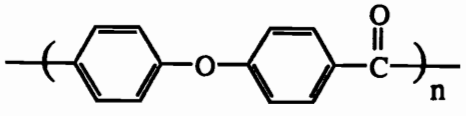

PAEK-II

The quenched, amorphous blends of PAEK-I and PEI displayed a single, sharp glass transition obeying the Fox equation, indicative of miscibility. The melting points and glass transitions of isothermally crystallized (300°C) samples are depicted in Table 14. Little variation of the melting point with composition was observed, however, the glass transition increased with PEI incorporation. Likewise, the annealed and crystallized blends exhibited a significant increase in strength and modulus accompanied by a decrease in ultimate elongation, although maximum toughness was experienced at intermediate compositions. The incorporation of the PAEK into the blends clearly also improved the environmental stress crack resistance of PEI in aromatic hydrocarbons (toluene) and chlorinated aliphatic hydrocarbons (trichloroethylene). Crystallized blends of PAEKs I and II have also been investigated (242).

Table 14: Glass and melting transitions of miscible blends of poly(aryl ether ketone) with polyetherimide (240)

Weight % PAEK-I	Tg, °C	Tm, °C
100	142	343
80	155	340
70	161	340
60	168	340
50	176	340
40	183	340
0	215	340

Miscible blends of a sulfonated poly(ether ether ketone), PEEK™ from ICI (structure PAEK-I in previous study) with the PEI Ultem 1000 and a poly(amide imide) (PAI), Torlon™ 4000T from Amoco, have also been investigated (243). PEEK exhibits a glass transition of 143°C and melting transition of 343°C, although sulfonated PEEK is completely amorphous, except at very low sulfonation levels. The PAI exhibits a glass transition of 273°C. The glass transitions as a function of composition are displayed in Figure 11. For nearly all compositions in both blends, the experimentally determined glass transitions were higher than the value calculated by the Fox equation. Since the nonsulfonated PAEK-I/PEI blends of the previous study do not show this deviation, the presence of strong intermolecular interactions is implied.

Hedrick has investigated the effect of structural variations of the PAEK component on the miscibility with PEI, finding that blends with the following PAEKs were immiscible (244):

- Bisphenol A and dichlorodiphenylsulfone (Udel™, Amoco)
- Bisphenol A and difluorobenzophenone
- Bisphenol S and difluorobenzophenone
- Hydroquinone (50%), biphenol (50%) and difluorobenzophenone, and
- poly(ether ketone ketone ether)

Hedrick has also investigated the effect of structural variations of the polyimide component on the miscibility with PEEK (244). This aspect is qualitatively covered as part of this research (section 4.12). The blends were based upon PEEK and a novel polyimide based on benzophenone tetracarboxylic dianhydride and 4, 4'-[1, 4-phenylene-bis-(1-methyl ethylidene)] bisaniline (Bis P, section 3.3.4). The polyimide was molecular weight controlled to 25,000 g/mole (<Mn>) by the addition of phthalic anhydride to enhance melt

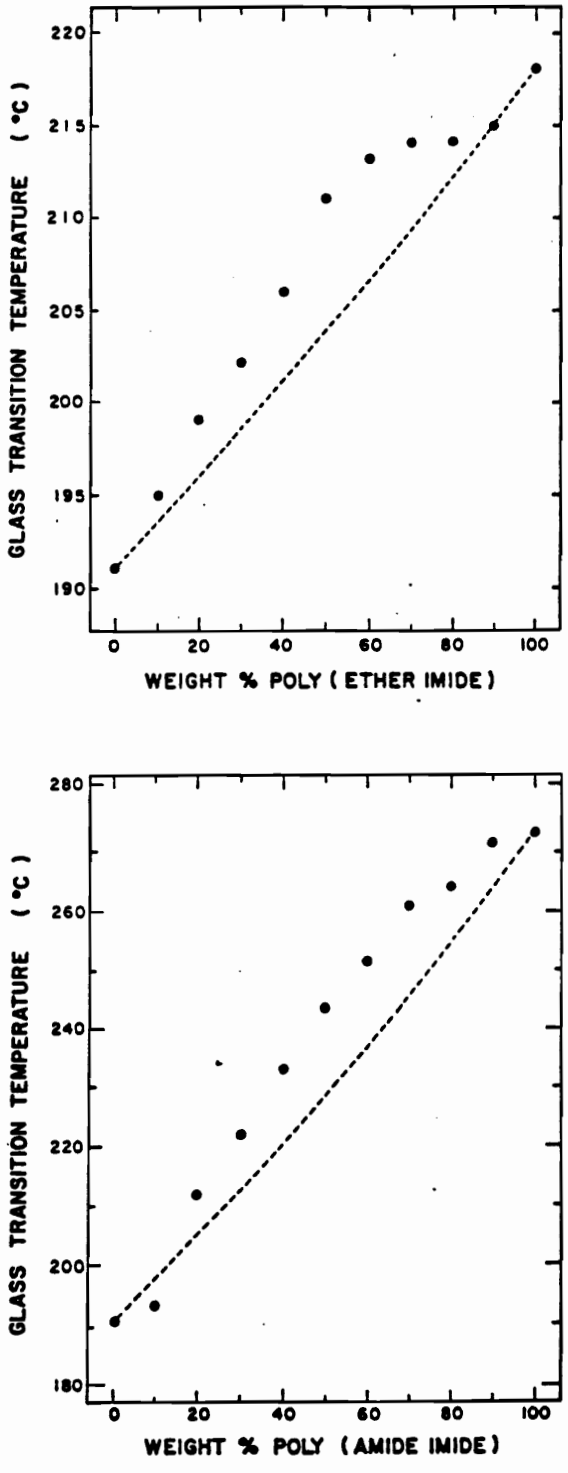

Figure 11: Glass transitions of blends of sulfonated PEEK and polyetherimide (upper) and poly(amide imide) (lower) (243)

processability. The thermal transitions of the quenched, amorphous miscible blends are listed in Table 15. Similar to the results of the PAEK/PEI blend study, the melting transitions were relatively unaltered by the compositional variations of the blends. Crystallinity of the PEEK component of the blends was suppressed most probably due to the rigidity of the polyimide component and its high molecular weight of 25,000 grams per mole. Blends of PEEK with a polyimide of the same composition but lower molecular weight of 15,000 grams per mole did exhibit some crystallinity when slow cooled from the amorphous melt.

Blends of General Electric's poly(siloxane ether imide) copolymer with polycarbonate and PEI have also been reported, to capitalize on the benefits of siloxane incorporation (245, 246). Spectroscopic studies are currently underway in all of these research efforts to determine the nature of the interactions between poly(aryl ether ketone)s and polyimides.

Miscible blend technology has been explored as a means of generating polymeric matrix resins for advanced aerospace, fiber reinforced composite and adhesive applications, which are readily processable by conventional techniques, yet stable to 700°F (371°C). In particular, polybenzimidazole (PBI) was found to be miscible with a range of aromatic polyimides, including thermoplastic polyimides (247-253). PBI possesses an unusually high glass transition of ~420°C, high temperature mechanical properties, and solvent resistance, although it lacks true thermoplastic processability and has poor thermal oxidative stability (256, 257). Miscibilites of PBI and the polyimides Ultem 1000 (249, 252-254), Ciba Geigy's XU 218 (Tg 320°C) (251, 254), Mitsui Toatsu's LARC-TPI (Tg 270°C) (248, 250), and Dow Chemical's 2080 (Tg 310°C) (247, 252, 254) have been

Table 15: Glass transitions of amorphous blends of poly(ether ether ketone) (PEEK) and molecular weight controlled (25,000 g/mole) polyimide (PI) based upon benzophenone tetracarboxylic dianhydride and 4, 4'-[1, 4-phenylene-bis-(1-methyl ethylidene)] bisaniline; crystallization suppressed with high molecular weight polyimide (244)

Glass transitions of amorphous miscible PEEK/Polyimide Blends

Composition		Glass Transition, °C	
% PEEK	% PI	Experimental	Theoretical*
100	0	143	----
75	25	171	167
50	50	197	194
25	75	226	225
0	100	265	----

* Fox Equation

demonstrated. The structures of these thermoplastic polyimides were indicated in section 2.3.0. The structure of PBI is illustrated in Figure 12.

Miscibility in the blends was attributed to specific interactions. Specifically, three sources of the interactions were postulated as: (a) hydrogen bonding between the carbonyl groups of the imide ring and the amine group of the imidazole ring, (b) π-orbital interactions between the imide and imidazole rings, or (c) charge transfer interaction between the phthalimide and benzimidazole fused ring systems. The composition dependent bands of the amine stretching of PBI and the carbonyl stretching of Ultem were monitored by fourier transform infrared spectoscopy (FT-IR) and used to elucidate the nature of the interactions. Phase separation in the blends occurred at temperatures greater than their respective glass transitions, however. The glass transitions of blends of PBI and Ultem™ 1000 are indicated in Figure 12 (254).

Blends of PBI with XU 218 exhibited inferior thermal oxidative stability relative to the PBI/Ultem blends. Additionally, the PBI/Ultem blends experienced accelerated degradation at 450°C relative to the weight loss incurred by either homopolymer alone. As determined by a degradation study of labelled polymers monitored by FT-IR, the imidazole or aromatic amine degradation products of PBI appeared to catalyze the decomposition of Ultem, and in particular, attack the ether linkage. Substitution for Ultem by a polyimide partially comprised of the hexafluoroisopropylidene moiety along its backbone improved thermal oxidative stability, as well as lowered water sorption and enhanced thermoplastic flow behavior. Benzophenone tetracarboxylic dianhydride was also incorporated into this improved polyimide to promote miscibility with PBI by specific interactions (253).

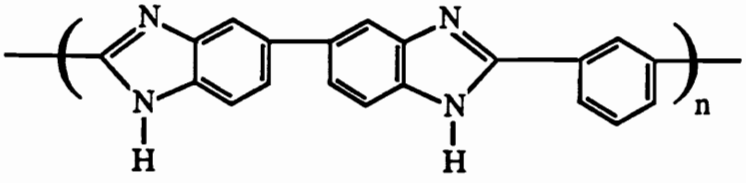

Poly[2, 2'-(m-phenylene)-5, 5'-bibenzimidazole] (PBI)

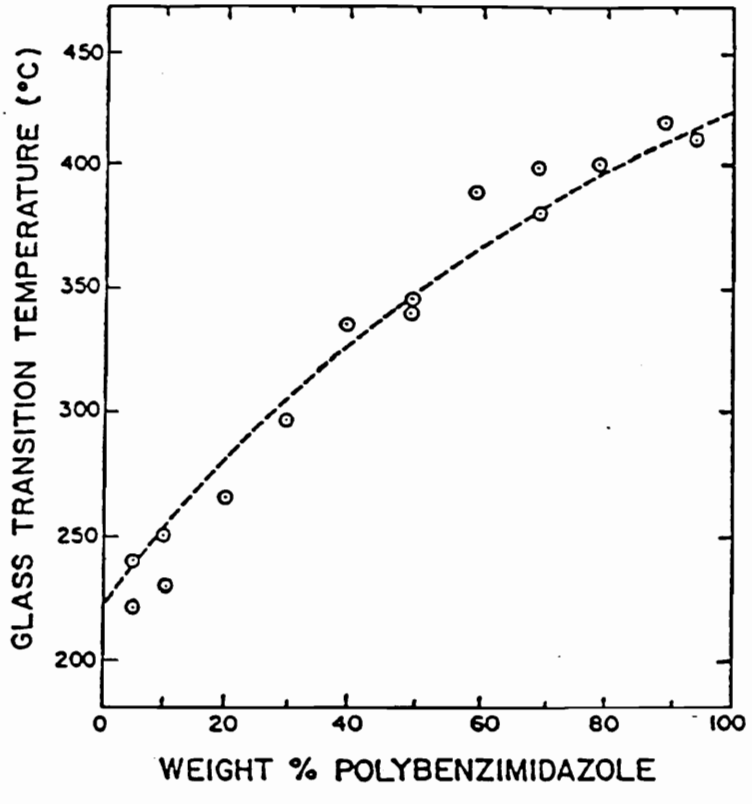

Figure 12: Glass transitions of miscible blends of polybenzimidazole with Ultem™ 1000 (254)

As a means of obtaining a combination of properties such as good adhesion, high temperature dimensional stability, mechanical properties characteristic of a tough material, and low thermal expansion coefficient, an effort to generate molecular composites by blending rigid polyimides with more flexible polyimides was attempted. Due to the difficulty of blending high molecular weight, high glass transition, rigid polyimides, however, the polymers were mixed in their poly(amic acid) form (258, 259). Dynamic mechanical analysis and optical microscopy, as well as qualitative indications of turbidity of the solutions, indicated that the dynamic nature of the poly(amic acid)s induced randomization, yielding a copolymer, rather than a blend (258). The degree of phase separation in the cured polyimide films was found to depend on the chemical randomization process and the interaction energy between the polymer segments. Composite properties have been evaluated for a blend of poly(amic acid)s based on benzophenone tetracarboxylic dianhydride (260). The diamines were 3, 3'-diaminodiphenyl sulfone (NASA Langley polyimidesulfone) and 3, 3'-diaminobenzophenone (LARC-TPI). An attempt to generate molecular composites by blending liquid crystalline polyesters with the polyetherimide Ultem has also been attempted. (261)

2.6.3 Semi-interpenetrating polymer networks (IPNs)

A semi-interpenetrating polymer network is a combination of polymers in network form, where at least one of the polymers has been polymerized and/or crosslinked in the immediate presence of the other (262). While ideally the polymers should interpenetrate on the molecular level, actual interpenetration may be limited by phase separation. IPNs have been explored as a means of enhancing the toughness of brittle crosslinked networks, such as crosslinked addition imides or epoxies, by incorporating tough thermoplastics (43, 263-

269). They may also exhibit improved processability relative to that of the high molecular weight thermoplastic. The concept of IPNs is illustrated in Figure 13 (268).

2.7.0 Requirements for electronics packaging applications

Polyimides are increasingly being used in the electronics industries for a variety of applications: as fabrication aids such as photoresists, planarization layers, and ion implant masks, as passivant overcoats and interlevel insulators, as adhesives, and as substrate components (270). The technology requirements vary depending on the specific application, however, the properties of polyimides for electronic applications should include (271):

- Thermal stability to withstand processing temperatures as high as 400°C
- Good mechanical properties and adhesion to the substrate
- Excellent insulating capabilities
- Chemical resistance to process solvents

2.7.1 Dielectric constant

Commerically available polyimides generally have dielectric constants in the range of 3.2 to 4.0, depending upon the freqency of evaluation and the level of sorbed water (272, 273). St. Clair has studied the structure-to-property relationships of highly insulative, low dielectric constant polyimides (273). Dielectric constants less than 3.2 were obtained by reducing the interactions between the linear polyimide chains and by the incorporation of fluorine into the polyimide backbone (Table 16).

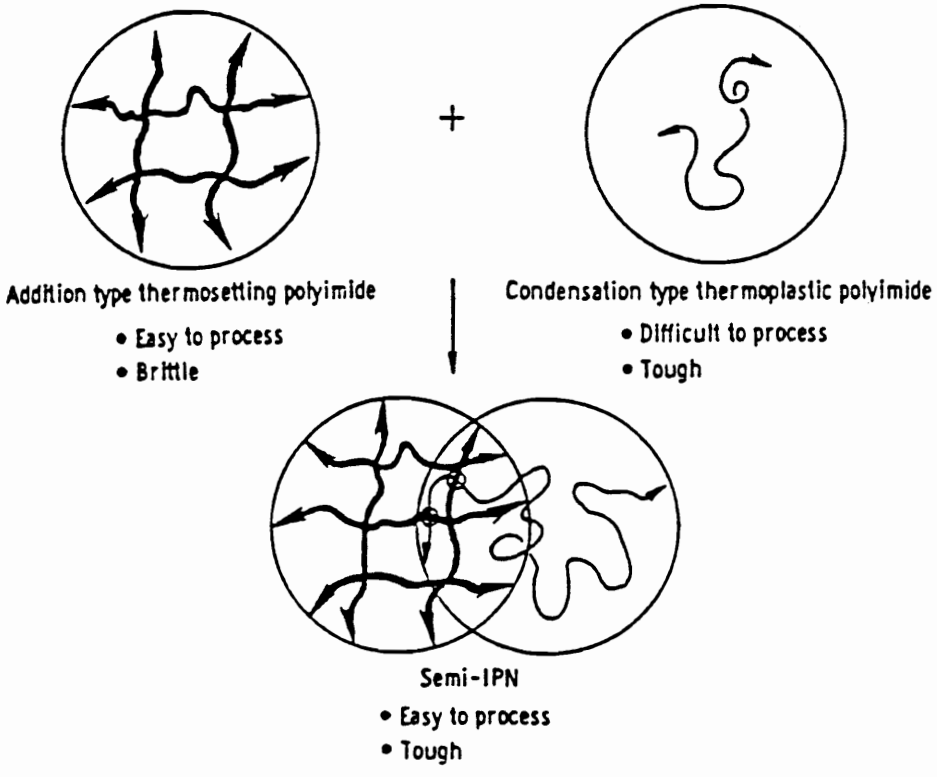

Figure 13: Concept of semi-interpenetrating polyimide networks (268)

Table 16: Dielectric constants for polyimides (273)

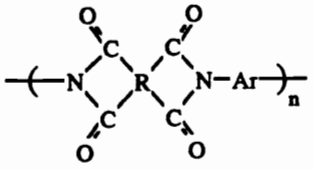

POLYMER	DIANHYDRIDE R	DIAMINE Ar	DIELECTRIC CONSTANT at 10 GHz
PMDA + 4,4'-ODA (KAPTON®)		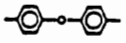	3.22(3.25)
PMDA + 3,3'-ODA		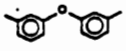	2.84
BTDA + 4,4'-ODA	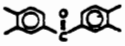	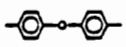	3.15
BTDA + 3,3'-ODA	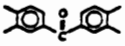	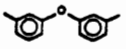	3.09
ODPA + 4,4'-ODA	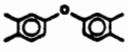	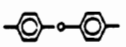	3.07
ODPA + 3,3'-ODA	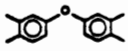	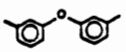	2.99
HQDEA + 4,4'-ODA	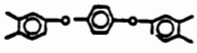	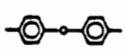	3.02
HQDEA + 3,3'-ODA	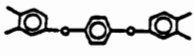	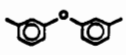	2.88
BDSDA + 4,4'-ODA	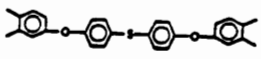	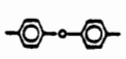	2.97
BDSDA + 3,3'-ODA	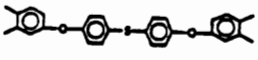	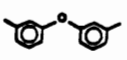	2.95
6FDA + 4,4'-ODA	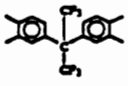	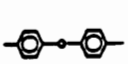	2.79
6FDA + 3,3'-ODA	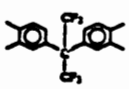	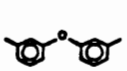	2.73

2.7.2 Thermal coefficient of expansion (TCE)

Numata has investigated the relationship of molecular structure to the thermal coefficients of expansion for a series of polyimides, as indicated in Table 17 (274). In general, the low thermal coefficient polyimides (boxed) possessed linear backbones and were generally composed of pyromellitimide and biphenyl moieties, which do not have flexible linkages. The thermal coefficients of expansion for polyimides typically ranged from 3 to 6 X 10^{-5} K^{-1}. The polyimides with rigid, linear backbones, however, exhibited values in the range of inorganic materials.

2.8.0 Requirements of aerospace applications

The conditions in which space structures operate are exteme and dynamic (275-280). Space materials may be exposed to radiation bombardment by protons, electrons, and the full solar UV spectrum, vacuum from 10^{-6} to 10^{-17} Torr, and thermal cycling from -160 to +120°C. The environment around the Space Shuttle consists of a gaseous contaminant "cloud" due to surface outgassing, exacerbated by solar heating and enhanced by thruster firings. In the low earth orbit (LEO), the primary atmospheric contamination is atomic oxygen (Figure 14). Although the number densities of any of the atmospheric constituents at typical spacecraft operating altitudes are low, the high orbital speed produces flux densities large enough (10^{13} to 10^{15} atoms per cm^2 per second) for interaction with surfaces to produce drag effects and changes in optical and physical properties by reflection, adsorption, or chemical reactions. These interactions, which occur at orbital velocities of 8 km per second corresponding to an oxygen atom kinetic energy of 5.03 eV (~500 kJ per mole), are manifested as selective charging of spacecraft surfaces, a ram-direction surface glow which is observed to extend more than 20 cm from the Shuttle

Table 17: Thermal expansion coefficients for polyimides (274)

DIAMINE	ANHYDRIDE		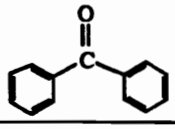 (unit X 10^5 K^{-1})	
		—	2.10	0.26
		3.20	2.94	4.00
		—	3.95	3.19
		0.04	2.59	0.58
		3.48	3.95	4.00
		1.61	—	—
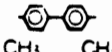		0.59	2.17	0.54
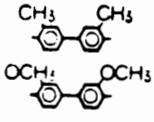		0.20	1.54	0.56
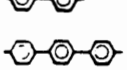		1.37	4.91	4.64
		0.56	1.83	0.59
		—	—	1.72
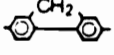		1.58	1.60	1.13
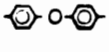		2.16	4.28	4.56
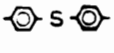		4.15	5.24	4.61
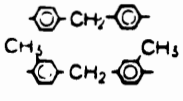		4.57	4.50	4.18
		5.76	5.36	4.85
		—	2.61	1.00
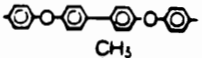		5.33	5.43	5.32
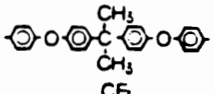		5.01	5.39	5.69
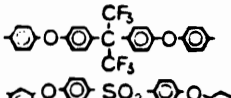		4.57	5.47	5.61
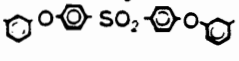		5.14	—	4.90

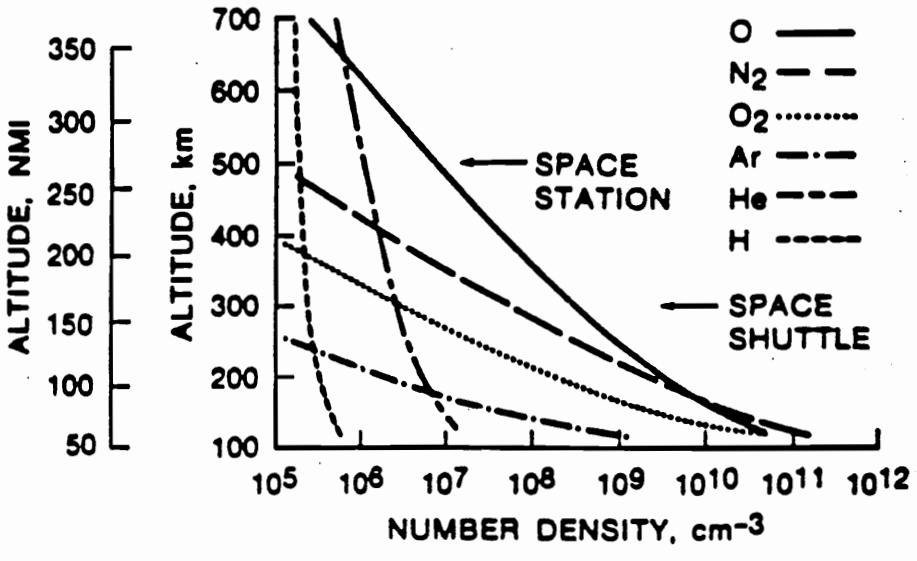

Figure 14: Atmospheric composition as a function of altitude in the low earth orbit (280)

surface, and from a materials design point of view, surface recession and, therefore, mass loss which arises from oxidation of the materials involved.

Several experiments have been conducted on Space Shuttle missions to quantify material degradation caused by interactions with atomic oxygen . The extent of mass loss is directly proportional to the reaction rate with the exposed material and integrated flux (fluence), which is, in turn, dependent on many parameters, such as altitude and life of the spacecraft, attitude of the surface relative to the orbital velocity vector, solar activity, and possible synergistic effects due to the Shuttle environment (i. e., plasma, surface charging,...). Thus, the efficiency of the interaction is expressed as the volume of material lost per incident oxygen atom, derived by normalizing the material recession by exposure fluence. Experiments on three missions, Space Transportation Systems STS-5, STS-8, and STS-41-G, provide all of the quantitative data available to date (179, 281-284). Results of atomic oxygen interactions with selected materials, representing data from STS-8, are reported in Table 18 (186). Of the two general classes of materials, metals and non-metals, the metals are the least reactive to atomic oxygen. More than 20 metal surfaces were exposed during the Shuttle flights, and only carbon, silver, and osmium interacted with sufficiently high efficiencies to produce macroscopic changes. Generally, all of the other metals exhibited significantly lower interaction rates.

Generally, all organic polymeric materials commonly used on spacecraft surfaces (epoxy, polyurethane, polyamide, polyimide) were reactive with the LEO environment. Oxidation occurred due to the rupture of primary bonds, which subsequently led to chain scission and loss of polymer properties. Hydrogen abstraction and hydroperoxide formation have been defined as the rate controlling step in oxidation by atomic oxygen attack (285). Therefore,

Table 18: Reaction efficiencies of selected materials with atomic oxygen in low earth orbit (186)

Material	Reaction Efficiency, cm^3/atom
Kapton	3×10^{-24}
Mylar	3.4
Tedlar	3.2
Polyethylene	3.7
Polysulfone	2.4
Graphite/epoxy	
1034C	2.1
5208/T300	2.6
Epoxy	1.7
Polystyrene	1.7
Polybenzimidazole	1.5
25% Polysiloxane/45% Polyimide	0.3
Polyester 7% Polysilane/93% Polyimide	0.6
Polyester	Heavily attacked
Polyester with Antioxidant	Heavily attacked
Silicones	
RTV-560	0.2*
DC6-1104	0.2*
T-650	0.2*
DC1-2577	0.2*
Black paint Z306	0.3-0.4*
White paint A276	0.3-0.4*
Black paint Z302	2.03*
Perfluorinated polymers	
Teflon, TFE	<0.05
Teflon, FEP	<0.05
Carbon (various forms)	0.9-1.7
Silver (various forms)	Heavily attacked
Osmium	0.026

the oxidation rate depends on the types of bonds present in the polymer backbone, although reaction efficiency does not seem to be strongly dependent on chemical structure (186). However, perfluorinated polymers such as Teflon and poly(siloxane imide) segmented copolymers, which contain much stronger bonds than polyethylene, are considerably more stable than the wholly organic polymers, by at least a factor of 50 (14, 32, 185, 186, 286, 287). In fact, their reaction rates are considered low enough for use as protective coatings.

Factors such as the degree of crystallinity and permeability to oxygen can also affect polymer stability to atomic oxygen. Oxides or less reactive additives lower the reactivity of polymers by shadowing the organic matrix from the incoming ambient oxygen atmosphere. However, the additive particles are not covalently bound into the organic matrix and may be lost in time because of interactions with scattered atomic oxygen (186). The same problem of long term stability occurs with coatings which exhibit poor adhesion to the substrate. The use of the conventional t-butylphenol type antioxidants has proven totally ineffective in improving the stability of organic materials in the LEO (288). In addition to the problem of mass loss and erosion, further concern has developed over oxygen atom induced surface modification resulting in the change of optical, thermal, or conductive properties of spacecraft materials.

The use of silicon containing surface layers as a barrier against aggressive oxygen species is not entirely new. In 1980, Taylor and Wolf postulated that when locked into a suitable host by incident radiation, silicon containing materials would be converted to their metal oxide by oxygen reactive ion etching (RIE), a common lithographic process (289, 290):

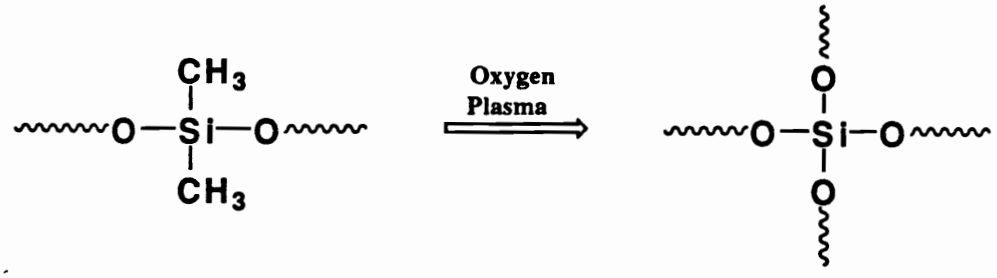

Since the silicon oxide is nonvolatile, a protective shield or coating of oxide would be left behind, thus preventing the etching of material beneath it. Shifts in binding energy as revealed by X-ray photoelectron spectroscopy confirm this transformation (14, 32, 286, 291), and Auger spectroscopy has been used to determine the oxide film thickness of 100 to 200 Å (292). This transformation to a stable, ceramic-like silicate structure was used to explain the low and even nonexistent etch rates of organometallic polymers in oxygen plasma, as documented in the early literature of the electronics industry (175, 176, 289, 290, 292-296). Figure 15 illustrates the effect of side chain silicon incorporation on the stability of poly(methyl methacrylate) to oxygen RIE (173).

Numerous siloxane and silane-containing polymeric systems have subsequently been developed for optical lithography applications (292, 297-301). Studies have concentrated on silicon containing materials primarily because of their general availability and the ease with which a variety of structures can be synthesized. The NASA Space Transportation System experiments have also shown that poly(siloxane imide) segmented copolymers are promising candiates for atomic oxygen stable matrix resins, coatings, and structural adhesives (32, 185, 302). Similar results have been obtained by Lockheed using an oxygen plasma reactor which simulates the effects associated with the LEO environment (285).

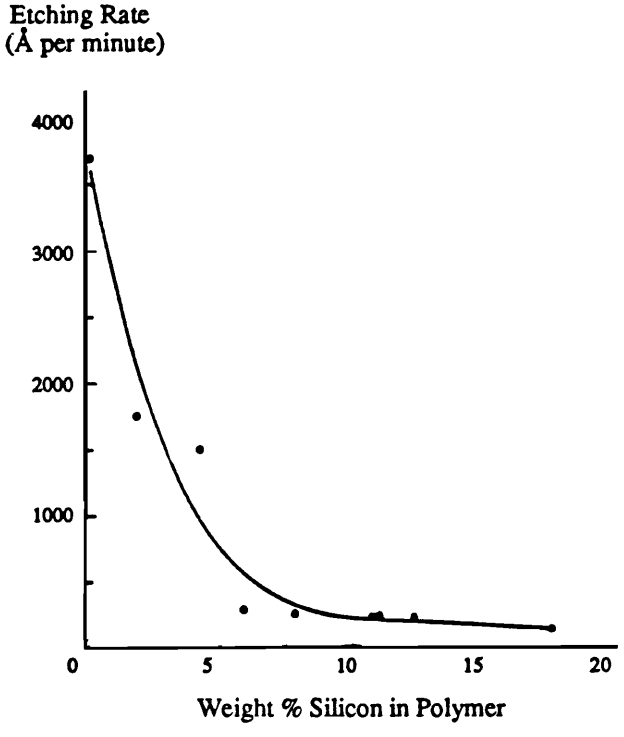

Figure 15: Etching rate versus silicon content in poly(methyl methacrylate) resins (173)

An understanding of the chemical and physical processes that occur during atomic oxygen degradation is required to provide accurate predictions of the useful lifetimes of materials in the LEO. Therefore, ground-based energetic oxygen facilities for accelerated materials testing have been developed which simulate, to varying degrees, the LEO environment. These oxygen sources may be considered as three basic types (276). The first of these are the asher sources, where oxygen atoms and other oxygen species (plasma) are formed by a variety of discharge techniques, and usually possess relatively low kinetic energies (<1eV). These reactors generally operate at pressures appreciably higher than those experienced in the LEO, and so more backbone scission is required before volatilization (303). The second type of source exploits ion beam neutralization. A beam of positive or negative oxygen ions is field accelerated to the desired energy and then neutralized to produce the desired oxygen atom beam. These sources are straightforward and can produce the desired energy of 5 eV, but are limited in ultimate flux by coulombic repulsion of the ion beams. In general, accelerated testing methods relying on these types of oxygen sources show a greater dependence on polymer structure than the LEO exposure data. Thus, the erosion processes in the LEO are more complex, and the mechanisms of degradation are somewhat different, although stability trends may be reasonably obtained by exposure to these types of sources. The third type of oxygen atom source utilizes laser heating to produce a high temperature gas which is subsequently expanded, thus converting the thermal energy to directed velocity (276). A pulsed laser was utilized in this research, although continuous wave lasers may also be used. Laser oxygen sources can conceivably more exactly replicate the high energy, high fluence, and low vacuum of the LEO, although utilization of the laser oxygen atom source is still in its early stages.

CHAPTER 3

EXPERIMENTAL TECHNIQUES----------

3.1.0 Solvent Purification

A variety of solvents were employed in the synthesis of monomers, oligomers, and polymers, and for solubility studies. In order to obtain controlled, high molecular weight polymers, solvent impurities, particularly water, were isolated by distillation. The solvents for synthetic reactions were allowed to stir over phosphorous pentoxide (P_2O_5) for at least five hours, refluxed for approximately one hour, and then fractionally distilled from the apparatus illustrated in Figure 16. Some distillations, particularly for high temperature boiling solvents, were conducted under reduced pressure. Distillations which did not require vacuum were conducted with a low nitrogen flow through the apparatus. In all cases, the constant boiling middle fraction was collected in a round bottom flask, sealed with a rubber septum, and stored under low nitrogen pressure. Water contents of the distilled solvents were determined by Karl Fisher coulamatic titrations (3.12.1) and considered acceptable for polymerizations if less than 150 ppm. Solvent transfer during polymerization was generally conducted via syringe techniques. Solvents for solubility studies were not typically distilled, but rather used as received. Structures of the most commonly used solvents are listed in Table 19.

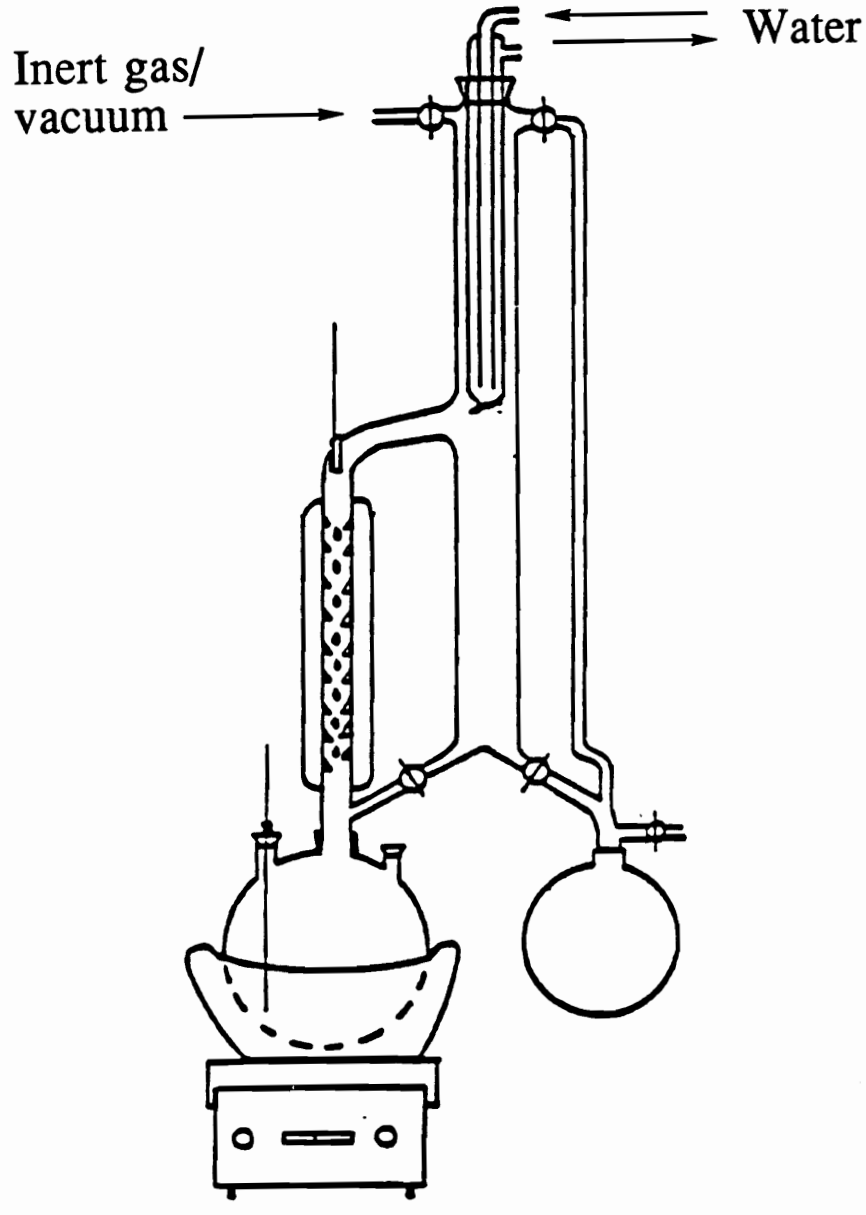

Figure 16: Apparatus used for solvent distillation

Table 19: Common solvents for polyimide synthesis and solubility studies

STRUCTURE	SOLVENT	ACRONYM	BP, °C
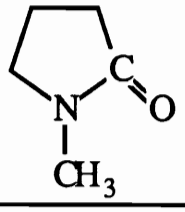	1-Methyl-2-Pyrrolidinone	NMP	82 at 10 mm
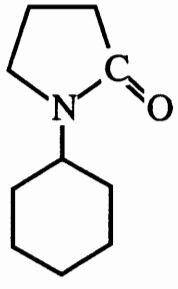	1-Cyclohexyl-2-Pyrrolidinone	CHP	154 at 7 mm
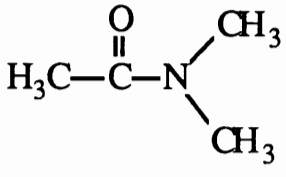	N,N-Dimethyl-acetamide	DMAc	166
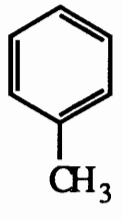	Toluene	Tol	111
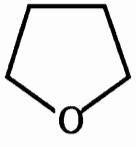	Tetrahydro-furan	THF	67

3.2.0 Anhydrides

3.2.1 3, 4, 3', 4'-biphenyltetracarboxylic dianhydride (BPDA)

Supplier(s): Chriskev (Ube Industries)
Empirical Formula: $C_{16}H_6O_6$
Molecular Weight: 294
Melting Point (pure), °C: 300
Structure:

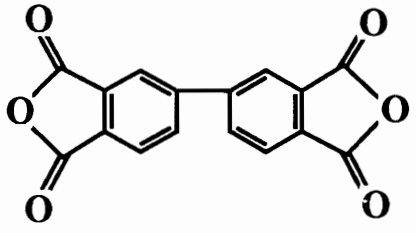

Purification: BPDA was received as a light grey powder and used as received, and stored in a dessicator between uses.

3.2.2 Pyromellitic dianhydride (PMDA)

Supplier(s): Allco, Chriskev, Aldrich
Empirical Formula: $C_{10}H_2O_6$
Molecular Weight: 218.12
Melting Point (pure), °C: 285.6
Structure:

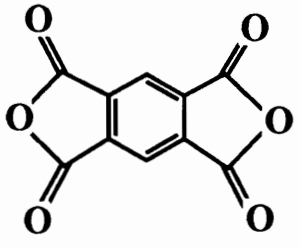

Purification: PMDA was sublimed with the oil bath setting at 260°C under full vacuum.

3.2.3 *Benzophenone tetracarboxylic dianhydride or 4, 4'-carbonyl diphthalic anhydride* (BTDA)

Supplier(s): Allco, Chriskev
Empirical Formula: $C_{17}H_6O_7$
Molecular Weight: 322.23
Melting Point (pure), °C: 225.4
Structure:

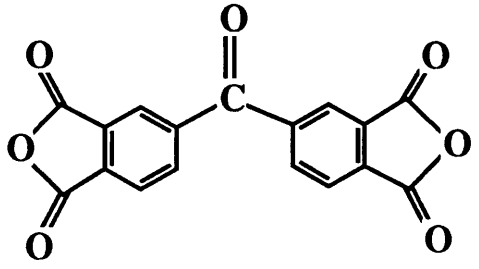

Purification: Ultra-high purity BTDA was used as received from the supplier, although lower grade BTDA may be purified by a number of techniques, notably recrystallization from acetic anhydride, sublimation, and water-free acetone washing.

3.2.4 *4, 4'-oxydiphthalic anhydride or 5, 5'-oxybis-1, 3-isobenzofurandione* (ODPA)

Supplier(s): Occidental Chemical Corporation
Empirical Formula: $C_{16}H_6O_7$
Molecular Weight: 310.23
Melting Point (pure), °C: 228
Structure:

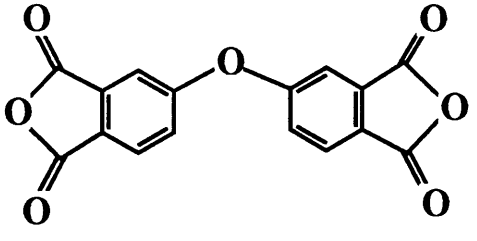

Purification: OPDA was received as an off-white powder and used without further purification to obtain high molecular weight polymers. Alternatively, this monomer could be sublimed at an oil bath temperature of ~240°C in order to obtain pure white crystals. Full vacuum was necessary achieve sublimation prior to degradation.

3.2.5 Sulfonyl bis(phthalic anhydride) (SDA)

Supplier(s): Amoco Research Center
Empirical Formula: $C_{16}H_6O_8S_1$
Molecular Weight: 358
Melting Point (pure), °C: no detectable melting point up to 260°C
Structure:

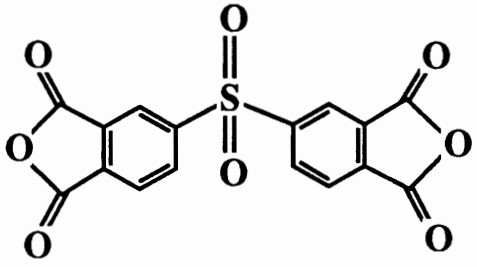

Purification: SDA was received as an off-white powder and used without further purification. SDA was stored under rigorously dry conditions between uses.

3.2.6 5, 5'-[2, 2, 2-Trifluoro-1-(trifluoromethyl) ethylidene] bis-1, 3-isobenzofuranedione (6F)

Supplier(s): Hoechst Celanese Corporation
Empirical Formula: $C_{19}H_6F_6O_6$
Molecular Weight: 444
Melting Point (pure), °C: 247
Structure:

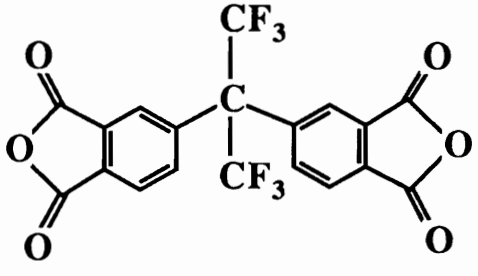

Purification: Polymer and electronic grade 6F were used as received to obtain high molecular weight polyimides. Electronic grade 6F was a higher quality monomer, as indicated by melting point determinations, and yielded superior molecular weight control. Polyimides for blending studies with polybenzimidazole and for rheological investigations were synthesized with the highest purity monomer.

3.2.7 Maleic anhydride (MA)

Supplier(s): Aldrich Chemical Corporation
Empirical Formula: $C_4H_2O_3$
Molecular Weight: 98.06
Melting Point (pure), °C: 56
Structure:

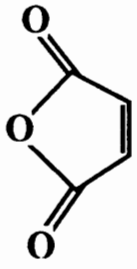

Purification: MA was sublimed at the oil bath setting at 120°C and under full vacuum, yielding pure, white crystals which were dried overnight at 60°C in a vacuum oven.

3.2.8 Phthalic anhydride (PA)

Supplier(s): Aldrich Chemical Corporation
Empirical Formula: $C_8H_4O_3$
Molecular Weight: 148.12
Melting Point (pure), °C: 134
Structure:

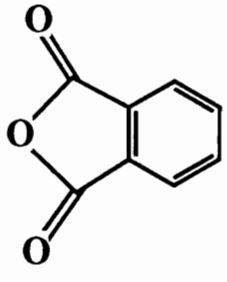

Purification: PA was sublimed under full vacuum at an oil bath temperature of ~130°C, and dried overnight at 50°C in a vacuum oven.

3.3.0 Diamines

3.3.1 Synthesis of 1, 4- (3-aminophenoxy) 2, 3, 5, 6-tetrafluorobenzene (4F)

Reaction:

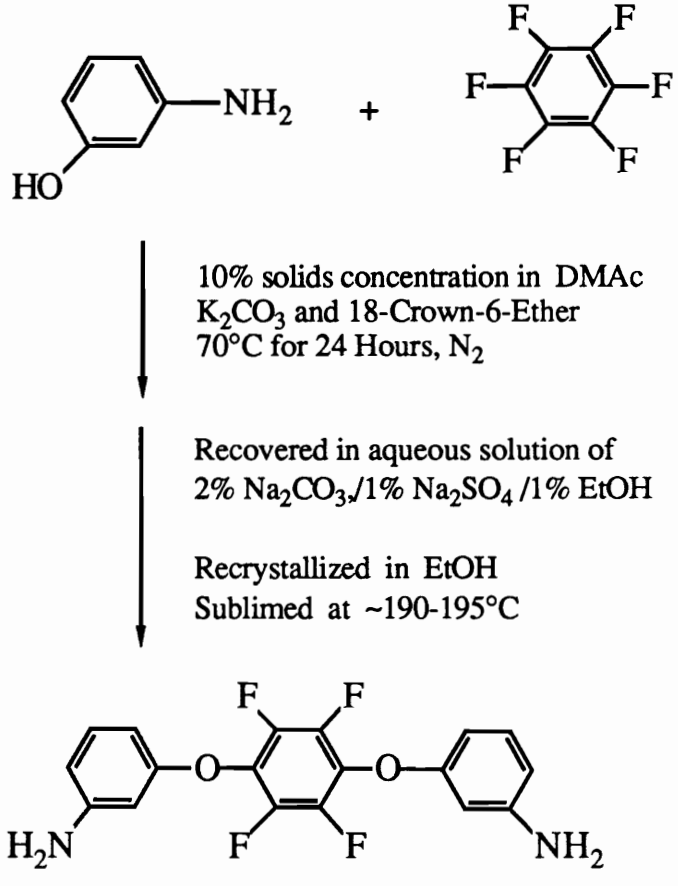

Molecular weight 364.3 g/mole

To a solution of hexafluorobenzene (9.303 grams, 0.050 mole) and 3-aminophenol (10.913 grams, 0.100 mole) in 200 ml of DMAc was added K_2CO_3 (29.64 grams, 0.214 mole) and 18-crown-6-ether (370 grams, 0.014 mole). The heterogeneous mixture, under nitrogen, was heated to 70°C and held for 24 hours. The color changed from light yellow to light green after 2 to 3 hours, and to greenish brown at the end of the reaction. The reaction mixture was cooled to room temperature and poured into 2 liters of an aqueous

solution of 2 percent Na_2CO_3, 1 percent Na_2SO_4, and 1 percent ethanol. The pink tan solid was filtered, washed with distilled water, and dried. The product was recrystallized from ethanol at a concentration of 15 ml per product gram, with charcoal or Celite, concentrated to half of the original volume, filtered, and dried. As a final purification procedure, the product was sublimed at an oil bath temperature of 190 to 195°C to yield a pure white solid in flake form. The melting point of the pure material was 180 to 182°C. Structure was determined by fluorine-19, carbon-13, and proton nuclear magnetic resonance spectroscopy (NMR). (*procedure credited to Dr. Justin W. Diehl, Chemistry Department, St. Bonaventure's University, St. Bonaventure, New York, 14778*)

3.3.2 Synthesis of bis(3-aminophenoxy-4'-phenyl) phenyl phosphine oxide (PO) Reaction:

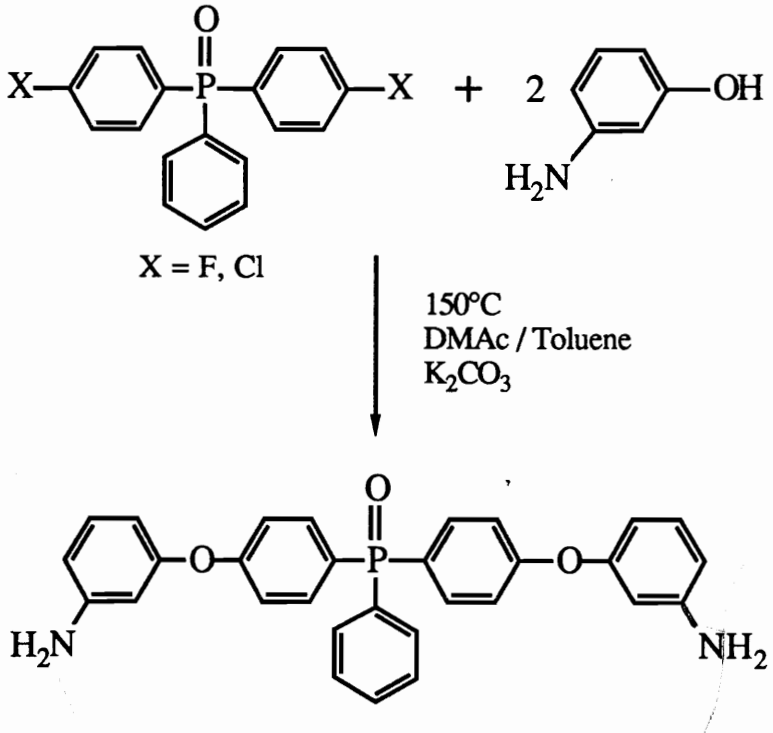

Molecular weight 492 g/mole

The monomers POX and m-AP were added in a 2:1 molar ratio to a flask equipped with a mechanical stirrer, inert gas inlet, thermometer, and Dean Stark trap fitted with a condenser and drying tube (Figure 17). The monomers were dissolved to a 30 w/v % solids concentration in a cosolvent system of DMAc (70 v. %) and toluene (30 v. %). Five mole percent excess K_2CO_3 was then added to the flask. The reaction mixture was heated to 140°C, maintained for 12 hours, then raised to 148°C while a fast inert gas flow to expelled toluene from the reaction flask. After cooling to ~90°C, the mixture was filtered through a glass sintered funnel to remove any inorganic salts. The homogeneous solution was reduced 25 % in volume by applying vacuum, and allowed to cool to room temperature undisturbed. After ~4 hours at room temperature, crystals of the monomer began to precipitate; precipitation proceeded for 18 hours. The crystals were recovered by filtration, air dried, then redissolved at 65°C in DMAc (35 w/v % solids concentration). Undisturbed slow cooling to room temperature allowed precipitation of the purified product. The filtered recovery was greater than 90 percent when POF was used, and approximately 60 percent for POCl. The recovered product was dried at 70°C under vacuum for 12 hours. Proton NMR indicated the presence of residual DMAc after these drying conditions. DMAc was more efficiently removed by dissolving the dried product in THF (20 to 25 w/v % solids concentration), precipitating in stirring hexane, and drying at 70°C under vacuum for 12 hours. A DSC scan of the dried, off-white crystalline final product indicated no melting transition, but rather a weak second order transition similar to a glass transition occurring at 75°C. (*procedure credited to Dr. Attila Gungor, Chemistry Department, Virginia Polytechnic Institute and State University, Blacksburg, Virginia 24061)*

3.3.3 4, 4'-isopropylidene dianiline (Bis A)

Supplier(s): Air Products and Chemicals, Inc.
Empirical Formula: $C_{15}H_{18}N_2$
Molecular Weight: 226
Melting Point (pure), °C: 132
Structure:

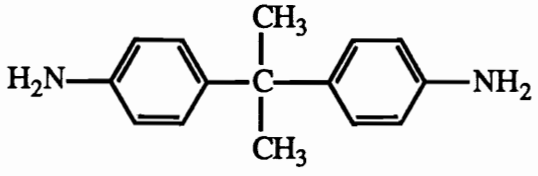

Purification: Bis A was received as a high purity white powder and used as received.

3.3.4 4, 4'-[1, 4-phenylene-bis-(1-methyl ethylidene)] bisaniline (Bis P)

Supplier(s): Air Products and Chemicals, Inc., Shell Chemical Company (EPON HPT™ Curing Agent 1061)
Empirical Formula: $C_{24}H_{28}N_2$
Molecular Weight: 344
Melting Point (pure), °C: 165
Structure:

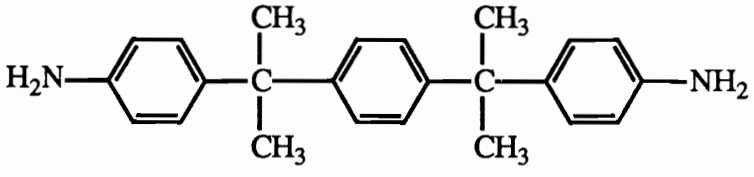

Purification: Bis P was received as a high purity white powder and used as received.

3.3.5 m-aminophenol (m-AP)

Supplier(s): Aldrich
Empirical Formula: $C_6H_7N_1O_1$
Molecular Weight: 109.13
Melting Point (pure), °C: 126
Structure:

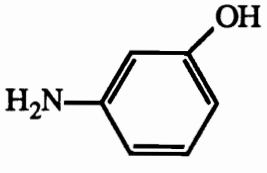

Purification: m-AP was sublimed at an oil bath setting of 130°C and full vacuum.

3.3.6 *3, 3'-diaminodiphenyl sulfone* (m-DDS)

Supplier(s): Aldrich, Chriskev, FIC, Kennedy and Klim
Empirical Formula: $C_{12}H_{12}N_2O_2S_1$
Molecular Weight: 248.3
Melting Point (pure), °C: 173
Structure:

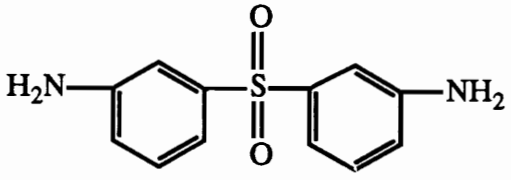

Purification: m-DDS was recrystallized from deoxygenated methanol according to the following technique: one liter of methanol in an erlenmeyer flask was purged with nitrogen for at ~5 hours, then heated to boiling. While stirring with a magnetic stir bar, m-DDS was slowly added until a dark amber saturated solution was obtained. Distilled water (~5 ml) was added slowly into the hot solution to affect precipitation. Stirring was stopped and the flask was allowed to slowly cool to room temperature. White crystals were isolated by vacuum filtration, washed with cold deoxygenated methanol, crushed, dried at 80°C in a vacuum oven for at least 12 hours, and then stored in a dessicator.

3.3.7 *4,4'-diaminodiphenyl sulfone* (p-DDS)

Supplier(s): Kennedy and Klim (99.6% purity)
Empirical Formula: $C_{12}H_{12}N_2O_2S_1$
Molecular Weight: 248.3
Melting Point (pure), °C: 180
Structure:

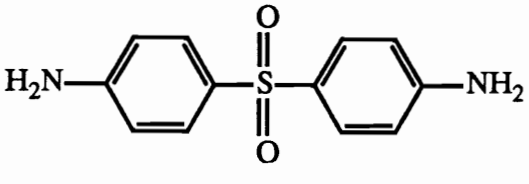

Purification: p-DDS was received as a light tan powder, and recrystallized by the same procedure as used for m-DDS, with sodium dithionite used as an antioxidizing agent.

3.4.0 Other monomers

3.4.1 Bis(4-fluoro or chlorophenyl) phenyl phosphine oxide (POX)

Supplier(s): Hoechst Celanese (POF) and AKZO (POCl)
Empirical Formula: $C_{18}H_{13}O_1F_2P_1$ or $C_{18}H_{13}O_1Cl_2P_1$
Molecular Weight: 314 (POF) or 347 (POCl)
Melting Point (pure), °C: 128 (POF) or 108.5 (POCl)
Structure:

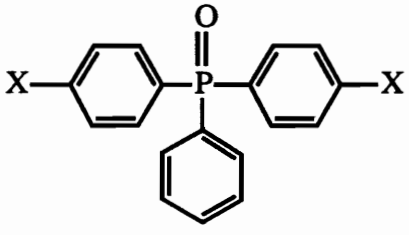

X = F, Cl

Purification: Both POF and POCl were received as a high purity white powders, and used as received.

3.4.2 4, 4'-Dichlorodiphenyl sulfone (DCDPS)

Supplier(s): Amoco Chemical Company
Empirical Formula: $C_{12}H_8O_2Cl_2S_1$
Molecular Weight: 228.27
Melting Point (pure), °C: 148
Structure:

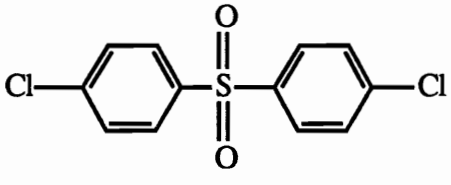

Purification: DCDPS was recrystallized from a ~60 w/v percent toluene solution. A small amount of activated charcoal was added and allowed to stir for 30 minutes. The solution was filtered through Celite™, and the clear filtrate was reduced in volume and allowed to cool slowly to room temperature. The white precipitated crystals were filtered, washed with cold toluene, and dried at 90°C under vacuum for at least 12 hours. DCDPS was typically received in high purity and the use of Celite™ was not necessary.

3.4.3 2, 2-bis (4-hydroxyphenyl) propane (Bisphenol A)

Supplier(s): Dow Chemical Company
Empirical Formula: $C_{15}H_{16}O_2$
Molecular Weight: 228.27
Melting Point (pure), °C: 124
Structure:

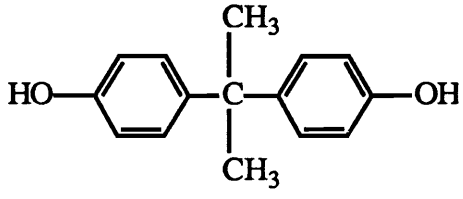

Purification: Bisphenol A was recrystallized from a 25 w/v percent toluene solution. The solution was heated to 100°C with stirring and a small amount of activated charcoal was added. Another 100 ml toluene (per ~200 grams of Bisphenol A) was added to dilute the solution, allowing for easy filtration. The solution was stirred for 30 minutes, filtered through a porcelain buchner funnel using Celite™ to remove the charcoal, reheated to reduce the volume, and then slowly cooled to room temperature. The white cyrstals were filtered and dried under vacuum at 50°C for ~12 hours, then crushed and dried again for at least 8 hours at 90°C in a vacuum oven. Use of the activated charcoal was not always necessary as the as-received Bisphenol A was typically of high purity.

3.4.4 4, 4'-Difluorobenzophenone (DFBP)

Supplier(s): ICI, Americas or Amoco Chemical Corporation
Empirical Formula: $C_{13}H_8O_1F_2$
Molecular Weight: 218.12
Melting Point (pure), °C: 124
Structure:

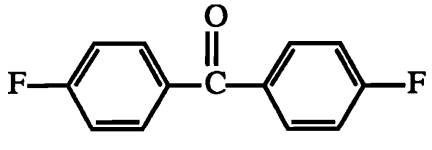

Purification: DFBP was received as a high purity, white powder and used as received.

3.4.5 *Bis(3-aminopropyl) tetramethyldisiloxane* (DSX)

Supplier(s): Petrarch Systems, Inc.
Empirical Formula: $C_{10}H_{28}N_2O_1Si_2$
Molecular Weight: 248
Melting Point (pure), °C: ----
Structure:

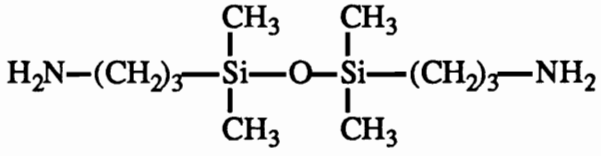

Purification: DSX was obtained as a high purity liquid and used as received.

3.4.6 *Octamethylcyclotetrasiloxane* (D_4)

Supplier(s): Petrarch Systems, Inc. or Union Carbide
Empirical Formula: $C_8H_{24}O_4Si_4$
Molecular Weight: 296
Melting Point (pure), °C: ----
Structure:

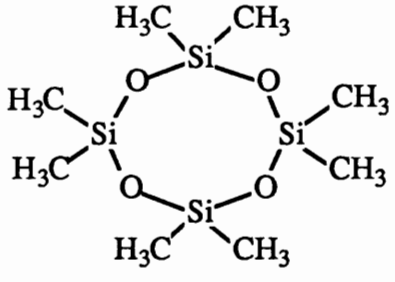

Purification: D_4 was obtained as a high purity, colorless liquid and used as received.

3.5.0 Oligomer Synthesis

3.5.1 Polydimethylsiloxane (PSX)

Reaction:

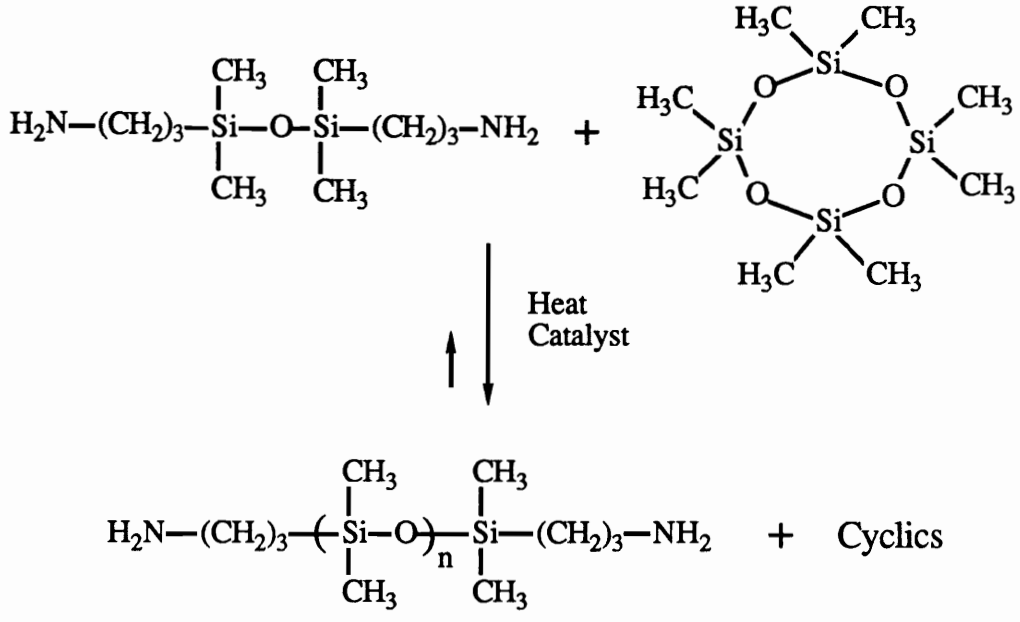

- Cyclics are removed via vacuum stripping.
- Catalyst must be neutralized for maximum stablility.
- <Mn> is controlled at equilibrium by the initial ratio of D_4 to DSX.
- Other endgroups are possible with appropriate DSX and catalyst.
- Actual <Mn> is determined by titration of amine endgroups or ^1H NMR.

The difunctional polydimethylsiloxane oligomers were synthesized in bulk by the ring opening equilibration of aminopropyl disiloxane (DSX) and the cyclic siloxane tetramer, octamethylcyclotetrasiloxane (D4). The molecular weight of the siloxane oligomer was controlled by the initial ratio of the tetramer to the disiloxane. The simple calculation for one mole of siloxane oligomer, which may be scaled to an alternate batch size, follows:

grams D4 required = Desired siloxane oligomer molecular weight (g/mole) - molecular weight DSX (248.5 g/mole)

where the molecular weight of D_4 is 296.6 g/mole. The reaction was conducted in a three necked round bottom flask equipped with a mechanical stirrer, condenser, inert gas inlet, thermometer and drying tube. The disiloxane and cyclic tetramer were added to the flask and heated to 80°C with stirring and an inert gas flow. The catalyst, tetramethylammonium siloxanolate or tetramethylammonium hydroxide pentahydrate, was then added at an approximate concentration of one tenth mole percent, based on the molar concentration of D_4, or one tenth weight percent. The reaction was maintained at 80°C for 48 hours to ensure complete equilibration. To decompose the catalyst after the equilibration was complete, the reaction temperature was increased to 150°C for three hours. Flow of the inert gas was increased to efficiently remove the gaseous, inert by-products. After cooling, the viscous product was transferred to a Kugelrohr vacuum distillation apparatus and stripped of the cyclic equilibrates at 0.5 torr and 130°C. Determination of the final product molecular weight was conducted by potentiometric titration of the primary amine endgroups with 0.1 N alcoholic HCl.

3.5.2 Poly(aryl ether)s: sulfones and ketones (PSF, PEK)

Reaction:

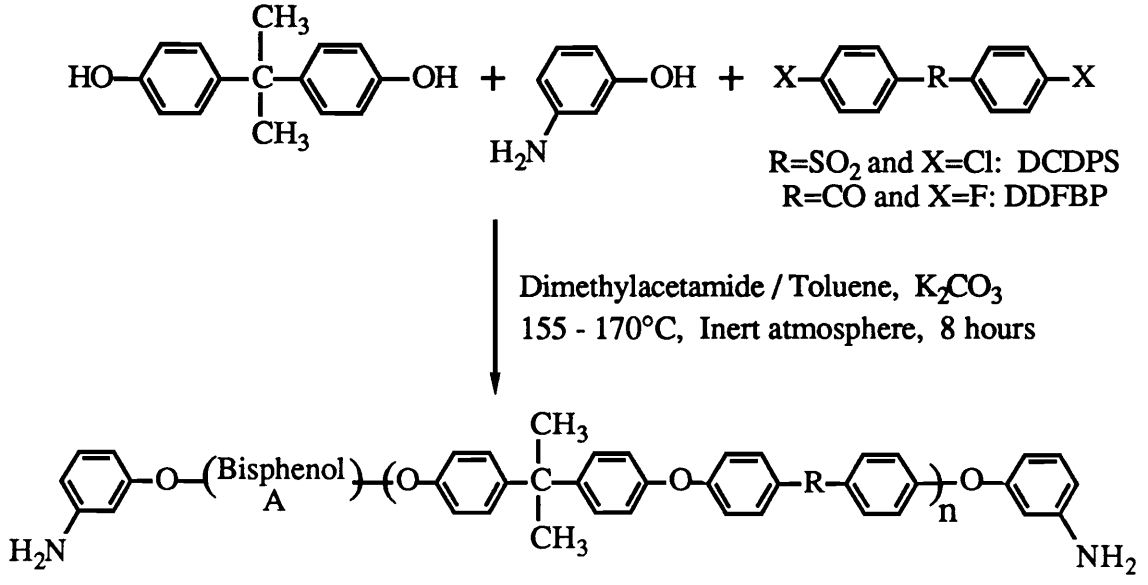

If R = SO_2, Poly(aryl ether sulfone) oligomer (PSF)
If R = CO, Poly(aryl ether ketone) oligomer (PEK)

Purified Bisphenol A, dichlorodiphenylsulfone (DCDPS) or difluorobenzophenone (DFBP), and m-aminophenol (m-AP) were charged to a three necked flask equipped with a mechanical stirrer, thermometer, inert gas inlet, and Dean Stark trap fitted with a condenser and drying tube (Figure 17). The quantities of the reactants were determined according to the Carothers equation (3.7.0). The reactants were dissolved in NMP (70%) and toluene (30%) to 15% solids concentration. Ten molar percent excess crushed and dried K_2CO_3 was added and the solution was heated to 150°C to dehydrate the system. After approximately 3 hours, the reaction was heated to 170°C for 8 hours and became viscous and green. To remove the inorganic salts, the reaction was filtered after cooling to ~80°C, and then coagulated in alcohol. Isopropanol (IPA) was used for oligomers with <Mn> < ~5,000 g/mole or methanol for <Mn> > ~ 5,000 g/mole. The alcohol solution was acidified with a few drops of glacial acetic acid and then filtered, washed with more

alcohol, and allowed to dry. The precipitated oligomer was stirred in hot water for several hours, refiltered, washed with more alcohol, and then dried under vacuum for at least 8 hours at 60 to 80°C. After drying, the oligomer was redissolved in methylene chloride, and the filtration and washing procedures were repeated to ensure that all dissolved inorganic salts were removed. Finally, the oligomer was dried under vacuum at 100°C for at least 15 hours.

3.5.3 Imide oligomers

Imide oligomers based upon 6F and Bis A with controlled molecular weight and maleimide endgroups were synthesized by a two step reaction. The same procedure as employed for the synthesis of the higher molecular weight analogue amic acids (3.7.1) was used to generate the 6F-Bis A amine terminated imide oligomers. Thus, a calculated excess of the Bis A diamine, as determined by the Carothers equation, was added to a stirring solution of the 6F dianhydride in DMAc, yielding the low molecular weight species. Higher solids contents of 20 percent could be used for this reaction due to the increased solubility of the low molecular weight species and incorporation of the 6F moiety. Solution imidization and the polymer recovery procedure were as described for the higher molecular weight analogues (3.8.2). The amine endgroups of the dried, recovered polymer were titrated with 0.02 N HBr (3.12.2) to determine the actual molecular weight and amount of maleic anhydride (MA) needed for quantitative end-capping, i.e., 2 moles MA per mole of oligomer. The second step involved the addition of MA and solution imidization of the amic acid end groups at 130°C. A lower solution imidization temperature was used to avoid crosslinking of the MA. Thus, the stoichiometric amount of MA plus 5 or 10 mole percent excess (for $\langle Mn \rangle \leq 10{,}000$ g/mole and > 10,000 g/mole, respectively) was added to enough prewarmed (130°C) cosolvent solution of DMAc (80%) and CHP (20%) to yield a final solids concentration of 15 to 17 w/v percent. The reaction was allowed to proceed

for 14 hours. The oligomer was recovered by precipitating in vigorously stirring methanol (~30%)/water (~70%) and dried in a vacuum oven at 100°C for 48 hours. The maleimide endgroups were subsequently thermally reacted to form a network structure (3.9.0).

3.6.0 Molecular weight and endgroup control of polyimides via the Carothers equation

The theoretical calculations for molecular weight and end group control in step growth polymerizations are embodied in the Carothers equation. To properly control the polymer molecular weight, the stoichiometric imbalance of the difunctional monomers or of the monofunctional monomer must be precisely adjusted. A derivation of associated useful equations is presented here for the condensation reaction of anhydrides with amines to form polyimides. A more complete derivation of the Carothers equation is described in basic polymer texts (117, 118).

The Carothers equation relates the extent of reaction and degree of polymerization to the average functionality of the polymerizing system:

$$X_n = \frac{2\ N_o}{(2\ N_o - N_o\ p\ f_{av})} = \frac{2}{(2 - p\ f_{av})}$$

where X_n is the number average degree of polymerization, related to the desired polymer molecular weight, M_d, by

$$X_n = 2\ DP = 2\ \frac{M_d}{\text{molecular weight of the repeat unit } (M_{ru})}$$

and N_o is the initial moles of monomers, p is the extent of reaction, and f_{av} is the average number of functional groups per monomer molecule which can react. In the context of the polymerization of anhydrides and amines to obtain polyimides, the number average degree of polymerization, Xn, is twice the number of repeat units in the polymer molecule, DP,

because each repeat unit contains the residue of two monomers. For complete conversion of monomer to polymer (p = 1) in a wholly difunctional system (f_{av} = 2), the molecular weight is predicted to become infinite. Thus, any stoichiometric deviation which decreases the average functionality to less than 2 will lower the polymer molecular weight. Molecular weight may be related to the stoichiometric imbalance, r:

$$Xn = \frac{(1 + r)}{(1 - r)}$$

The stoichiometric imbalance, r, is defined to always be less than 1.00, and may be established for two different situations: for offset stoichiometry such that anhydride or amine endgroups will be obtained, or with the addition of a monofunctional reagent which may have either reactive or nonreactive endgroups. Thus, the incorporation of a monofunctional reagent such as maleic anhydride will yield a functionalized oligomer, whereas the use of phthalic anhydride will yield nonreactive phthalimide endgroups. Similarly, amine endgroups may be obtained by offsetting the stoichiometry with an excess of diamine over dianhydride.

When excess difunctional B monomer is used to offset stoichiometry and achieve B endgroups,

$$r = \frac{\text{moles of difunctional A monomer}}{\text{moles of difunctional B monomer}}$$

On the other hand, if a monofunctional reagent with a B endgroup is incorporated,

$$r = \frac{\text{moles of difunctional A monomer}}{\text{moles of difunctional B monomer + moles of monofunctional B monomer}}$$

The moles of difunctional A monomer may be arbitarily established as 1; the moles of difunctional B monomer may then be defined as r, and the above equation may be solved for the moles of monofunctional B monomer required to limit molecular weight to M_d. This approach dictates that the number of A functional groups equals the number of B functional groups, with the polymer endgroups determined by the nature of the monofunctional reagent. To obtain a sufficient total batch size, these values may be scaled accordingly.

3.7.0 Synthesis of poly(amic acid)s

The polyimides of this research were synthesized by the classic two-step procedure which initially involved the synthesis of a soluble amic acid intermediate from aromatic dianhydrides and aromatic diamines, yielding homopolymers. When difunctional, amine terminated oligomers were also employed, copolymers were obtained. Typically, an anhydride or amine terminated monofunctional reagent was added to control molecular weight and end groups. As described in section 3.8.0, the amic acid intermediates were cyclodehydrated by two different methods, in bulk or in solution, to afford the polyimide homo- or copolymers.

3.7.1 Synthesis of homopolymer (amic acid)s

The amic acid intermediates were synthesized in a 3 necked, round bottom flask equipped with a mechanical stirrer, inert gas inlet, and drying tube at a final solids concentration of 15 to 20 w/v percent. To ensure the elimination of moisture, this equipment was dried in a forced air convection oven at ~150°C, flame dried after assembly, and purged with inert gas prior to beginning the reaction. A low flow of inert gas was maintained through the apparatus during the entire reaction. As each of the monomers were added, the weighing

pan, paper or vial would be rinsed with solvent to ensure that quantitative transfer into the flask occurred. The calculated amount of the diamine was added first into the flask in powder form, and enough solvent was added as a rinse to completely dissolve the diamine with stirring. NMP was typically the solvent of choice. To circumvent the insolubility of Bis P in NMP, DMAc could be used when Bis P containing polyimides were synthesized. Alternatively, the Bis P could be added to a stirring solution of NMP prewarmed to 60°C by a warm water bath. The bath would be removed just prior to adding the remaining monomers. If a monofunctional reagent were used, it would be added next, with the same rinsing procedure of the weighing pan. Finally, the powdered dianhydride would be slowly added to the stirring solution, ensuring that each previous addition of dianhydride had dissolved before more was added. A cold water or water/ice bath was used to maintain the reaction temperature at ambient or lower, particularly for reactions which were moderately exothermic upon the addition of the dianhydride. The amic acid reaction was stirred for at least 3 hours, and then either immediately imidized or stored in a sealed, nitrogen blanketed bottle at ~-10°C until needed.

3.7.2 Determination of quantities of reactants for the synthesis of copolymer (amic acid)s

Typical copolymerizations were conducted with monomeric aromatic diamines and dianhydrides, an oligomeric diamine such as a polydimethylsiloxane or poly(aryl ether), and a monofunctional reagent to control molecular weight and endgroups, such as phthalic anhydride. In these instances, the determination of the quantities of the monomers and oligomeric species became more complex than for homopolymerizations. Advantageously, mathematical relationships between the reaction variables could be derived from the fundamentals of polymer chemistry. Simultaneous solution of these relationships yielded an equation based upon the known or desired variables which allowed for the simple

determination of the quantities of reactants. The derivation is based upon the following input variables:

P:	weight fraction of the diamine oligomer
MWDianh:	molecular weight of the dianhydride monomer
MWDiam:	molecular weight of the diamine monomer
MWOlig:	molecular weight of the diamine oligomer
B:	total batch weight desired, grams

The following abbreviations are useful: g: grams and m: moles.

$$gDianh = (MWDianh)(mDianh) \tag{1}$$

$$mDianh = mOlig + mDiam = \frac{gOlig}{MWOlig} + \frac{gDiam}{MWDiam} \tag{2}$$

Substituting (2) into (1):

$$gDianh = MWDianh \left(\frac{gOlig}{MWOlig} + \frac{gDiam}{MWDiam}\right) \tag{3}$$

$$gOlig = BP = \frac{(gDianh + gDiam)\,P}{(1 - P)} \tag{4}$$

Substituting (4) into (3), rearranging, and defining

$$X = \frac{(MWDianh)(P)}{(MWOlig)(1 - P)} \quad (5) \quad \text{and} \quad Z = X + \frac{MWDianh}{MWDiam} \quad (6)$$

$$gDianh = gDiam \left(\frac{Z}{1 - X}\right) \tag{7}$$

Finally, using the relationship of B = gDianh + gDiam + gOlig, and equation (4), and rearranging: $gDiam = B(1 - P) - gDianh$ (8)

Substituting equation (8) into equation (7) and rearranging:

$$gDianh = \frac{BZ(1 - P)}{1 - X + Z} \tag{9}$$

Equation (9) defines the grams of dianhydride to be used to synthesize a total batch of B grams, based upon known and desired variables. Once equation (9) is solved, the quantities of the difunctional, amine terminated oligomer and the monomeric aromatic diamine may be calculated by equations (4) and (3), respectively. The weights of the individual reactants may be easily converted to molar quantities by dividing by molecular weight, as defined in equation (1). The molar quantities of the reactants serve as the basis for determining the molecular weight of the repeat unit of the amic acid copolymer, because the dianhydride may react with either the monomeric aromatic diamine or the amine terminated oligomer. Thus,

$$M_{ru} = \frac{(mDiam)(MWDianh + MWDiam) + (mOlig)(MWDianh + MWOlig)}{(mDiam + mOlig)} \qquad (10)$$

Once the molecular weight of the repeat unit is calculated according to equation (7), the amount of monofunctional reagent may be determined by using the Carothers equation, as described in section 3.6.0.

3.7.3 Sample calculation for the determination of the quantities of reactants for the synthesis of a poly(dimethylsiloxane imide) segmented copolymer based on BTDA and Bis P, with 40 weight percent aminopropyl terminated polydimethylsiloxane; siloxane oligomer molecular weight is 3644 g/mole; PA is added to control molecular weight of the copolymer to 25,000 g/mole

First, the molar ratios of each of the starting materials must be determined by employing equation (8). The variables are defined as follows:

P:	weight fraction of the diamine (siloxane) oligomer	= 0.40
MWDianh:	molecular wt of the dianhydride monomer (BTDA)	= 322.23
MWDiam:	molecular weight of the diamine monomer (Bis P)	= 344
MWOlig:	molecular weight of the diamine oligomer (siloxane)	= 3644
B:	total batch weight desired, grams	= 50

The values for X and Z are determined from equations (5) and (7), respectively:

$$X = \frac{(MWDianh)(P)}{(MWOlig)(1 - P)} = \frac{(322.23)\ (0.40)}{(3644)\ (0.60)} = 0.0590 \qquad (5)$$

$$Z = X + \frac{MWDianh}{MWDiam} = 0.0590 + \frac{322.23}{344} = 0.0590 + 0.9367 = 0.9957 \qquad (7)$$

Then, equations (8) and (1) may be used to determine the grams and moles of BTDA needed for a 50 grams batch size of the stated composition:

$$gDianh = \frac{BZ\ (1 - P)}{1 - X + Z} = \frac{(50)\ (0.9957)\ (0.60)}{(1 - 0.0590 + 0.9957)} = 15.4237 \text{ grams BTDA} \qquad (8)$$

$$(mDianh) = \frac{gDianh}{MWDianh} = 0.0479 \text{ moles BTDA} \qquad (1)$$

Equation (4) defines the grams of PSX and Bis P, which may be converted to moles by the relationship described in equation (1):

gOlig = BP = (50) (0.40) = 20 grams siloxane = 0.0055 moles PSX, and

$$20 = \frac{(gDianh + gDiam)\ P}{(1 - P)} = \frac{(15.4237 + \text{grams Bis P})\ (0.40)}{0.60} \qquad (4)$$

so the quantity of Bis P = 14.5763 grams = 0.0424 moles Bis P. Notice that the moles of diamine (PSX and Bis P) equals the moles of dianhydride, i.e., 0.0055 + 0.0424 =

0.0479, and the calculated batch size is indeed 50 grams, i.e., 20.000 + 14.5763 + 15.4237.

The first step in determining the amount of monofunctional reagent to add, in this case PA, is to determine the molecular weight of the copolymer amic acid repeat unit, as defined previously in equation (9):

$$M_{ru} = \frac{(mDiam)(MWDianh + MWDiam) + (mOlig)(MWDianh + MWOlig)}{(mDiam + mOlig)} =$$

$$\frac{(0.0424)(322.23 + 344) + (0.0055)(322.23 + 3644)}{0.0424 + 0.0055} = 1045 \text{ g/mole} \qquad (10)$$

Then, by application of the Carothers equation (section 3.6.0) for a desired molecular weight of 25,000 g/mole,

$$X_n = 2\,\frac{M_d}{M_{ru}} = \frac{50000}{1045} = 47.8469 = \frac{(1 + r)}{(1 - r)}, \quad \text{so } r = \frac{(X_n - 1)}{(X_n + 1)} = 0.9591$$

Because PA, an anhydride monofunctional reagent is used to control molecular weight and endgroups, r is defined as:

$$\frac{\text{moles of difunctional A [0.1 mole diamine (Bis P and siloxane)]}}{\text{moles of difunctional B (0.09591 mole BTDA) + moles of monofunctional B (PA)}}$$

yielding a value of 0.0084 moles of PA per 0.1 mole of diamine and 0.09591 mole of BTDA. The 0.1 mole of diamine is prorated on a molar basis between the Bis P and PSX. These quantities can easily be converted to weights by multiplying by molecular weight, and the batch size may be scaled accordingly. Thus, for a total batch size of 50 grams, the calculated quantities are as follows:

	grams	moles
BTDA	14.7869	0.0459
Bis P	14.5668	0.0423
PSX	20.0511	0.0055
PA	0.5953	0.0040
TOTAL	50.0001	0.0977

Notice that within the error of the calculations, the number of anhydride functional groups is equal to the number of amine functional groups, ensuring that the polymer chain ends should be phthalimide.

3.7.4 Synthesis of poly(siloxane amic acid)s

Due to the different solubility characteristics of the polydimethylsiloxane oligomer and the aromatic imide component, the poly(siloxane amic acid)s were synthesized by a modified technique similar to the procedure described for the synthesis of the polyimide homopolymer amic acids (3.7.1). The same reaction apparatus was used in both cases. First of all, a cosolvent system of NMP or DMAc with THF was used to accomplish homogeneous copolymerization. Typically, cosolvent volume ratios of 50:50 to 70:30 amide solvent to THF were used, with more THF being needed for high concentrations of the siloxane oligomer (> 20 weight percent) or for high siloxane molecular weights (>4,000 g/mole). The order of addition of the monomers was changed so that the first reaction step involved the slow addition of the siloxane oligomer to a stirring solution of the dianhydride which had been dissolved in an appropriate amide solvent and THF. After reacting for ~15 minutes, the monofunctional reagent was added. The diamine in powder form was added in small increments, ensuring that the previous increment had dissolved before adding the next. Solids concentrations of 15 w/v percent or less were typically needed, due to the large amount of THF and/or NMP needed to keep the polymerization

homogeneous at all times. As for the synthesis of the homopolymer amic acids, the poly(siloxane amic acid)s were allowed to stir for at least 3 hours, usually longer, under a low flow of inert gas, and either immediately imidized or stored appropriately.

3.7.5 Synthesis of poly(aryl ether amic acid)s

The poly(aryl ether amic acid)s were synthesized in the same apparatus as used for the synthesis of homopolymer and siloxane imide amic acids. Like the poly(siloxane amic acid)s, the order of addition was to add the oligomer, in this case an aryl ether, to a stirring solution of the dianhydride in an amide solvent (NMP). Due to the similar solubilities of the aryl ether and imide components, however, only one solvent was necessary to achieve homogeneous copolymerization. After ~ 15 minutes, the monofunctional reagent was added, followed by the slow addition of the aromatic diamine monomer in powder form. A solids concentration of 15 to 17 w/v percent was used. The reaction proceeded for at least 3 hours under a low flow of inert gas, and was either immediately imidized or stored appropriately.

3.8.0 Imidization of poly(amic acid)s

Conversion of the poly(amic acid) intermediates to the fully cyclized polyimide could be accomplished by a number of different techniques. Two techniques for imidization were used in this research, namely, the bulk thermal and solution imidizations, although chemical means and microwave energy could also be employed.

3.8.1 Bulk thermal imidization

The most common method of imidization involved casting the amic acid solution onto a glass plate and removing the solvent in a vacuum oven at 100°C for several hours. To

complete the cyclization/ dehydration and remove residual solvent, the films were then subjected to scheduled heating in a forced air convection oven at 100, 200 and 300°C for an hour at each temperature. If the glass transition temperature of the fully cyclized polyimide was known to be significantly less than 300°C, a lower final imidization temperature of approximately Tg was chosen.

3.8.2 Solution imidization technique

Solution imidizations were conducted in a 3 or 4 necked flask equipped with a mechanical stirrer, inert gas inlet, thermometer and Dean Stark trap with a condenser and drying tube. The apparatus, illustrated in Figure 17, was heated by an oil bath (~170°C) on a hot plate-stirrer, with copper coils and a type J thermocouple in the bath. If cooling was required, a solenoid valve was activated by an Omega temperature controller CN 9000, which allowed air to flow through the copper coils. The amic acid solution was added into the flask, which contained enough prewarmed (~150°C) cosolvent mixture of CHP (20%) and NMP (80%), if needed, to allow for a final solids concentration of ~15 percent. The reaction temperature was regulated at ~160°C, and never allowed to fall below 120°C while adding the amic acid solution. A moderately fast inert gas flow was maintained during the ~20 hour reaction time. The polyimide was recovered by precipitating the solution into a ~10 fold excess of a rapidly stirring methanol (~40%)/water(~60%) mixture, filtering in a sintered glass funnel, rinsing with more methanol/ water, and air drying for several hours. The coagulated polymer was then placed in a vacuum oven and the temperature was slowly increased to ~200°C and maintained for ~18 hours.

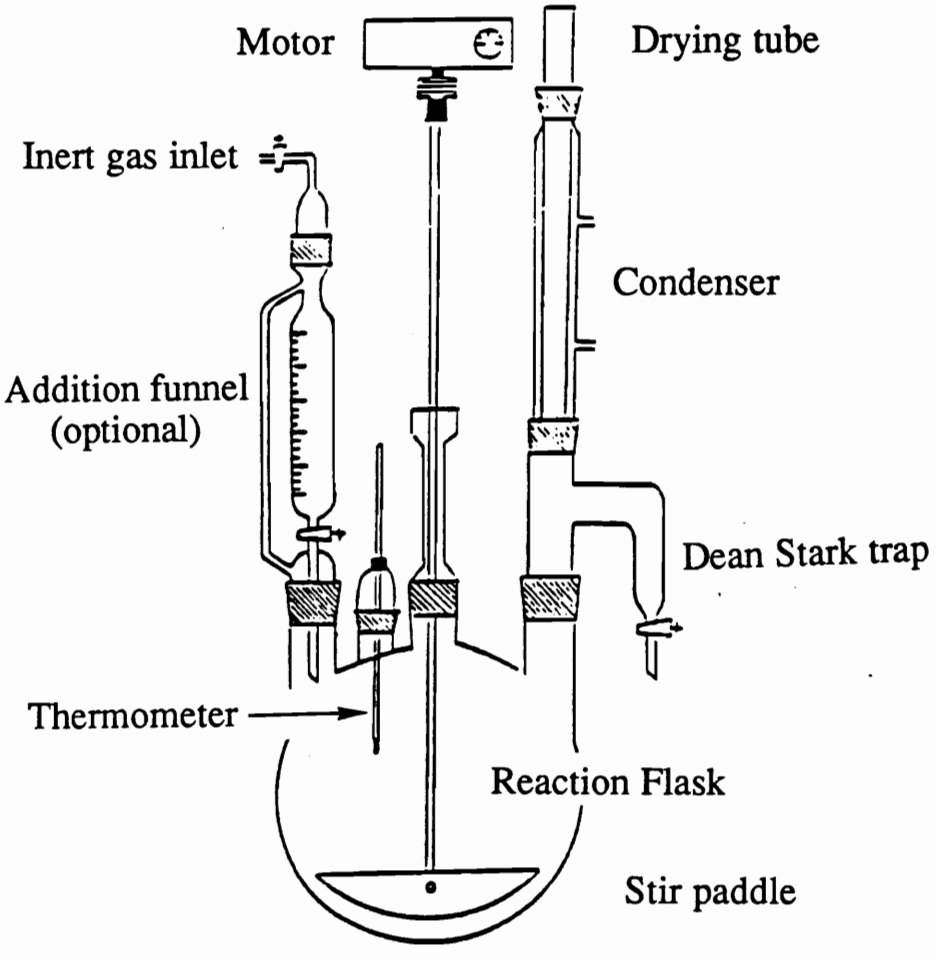

Figure 17: Solution imidization apparatus

3.9.0 Crosslinking of reactive maleimide endgroups

The imide oligomers with reactive maleimide endgroups were crosslinked to form network structures by two techniques. For oligomers with <Mn> > 10,000 g/mole, 20 to 25 w/v percent solids solutions of the oligomer in DMAc were cast unto a clean, dry glass plate, slowly heated in a vacuum oven over several hours to 200°C, and held for several hours. A final curing step at 300°C in a forced air convection oven for 12 hours yielded tough films which were insoluble in NMP or DMAc. A melt pressing technique was also used to cure the oligomers. Dry, powdered oligomers were compacted in a PHI hydraulic press at 400 psi between steel plates lined with Teflon sheets. The temperature of the press plates was slowly increased to 300°C and held for several hours. The films were then placed onto a glass plate and placed in a 300°C forced air convection oven for 12 hours, yielding tough films which were insoluble in NMP or DMAc.

3.10.0 Preparation of films of solution imidized polyimides

Films of solution imidized polyimides were prepared by dissolving the dried polymer in NMP with stirring or vigorous shaking at room temperature. Heating to affect solvation was not desirable. The highest solids concentration which yielded homogeneous solutions was desired, usually a maximum of 20 to 25 w/v percent. Solution stability was limited, particularly at high solids concentrations, or for solutions which had been heated to affect solvation, or for solutions of the more relatively rigid, high molecular weight homopolyimides. For example, 15 w/v percent solutions of BTDA-m-DDS in NMP were found to irreversibly solidify and become opague after ~2 to 3 hours. In some cases, endcapping with phthalic anhydride enhanced solution stability, although this was not always the case. The homogeneous solutions were cast onto a clean, dry glass plate and levelled to a constant thickness of 0.025 or 0.030 inch with a doctor's blade. The films

were placed in a vacuum oven, and the temperature was slowly increased to 200°C and held for ~12 hours. The films were then dried under vacuum at ~Tg for at least 4 hours.

3.11.0 Preparation of polymer blends

Blends of novel polyimides were made with other polymers by either melt or solution blending.

3.11.1 Polybenzimidazole (PBI) *blends*

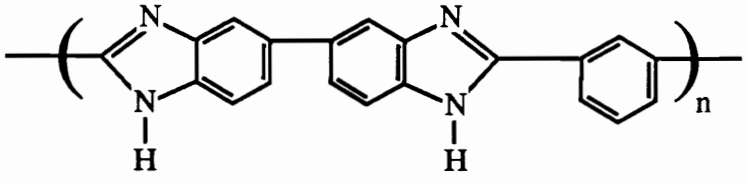

Tg 430°C

Blending of dry PBI powder with the polyimide homopolymer and copolymers was accomplished by combining individual solutions of the components, each at a concentration of approximately 10 to 15 weight percent in dimethylacetamide, in a blender with vigorous stirring. Films were solution cast onto glass plates and dried at 65°C under moderate vacuum for 2 days in order to remove most of the solvent. Further staging under vacuum at 120°C for 2 days and 300°C for 3 days yielded solvent-free films, as determined by DMTA and TGA. The polyimides used for this blending study were based upon BTDA, m-DDS and PSX (<Mn> = 800 or 950 grams per mole.) The PBI used for the initial blending work was not endcapped. To limit molecular weight and thereby improve thermoplastic melt flow behavior, continuing studies were conducted with PBI endcapped with 2 mole percent phenyl benzoate.

3.11.2 *Poly (ether ether ketone)* (PEEK) *blends*

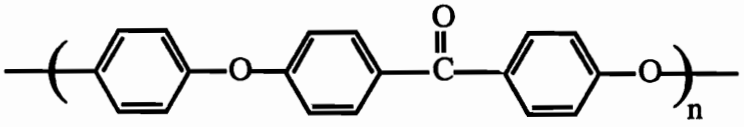

Tg 143°C, Tm 343°C

Blending of PEEK with the polyimide homopolymers and copolymers could not be accomplished by solution techniques, due to the semi-crystalline nature of PEEK. Rather, a Rheomix intensive shear mixer was employed. Dry blended powders of the components were added to the mixer chamber, which was set at 350°C, and blended for 7 minutes under intensive shearing conditions. The molten blend was removed quickly from the mixing chamber, melt pressed (350°C, 400 psi) into films, and quickly quenched by total immersion into a cold water bath. The polyimides used for this blending study were based upon BTDA, Bis P, PSX (<Mn> = 2465 grams per mole), and PA. The incorporation of PA was used to improve flow properties by limiting the overall molecular weight to typically 25,000 grams per mole. The PEEK was grade 380P, in pellet form, of medium grade viscosity, and suitable for general purpose extrusion.

3.11.3 *Poly(ether ketone)* (PEK) *blends*

Blends of Bisphenol A-difluorobenzophenone based PEK (18,000 <Mn> obtained by adding an excess of difluorobenzophenone) and polyimide homopolymers and copolymers were attempted by solubilizing dry blends of the components in NMP or DMAc at a solids concentration of 15 weight percent. The solutions were coagulated in rapidly stirring methanol to yield fibrous, off-white powders. The powders were dried under vacuum at ~200°C for a minimum of 12 hours, then melt pressed into clear, light amber films.

Independent of the blend composition, DSC scans indicated two distinct glass transitions corresponding to the PEK and polyimide components, respectively. Thus, this solution blending method proved unsuccessful in obtaining miscible blends of these two components.

3.12.0 Characterization of solvents, monomers, oligomers, polymers and blends

3.12.1 Solvent water contents

Solvent water contents were determined by Karl Fisher Model 447 Coulamatic titrator (Fisher Scientific, Inc.) The typical sample volume was ~0.6 ml, with a persist time of 30 seconds. Solvents were considered acceptable for use for polymerizations if the water content was less than 150 ppm.

3.12.2 Potentiometric endgroup titration

Titrations of functional monomers and oligomers were performed on either a Fisher Scientific Titrimeter II or MCI GT-05 (COSA Instruments Corporation) automatic potentiometric titrator. The samples were accurately weighed into a 150 ml beaker, and 50 to 70 ml of solvent were added. Mild stirring by a magnetic stir bar effected complete solvation. Sample quantities were chosen to require ~2 to 4 ml of titrant. When the sample was completely dissolved, the electrodes were inserted into the solution and the titration begun. A blank titration (solvent only) was performed under similar conditions by titrating the exact volume of solvent used with the same titrant until the endpoint potential was reached. The blank volume was subtracted from the endpoint value.

The aryl ether oligomers based upon Bisphenol A and amine terminated imide oligomers based upon 6F and Bis A (diamine) were dissolved in a chlorobenzene (66)/glacial acetic

acid (34) cosolvent mixture and titrated potentiometrically with 0.02 N anhydrous HBr in glacial acetic acid. The HBr solution was standardized by titrating potassium hydrogen phthalate in glacial acetic acid with crystal violet as the indicator. The siloxane oligomers were dissolved in IPA and titrated with 0.10 N methanolic HCl. The average of a minimum of three titrations was used to determine the molecular weight of each sample.

3.12.3 Determination of monomers' melt temperatures

Monomer purity was assessed by detemining melt temperatures on a Lab Devices Mel-Temp II (Holliston, Mass).

3.12.4 Intrinsic viscosity ([*n*])

Relative molecular weights of oligomers and polymers were determined by intrinsic viscosity measurements in distilled NMP at 25°C. A Cannon-Ubbelohde viscometer was used with a sufficient capillary size to yield flow times greater than 100 seconds. Four concentrations were analyzed and linear regression to zero concentration yielded the intrinsic viscosity values. Intrinsic viscosity values are in units of deciliters per gram.

3.12.5 Gel permeation chromatography (GPC)

GPC was used to investigate the molecular weights and molecular weight distributions of polyimide homopolymers and copolymers which were soluble in THF or methylene chloride. A Waters 150C instrument, a Viscotek differential viscometer detector Model 100, and six Permagel columns ranging in size from 500Å to 10^6Å were used. The samples were dissolved in HPLC grade solvent at a concentration of ~0.1 w/v percent, and injected at a flow rate of ~1 ml per minute. Analyses were performed at 30°C. Molecular weights were determined using a universal calibration curve.

3.12.6 Fourier transform infrared spectroscopy (FTIR)

The amic acid to imide transformation was monitored by FTIR using a Nicolet MX-1 spectrophotometer. Samples were removed during the course of the imidization to monitor the progress of the transformation, or at its completion to ensure quantitative conversion. The reaction solution was either cast as a thin free standing film, or onto KBr pellets, and dried in a vacuum oven at 70°C for one hour to remove a large amount of solvent. FTIR scans indicated that no imidization occurred under these conditions. The disappearance of the amic acid peak at 1546 cm^{-1} and the appearance of the imide peak at 1778 and 725 cm^{-1} were taken as evidence that imidization had proceeded quantiatively.

3.12.7 Proton nuclear magnetic resonance spectroscopy (NMR)

NMR was particularly useful in yielding chemical composition information for the poly(siloxane imide) segmented copolymers. A Bruker 270 MHz instrument was used for obtaining quantitatively integrated spectra. The copolymer samples were extracted with hexanes in a Soxhlet extractor for at least 12 hours, then dried in a vacuum oven at ~200°C for 12 hours. The samples were then dissolved in deuterated DMSO or deuterated chloroform at a solids concentration of ~ 3 to 5 percent. Methylene chloride was used as the lock reference because the tetramethylsilane resonance was not base line resolved from the polydimethylsiloxane resonances in the samples. The ratio of the area of the siloxane methyl peaks (0 ppm) to the area of another distinct peak, such as the aromatic protons (~7 to 8 ppm) or methyl protons of the imide component (~1.6 ppm for Bis P containing imides), was used to determine the actual amount of siloxane incorporated into the polymer backbone, as contrasted with the amount of siloxane charged to the reaction.

The theoretical ratio of the protons arising from the distinct peak to the siloxane protons was calculated as follows. The siloxane protons were determined by dividing the siloxane oligomer molecular weight by the molecular weight of the polydimethylsiloxane repeat unit (74 g/mole), and multiplying by 6, the number of protons per repeat unit. This value represents the number of siloxane protons per siloxane-containing repeat unit. When multiplied by the fractional molar percent of siloxane, the weighted (molar basis), theoretical number of siloxane protons in the copolymer repeat unit is obtained [PSX(th)]. The number of protons arising from one mole of the monomer(s) associated with the distinct peak is multiplied by the fractional molar percent of this monomer(s). For example, one mole of Bis P contains 12 protons, but Bis P only constitutes 30 molar percent of the total reaction. Thus, 12 X 0.30 is the weighted, theoretical number of protons giving rise to the distinct "Bis P" peak at ~ 1.6 ppm [DP(th)]. The theoretical ratio (TR) of the protons arising from the distinct peak to the siloxane protons is thus [DP(th)] ÷ [PSX(th)].

The actual ratio (AR) of the protons arising from the distinct peak to the siloxane protons is simply the ratio of their respective integrated peak intensities. This actual ratio (AR) divided by the theoretical (TR) ratio determines the amount of siloxane actually incorporated into the polymer backbone.

3.12.8 Solubility

Solubilities of the homopolymers and copolymers were evaluated in a wide variety of solvents. The dried polymer films or powders were dissolved in the appropriate solvent at a solids concentration of 10 w/v percent and stirred or shaken vigorously. If ready solubility was not apparent, the samples were allowed to stir for longer periods of time or

diluted with more solvent to a lower solids concentration of ~5 w/v percent. Solubilities were ranked as "Soluble" if a clear solution was obtained shortly after solvation, "Marginally Soluble" if a turbid solution was obtained, or "Insoluble" if solid particles remained in the solution even after prolonged vigorous stirring and mild heating at 60°C.

3.12.9 Thermal Characterization: differential scanning calorimetry (DSC), *thermal gravimetric analysis* (TGA), *thermal mechanical analysis* (TMA)

DSC was used to determine glass transition tempeatures with either a Perkin-Elmer DSC-4 or a DuPont 912 connected to a DuPont 2100 Thermal Analyst. Temperature ramping was 10°C per minute with reported values being obtained from a second scan after heating and cooling. Rapid cooling was typically used between scans for amorphous materials, whereas the semi-crystalline blends of PEEK and novel polyimides were slow cooled at a rate of 2°C per minute between the first and second scans . The glass transition temperature was defined as the midpoint of the slope change from the baseline. The Perkin-Elmer instrument covered a temperature range of -150°C to 300°C, with scanning performed in two steps. Subambient runs from -150°C to room temperature were obtained by cooling the sample chamber with liquid nitrogen in a helium gas atmosphere, which prevented condensation. Ambient scans were run in a nitrogen atmosphere. TGA was performed on a Perkin-Elmer TMS-2 or a DuPont 951 instrument on samples in either thin film or powder form. Scans were run at 10°C per minute in a flowing air or nitrogen atmosphere. The gas flow rate was set at 10 ml per minute. The TGA char yield at 700°C of the poly(siloxane imide) segmented copolymers was a realistic estimate of the amount of siloxane acually incorporated into the copolymer backbone. TMA was performed on a Perkin-Elmer TMS-2 instrument on samples in film form. Scan conditions for TMA and TGA were the same.

3.12.10 Dynamic mechanical thermal analysis (DMTA)

Dynamic mechanical thermal analysis was used to determine the thermal-mechanical behavior of some specimens. A Polymer Laboratories instrument was used at a frequency of 1 Hz and a typical temperature ramping rate of 5°C per minute.

3.12.11 Mechanical properties

Both Instron models 1122 or 1123 were used to determine the room temperature mechanical behavior of dogbone shaped film specimens cut from a steel rule die (ASTM-638 IV) against a polyethylene cutting board. The specimen gauge length was 10 mm and the width was 2.76 mm. Sample thicknesses were ~0.003 to 0.007 inch. The crosshead extension rate was either 5 mm per minute for the poly(siloxane imide) segmented copolymers, or 0.5 inch per minute for the homopolyimides. Reported results are an average of 3 to 5 samples.

3.12.12 Adhesive and durability properties

Adhesive and durability properties were determined on single lap shear specimens in several different environments of varying temperature and humidity. Films of solution imidized homopolymers or copolymers were typically prepared by melt press methods (3.8.0), although solution casting was sometimes used. The films were then layered together to yield an overall thickness of 0.023 to 0.033 cm and pressed between two primed titanium adherends using the following bonding cycle:

Room temperature to 325°C, apply 1.4 MPa (200 psi) at 280°C
Hold for 15 to 60 minutes at 325°C
Cool under pressure to room temperature.

The titanium adherends were prepared by sandblasting, treating with a Pasa Jell 107 acid etch, ultrasonically cleaning, and immediately priming with a coating of a solution (15 percent solids concentration in NMP) of the fully imidized homopolymer or copolymer adhesive.

3.12.13 Dielectric properties

Dielectric properties were determined on a Hewlett Packard Network Analyzer 8510 over the frequency range of 12.5 to 18.0 GHz with a P band waveguide. The sample specimens were assessed after being dried in a vacuum oven for a minimum of 12 hours near the glass transition of the polymer. As a comparison, a Kapton sample was also assessed after remaining at ambient conditions for an extended time. The specimen size was approximately 1 cm by 0.5 cm. The scans were run at room temperature in an air atmosphere, although operation up to 165°C and in different environments over the frequency range of 45 MHz to 26 GHz was also possible.

3.12.14 Oxygen plasma stability

A Plasmod "asher" unit from the Tegal Corporation (Richmond, California) was used to determine the stability of the polyimide homopolymers and particularly the siloxane containing copolymers in an aggressive oxygen environment. One square inch thermally imidized film samples were placed into the Plasmod environmental chamber under a reduced pressure of 150 millitorr and an oxygen flow rate of 30 cc per minute. The siloxane rich surface (i.e., air-polymer surface) of the copolymers was placed facing upwards. An applied radio frequency of 50 MHz caused the oxygen plasma to be generated within the chamber. Exposure time to the plasma was limited to 45 minutes. The film surfaces were characterized by weight loss measurements, XPS and SEM to

determine any physico-chemical changes which may have occurred during exposure to the aggressive oxygen plasma.

3.12.15 Atomic oxygen stability

In order to more closely mimic the aggressive environment present in the low earth orbit (LEO), atomic oxygen stability tests were performed at Physical Sciences, Inc. (Andover, Massachusetts). Their facilities employ a high power pulsed carbon dioxide laser to generate high flux, high velocity pulses of pure oxygen atoms to bombard the sample specimens in a 20 cm diameter vacuum test chamber. The exposure time for the eight test specimens was chosen to correspond to one week of LEO exposure. The specimens were placed in the chamber with their siloxane-rich surface oriented toward the incoming atomic oxygen (278). The test conditions are specified in the following table:

Chamber Base Pressure	2×10^{-5} Torr
Nozzle Pulse Repetition Rate	1.4 Hz
Average Velocity	8 km per second
Distance from throat to sample	40 cm
Area of Beam at Sample	300 cm^2
Nominal Area exposed on target	6.4 cm^2 (-10%)
Number of Pulses	54360
Number of O-atoms per Pulse (Theory)	2×10^{19} atoms
Number of O-atoms per Pulse (Kapton)	5×10^{17} atoms
Average Pulse Fluence on Target (Theory)	6.7×10^{16} atoms per cm^2
Average Pulse Fluence on Target (Kapton)	6.7×10^{16} atoms per cm^2
Total Integrated Flux (Theory)	3.6×10^{20} atoms per cm^2
Total Integrated Flux (Kapton)	3.6×10^{20} atoms per cm^2

3.12.16 Water sorption studies

Water sorption studies were conducted by immersing thin dry (to constant weight) film samples in distilled water at room temperature and removing the samples at periodic intervals, blotting dry and weighing to determine water uptake.

3.12.17 X-ray photoelectron spectroscopy (XPS)

A Kratos XSAM-800 x-ray spectrometer with a Mg x-ray source was used to determine the surface composition of the copolymer films. Samples were prepared by spin-coating (at 3000 rpm) the amic acid intermediate in its reaction solution onto ferrotype plates which had been washed thoroughly in hexane. The samples were covered with a watchglass to prevent contamination during bulk thermal imidization in a forced air convection oven. After imidization, the samples were washed three times in hexane and placed in clean glass containers with glass lids. Analysis was performed on a Kratos instrument at exit angles of 15° and 90°. The 15° grazing angle yields compositional data from depths of ~10 to 20 Å, whereas the 90° normal angle samples depths of ~70 to 100 Å.

3.12.18 Scanning electron microscopy (SEM)

An ISI Super III scanning electron microscope was used to examine the surface topography of gold-palladium coated samples at magnifications up to 10,000X. Alternatively, a Philips EM-420 Scanning Transmission Electron Microscope (STEM) could also be used to obtain magnifications up to 25,000X with high resolution. The ISI Super III SEM was used for examining the surface morphology of samples exposed to oxygen plasma; the Philips EM-420 was used for surface morphological investigations of atomic oxygen exposed samples.

3.12.19 Transmission electron microscopy (TEM)

Samples of the poly(siloxane imide) segmented copolymers for TEM were either sectioned on a Reichert cryo-ultramicrotome or solution cast from chloroform as thin films on water. The microtome sample holder was cooled to ~ -100°C and the diamond knife to ~ -90°C with liquid nitrogen gas. The sample temperatures were slightly above the Tg of the siloxane component of the copolymers. The liquid used in the knife boat was methanol, a non-solvent for the copolymers which were studied. The liquid allows for easy transfer of the sectioned sample onto a copper mesh grid. Solvent cast thin films were prepared by dissolving the dried polymer sample in chloroform at a 5 w/v percent solids concentration. The solution was cast as droplets from a syringe onto distilled water, readily forming a thin film. The thin film, usually gold or silver in color corresponding to thicknesses of ~500 to 100 Å, was transferred to a copper mesh grid. The sections or films on the grids were dried under vacuum prior to TEM analysis. A Philips EM-420 Scanning Transmission Electron Microscope (STEM) was operated in the transmission mode at 100 kV. Siloxane-rich phases of the order of 40 to 100 nm could be confirmed with a Tracor Northern TN-500 energy dispersive x-ray spectrometer.

3.12.20 Rheological properties

Rheological behavior of the polyimide homopolymers and copolymers was assessed by performing temperature-frequency sweeps in an air atmosphere on a Rheometrics RMS-800 parallel plate rheometer with a Dynamic Spectrometer Model RDS-II. Frequency was varied from 0.1 to 100 radians per second; the temperature range differed for each polymer sample, up to 380°C. Strain was held constant. Plots of complex viscosity versus frequency were generated for each sample at each temperature.

3.13.0 Suppliers

Air Products and Chemicals, Inc.
P. O. Box 2662
Allentown, Pennsylvania 18001

Aldrich Chemical Company
940 West Saint Paul Avenue
Milwaukee, Wisconsin 53233

Allco Chemical Company
P. O. Box 6200 B
Pittsburg, Kansas 66762

Chriskev Corporation
5109 West 111th Terrace
Leawood, Kansas 66211

FIC Resins Corporation
333 Market Street
San Francisco, California 94105

Fisher Scientific
3315 Atlantic Avenue
Raleigh, North Carolina 27629

GAF Corporation, Chemicals Group
140 West 51st Street
New York, New York 10020

Hoechst Celanese
86 Morris Avenue
Summit, New Jersey 070901

Imperial Chemical Industries, Americas (DFBP)
Route 202
Wilmington, Delaware 19897

Imperial Chemical Industries, Fiberite (PEEK)
2055 East Technology Circle
Tempe, Arizona 85284

H. S. Bancroft Corporation (Pasa Jell 107)
Rockhill Road
Cherry Hill, New Jersey 08003

Occidental Chemical Corporation
2801 Long Road
Grand Island, New York 14072

Petrarch Systems, Inc.
2731 Bartam Road
Bristol, Pennsylvania 19007

Union Carbide Corporation
Old Ridgebury Road
Danbury, Connecticut 06817

CHAPTER 4

RESULTS AND DISCUSSION----------

4.1.0 Nomenclature

An unmistakable identification of each polyimide system must be made to promote a clear, easy discussion of polyimide structure-property relationships. The nomenclature to describe each polymer system will consist of a complete listing of the monomers and oligomers employed in its synthesis, starting with the dianhydrides, then diamines, followed by monofunctional reagents with the theoretical number average molecular weight in parentheses. Polyimide systems consisting of monomers, and even multiple dianhydride monomers and/or multiple diamine monomers will be referred to as homopolymers, although a polyimide comprised of multiple monomers could be more properly described as a copolymer. In the case of multiple monomers, a corresponding molar percentage of the total dianhydride or diamine content will be indicated. Polyimide systems consisting of monomers and oligomers, either polysiloxanes (PSX) or poly(aryl ether)s (PSF or PEK, for polysulfones or polyketones, respectively), will be referred to as copolymers. Their nomenclature will consist of an extra term which encompasses the weight percentage of the oligomer relative to the total copolymer, the oligomer type (PSX, PSF, PEK), then the oligomer molecular weight. Thus, the designation:

BTDA (50) 6F (50)-mDDS-20 PSX 5000-PA(25,000)

defines a copolymer with phthalimide endgroups and a 25,000 g/mole <Mn>. It is composed of an equimolar amount of two monomeric dianhydrides: BTDA and 6F, and the only monomeric diamine is m-DDS. The 5,000 g/mole polydimethylsiloxane segment comprises 20 percent of the total copolymer weight.

4.2.0 Synthesis of polyimide homopolymers and copolymers

The synthetic procedure for the polyimide homopolymers and copolymers was well established by Summers (14), who primarily worked with BTDA and m-DDS based poly(siloxane imide) segmented copolymers. For specific information regarding sample reactions, other synthetic issues, or the kinetics of the imidization reaction, the reader is referred to his work. The focus of this research was on the structure-property relationships of polyimides of greater compositional variations, including not only homopolyimides containing multiple dianhydride and/or multiple diamine monomers, but polysiloxane and polyaryl ether segmented copolymers as well. Blends of polyimide homo- and copolymers with polybenzimidazole or poly(ether ether ketone) were also investigated for miscibility and for their unique, high performance properties.

One synthetic aspect worthy of emphasis is the use of the cosolvent system, NMP and THF, to solubilize the reacting poly(siloxane amic acid)s. More THF was necessary to solubilize species containing more siloxane, higher siloxane molecular weights, or other aromatic monomers which exhibited at least partial, if not complete solubility in THF, such as Bis P or 6F. Independent of the amount or molecular weight of the polysiloxane oligomer, BTDA-Bis P based copolymers typically required approximately 10 w/v percent solids concentration in THF (70 to 80%):NMP (30 to 20%). Occasionally, some poly(siloxane amic acid)s would not form *entirely* clear solutions even at this low solids concentration with an excess of THF. The amic acid solutions would be *almost* clear, however, they would look opalescent. Thus, proton NMR was an exceptionally useful tool in determining the amount of polysiloxane oligomer actually incorporated into the copolyimide backbone. For instance, the poly(amic acid) for BTDA-Bis P-40 PSX 3650-PA (25,000) displayed such an opalescence, indicating that perhaps quantitative

incorporation of the siloxane oligomer would not be achieved. In Figure 18, its proton NMR spectrum, alongside the NMR spectra of the corresonding homopolymer, indicates that 95 percent of the siloxane was incorporated, or 38 percent overall. Proton NMR spectra of a series of poly(siloxane imide) segmented copolymers which were extracted for 72 hours in hexanes were compared to the NMR spectra of samples which were not extracted, indicating that the typical precipitation procedure in a ten-fold excess of methanol and water was sufficient to remove residual, unreacted polysiloxane oligomers. The differences in calculated siloxane contents between extracted and unextracted samples was less than ~1 percent. Additionally, the char yield at 750°C by TGA in flowing air corresponded to the weight percent of siloxane incorporated into the copolymer backbone.

4.3.0 Solubility

One of the major endeavors of this research was to solubilize the normally intractable high molecular weight polyimides by the judicious choice of monomers and oligomers while maintaining good ductility and high glass transition values. Previous work by Summers had shown that for certain monomer combinations, the solution imidized materials were markedly more soluble than their bulk imidized analogues, although the glass transitions of the solution imidized systems were only marginally lower by approximately 5°C. Gel permeation chromatographs (GPC) alluded to the differences in solubility between the bulk and solution imidized systems. The typical unimodal GPCs of the bulk imidized polyimides exhibited a low molecular tail, contrasted with the expected unimodal Gaussian distribution of the solution imidized versions. This skewed molecular weight distribution suggested possible abnormal side reactions were occurring at the high temperatures (300°C) required for quantitative bulk imidization. Consequently, the solution technique was the favored imidization method.

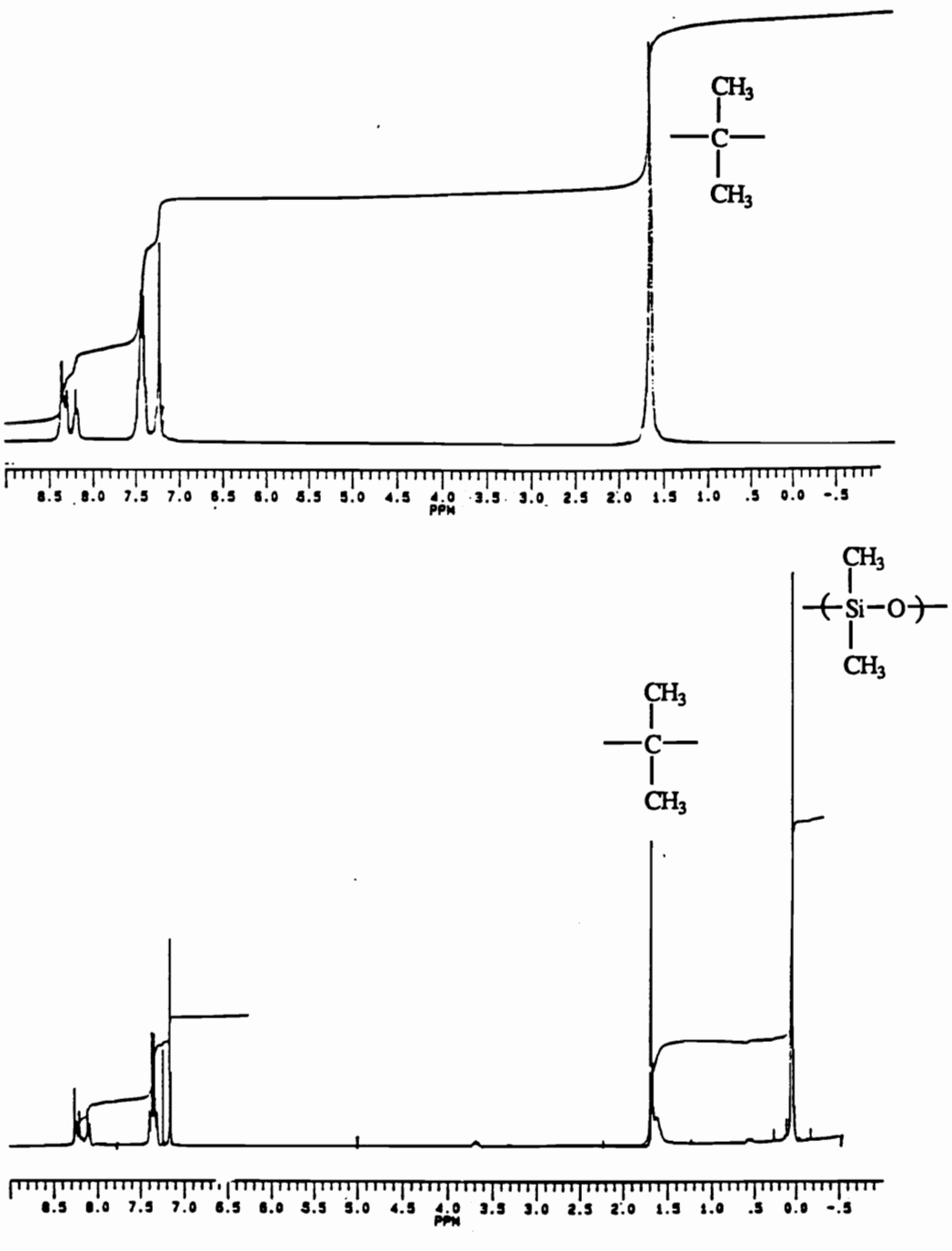

Figure 20: Proton NMR spectra of BTDA-Bis P-PA (25,000) homopolyimide (upper) and BTDA-Bis P-38 PSX 3650-PA (25,000) poly(siloxane imide) segmented copolymer (lower)

4.3.1 Solubilities of homopolyimides

Table 20 indicates the solubilities of some high molecular weight, solution imidized polyimide homopolymers; some are based upon less polar monomers such as bisaniline diamines or the 6F dianhydride. Utilization of these monomers, rather than the more polar BTDA or m-DDS, yielded more soluble polyimide systems. Homopolyimides based upon the triphenyl phosphine oxide (PO) diamine were also synthesized. Due to the limited supply of the starting material (POF), very little PO diamine was available for use. Consequently, these homopolyimides could only be imidized in bulk, and attained only moderate molecular weights due to a small amount of solvent impurities, as judged by the quality of the imidized films. Nevertheless, bulk imidized BTDA-PO and 6F-PO, and solution imidized PMDA-PO were readily soluble in NMP. The bulk imidized 6F-m-DDS (50) PO (50) polyimide was highly soluble in NMP as well, although a minute gel fraction may have remained. The enhanced solubility of PO containing systems is attributed to the high content of the flexibilizing ether linkage. Polyimides based on the 4F diamine were expected to exhibit enhanced solubility due to the presence of the fluorine groups and flexible ether linkages, however, these polymers, BTDA-4F and 6F-4F, showed only a marginal improvement in solubility over the m-DDS containing anologues. Although not indicated in Table 20, attempts to synthesize other PMDA-based polyimides by solution imidization were unsuccessful. Both PMDA-Bis P and PMDA (50) 6F (50)-Bis P poly(amic acid)s precipitated out of solution prematurely, although some imidization had occurred. Likewise, attempts to synthesize high molecular weight SDA- and BTDA-p-DDS polyimides were similarly unsuccessful. Accordingly, these systems were only imidized in bulk.

Table 20: Solubilities of solution imidized polyimide homopolymers: Sol: soluble; MS: marginally soluble; IS: insoluble; asterisk (*) indicates bulk imidized sample; symbol (†) indicates slightly hazy solution

Polyimide System	NMP	THF	CH_2Cl_2	øCl	Tol
BTDA-m-DDS	Sol	IS	IS	IS	IS
BTDA-Bis A	Sol	IS	Sol	IS	IS
BTDA-Bis P	Sol	MS	Sol	MS	IS
BTDA-PO*	Sol	IS	IS	IS	IS
BTDA-4F	Sol	IS	IS	IS	IS
6F-m-DDS	Sol	Sol	Sol	IS	IS
6F-Bis A	Sol	Sol†	Sol	Sol†	IS
6F-Bis P	Sol	Sol	Sol	Sol	Sol
6F-PO*	Sol	Sol	Sol	IS	IS
6F-4F	Sol	Sol	Sol	IS	IS
6F-p-DDS	Sol	Sol	Sol	IS	IS
6F (50) BTDA (50)-PO*	MS	IS	IS	IS	IS
ODPA-Bis A	Sol	----	Sol	----	IS
ODPA-Bis P	Sol	Sol†	Sol	Sol†	IS
SDA-m-DDS	Sol	IS	IS	IS	IS
SDA-Bis P	Sol	IS	MS	IS	IS
PMDA-PO	Sol	---	---	---	---

4.3.2 Solubilities of poly(siloxane imide) and poly(aryl ether imide) segmented copolymers

Solubilities of a series of siloxane and aryl ether containing copolymers were evaluated in a variety of solvents, as indicated in Tables 21 and 22, respectively. Solubility of the BTDA-m-DDS based poly(siloxane imide) segmented copolymers was primarily a function of the concentration of the siloxane oligomer. At concentrations equal to or greater than 10 weight percent, all solution imidized copolymers were soluble in dipolar, aprotic solvents such as NMP and DMAc. Copolymers containing higher percentages of siloxane were soluble in a wider range of solvents, such as THF, diglyme, and methylene chloride. Intrinsic viscosities of the copolymers ranged from 0.50 to 1.88 dl per gm, indicating that high molecular weight copolymers were obtained over the entire composition range. The poly(aryl ether imide) segmented copolymers displayed a remarkably high degree of solubility, however, the homopolymer, BTDA-Bis P, was one of the more relatively soluble polyimides itself. The intrinsic viscosities for these copolymers were relatively low, reflecting that the copolymer molecular weight was controlled to ~25,000 g/mole. GPCs in chloroform, run with the viscosity detector and universal calibration curve, indicated that the actual molecular weights for these copolymers were in the range of 16,000 to 22,000 g/mole. Tough, ductile films were obtained, indicating that the molecular weight was indeed above the critical value for obtaining good physical properties.

Table 21: Solubilities of solution imidized poly(siloxane imide) segmented copolymers: Sol: soluble; MS: marginally soluble; IS: insoluble; asterisk (*) indicates slightly hazy solution

Polyimide System	NMP	THF	CH_2Cl_2	øCl	Tol
BTDA-m-DDS-10 PSX 950	Sol	IS	IS	IS	IS
BTDA-m-DDS-20 PSX 950	Sol	IS	IS	IS	IS
BTDA-m-DDS-40 PSX 950	Sol	Sol	Sol	Sol	Sol*
BTDA-m-DDS-60 PSX 950	Sol	Sol	Sol	Sol	Sol*
BTDA-Bis A-10 PSX 2500	Sol	MS	Sol	MS	IS
BTDA-Bis A-20 PSX 2500	Sol	Sol	Sol	Sol	MS
BTDA-Bis P-10 PSX 2500	Sol	Sol	Sol	MS	IS
BTDA-Bis P-20 PSX 2500	Sol	Sol	Sol	Sol	MS
BTDA-Bis P-30 PSX 2500	Sol	Sol	Sol	Sol	Sol*
BTDA-Bis P-50 PSX 2500	Sol	Sol	Sol	Sol	Sol
6F-Bis A-10 PSX 2500	Sol	Sol	Sol	Sol	MS
ODPA-Bis P-10 PSX 1150	Sol	Sol	Sol	Sol	----

Table 22: Solubilities of solution imidized poly(aryl ether imide) segmented copolymers based on BTDA and Bis P, with molecular weight controlled to 25,000 g/mole by the addition of phthalic anhydride: Sol: soluble; MS: marginally soluble; IS: insoluble

Poly(sulfone imide) System	NMP	CH_2Cl_2	THF
BTDA-Bis P Homopolyimide	Sol	Sol	MS
10 PEK 6580	Sol	Sol	MS
30 PEK 6580	Sol	Sol	MS
50 PEK 6580	Sol	Sol	almost Sol
10 PSF 6050	Sol	Sol	MS
30 PSF 6050	Sol	Sol	MS
50 PSF 6050	Sol	Sol	MS
95 PSF 6050 (no Bis P)	Sol	Sol	almost Sol

4.3.3 Influence of molecular weight on adhesive and melt flow properties

Solubility and processablity were further enhanced by controlling the overall molecular weight. Table 23 illustrates that incorporation of a monofunctional reagent, in this case phthalic anhydride, indeed limited molecular weight, as determined indirectly by intrinsic viscosity values. Presumably, most of the end groups were phthalimide in nature, as depicted in Figure 19, although this was not quantitatively demonstrated. The use of controlled molecular weights offers two pertinent advantages for thermoplastic processing and adhesive applications. First of all, lower molecular weight samples exhibit better and more stable melt flow properties and consequently, superior bond consolidation. Secondly, non-functional phthalimide end groups are unreactive towards potential post-reactions which could occur during bond formation. Such post-reactions could inhibit good wetting of the adherend which might prevent adequate bond consolidation. Furthermore, the presence of functional end groups (anhydride and especially amine) decreases the thermal stability of polyimides markedly (37).

The effect of molecular weight and endgroup control on the adhesive properties of a BTDA-Bis P-PA based polyimide is demonstrated in Table 24. High single lap shear strengths of ~27 MPa were obtained in two cases: for the homopolymer with the controlled molecular weight of 30,000 g/mole and for the copolymer with 30 weight percent siloxane (PSX <Mn> = 2500 g/mole). These high lap shear strengths indirectly indicated that good melt flow and bond consolidations were obtained, particularly when considered relative to the homopolymer with uncontrolled molecular weight and end groups (11.7 MPa only). The 10,000 and 20,000 g/mole molecular weight controlled homopolymers exhibited somewhat lower lap shear strengths than the 30,000 g/mole analogue, because molecular entanglements responsible for excellent physical properties were somewhat lower in these

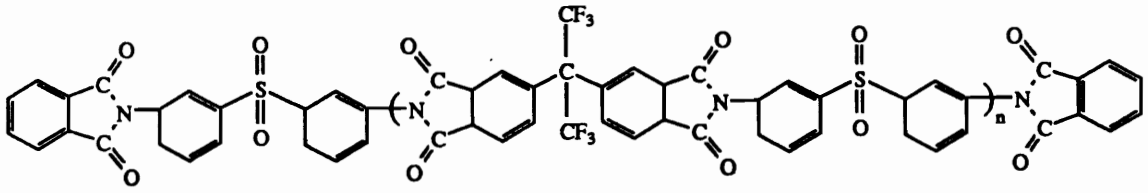

Figure 19: Polyimide homopolymer based on 6F and m-DDS with phthalimide endgroups

Table 23: Molecular weight and endgroup control of 6F-m-DDS homopolyimides by incorporation of phthalic anhydride

Desired <Mn>	Mole percent Phthalic Anhydride	[*n*]
5,000	7.0	0.11
10,000	3.5	0.23
20,000	1.8	0.37
30,000	1.2	0.40
∞	----	1.08

Table 24: Single lap shear strengths for a series of molecular weight and endgroup controlled BTDA-Bis P-PA polyimides and a corresponding poly(siloxane imide) segmented copolymer with 30 weight percent siloxane of 2500 g/mole molecular weight

10,000	3.3	0.27	17.9 (2600)
20,000	1.7	0.33	25.5 (3700)
30,000	1.1	0.43	28.3 (4100)
∞	----	0.65	11.7 (1700)

BTDA-Bis P-30 PSX 2500 poly(siloxane imide) segmented copolymer

∞	----	0.74	27.6 (4000)

cases. However, these samples still exhibited superior adhesive performance relative to the uncontrolled molecular weight homopolymer. That the 30 weight percent siloxane copolymer could attain a lap shear strength comparable to the homopolymer attests to the fact that good melt flow resulting in good bond consolidation is a major factor in obtaining optimal adhesive performance.

4.3.4 Solubility and molecular weight control of addition imide oligomers

The issue of solubility also involves the need for a wide range of appropriate *environmentally acceptable* solvents for coating applications of the polyimide homo- and copolymers. Solvents such as gamma butryolactone, propylene carbonate and dibasic esters would be particularly attractive for electronic coatings applications. By controlling molecular weight with the incorporation of maleic anhydride and employing a polyimide system which was already highly soluble in a range of solvents, namely 6F-Bis A, addition imide oligomers which were soluble in an even wider variety of solvents than their linear high molecular weight analogues were obtained, as indicated in Table 25. Solubilities were determined at higher solids concentrations ranging from ~ 15 to 50 w/v percent. These oligomers could be subsequently crosslinked by thermal or electromagnetic (microwave) means to obtain crosslinked networks. In their crosslinked state, these systems were solvent insensitive relative to their high molecular weight, uncrosslinked analogues.

The synthesis of the 6F-Bis A series of imide oligomers was conducted in two steps. First, the amine terminated oligomers were synthesized by offsetting the stoichiometry in favor of the diamine and conducting the standard poly(amic acid) synthesis and solution imidization. The oligomers were isolated by coagulation in a ten-fold excess of distilled water, dried under vacuum, and titrated to determine their number average molecular

Table 25: Solubilities of 6F-Bis A-MA imide oligomers: Sol: soluble; MS: marginally soluble; IS: insoluble; asterisk (*) indicates that 40,000 g/mole <Mn> polyimide is phthalic anhydride endcapped

Oligomer <Mn>	NMP, DMAc, DMSO, THF, CH_2Cl_2, CH_3Cl	Propylene Carbonate	Amyl Acetate
5,000	Sol	Sol	Sol
10,000	Sol	Sol	IS
15,000	Sol	Sol	IS
20,000	Sol	MS	IS
40,000*	Sol	IS	IS

weights. As depicted in Table 26, the titrated molecular weights were in good agreement with the theoretical values. Intrinsic viscosity values corresponded with the expected trend. Several samples were analyzed by GPC with a viscosity detector and universal calibration curve. For instance, the actual molecular weight as determined by GPC for the fully imidized 6F-Bis A (10,000) sample was 12,500 g/mole (Figure 20). The polydispersity was 2.08, as expected for step growth polymerizations. The Mark-Houwink parameters, which provide information about the shape of the polymer in solution, were calculated to be 'k' = 0.0366 and 'a' = 0.61. The 'a' exponent of 0.61 is similar to other carbon based polymers in good solvents. Higher values of the 'a' exponent would be indicative of more rigid or extended conformations.

4.4.0 Thermal Properties

4.4.1 Glass transitions and morphologies of homopolyimides and poly(siloxane imide) segmented copolymers

The upper glass transitions of solution imidized, high molecular weight polyimide homopolymers and poly(siloxane imide) segmented copolymers are listed in Table 27, as determined by DSC. The upper glass transitions of the copolymers were found to be a function of both the level of incorporated siloxane as well as the siloxane molecular weight, generally increasing with greater siloxane oligomer molecular weight and lower siloxane incorporation. In many cases, the copolymers' upper transitions were only slightly depressed relative to the controls, particularly for the case of the polar polyimide BTDA-m-DDS, indirectly indicating that good microphase separation was achieved. For the BTDA-m-DDS-PSX series, the lower temperature siloxane transition was difficult to detect by DSC for low levels of siloxane incorporation, i.e., less than 20 weight percent. At greater levels of incorporation, however, the transition was detected by both DSC and DMTA

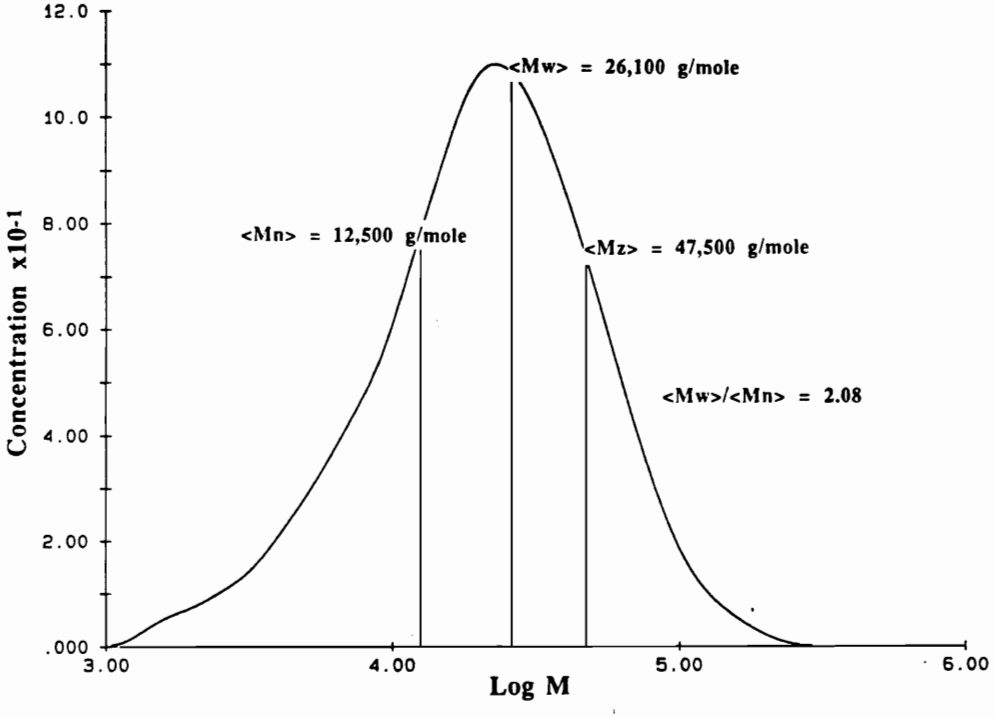

Figure 20: Molecular weight distribution as determined by gel permeation chromatography (THF, 30°C) with a viscosity detector for 6F-Bis A-MA addition imide oligomer with theoretical <Mn> = 10,200 g/mole

Table 26: Molecular weight data for 6F-Bis A based addition imide oligomers; asterisk (*) indicates sample from Figure 22 (MA endcapped) with <Mn> = 12,500 g/mole (theoretical <Mn> = 10,200 g/mole)

Amine Term. Olig. Theoretical <Mn>	Amine Term. Olig. Titrated <Mn>	MA Terminated Oligomer, [*n*]
5,000	6,470	0.187
10,000	10,200	0.342*
15,000	14,950	0.435
20,000	19,840	0.512
40,000	--------	0.811

Table 27: Upper glass transitions of polyimide homopolymers and poly(siloxane imide) segmented copolymers; asterisk (*) indicates bulk imidized samples

Polyimide System	[*n*]	Tg, °C
BTDA-m-DDS	1.36	265
BTDA-m-DDS-10 PSX 900	1.88	251
BTDA-m-DDS-10 PSX 2,100	0.73	260
BTDA-m-DDS-10 PSX 5,000	0.71	264
BTDA-m-DDS-10 PSX 10,000	0.73	266
BTDA-m-DDS-20 PSX 900	0.67	240
BTDA-m-DDS-40 PSX 950	0.58	218
BTDA-Bis A	1.39	294
BTDA-Bis A-10 PSX 2,500*	-----	282
BTDA-Bis A-20 PSX 2,500*	-----	272
ODPA-Bis A*	-----	292
ODPA-Bis A-10 PSX 2,500*	-----	270
BTDA-Bis P	0.72	264
BTDA-Bis P-10 PSX 800*	0.60	241
BTDA-Bis P-10 PSX 2,500	0.65	258
BTDA-Bis P-20 PSX 2,500	-----	245
BTDA-Bis P-30 PSX 2,500	0.74	242
BTDA-Bis P-50 PSX 2,500	-----	205
SDA-Bis P	-----	280
ODPA-Bis P	0.66	265
ODPA-Bis P-10 PSX 1150	-----	234
SDA-m-DDS	0.30	265

Table 27, continued: Upper glass transitions of polyimide homopolymers and poly(siloxane imide) segmented copolymers; asterisk (*) indicates bulk imidized samples

Polyimide System	[*n*]	Tg, °C
6F-p-DDS	-----	331
6F-m-DDS	0.60	270
6F-Bis A	-----	295
6F-Bis A-10 PSX 2,500	-----	274
6F-Bis A-10 PSX 4,900	-----	282
6F-Bis P	0.50	267
6F-Bis P-10 PSX 800	0.79	232
6F-Bis P-10 PSX 10,000*	-----	262
BTDA-4F	1.42	213
6F-4F	0.85	219
BTDA-PO*	-----	212
BTDA-PO (50) m-DDS (50)-PO*	-----	231
6F-PO*	-----	222
PMDA-PO	-----	240

within the range of -106 to -123°C (Figure 21). Initial transmission electron micrographs of these solution imidized copolymers indicated siloxane microphase formation for a 10 weight percent siloxane copolymer with a 2,000 g/mole molecular weight siloxane segment (Figure 22, right). The domain size was relatively small, approximately 50 Å, and phase contrast was somewhat poor. This may have been due to the low siloxane molecular weight and its broad Gaussian distribution. Microphase separation was enhanced by increasing the siloxane molecular weight to 10,000 g/mole (Figure 22, left). Consequently, the phase contrast sharpened and the domain size increased to approximately 160 Å.

Although incorporation of less polar monomers such as the bisaniline diamines and 6F dianhydride enhanced solubility, the upper glass transitions of these homopolymers were relatively unchanged from the BTDA-m-DDS system. Incorporation of siloxane into Bis P and 6F based systems, however, more substantially depressed the upper glass transition than for the BTDA-m-DDS system. The siloxane component was more compatible with both the 6F and Bis P monomers, as judged by solubility in common solvents. Thus, enhanced misciblity of the siloxane component with the Bis P and 6F based imide component yielded this depression. More phase mixing occurred in this case and substantially decreased the glass transition than if better microphase separation had been obtained. Increasing the siloxane oligomer molecular weight caused the glass transition to increase, due to the thermodynamically favored formation of more homogeneous phases of the imide matrix and siloxane domains. Thus, for a polyimide based on BTDA and Bis P, almost identical upper glass transitions were obtained when either 10 percent siloxane of 800 g/mole molecular weight or 20 percent siloxane of 2,500 g/mole molecular weight was incorporated.

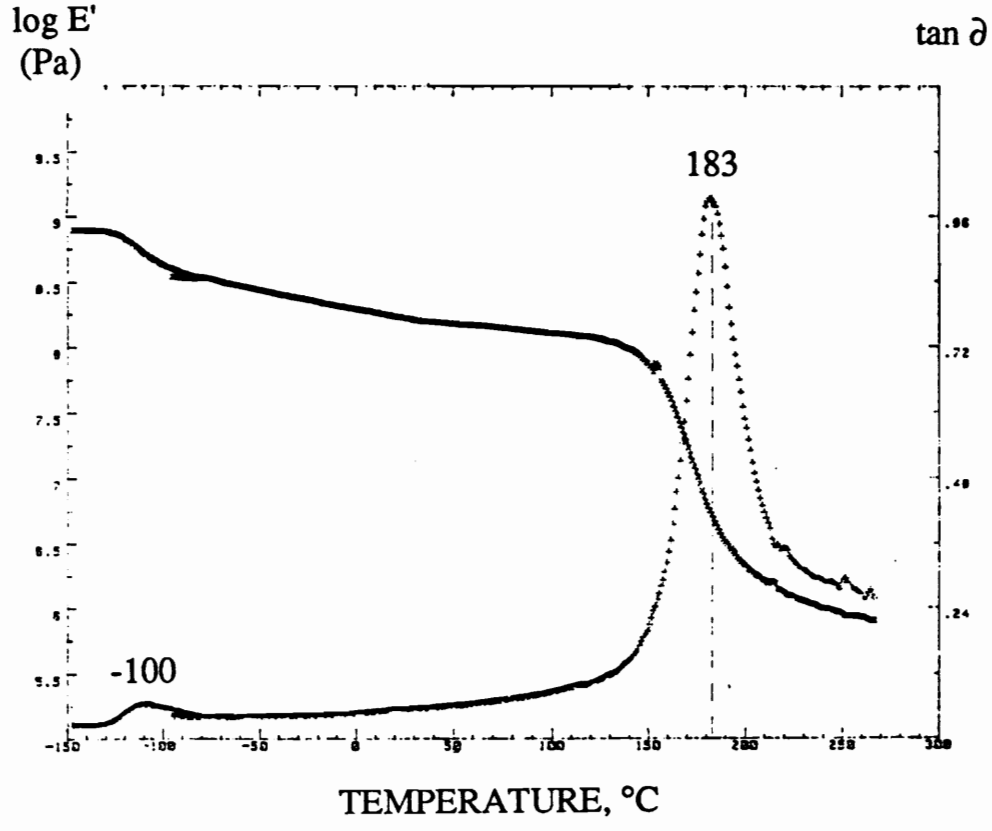

Figure 21: Dynamic mechanical thermal analysis of microphase separated BTDA-m-DDS-40 PSX 950 poly(siloxane imide) segmented copolymer, indicating imide (183°C) and siloxane (-106°C) phase transitions

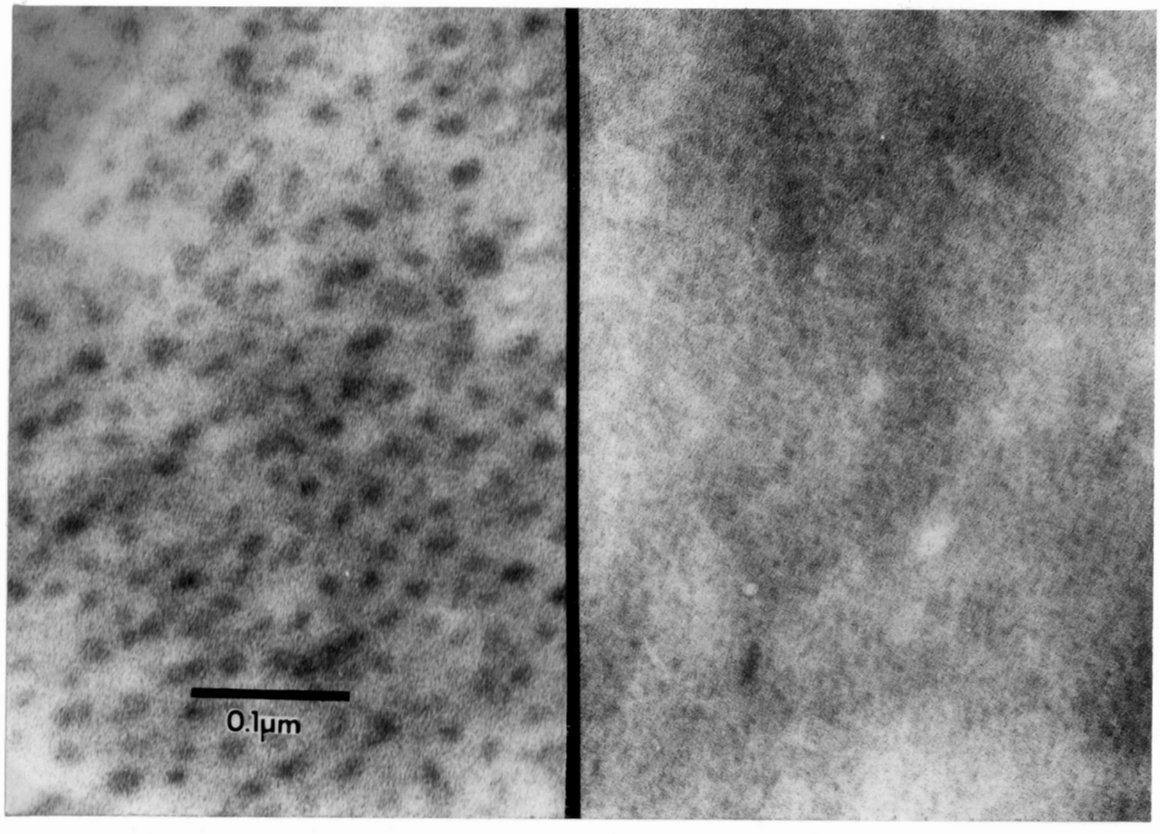

Figure 22: Transmission electron micrographs of BTDA-m-DDS-10 PSX poly(siloxane imide) segmented copolymers with siloxane segment molecular weights of 2,000 (right) and 10,000 (left) g/mole (304)

Incorporation of the more flexible, ether containing diamines 4F and PO caused the glass transition values to decrease to approximately 220°C. Hergenrother, however, reports a glass transition of 258°C for a polyimide based upon BTDA and PO, where the PO is based on POF and the more symmetric *para*-aminophenol, rather than *meta*-aminophenol (58). As expected, incorporating more rigid monomers, such as m-DDS, increased the glass transition of the 6F-PO polyimide. Furthermore, a large enhancement of the glass transition, on the order of 50 to 60°C, was obtained by substituting the more rigid p-DDS isomer for the "kinked" m-DDS. Poly(siloxane imide) segmented copolymers based on 4F, PO and p-DDS have not yet been synthesized.

4.4.2 Glass transitions of poly(aryl ether imide) segmented copolymers

Glass transition values for the BTDA-Bis P based poly(aryl ether imide) segmented copolymers, as determined by DSC or DMTA, are listed in Table 28. The polysulfone and polyether ketone oligomer molecular weights were 6050 and 6580 g/mole, respectively, with glass transitions of ~160°C. High molecular weight poly(aryl ether)s of these general structures exhibited glass transitions of ~190°C. Unlike the poly(siloxane imide) segmented copolymers, the poly(aryl ether imide) copolymers generally exhibited only one glass transition. As expected, the polyether ketone based copolymers showed lower values than those based on polysulfone. If the diamine polarity was increased by using either Bis A or m-DDS rather than Bis P, phase separation occurred and two glass transitions were easily detected, as depicted in the DSC scans of Figures 23 and 24, respectively. The DMTA scan in Figure 25 for the BTDA-Bis A-30 PSF 6050 copolymer indicates a shoulder at 215°C corresponding to the polysulfone phase, and a major transition at 265°C corresponding to the imide phase.

Table 28: Glass transitions of BTDA-Bis P-PA (25,000) based poly(aryl ether imide) segmented copolymers; parentheses (-) indicate glass transition from DMTA, all others by DSC

Weight % PAE <Mn>	Tg, °C
BTDA-Bis P Homopolyimide	265
10 PSF 6050	250 (260)
30 PSF 6050	240 (245)
50 PSF 6050	229 (228)
95 PSF 6050	191
10 PEK 6580	239
30 PEK 6580	216
50 PEK 6580	195
BTDA-Bis A based 30 PSF 6050	205 / (215) / 265 (265)
BTDA-m-DDS based 30 PSF 6050	180 / 245

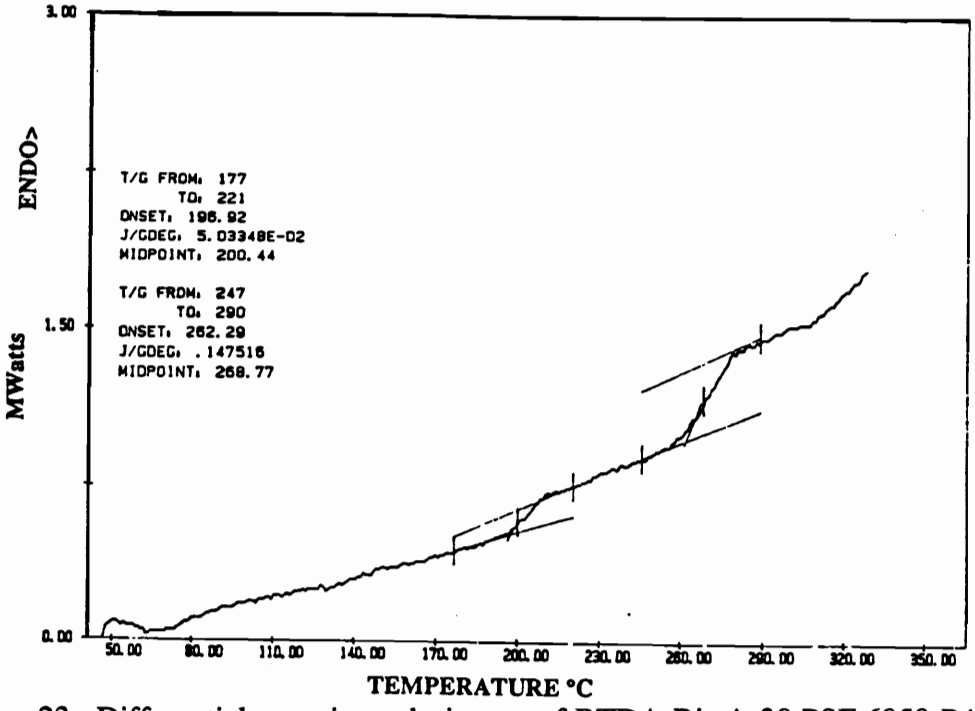

Figure 23: Differential scanning calorimetry of BTDA-Bis A-30 PSF 6050-PA (25,000) indicating two phase morphology

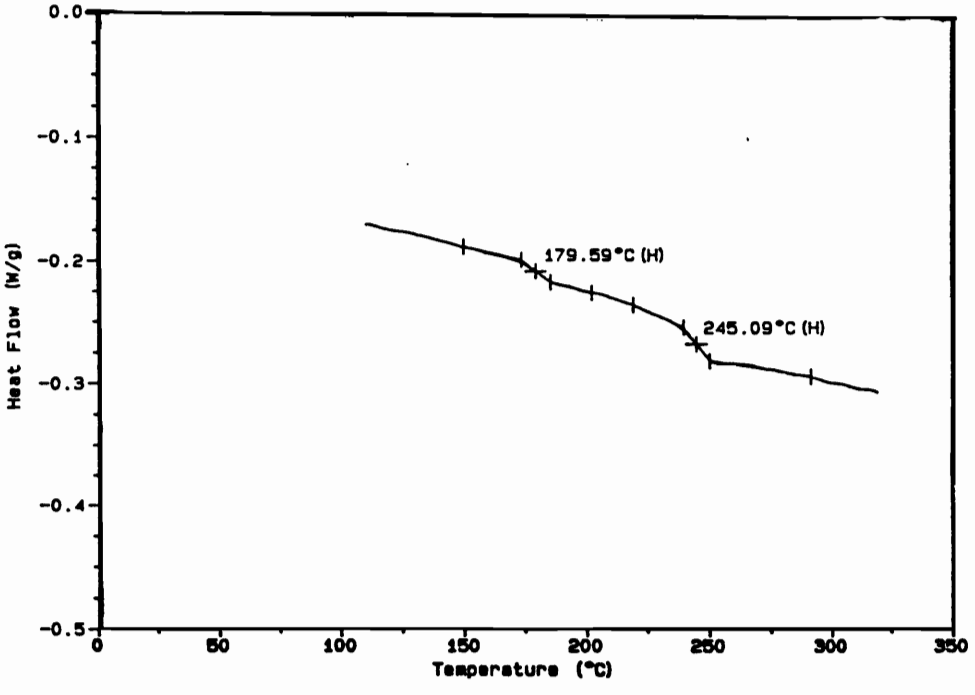

Figure 24: Differential scanning calorimetry of BTDA-m-DDS-30 PSF 6050-PA (25,000), indicating two phase morphology

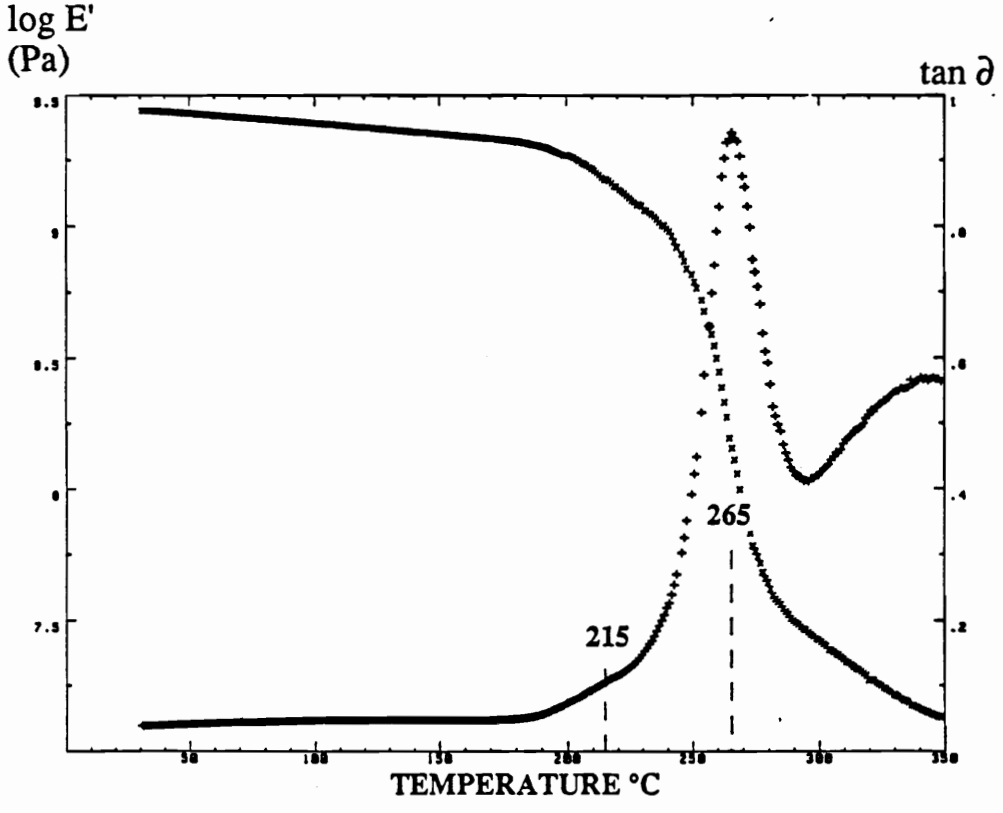

Figure 25: Dynamic mechanical thermal analysis of BTDA-Bis A-30 PSF 6050-PA (25,000) indicating two phase morphology; imide phase transition at 265°C and poly(aryl ether sulfone) phase transition at 215°C

4.4.3 Initial investigation of the thermal properties of crosslinked addition imides

Initial differential scanning calorimetry of the 6F-Bis A-MA addition imide series indicated that the glass transition values of the 5,000 and 10,000 g/mole samples increased slightly to ~300°C after being subjected to a thermally induced crosslinking step. Initial DMTA scans supported this value, however, the curing of these systems must be optimized before the ultimate properties may be determined.

4.4.4 Dynamic thermogravimetric analysis of homopolyimides, poly(siloxane imide), and poly(aryl ether imide) segmented copolymers

Dynamic thermal stability in an air environment was assessed by thermogravimetric analysis (TGA). All of the homopolymers exhibited excellent high temperature stability without incurring weight loss until at least 400°C, as depicted in Figure 26. The presence of the PO diamine in the polyimide backbone induced an interesting two-tiered TGA scan, which may be related to the well known anti-flame and anti-smoke properties of phosphorous containing polymers and additives (Figure 27, 305-309). Poly(siloxane imide) segmented copolymers' thermal stabilities were found to vary with the amount of the siloxane oligomer (Figure 28), as well as the siloxane oligomer molecular weight. This result was determined for a series of poly(siloxane imide) segmented copolymers based on BTDA and m-DDS. Poly(siloxane imide) segmented copolymers maintained good thermal stability, even at siloxane contents as high as 60 weight percent, however, degradation occurred at lower temperatures as the siloxane content was increased. The char yield was proportional to the siloxane content, suggesting that the silicate-type structure was the principal degradation product in an air atmosphere. As with phosphorous containing polyimides, this observation implies that siloxane containing polyimides are flame and smoke resistant. The slight but significant variation of initial weight loss temperature with

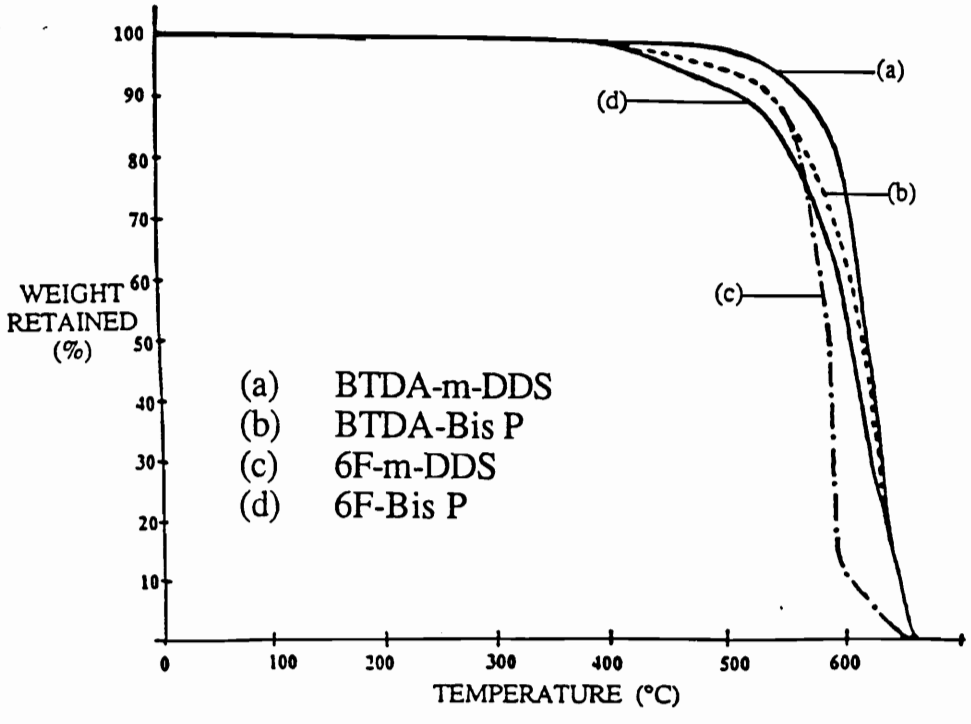

Figure 26: Thermogravimetric analysis in an air atmosphere of polyimide homopolymers

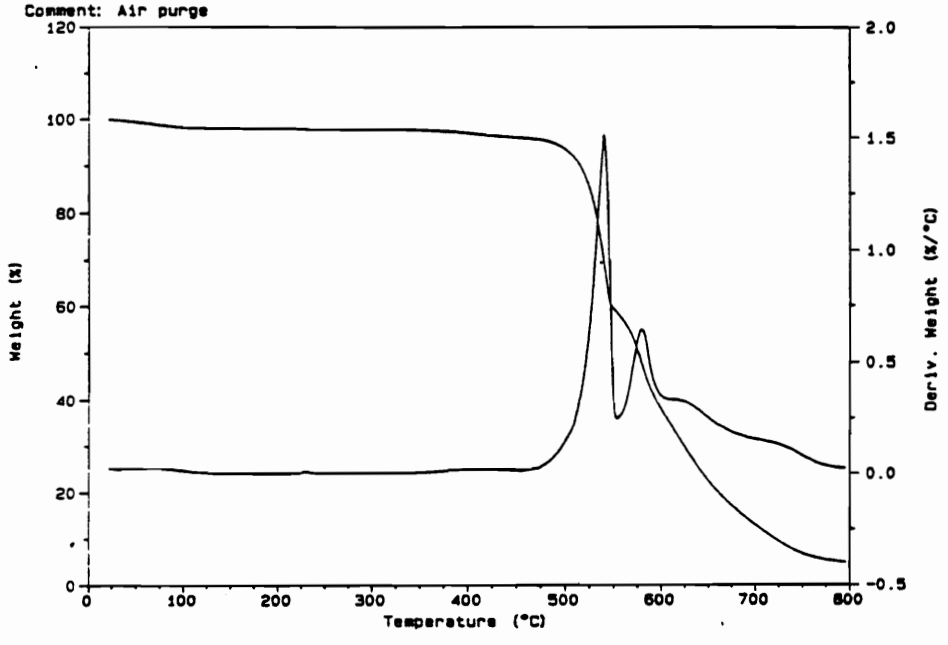

Figure 27: Thermogravimetric analysis in an air atmosphere of phosphorous containing BTDA-PO bulk imidized homopolyimide, indicating two-tiered degradation mechanism

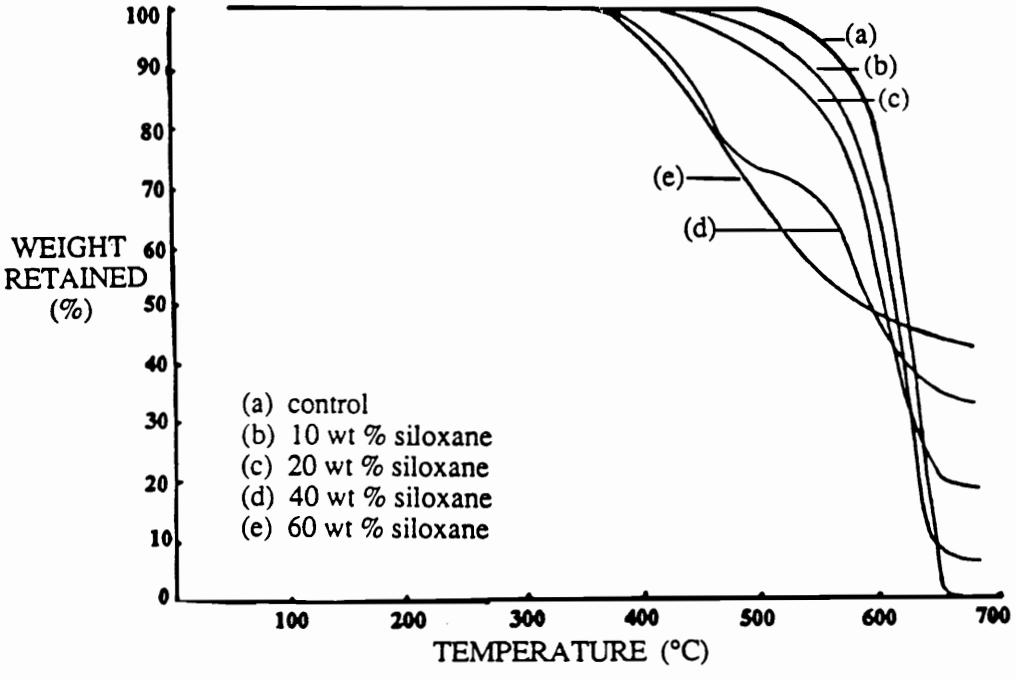

Figure 28: Thermogravimetric analysis in an air atmosphere of poly(siloxane imide) segmented copolymers, indicating char yield proportional to siloxane content; siloxane molecular weight was ~1000 g/mole

siloxane molecular weight was attributed to the preferential degradation of the aliphatic n-propyl linkages in the copolymer backbone. As the siloxane molecular weight was increased and the concentration of aliphatic linkages decreased, overall thermal stability was improved.

The thermal stability of poly(sulfone imide) segmented copolymers with a polysulfone molecular weight of 6050 g/mole is depicted in Figure 29. Initial weight loss occurred at approximately the same temperature (~400°C) for all of the copolymer compositions. No trend existed for correlating copolymer composition to the initial rate of weight loss, and surprisingly, the copolymers with the higher polysulfone contents showed slightly better high temperature thermal stability. The effect of the molecular weight of the polysulfone oligomer was not specifically explored.

4.5.0 Mechanical Properties

4.5.1 Initial stress-strain analysis of poly(siloxane imide) segmented copolymers

The mechanical properties of a series of bulk imidized BTDA-m-DDS based poly(siloxane imide) segmented copolymers were found to be a function of the amount of incorporated siloxane, as depicted in Figure 30. Thus, copolymers with high concentrations of siloxane (>50 weight %), where the siloxane was dominant in the continuous phase, behaved as thermoplastic elastomers. Copolymers containing low siloxane concentrations, on the other hand, behaved essentially as modified polyimides with siloxane domains interspersed throughout a continuous imide-dominant matrix. Variation of the siloxane segment molecular weight and the imide composition would modify the copolymer morphology and influence the stress-strain behavior as well, although this was not experimentally determined.

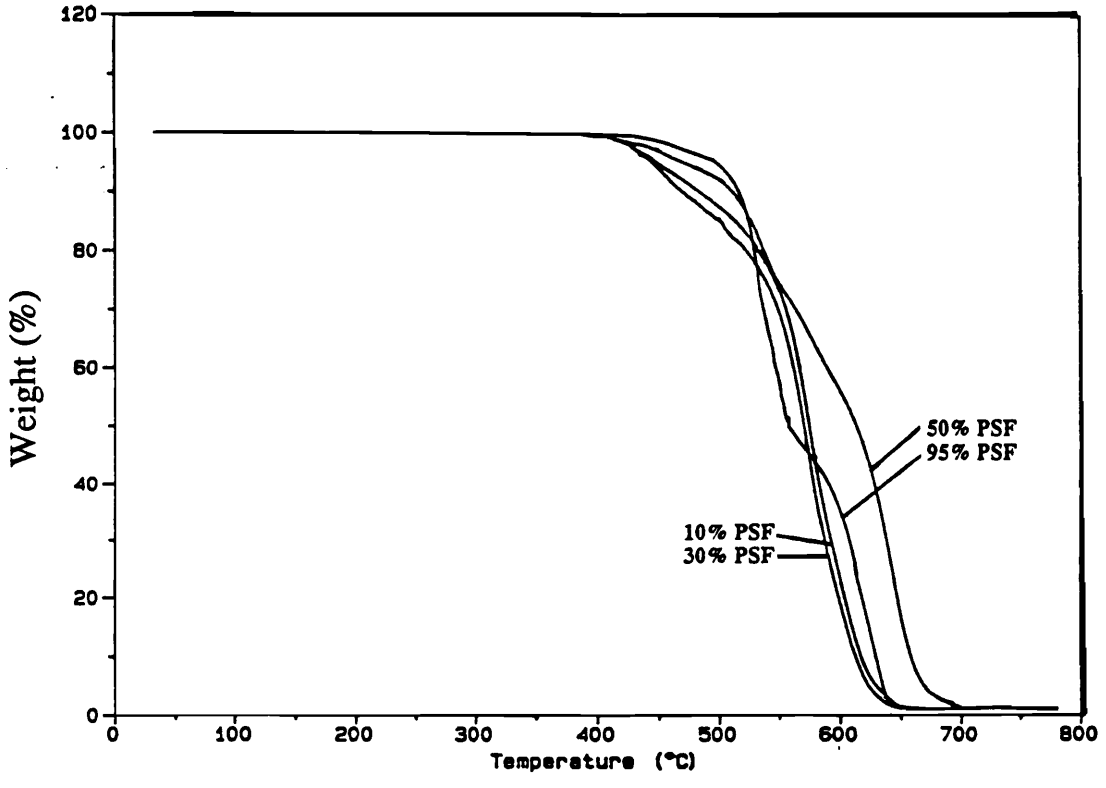

Figure 29: Thermogravimetric analysis of poly(sulfone imide) segmented copolymers as a function of polysulfone content; polysulfone segment <Mn> was 6050 g/mole

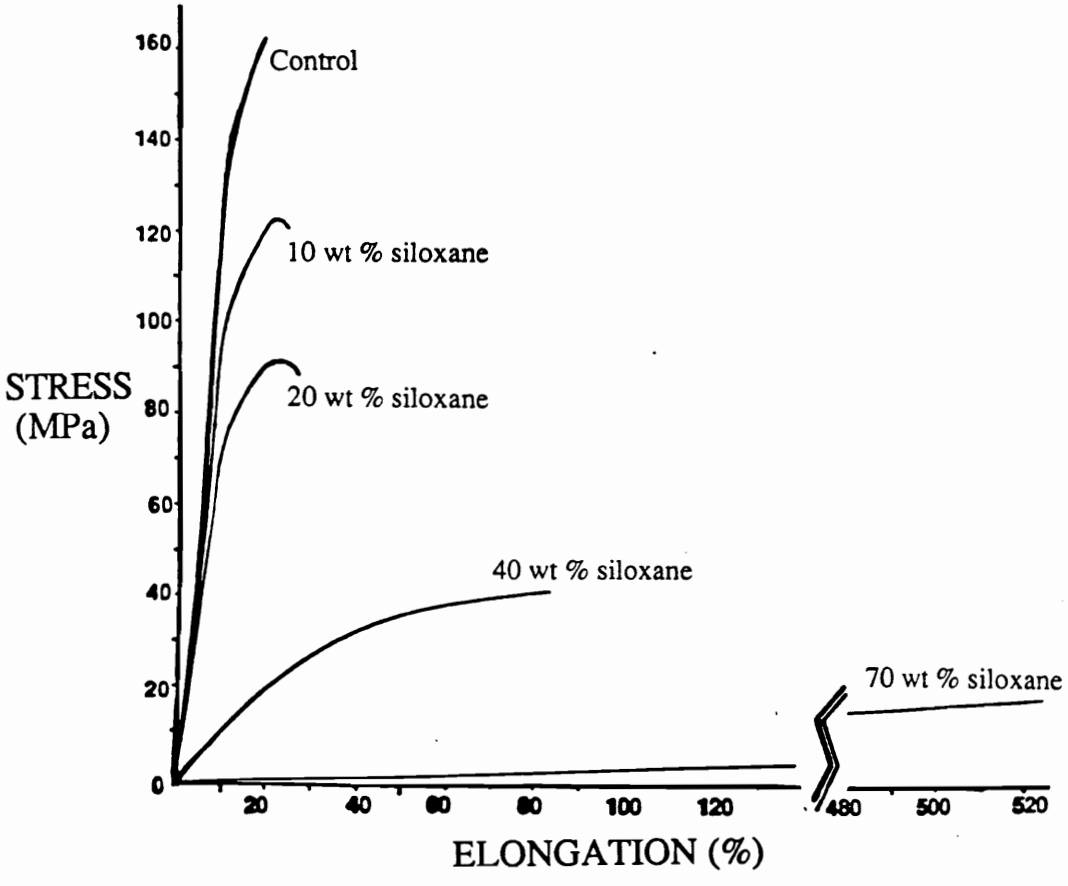

Figure 30: Initial stress-strain response of poly(siloxane imide) segmented copolymers based on BTDA and m-DDS, as a function of siloxane concentration; siloxane <Mn> was ~1000 g/mole

4.5.2 Initial stress-strain analysis of homopolyimides

Stress-strain analysis was also performed for a few bulk imidized homopolyimides, summarized below and in Figure 31. Although all of the homopolyimides had approximately the same moduli (480 - 550 MPa), the BPDA-Bis P exhibited a nearly linear stress-strain response compared with the more ductile behavior of the other systems. Thus, the BTDA-Bis P, BTDA-Bis A, and 6F-4F homopolyimides began to yield noticeably before failure, particularly the Bis P based system.

POLYIMIDE	STRESS (MPa) Yield	Break	STRAIN @ Break (%)
BPDA-Bis P	110	110	33
6F-4F	124	121	33
BTDA-Bis A	146	146	45
BTDA-Bis P	141	124	65

4.6.0 Surface analysis

Since the surface composition of these macromolecular materials is directly related to such properties as coefficient of friction and stability in aggressive environments, X-ray photoelectron spectroscopy (XPS or ESCA) was utilized to characterize the surface composition of the siloxane modified polyimide copolymers. By varying the angle of the sample relative to the analyzer, different depths of the polymer were sampled, such that a 15° grazing take-off angle characterized molecules from the uppermost surface (~10 to 20 Å) more so than molecules from the bulk. The 90° take-off angle, on the other hand, provided compositional information more characteristic of the subsurface regions (~ 50 to 70 Å).

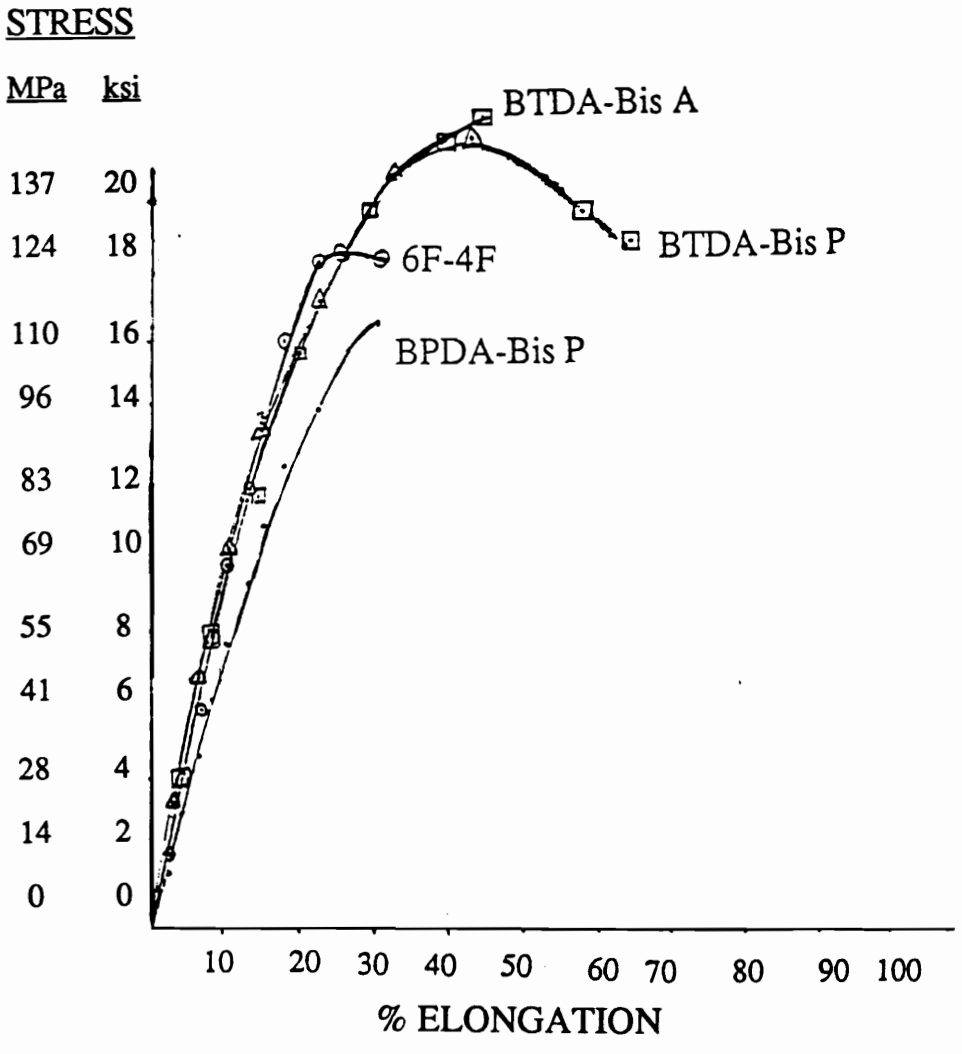

Figure 31: Initial stress-strain response of bulk imidized homopolyimides

4.6.1 Surface analysis of poly(siloxane imide) segmented copolymers

A wide scan spectrum of a BTDA-m-DDS-40 PSX 950 poly(siloxane imide) segmented copolymer is depicted in Figure 32. The results of the XPS experiment, tabulated in Table 29, conclusively demonstrate that the siloxane component dominated the surface of the copolymer. Furthermore, the extent of domination was independent of the weight percent of the siloxane incorporated into the copolymer. Thus, one is able to achieve a surface characteristic of the siloxane component while tailoring the physical properties to be characteristic of the bulk. The surface domination effect of the siloxane component is due to its relatively low surface energy. Thus, it is thermodynamically favored to migrate to the air or vacuum interface, to lower the overall surface energy of the system.

4.6.2 Surface analysis of poly(siloxane imide) segmented copolymers after exposure to atomic oxygen

The transformation of the siloxane surface to an inorganic silicate structure in aggressive oxygen environments may be documented by XPS. After exposure to atomic oxygen, the atomic abundance of oxygen increased, as depicted in the wide scan spectra of Figures 32 and 33 for the BTDA-m-DDS-40 PSX 950 poly(siloxane imide) segmented copolymer before and after exposure to atomic oxygen, respectively. (The experimental conditions were presented in section 3.12.15; section 4.7.2 details further experimental results.) The shift of the binding energy of the silicon 2p peak from 104.6 eV, corresponding to the siloxane, to 105.5 eV or greater, corresponding to a silicate structure, is further evidence of this conversion. Curve fitting and deconvolution of the silicon 2p peak are presented in Figure 34. This figure indicates that after exposure to atomic oxygen, the major component of the surface composition was a silicate structure. The accuracy of the curve fitting and deconvolution was verified in part by the fact that the full width at half height (FWHH) was

Table 29: X-ray photoelectron spectroscopy of poly(siloxane imide) segmented copolymers based on BTDA and m-DDS

Wt % PSX	PSX <Mn>	Take-off Angle, °	Wt % PSX at Surface
5	950	15	85
5	950	90	34
10	950	15	77
10	950	90	35
10	10,000	15	87
10	10,000	90	39
20	950	15	87
20	950	90	53
40	950	15	86
40	950	90	63

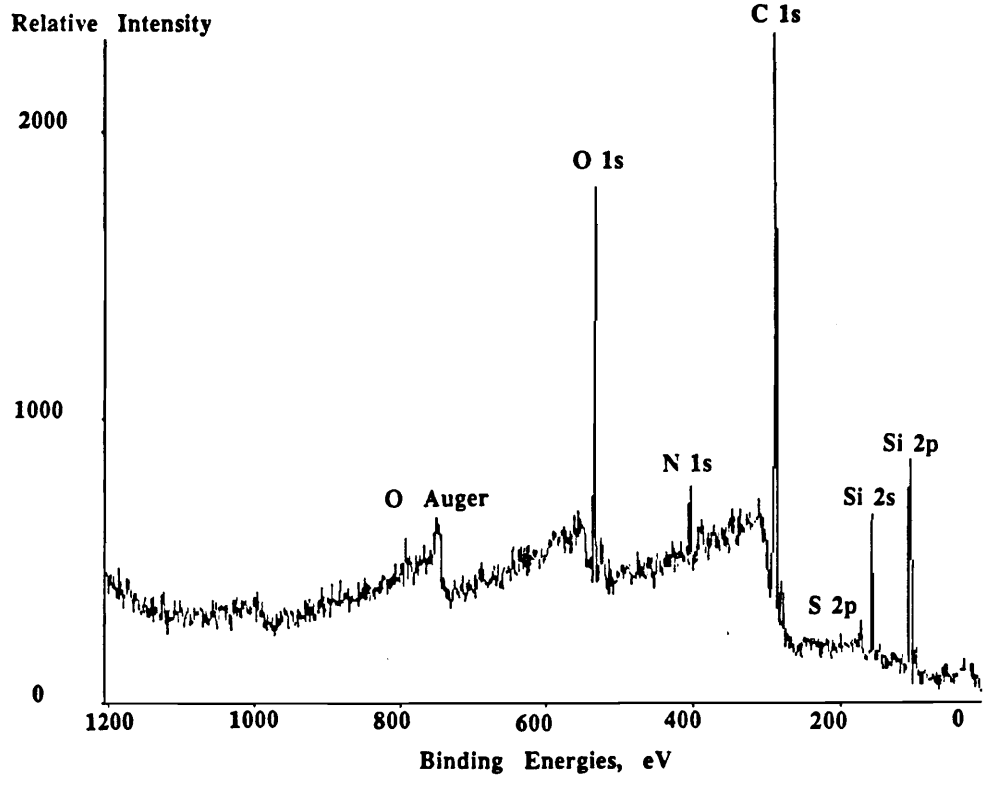

Figure 32: Wide scan spectra of BTDA-m-DDS-40 PSX 950 poly(siloxane imide) segmented copolymer before exposure to atomic oxygen (90° take-off angle)

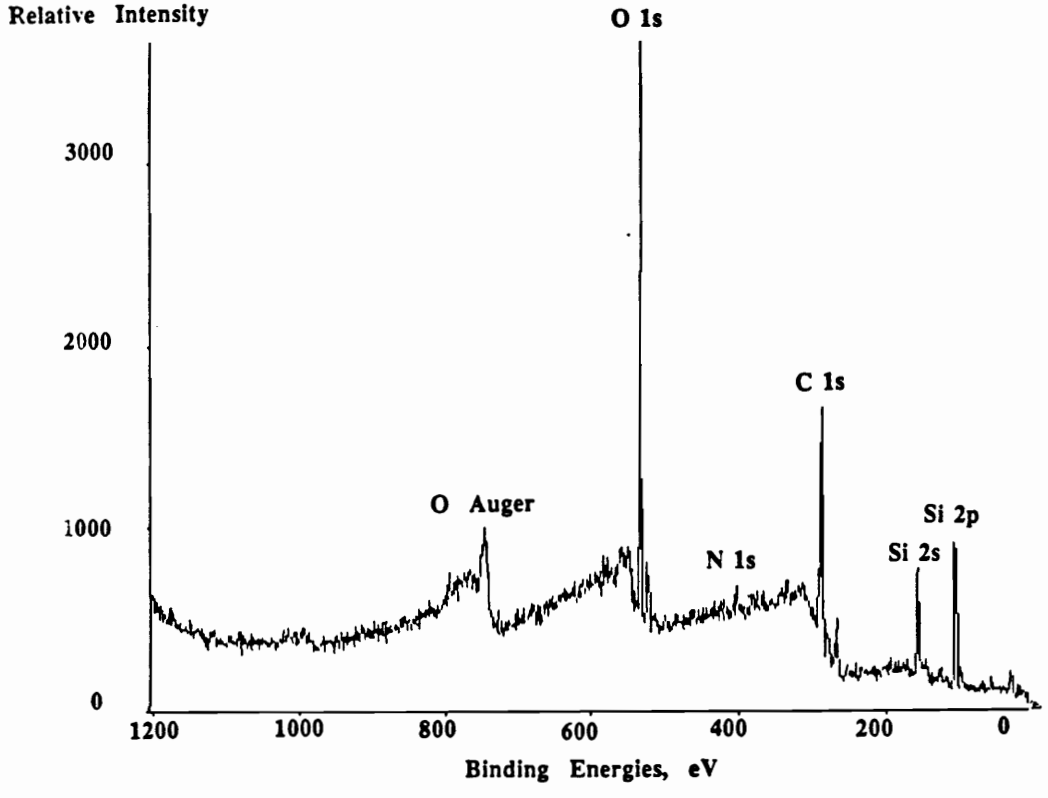

Figure 33: Wide scan spectra of BTDA-m-DDS-40 PSX 950 poly(siloxane imide) segmented copolymer after exposure to atomic oxygen (90° take-off angle) depicting increase in oxygen atomic abundance

PK	ENERGY	MAX	FWHH	AREA
1G	105.10	99.75	2.22	99.1

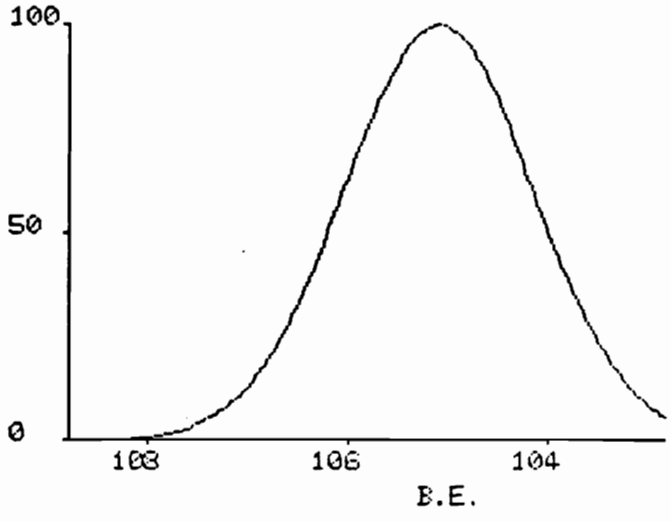

PK	ENERGY	MAX	FWHH	AREA
1G	106.10	74.00	2.22	59.0
2G	104.70	51.00	2.22	40.7

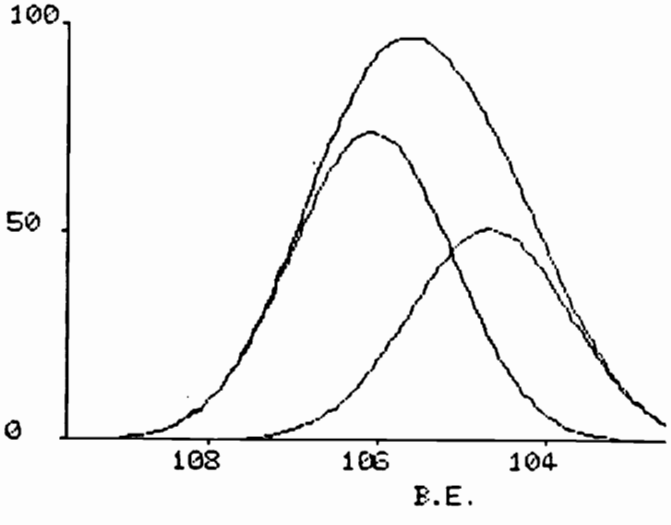

Figure 34: Curve fitting and deconvolution of silicon 2p peak of BTDA-m-DDS-40 PSX 950 poly(siloxane imide) segmented copolymer exposed to atomic oxygen, indicating presence of siloxane and silicate species (lower); upper spectra indicates silicon 2p peak before exposure to atomic oxygen

identical for the samples exposed and not exposed to the oxygen environment. Unfortunately, metallic (iron, aluminum) and fluorine contamination of the surfaces of other samples exposed to atomic oxygen prohibited accurate determination of their surface compositions. The source of the contamination was most probably from the atomic oxygen chamber, with the fluorine contamination originating from a Teflon reference standard. The surface analysis of all samples exposed to the atomic oxygen environment is detailed in the appendix.

4.7.0 Resistance to aggressive oxygen species

4.7.1 Oxygen plasma stability of homopolyimides and poly(siloxane imide) copolymers

As stated in the background information of Chapter 2, the conversion of polysiloxane to silicon dioxide in oxygen plasma has been documented within the literature as well as in our laboratories. In aggressive oxygen environments, the surface siloxane segments convert to a ceramic-like silicate (SiO_2) which provides a protective overlayer for the bulk material. This transformation is of critical interest to both the electronics and aerospace industries for the enhancement of oxygen plasma etch resistance and for the in situ formation of atomic oxygen resistant, protective coatings for organic space materials.

The oxygen plasma etch resistance was investigated for a series of poly(siloxane imide) segmented copolymers based on BTDA and m-DDS, as well as the oxydianiline (ODA) analogues. The copolymers had siloxane contents of 30 and 50 weight percent, with siloxane molecular weights of 1000 g/mole. Results of this so called "ashing" experiment are listed in Table 30. In every run, the BTDA-m-DDS-50 PSX 1000 sample lost no weight after exposure to this aggressive oxygen environment, and the ODA analogue performed similarly well. Interestingly, the ODA based systems were less resistant to

Table 30: Weight loss of BTDA-m-DDS and BTDA-p-ODA based poly(siloxane imide) segmented copolymers due to exposure to oxygen plasma

Polyimide System	Weight Loss (mg per sq. cm.)
Kapton	0.86
m-DDS-CONTROL	0.86
m-DDS-10 PSX 1000	0.75
m-DDS-20 PSX 1000	0.67
m-DDS-30 PSX 1000	0.24
m-DDS-50 PSX 1000	0
p-ODA-CONTROL	1.13
p-ODA-30 PSX 1000	0.30
p-ODA-50 PSX 1000	0.14
m-DDS-30 PSX 1000 coated on Kapton	0.35
m-DDS-50 PSX 1000 coated on Kapton	0.10

degradation than the m-DDS based copolymers. Additionally, the 30 weight percent siloxane copolymers lost more weight than the 50 weight percent siloxane copolymers, in both the m-DDS and ODA based systems. Consistently, Kapton lost more weight than either the m-DDS or ODA based copolymers. Coating Kapton with the m-DDS based copolymers enhanced the stability of the Kapton film to this environment, and the performance of the Kapton coated film resembled the performance of the siloxane modified polyimide which constituted the overcoat layer.

The scanning electron micrographs of the m-DDS based polyimide series presented on the following pages qualitatively depict the enhanced stability of the poly(siloxane imide) segmented copolymers to the oxygen plasma (Figures 35-37) . The micrographs were taken at magnifications of 1600 and 6400. Although not shown, all of the samples before exposure were relatively featureless, with smooth unmarred surfaces. The control exhibited severe microcracking and delamination (Figure 35), whereas the addition of 10 weight percent siloxane appeared to inhibit delamination (Figure 36), although some cracking still persisted. An even more significant improvement was obtained at the 20 weight percent level of siloxane incorporation, where delamination had not occurred and cracking was minimal (Figure 37).

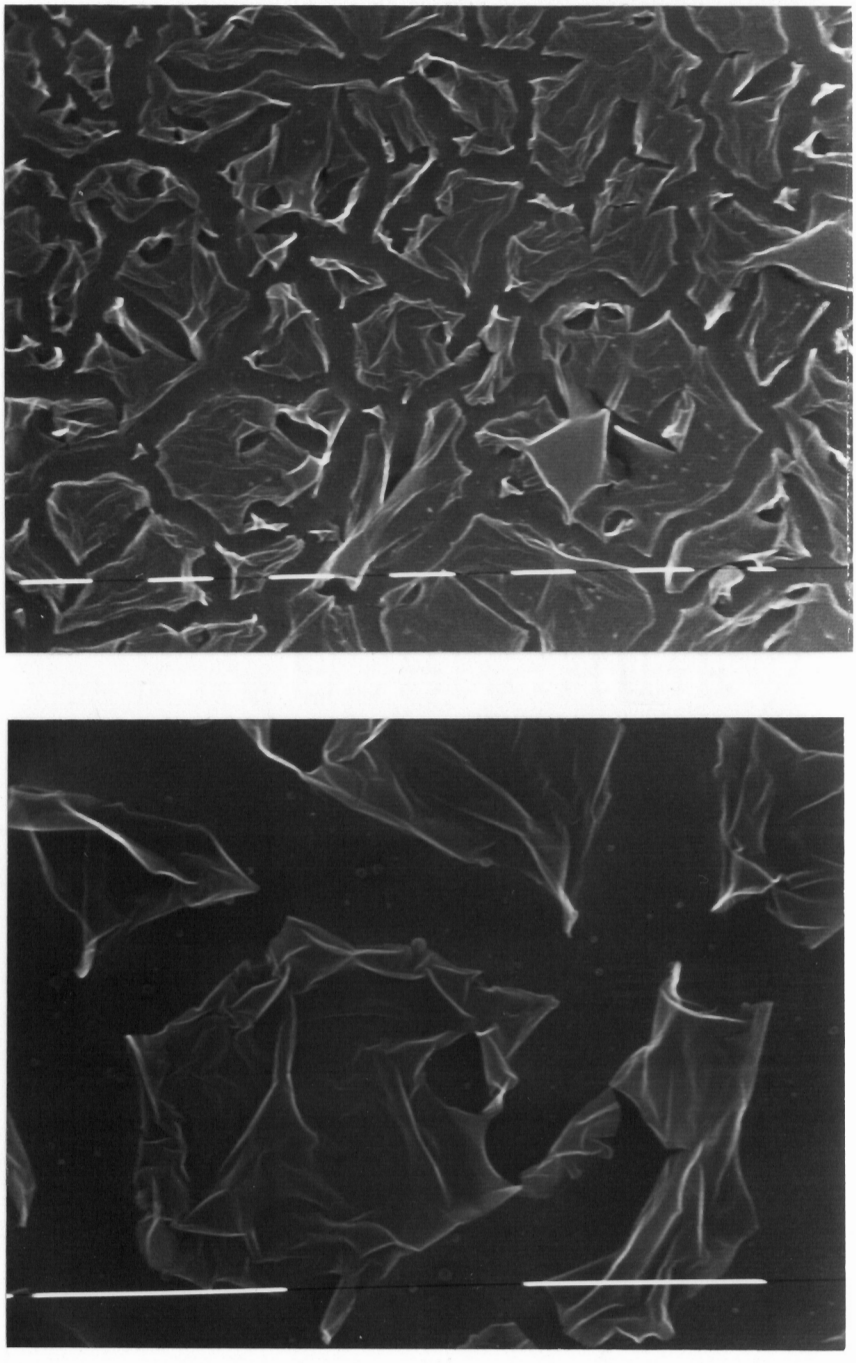

Figure 35: Scanning electron micrographs of BTDA-m-DDS homopolyimide after exposure to oxygen plasma at 1600 (upper) and 6400 (lower) magnifications

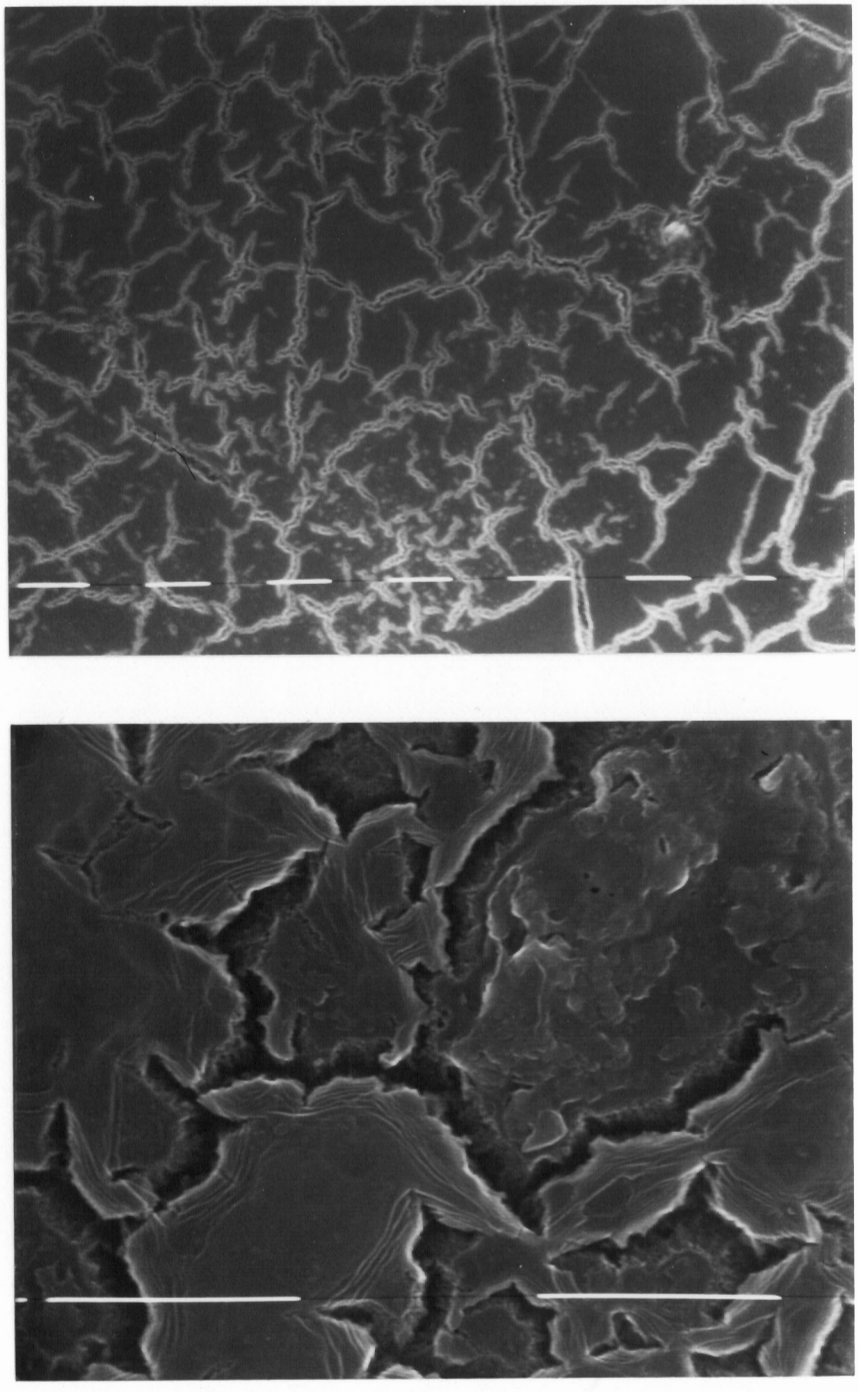

Figure 36: Scanning electron micrographs of BTDA-m-DDS-10 PSX 950 poly(siloxane imide) segmented copolymer after exposure to oxygen plasma at 1600 (upper) and 6400 (lower) magnifications

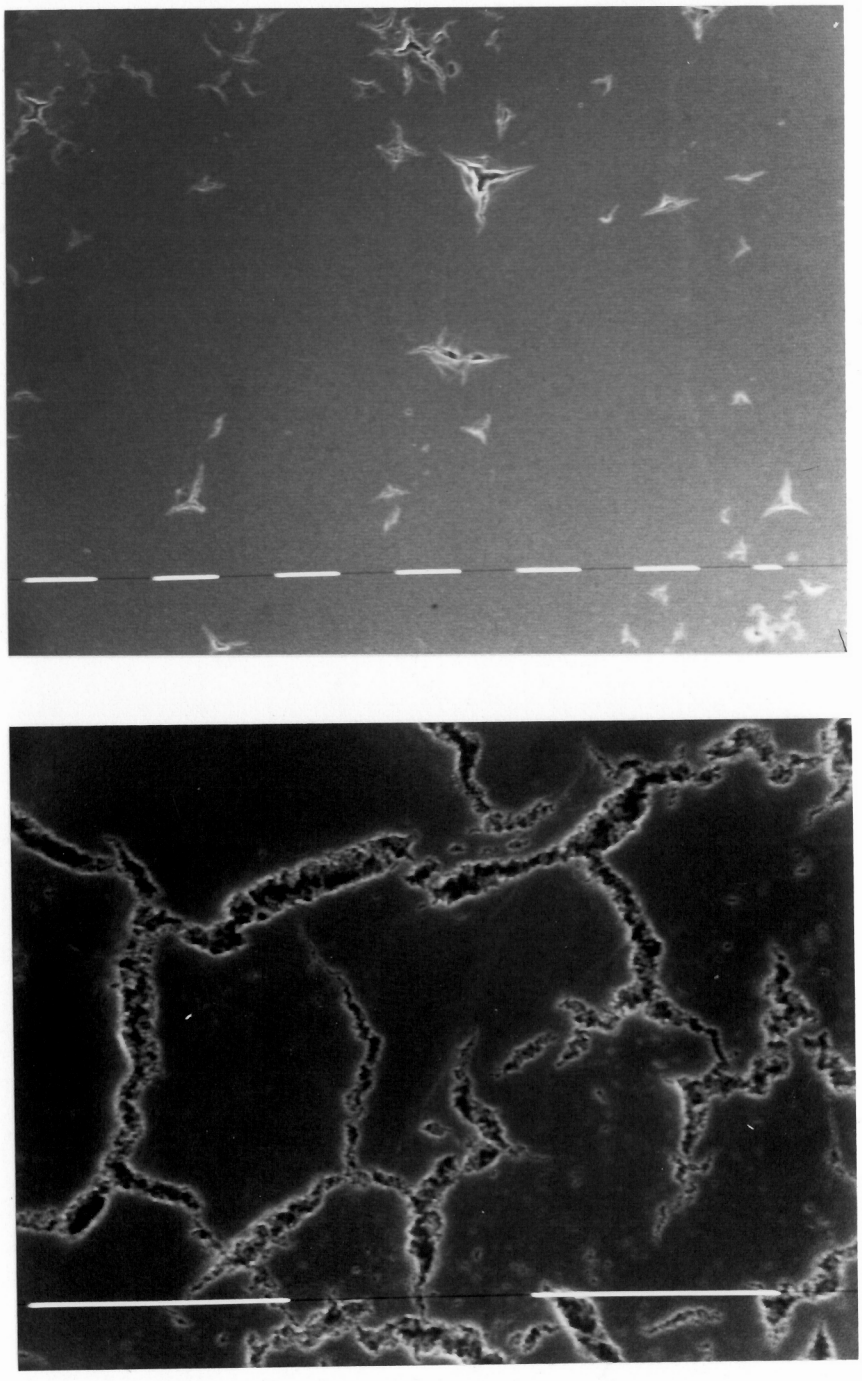

Figure 37: Scanning electron micrographs of BTDA-m-DDS-20 PSX 2000 poly(siloxane imide) segmented copolymer after exposure to oxygen plasma at 1600 (upper) and 6400 (lower) magnifications

4.7.2 Atomic oxygen stability of homopolyimides, poly(siloxane imide) copolymers, and blends with polybenzimidazole

In order to assess the feasibility of siloxane modified copolymers being used directly, as a component of, or as a coating for aerospace structures, a test environment more closely resembling that of the low earth orbit (LEO) was needed for materials evaluation. Typical "ashing" experiments may yield trends in materials stability in an oxygen plasma environment, however, they do not supply a *pure source of high energy atomic oxygen* at a *flux rate* similar to the LEO. Also, the *low pressure* of the LEO is not duplicated in the typical "ashing" experiment. Thus, exposure in the LEO is a more severe test of stability than just an "ashing" experiment, and mechanisms of materials failure in the two environments will differ.

The polymeric materials of interest for aerospace applications were miscible blends of polybenzimidazole (PBI) and the polyimide BTDA-m-DDS-40 PSX 950. The material properties (miscibility, glass transitions) are discussed in section 4.11. Eight different samples, homopolymers, copolymers and blends, were subjected to the equivalent of one week exposure to the LEO environment, and initially evaluated for weight loss and degradation of surface morphology. Additionally, all of the samples which were subjected to the atomic oxygen environment lost optical clarity. The siloxane containing samples, however, maintained a greater degree of optical clarity than samples which did not contain siloxane.

The weight loss data for these specimens are presented in Table 31. The absolute weight loss for a one square inch sample is quoted in grams and is, therefore, essentially normalized for exposed surface area. Consistently, homopolymers lost more weight than

Table 31: Weight loss incurred by homopolymers, poly(siloxane imide) segmented copolymers and blends with polybenzimidazole due to exposure to high energy, high flux atomic oxygen

Polymer System	Weight Loss x 10^4, gram
PBI	23.13
BTDA-m-DDS	14.01
BTDA-m-DDS-10 PSX 950 poly(siloxane imide) segmented copolymer	4.54
BTDA-m-DDS-40 PSX 950 poly(siloxane imide) segmented copolymer	+3.10 (gain)
Blend of BTDA-m-DDS-40 PSX 950 (75%) and PBI (25%); 30% overall PSX content	+2.95 (gain)
Blend of BTDA-m-DDS-40 PSX 950 (60%) and PBI (40%); 24% overall PSX content	+2.30 (gain)
Kapton	22.93
Kapton coated with ~1500 Å BTDA-m-DDS-40 PSX 950 poly(siloxane imide) segmented copolymer	5.96

siloxane containing systems. Although the minor weight *gains* for the siloxane systems may not be real, the trend was consistent in that systems with greater amounts of siloxane exhibited the greater weight gains. This result might be attributed to the proposed siloxane to silicate transformation. Even an angstrom level coating of the soluble, transparent poly(siloxane imide) copolymer (with 40 weight percent siloxane) onto Kapton remarkably enhanced the stability of Kapton to the aggressive oxygen environment. Scanning electron micrographs (SEMs) revealed that the coating was somewhat non-uniform, suggesting that even greater stability, comparable to that of the copolymer itself, may be obtained with improved coating techniques. The coating technique, therefore, offers a method of easily retrofitting existing spacecraft materials in order to avoid the surface erosion which is common to organic materials in the LEO environment.

The SEMs on the following pages depict the enhanced stability to the simulated LEO environment of the poly(siloxane imide) segmented copolymers, their blends with PBI, and a coating over Kapton. The SEMs at two magnifications of 1600 and 6600 are arranged in Figures 39 through 46. All of the samples before exposure resembled the micrographs of the BTDA-m-DDS-40 PSX 950 poly(siloxane imide) segmented copolymer in Figure 38, with an unmarred, relatively smooth surface. PBI experienced the most severe surface degradation and weight loss, comparable to Kapton, whereas the copolymers remained relatively stable. The blend systems qualitatively experienced surface degradation intermediate to their two components, but were significantly more stable than their wholly organic components alone. The surface active nature of the siloxane component ensured that the protective silicate structure dominated the surface, preventing further degradation of the bulk morphology.

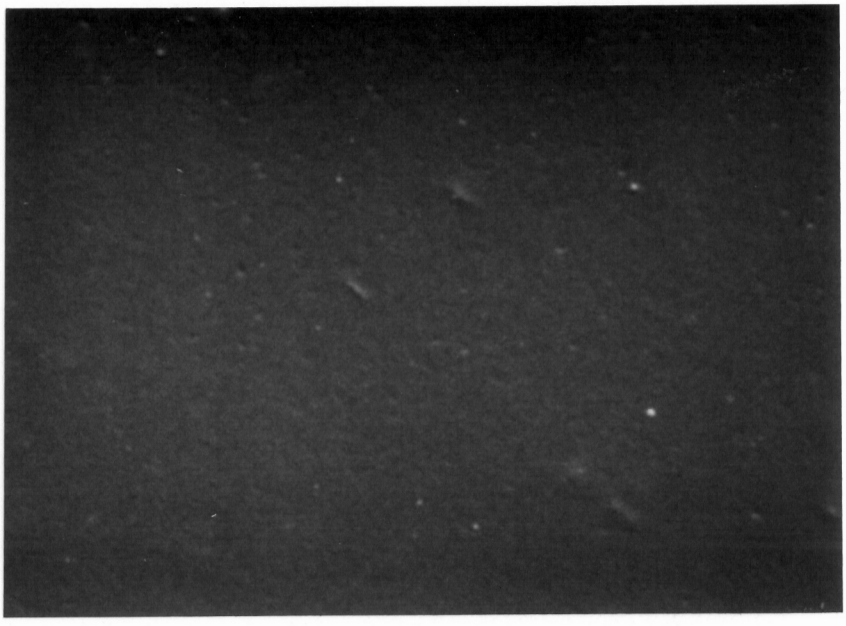

Figure 38: Scanning electron micrographs of BTDA-m-DDS-40 PSX 950 poly(siloxane imide) segmented copolymer *before* exposure to atomic oxygen at 6600 magnification

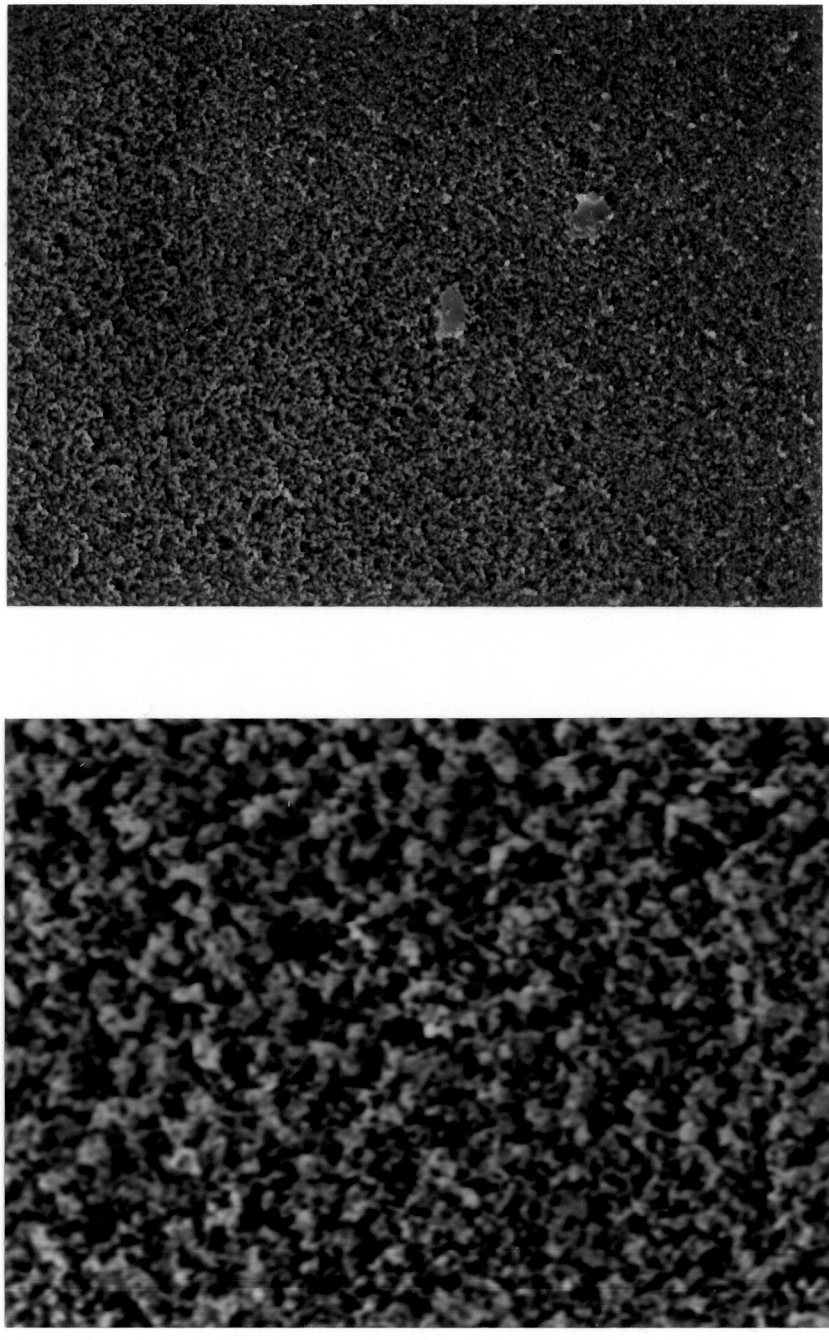

Figure 39: Scanning electron micrographs of polybenzimidazole after exposure to atomic oxygen at 1600 (upper) and 6600 (lower) magnifications

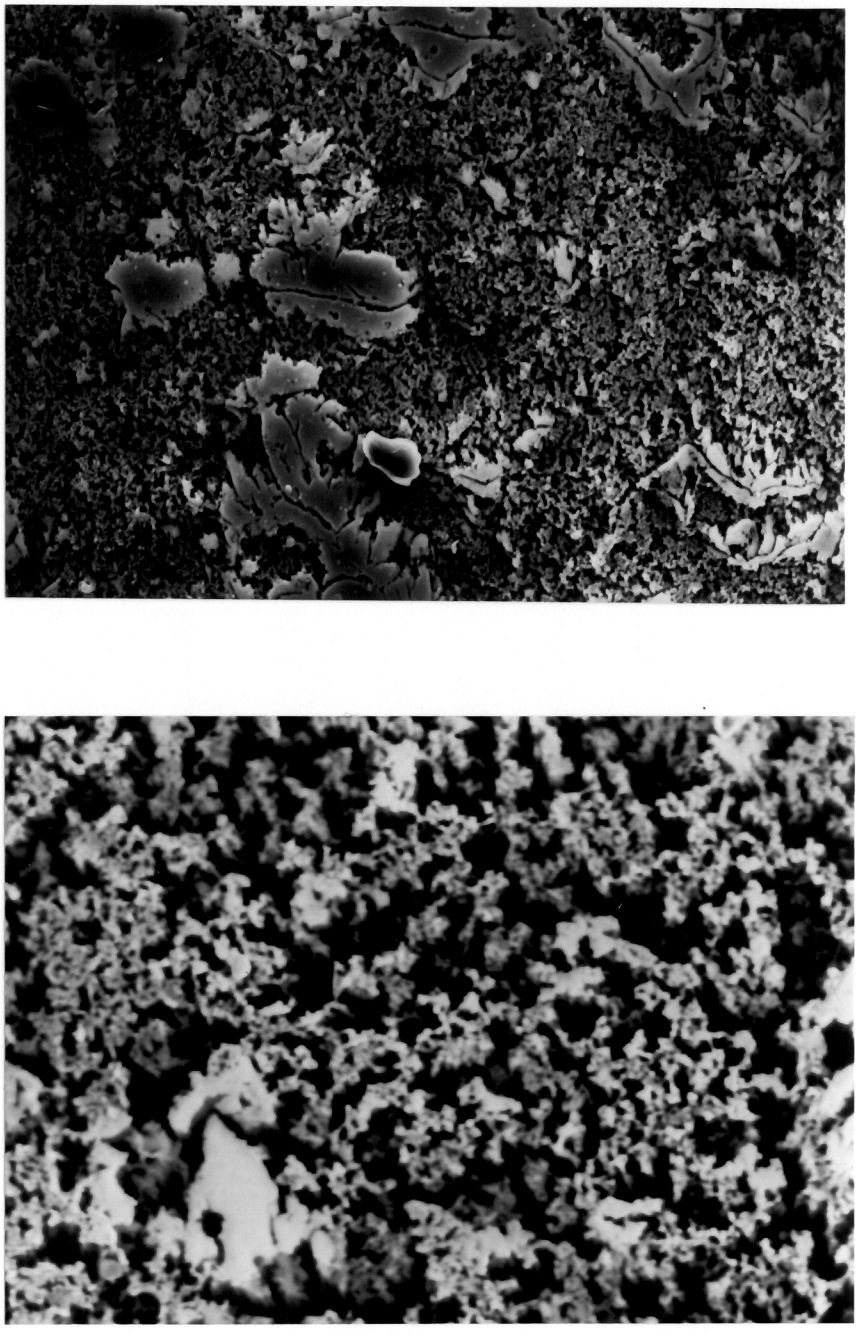

Figure 40: Scanning electron micrographs of Kapton after exposure to atomic oxygen at 1600 (upper) and 6600 (lower) magnifications

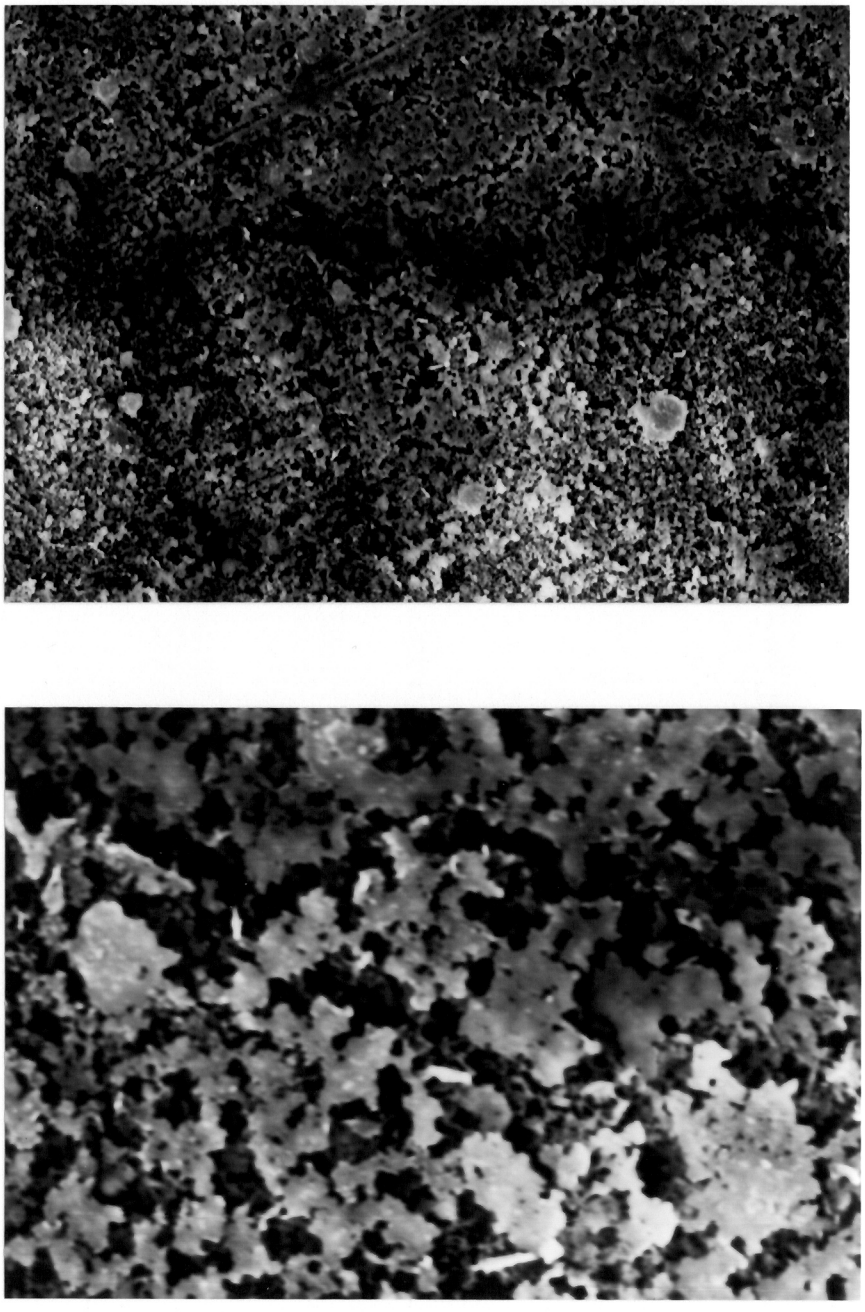

Figure 41: Scanning electron micrographs of BTDA-m-DDS polyimide homopolymer after exposure to atomic oxygen at 1600 (upper) and 6600 (lower) magnifications

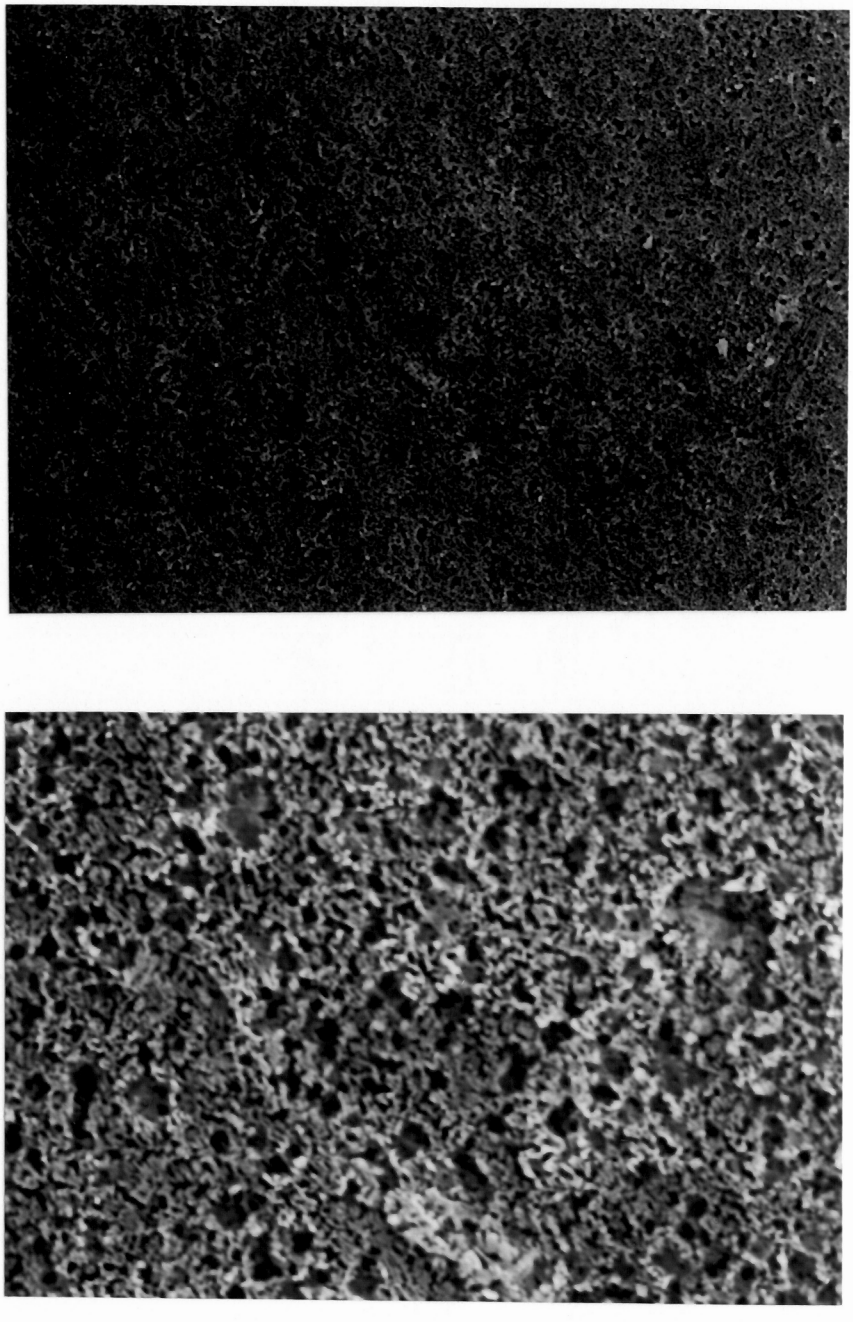

Figure 42: Scanning electron micrographs of BTDA-m-DDS-10 PSX 950 poly(siloxane imide) segmented copolymer after exposure to atomic oxygen at 1600 (upper) and 6600 (lower) magnifications

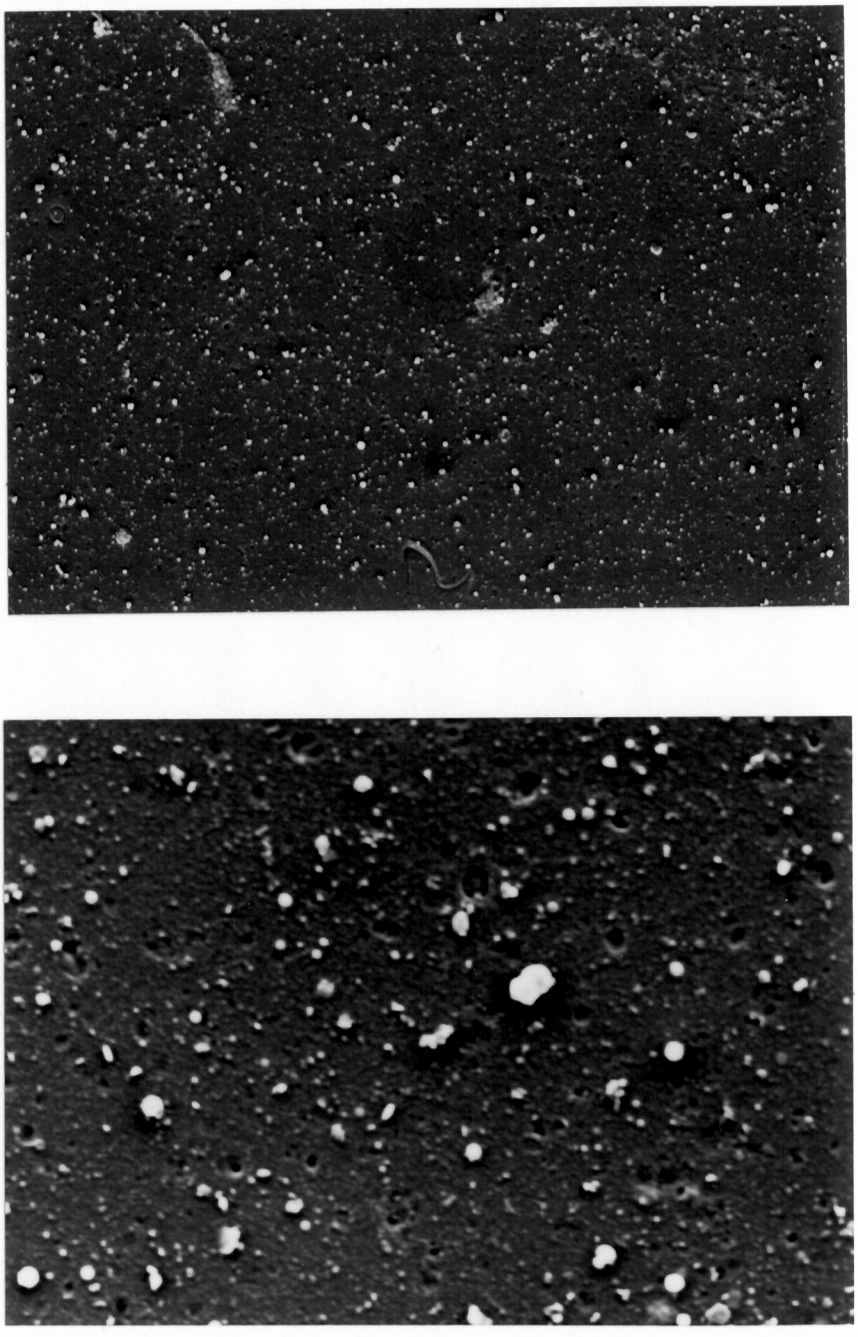

Figure 43: Scanning electron micrographs of BTDA-m-DDS-40 PSX 950 poly(siloxane imide) segmented copolymer after exposure to atomic oxygen at 1600 (upper) and 6600 (lower) magnifications

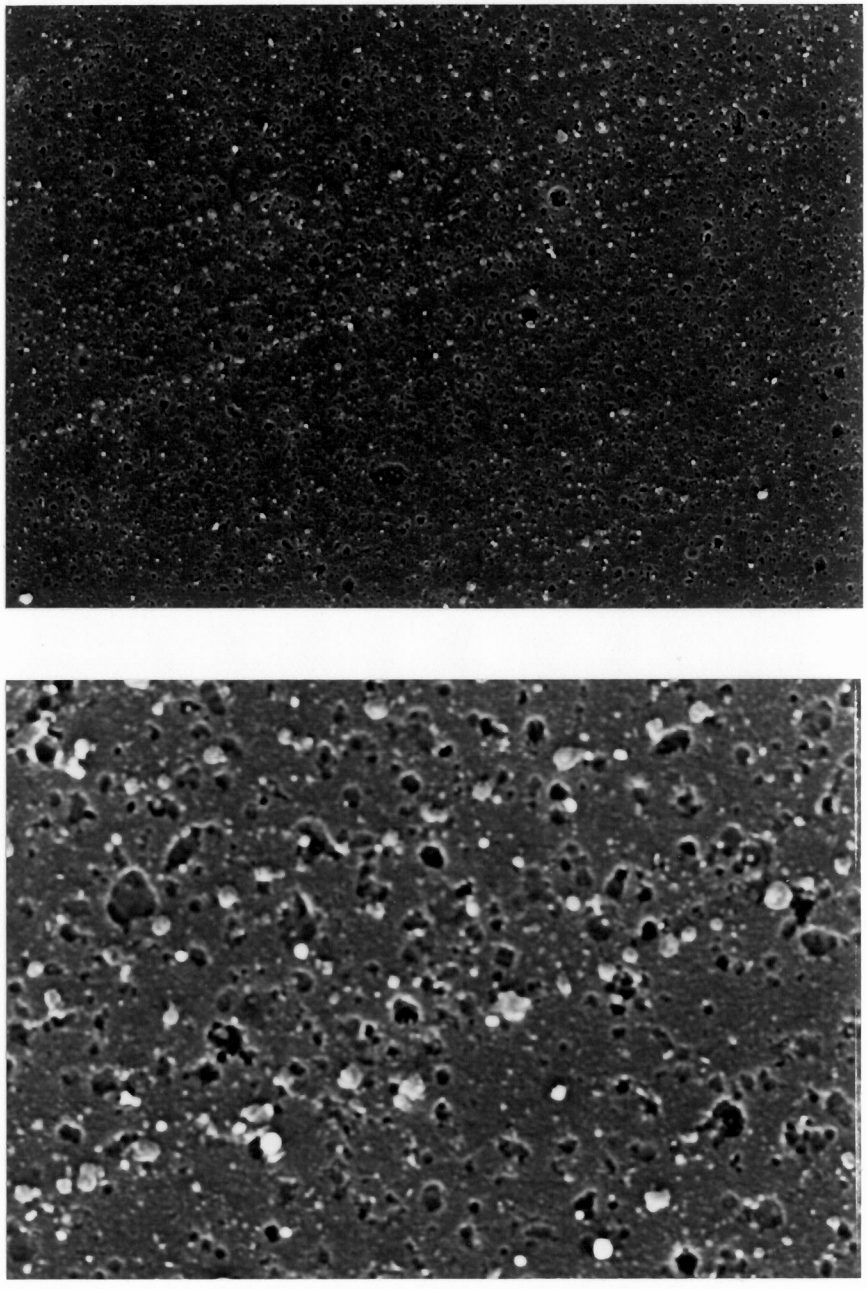

Figure 44: Scanning electron micrographs of a blend of polybenzimidazole (40 weight %) and BTDA-m-DDS-40 PSX 950 poly(siloxane imide) segmented copolymer (60 weight %); 24 percent overall PSX content; after exposure to atomic oxygen at 1600 (upper) and 6600 (lower) magnifications

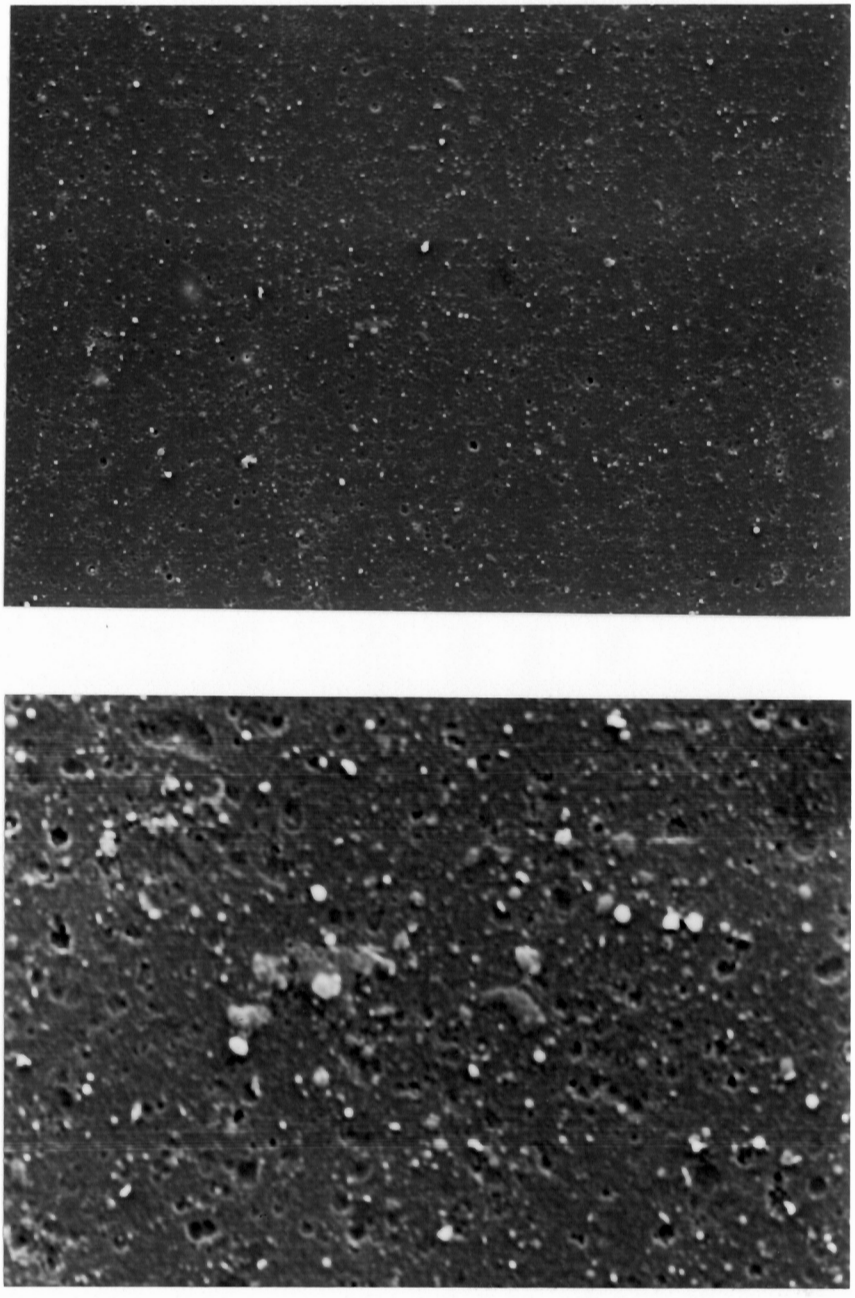

Figure 45: Scanning electron micrographs of a blend of polybenzimidazole (25 weight %) and BTDA-m-DDS-40 PSX 950 poly(siloxane imide) segmented copolymer (75 weight %); 30 percent overall PSX content; after exposure to atomic oxygen at 1600 (upper) and 6600 (lower) magnifications

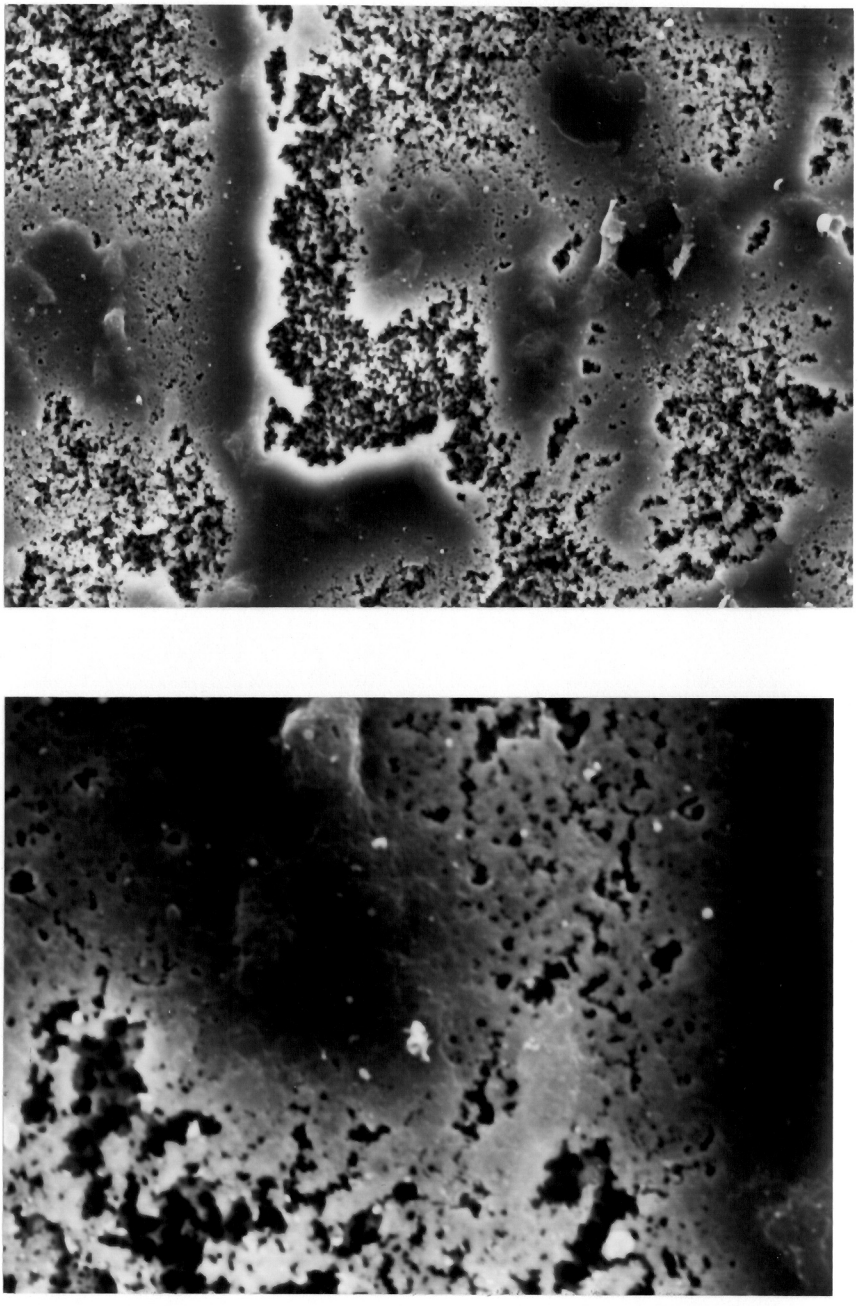

Figure 46: Scanning electron micrographs of Kapton coated with ~1500 Å BTDA-m-DDS-40 PSX 950 poly(siloxane imide) segmented copolymer after exposure to atomic oxygen at 1600 (upper) and 6600 (lower) magnifications

4.8.0 Dielectric Behavior

Another critical issue in this research was the possibility of controlling the dielectric behavior by molecular structure design of the homopolyimides and their siloxane modified counterparts. The dielectric behavior at 15 GHz for different homopolymer and copolymer systems is summarized in Table 32. The classic, commercially available Kapton (PMDA-ODA) system exhibited a dielectric constant of approximately 3.3 at 15 GHz. Introducing less polar diamines than ODA, such as Bis P, significantly decreased the dielectric constant to about 2.7. Bis P was found to decrease the dielectric constant for both BTDA and 6F based systems, as well, relative to the more commonly studied m-DDS diamine. Attempts to synthesize PMDA based soluble systems using the Bis P diamine were not successful, even when the 6F dianhydride comprised half of the dianhydride component on a molar basis. Thus, the PMDA-Bis P polyimide was only bulk imidized. The most dramatic reductions in the dielectric constant were obtained by utilizing the 6F dianhydride, where values approaching 2.5 were achieved. In some cases, incorporation of siloxane further reduced the dielectric constant. The dielectric behavior for these systems was relatively unchanged over the wide frequency range of 12.5 to 17.5 GHz, as indicated in Figure 47, although lower frequency behavior, i.e., 10 MHz, was not evaluated.

The dielectric behavior was also somewhat influenced by crosslinking, as demonstrated for the 6F-Bis A-MA crosslinked systems presented in Table 33. These samples were analyzed with different calibration and atmospheric conditions than for the results obtained in Table 32, therefore, Kapton was run as a reference. At 15 GHz under these conditions, Kapton displayed a slightly lower dielectric constant of 3.16. The 5,000 g/mole <Mc> sample displayed the lowest dielectric constant (2.52), and the 20,000 g/mole <Mc> sample, the highest (2.56). A 6F-Bis A high molecular weight, phthalic anhydride

Table 32: Dielectric constants at 15 GHz for a series of polyimide homopolymers and poly(siloxane imide) segmented copolymers; asterisk (*) indicates bulk imidized systems; all others were solution imidized

Polyimide System	Dielectric Constant at 15 GHz
PMDA-p-ODA* (Kapton™)	3.32
PMDA-p-ODA* (dry)	3.24
PMDA-Bis P*	2.70
PMDA (50) 6F (50)-Bis P	2.62
BTDA-m-DDS*	3.17
BTDA-m-DDS-10 PSX 800	3.09
BTDA-Bis A	3.10
BTDA-Bis P*	2.82
6F-m-DDS	2.87
6F-Bis P	2.62
6F-Bis P-10 PSX 800	2.61
6F-Bis P-10 PSX 800*	2.54
BTDA-4F	2.95
6F-4F	2.67
OPDA-Bis P	2.77

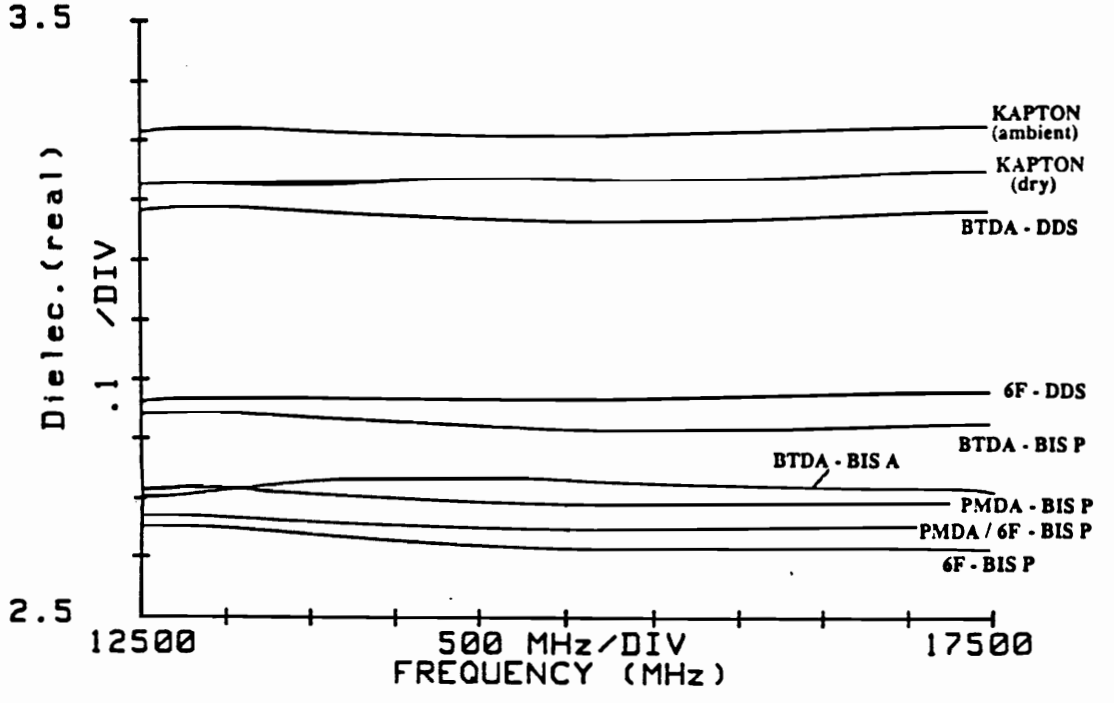

Figure 47: Dielectric constants as a function of frequency for polyimide homopolymers

Table 33: Dielectric constants of 6F-Bis A-MA addition imide oligomers which were thermally crosslinked

Imide Oligomer <Mn>	Dielectric Constant at 15 GHz
Kapton	3.16
40,000	2.58
20,000	2.56
15,000	2.56
10,000	2.55
5,000	2.52

terminated polyimide displayed a dielectric constant of 2.58. Although the variations were slight, the trend suggested that crosslinking may slightly reduce the dielectric constant.

4.9.0 Water sorption

4.9.1 Water sorption of homopolyimides

The trend of equilibrium water sorption as a function of polymer polarity was found to parallel that of the dielectric constant for a series of homopolyimides, presented in Figure 48. Thus, the most polar system with the highest dielectric constant, BTDA-m-DDS, was found to sorb the most water. As the polarity of the polyimide system decreased, water sorption decreased as well, with the 6F-4F polyimide having the lowest water sorption of the polyimides in this study.

Summers (14) had shown that incorporation of the less polar, hydrophobic polydimethylsiloxane oligomers into a polar BTDA-m-DDS backbone decreased the amount of water sorbed at equilibrium. Additionally, water sorption was found to be a function of the siloxane molecular weight, with copolymers comprised of the lower molecular weight oligomer sorbing slightly less water than if a higher segment molecular weight was used. This observation implied that the decrease in water sorption with siloxane incorporation was not only due to the siloxane surface functioning as a hydrophobic barrier, but was also due to limited diffusion throughout the partially miscible siloxane-imide matrix. An applied benefit of this result was realized in adhesive bonding studies in hot/wet environments. Durabilities of single lap shear joints were determined by Bott for a BTDA-m-DDS based copolyimide at 80°C in a 100 percent relative humidity environment (181-183). While the durability was enhanced three-fold by the incorporation of 10 weight percent siloxane, the room temperature ultimate strength (2900 psi) was

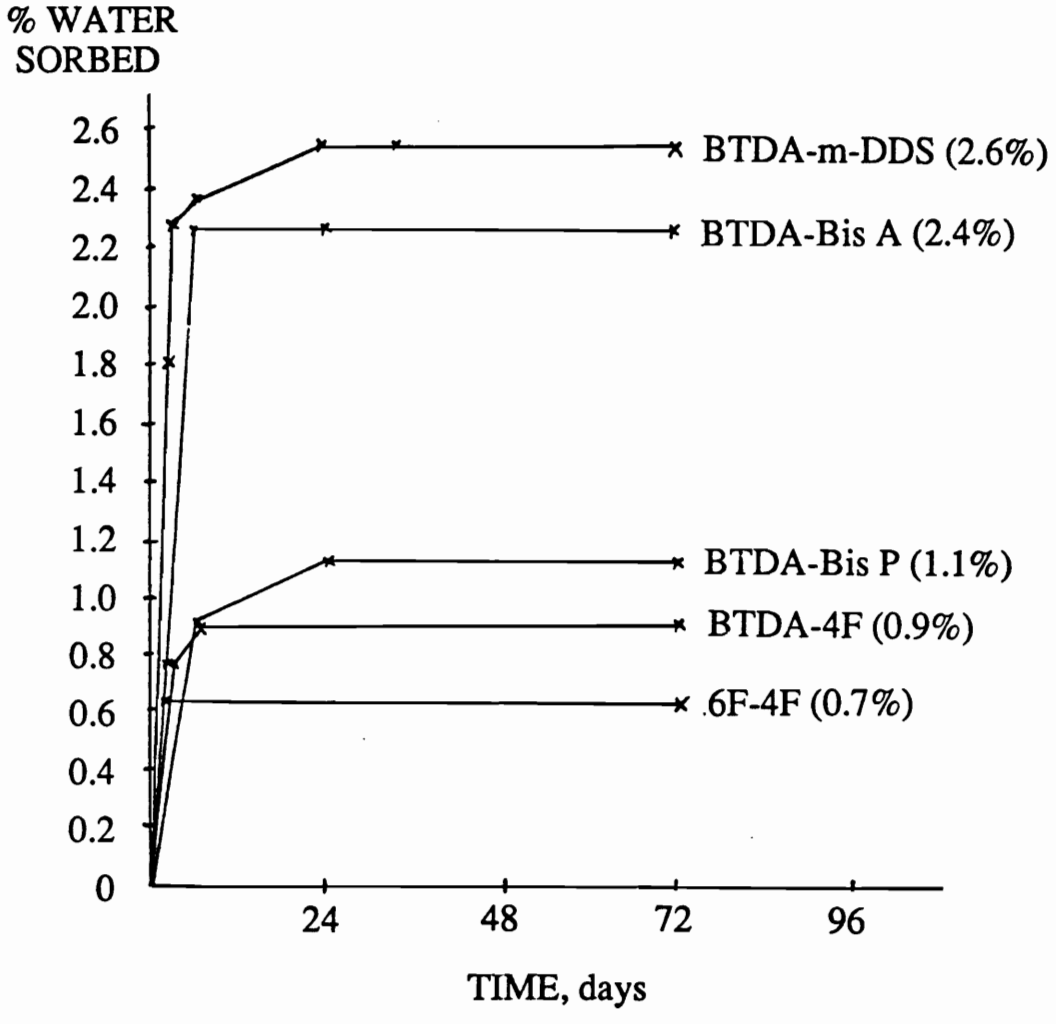

Figure 48: Water sorption for a series of polyimide homopolymers

almost identical to that obtained for the unmodified control (BTDA-m-DDS, 3000 psi).

4.9.2 Water sorption of polybenzimidazole blends

Sorption of large amounts of water can be particularly detrimental by plasticizing a polymer matrix and decreasing ultimate physical properties. Such is the case for polybenzimidazole (PBI), which is exceptionally hydrophilic due to the presence of the polar -NH group in its repeat unit. Specifically, the water sorption of PBI was reduced from its equilibrium value of 16 weight percent to approximately 2 percent by incorporating 60 percent of the BTDA-m-DDS-40 PSX 950 copolymer, or 24 percent siloxane overall. This blend displayed a glass transition in excess of 300°C. Thus, incorportion of siloxane not only benefits PBI's resistance to aggressive atomic oxygen, but also provides the advantage of lowering its water sorption dramatically, without a significant loss of its high thermal stability. This trend is delineated in Tables 34 and 35, for PBI blended with the BTDA-m-DDS homopolymer and the corresponding copolymer with 40 weight percent siloxane of 950 g/mole molecular weight.

4.10.0 Rheological Properties

4.10.1 Influence of molecular weight and composition varations on viscosity and shear stress

Some initial rheological investigations of solution imidized polyimides were performed to determine the improvement to processability by endcapping with phthalic anhydride and controlling molecular weight, and structural variations between the anhydrides BTDA and 6F. The effect of frequency and temperature changes on complex viscosity are presented in the log-log plot of Figure 49 for the solution imidized homopolymer 6F-m-DDS-PA (10,000). The high molecular weight analogue of this composition exhibited a glass

Table 34: Water sorption of blends of polybenzimidazole and BTDA-m-DDS homopolyimide

Weight % PBI	Weight % Homopolyimide	Water Sorbed %
100	0	15.7
75	25	12.7
56	44	10.6
25	75	-----
0	100	1.1

Table 35: Water sorption of blends of polybenzimidazole and BTDA-m-DDS-40 PSX 950 poly(siloxane imide) segmented copolymer

Weight % PBI	Wt % Copolyimide (Wt % PSX)	Water Sorbed %
100	0 (0)	15.7
86	14 (5.6)	13.2
66	34 (13.6)	8.4
40	60 (24.0)	2.4
0	100 (40.0)	0.6

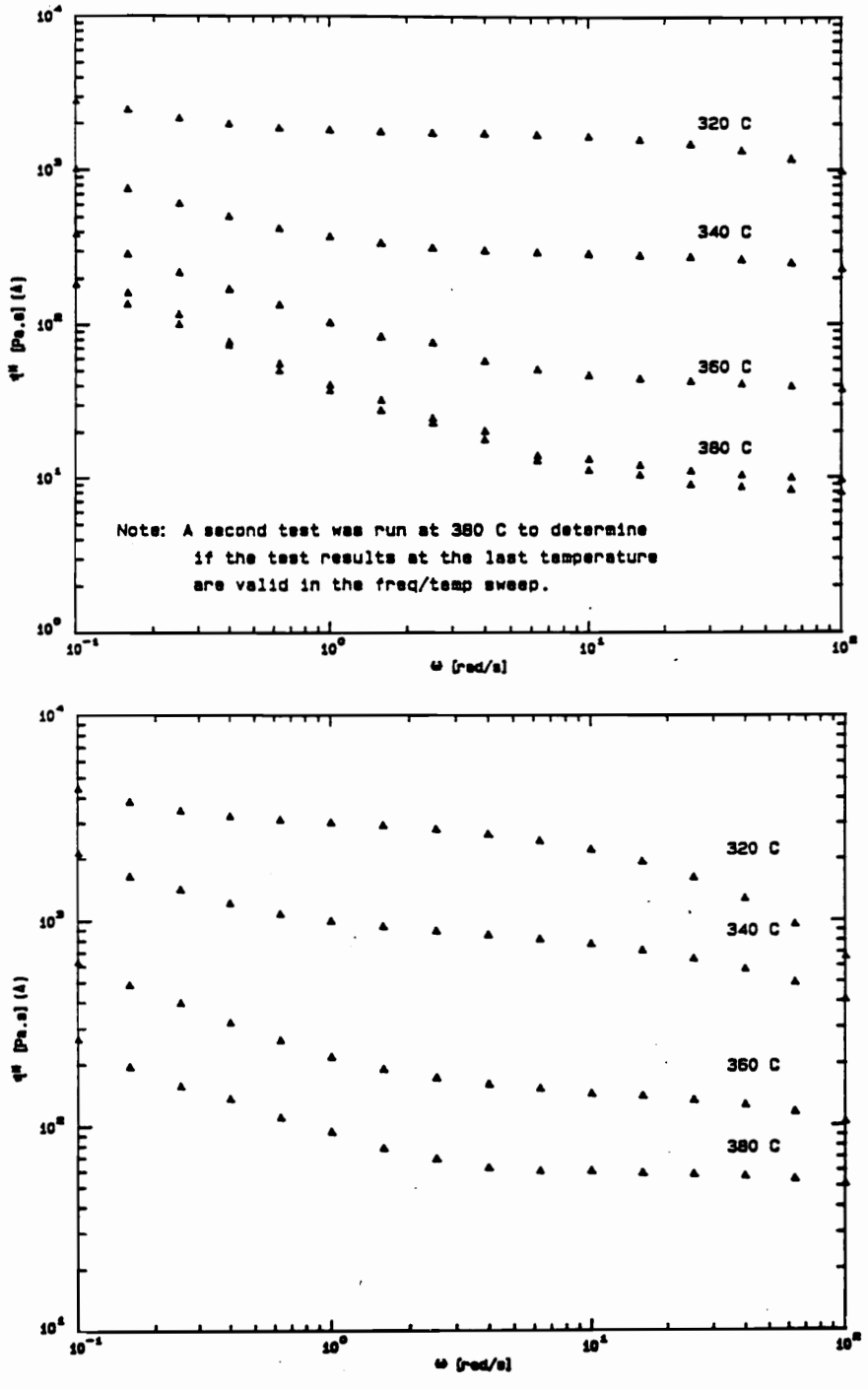

Figure 49: Complex viscosity as a function of temperature and angular frequency for 6F-m-DDS-PA (10,000) (upper), 6F (50) BTDA (50)-m-DDS-PA (10,000) (lower), both solution imidized

transition of 270°C. The experiment involved cycling a single sample through the entire frequency/temperature sweep, therefore, the sample was exposed to elevated temperatures for approximately 40 minutes. Another 'fresh' sample was run through the frequency sweep at only the highest temperature of 380°C to ascertain whether the viscosity response would be reproducible. The viscosity response was indeed identical for the two samples, indicating that no degradation had occurred while the initial sample was subjected to the entire range of temperatures and frequencies.

Also in Figure 49, the viscosity response is presented for a different composition of the same molecular weight, 6F (50) BTDA (50)-m-DDS-PA (10,000), clearly indicating that this sample possessed a higher viscosity at a given temperature than the analogue comprised of only 6F as the dianhydride component. Both of these samples, however, possessed low viscosities on the order of 100 to 1000 Pa.s at reasonable processing temperatures. The upper and lower portions of Figure 49, it should be noted, are plotted on different ordinate scales.

The viscosity response for a higher molecular weight, solution imidized polymer, 6F (50) BTDA (50)-m-DDS-PA (30,000), is presented in Figure 50. Clearly, this higher molecular sample exhibited a significantly higher viscosity than either of the lower molecular weight materials. Only at relatively high shear rates of 100 radians per second did the viscosity fall within a feasible range for processing by commercial means. The great dependence of viscosity on frequency indicated that this sample was highly shear thinning. Also, its viscosity was found to be somewhat independent of temperature within the range investigated.

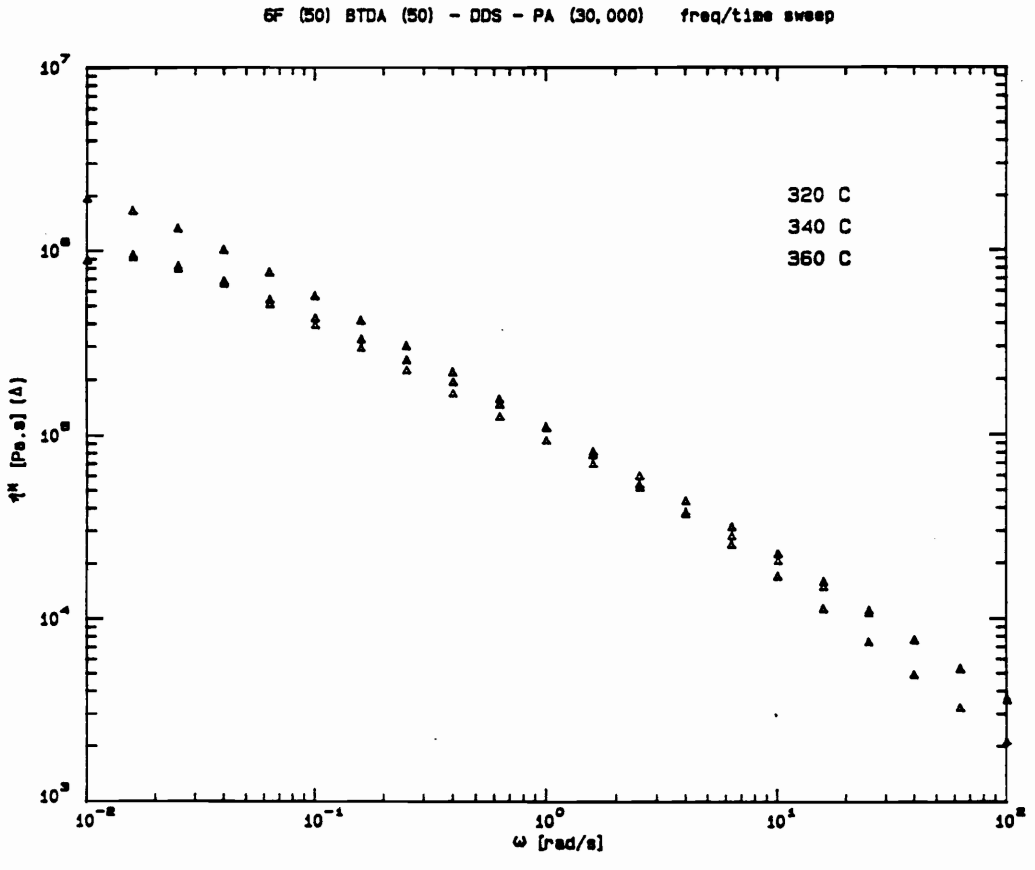

Figure 50: Complex viscosity as a function of temperature and angular frequency for solution imidized 6F (50) BTDA (50)-m-DDS-PA (30,000)

Some viscosity data were replotted in Figure 51 to illustrate shear stress as a function of applied frequency at 340°C for the 6F (50) BTDA (50)-m-DDS-PA samples of 10,000 and 30,000 g/mole molecular weights. As expected, the lower molecular weight sample exhibited a more Newtonian (linear) response according to the fundamental relationship of *Newton's law of viscosity*, Shear Stress = (Viscosity) (Shear Rate).

The experimental data at 340°C and 10 percent strain are summarized in Figure 52 for two compositions of varying dianhydride content, two molecular weights of 10,000 and 30,000 g/mole, and commercially available Ultem polyetherimide. As expected, the low molecular weight samples exhibited lower viscosities. Also, the incorporation of 6F over BTDA appeared to decrease viscosity. The laboratory synthesized polyimides possessed reasonable processability, as they were being tested at only 70°C above their glass transition temperature, whereas Ultem was 120°C higher than its glass transition.

4.10.2 Thermomechanical analysis

A comparison of the processability of a thermally versus solution imidized polyimide was attempted. Initial results indicated that the thermally imidized sample possessed a somewhat *lower* viscosity than its solution imidized analogue at a given temperature and frequency. Upon close examination, however, the thermally imidized sample was not found to flow between the parallel plates, indicating that the data were invalid. The inferior processability of thermally imidized samples may be inferred from simple TMA experiments for BTDA-m-DDS based poly(siloxane imide) segmented copolymers, as presented in Figure 53. These measurements also affirm that siloxane incorporation enhanced processability.

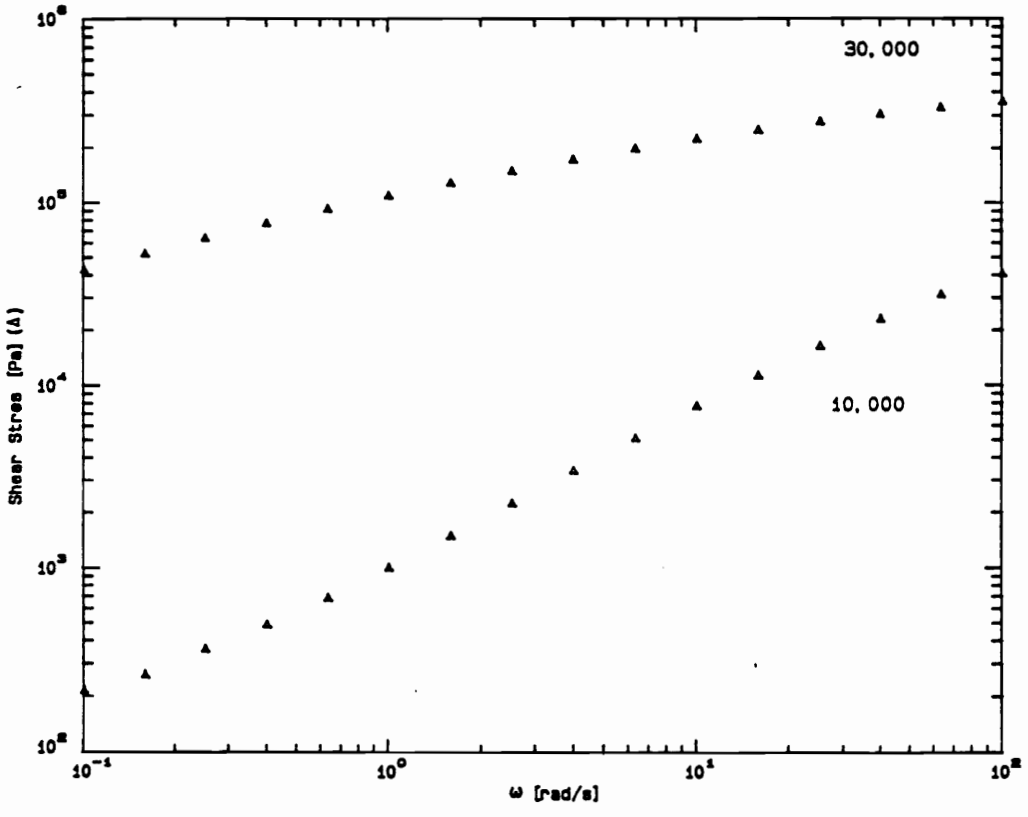

Figure 51: Shear stress versus angular frequency as a function of molecular weight for solution imidized 6F (50) BTDA (50)-m-DDS-PA at 340°C

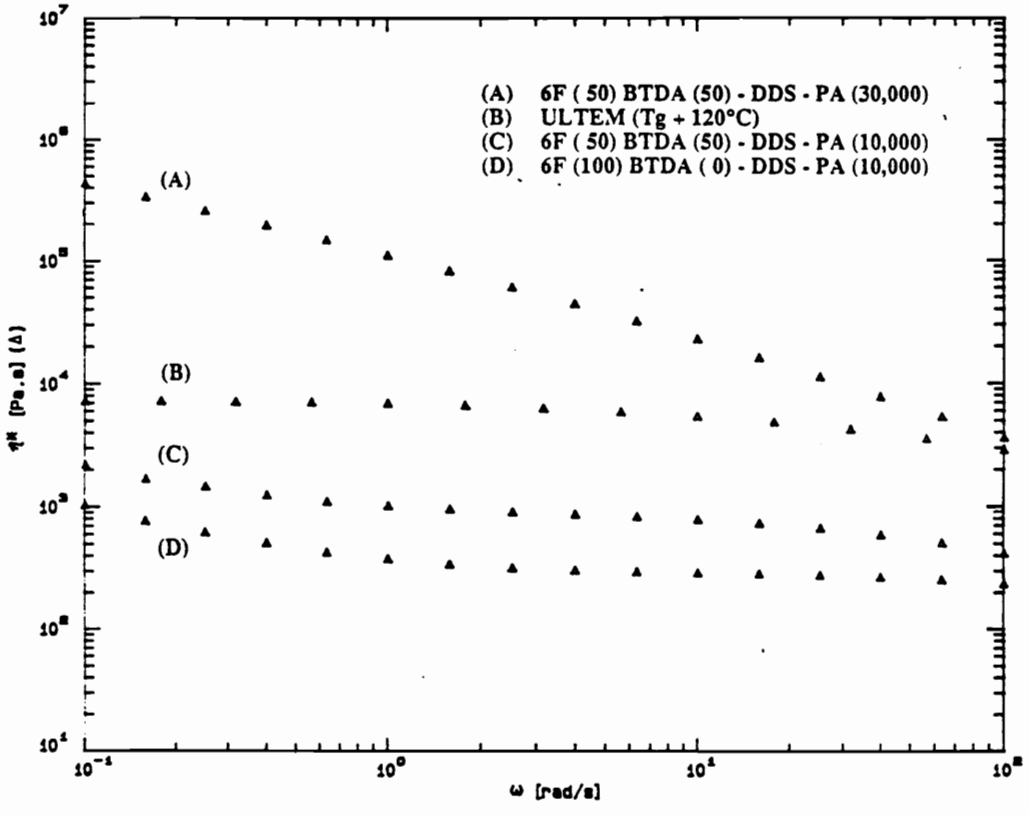

Figure 52: Summary of initial rheological investigation at 340°C of polyimides: variation of molecular weight and composition relative to commercially available Ultem

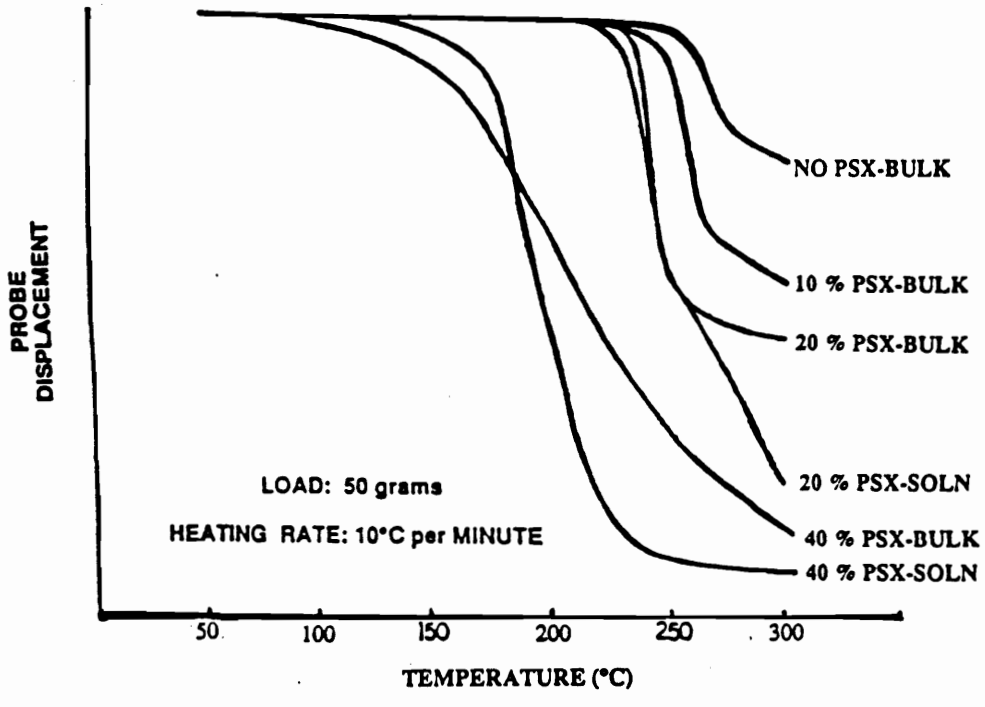

Figure 53: Thermal mechanical analysis of polyimide homopolymers and copolymers imidized in bulk or in solution, as indicated, with constant siloxane molecular weight of ~1000 g/mole

4.11 Blends of polyimides with polybenzimidazole (PBI)

Miscibility of the blends of the polyimide homopolymers and poly(siloxane imide) segmented copolymers based on BTDA and m-DDS with PBI was ascertained by a number of different techniques over a wide temperature range. The formation of clear, transparent films was the first evidence that these systems might be miscible and homogeneous. DMAc solutions and films of PBI blended with 6F-m-DDS-PA (25,000), on the other hand, were not clear, indicating immiscibility. Indeed, FTIR measurements have shown that the miscibility of BTDA based polyimides with PBI is due to specific interactions between the carbonyl group of the BTDA and the -NH group of PBI (247-253, 310). Scanning electron micrographs did not indicate any macrophase separation of the blend components. From DMTA, single, well defined tan ∂ relaxation peaks associated with the glass transition were observed in every instance (Figure 54).

The variation of the glass transition values as a function of the percent of PBI in the blends was found to positively deviate from the values expected from the simple Fox equation rule of mixtures. This phenomena may be attributed to the specific interaction of the BTDA carbonyl with the -NH group of PBI. Thus, the glass transitions of the blends varied between 430°C, the Tg for PBI, and 275°C for the polyimide homopolymer blend series, and 185°C for the BTDA-m-DDS-40 PSX 950 copolymer blend series. Even with 34 percent poly(siloxane imide) segmented copolymer, for instance, the glass transition of the blend with PBI was still remarkably high, at 381°C. Part of the complexity of the blend system's glass transition concerned the fact that the low molecular weight siloxane segment, at 950 g/mole, was only partially microphase separated. Tables 36 and 37 list the glass transitions of blends of PBI with BTDA-m-DDS based homopolyimides and poly(siloxane imide) segmented copolymers, respectively.

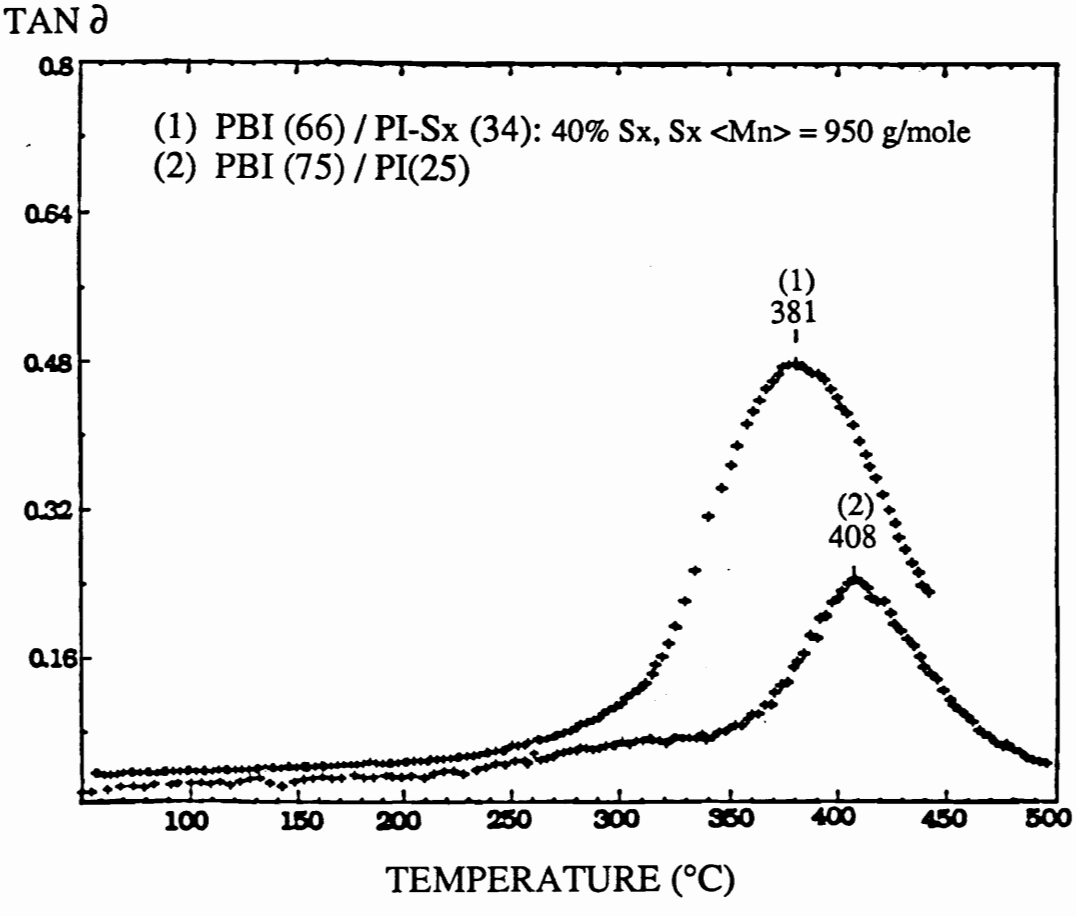

Figure 54: Dynamic mechanical thermal analysis of blends of polybenzimidazole with BTDA-m-DDS homopolyimide and BTDA-m-DDS-40 PSX 950 poly(siloxane imide) segmented copolymer

Table 36: Glass transitions of blends of polybenzimidazole and BTDA-m-DDS homopolyimide determined by dynamic mechanical thermal analysis

Weight % PBI	Weight % Homopolyimide	Tg, °C
100	0	430
75	25	408
56	44	377
25	75	300
0	100	275

Table 37: Glass transitions of blends of polybenzimidazole and BTDA-m-DDS-40 PSX 950 poly(siloxane imide) segmented copolymer determined by dynamic mechanical thermal analysis

Weight % PBI	Wt % Copolymer (Wt % PSX)	Tg, °C
100	0 (0)	430
86	14 (5.6)	394
66	34 (13.6)	378
40	60 (24.0)	339
0	100 (40.0)	185

4.12 Blends of polyimides with PEEK

Harris and Robeson (238-241) and Hedrick (244) have investigated the properties of PEEK-Ultem blends. Blend miscibility and thermal-mechanical properties as a function of structural variations of the polyimide component have been investigated in our laboratories by Hedrick and Arnold (244), and the aspect of miscibility will be outlined here. The following list describes the structural variations which give rise to a *single upper glass transition* for a 50:50 weight percent blend of the specified polyimide with PEEK. In the case of poly(siloxane imide) segmented copolymers, a lower transition corresponding to the siloxane phase may also be evident. All of the polyimides' molecular weights and endgroups were controlled by the addition of phthalic anhydride to enhance melt processability and miscibility. All of the "Comments" refer to the quenched *amorphous* films of the blends.

Bis P BASED POLYIMIDE	SINGLE UPPER Tg?	COMMENTS
BTDA-Bis P-PA (25,000)	Yes	Tough, clear films, Tm suppressed
BTDA-Bis P-PA (15,000)	Yes	Tough, clear films, Tm
BTDA-Bis P- 4 PSX 2500-PA (25,000)	Yes	Tough, clear films, Tm
BTDA-Bis P-20 PSX 3650-PA (25,000)	Yes	Tough, opaque films, Tm
BTDA-Bis P-40 PSX 3650-PA (25,000)	Yes	Poor physical properties, opaque, Tm
BTDA (50) 6F (50)-Bis P-PA (25,000)	Yes	Tough, clear films, Tm
6F-Bis P-PA (25,000)	Probably	Not tested yet

m-DDS BASED POLYIMIDE	SINGLE UPPER Tg?	COMMENTS
BTDA-m-DDS-PA (25,000)	No	Poor physical properties
BTDA (50) 6F (50)-m-DDS-PA (25,000)	No	"
BTDA (75) 6F (25)-m-DDS-PA (25,000)	No	"
6F-m-DDS-PA (25,000)	No	"

In Figure 55, a single, well defined tan ∂ relaxation peak of a DMTA scan is presented for the quenched, amorphous blend of PEEK (70%) and BTDA-Bis P-4 PSX 2500-PA (25,000) (30%), indicating that the components were indeed miscible. The DSC scans for the amorphous blend and its semi-crystalline version, obtained by slow cooling, are presented in Figure 56. Thus, blending a high glass transition polyimide with PEEK can raise the glass transition of the blend. The semi-crystalline nature of the PEEK component may be suppressed by the incorporation of a high molecular weight, more rigid polyimide, for example, in the 50:50 blend with BTDA-Bis P-PA (25,000) homopolymer. By lowering the molecular weight of the polyimide to 15,000 g/mole, the melting transition of the PEEK component became evident. Poly(siloxane imide) segmented copolymers were also miscible with PEEK, although at high siloxane contents the blends were no longer transparent. The incorporation of Bis P into the polyimide backbone appeared to promote miscibility, as m-DDS based polyimides were not miscible with PEEK, and 6F-Bis P polyimides were. Thermal and mechanical properties will be described in more detail by Hedrick (244).

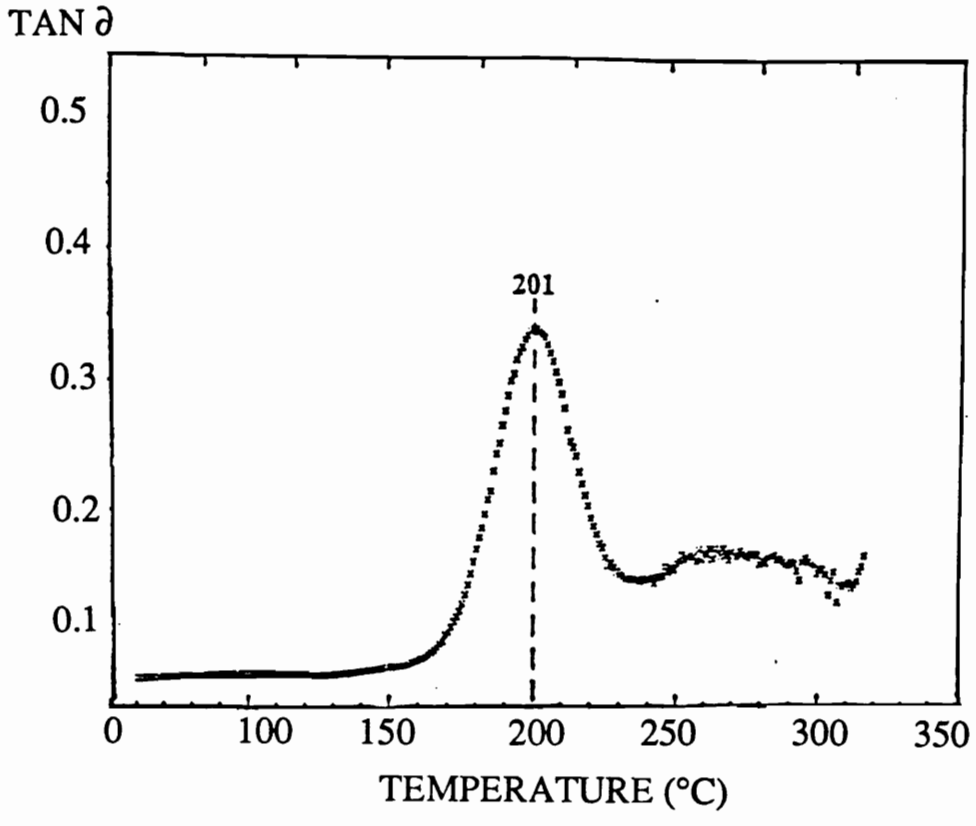

Figure 55: Dynamical mechanical thermal analysis of amorphous blend of 70 weight percent PEEK and 30 weight percent BTDA-Bis P-4 PSX 2500-PA (25,000) poly(siloxane imide) segmented copolymer

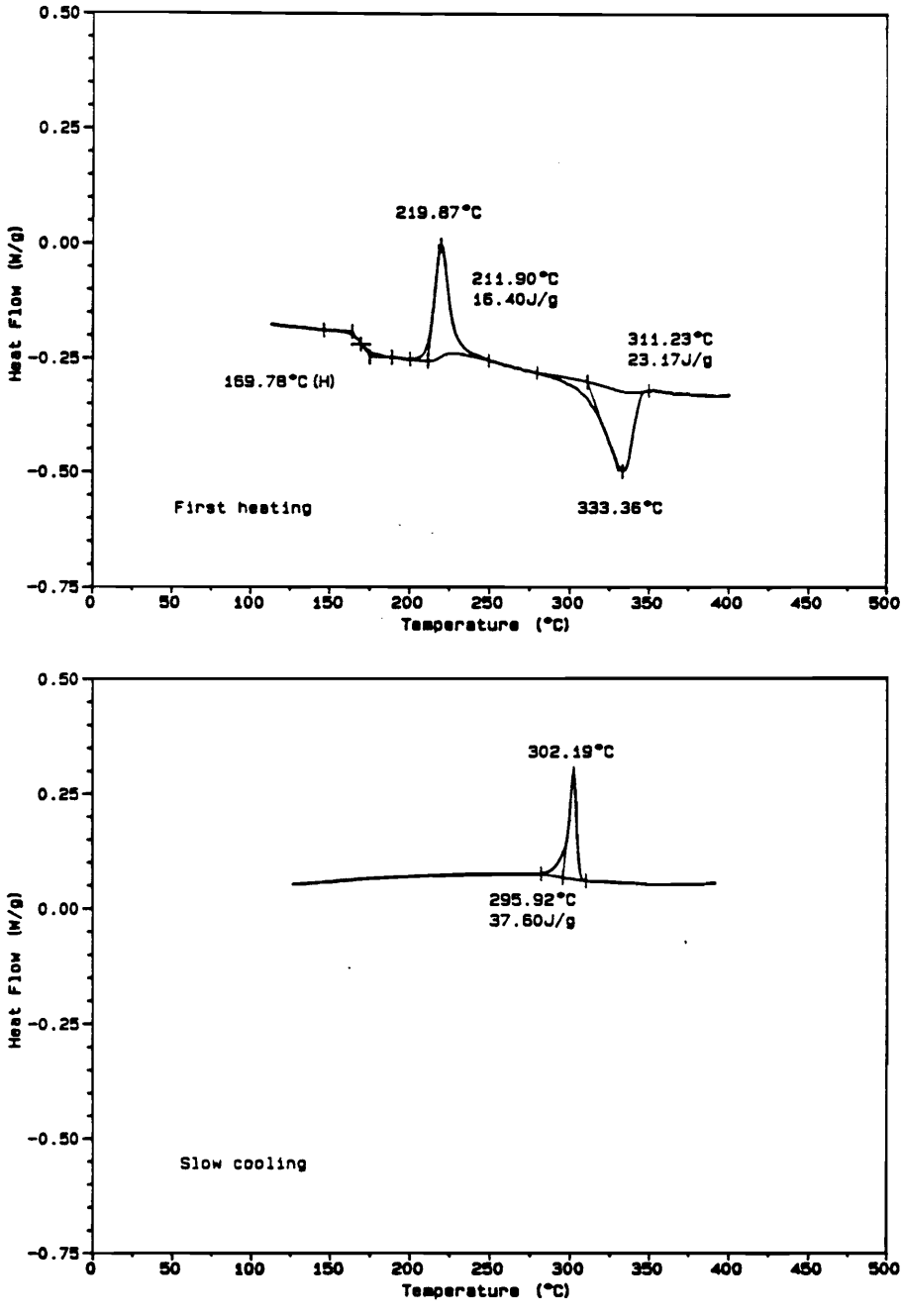

Figure 56: Differential scanning calorimetry of blend of 70 weight percent PEEK and 30 weight percent BTDA-Bis P-4 PSX 2500-PA (25,000) poly(siloxane imide) segmented copolymer: First heat of amorphous sample (upper), followed by slow cooling (lower), and second heat (next page)

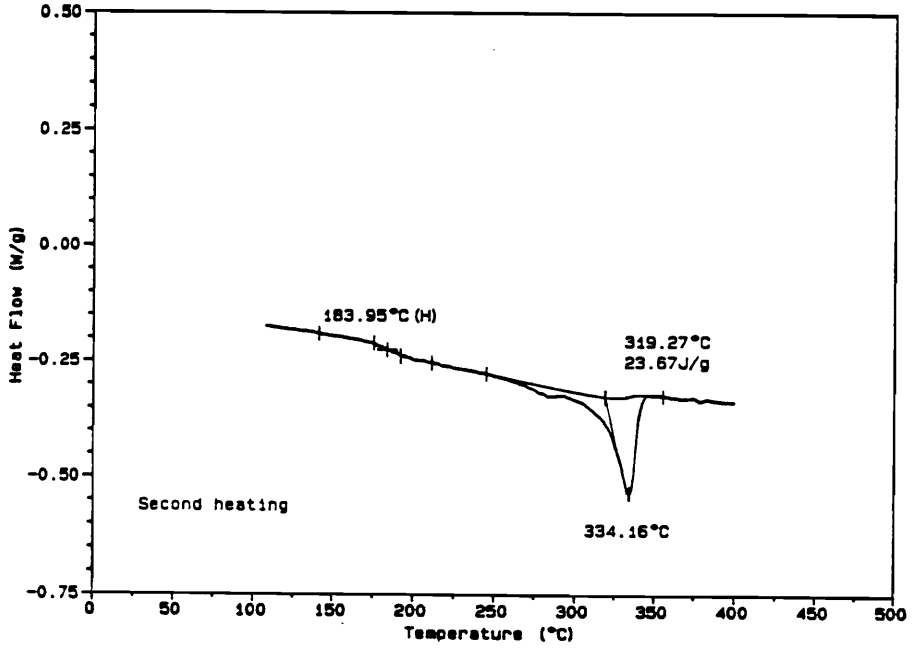

Figure 56, continued: Differential scanning calorimetry of blend of 70 weight percent PEEK and 30 weight percent BTDA-Bis P-4 PSX 2500-PA (25,000) poly(siloxane imide) segmented copolymer: First heat of amorphous sample and slow cooling (previous page), and second heat (above)

4.13 Molecular modelling of imide repeat units

Low energy conformations of various imide repeat units were calculated using Polygen's Quanta/CHARM molecular modelling facility. The imide repeat units were based upon a variety of dianhydrides and diamines. The dianhydrides were generally bis(phthalic anhydride)s with ether (ODPA), carbonyl (BTDA), sulfone (SDA), or hexafluoroisopropylidene (6F) linking units. The diamines were generally isomeric bis(aniline)s with similar linking units. The resulting structures gave qualitative evidence for the structure-property relationships of the polyimides which had been synthesized as part of this research. Modelling efforts demonstrated that the low energy conformers of the imide repeat units constructed from more rigid monomers, such as the biphenyl dianhydride (BPDA) or para-linked diamines were linear and planar. Experimentally, as discussed in preceeding sections, the corresponding polyimides exhibited high glass transition temperatures and were typically insoluble. On the other hand, the corresponding low energy conformers of the imide repeat units constructed from the more flexible dianhydrides, such as those with hexafluoroisopropylidene or ether linking units and meta-linked diamines, exhibited "kinks" in the backbone and were typically not planar. Polyimides synthesized with these more flexible monomers were generally more soluble, even when fully imidized. The low energy conformers of various imide repeat units are depicted in Figure 57.

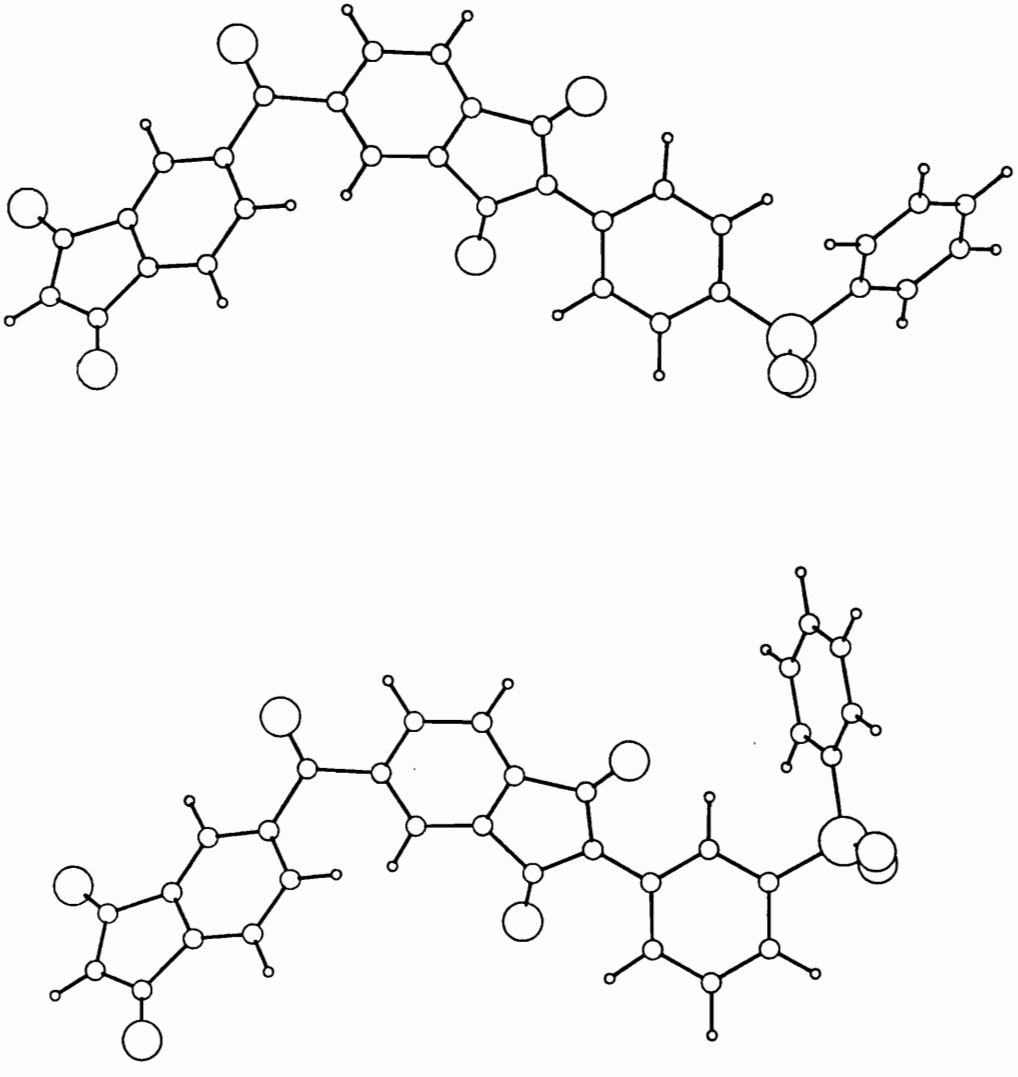

Figure 57: Low energy conformers of BTDA-p-DDS (upper) and BTDA-m-DDS (lower) imide repeat units

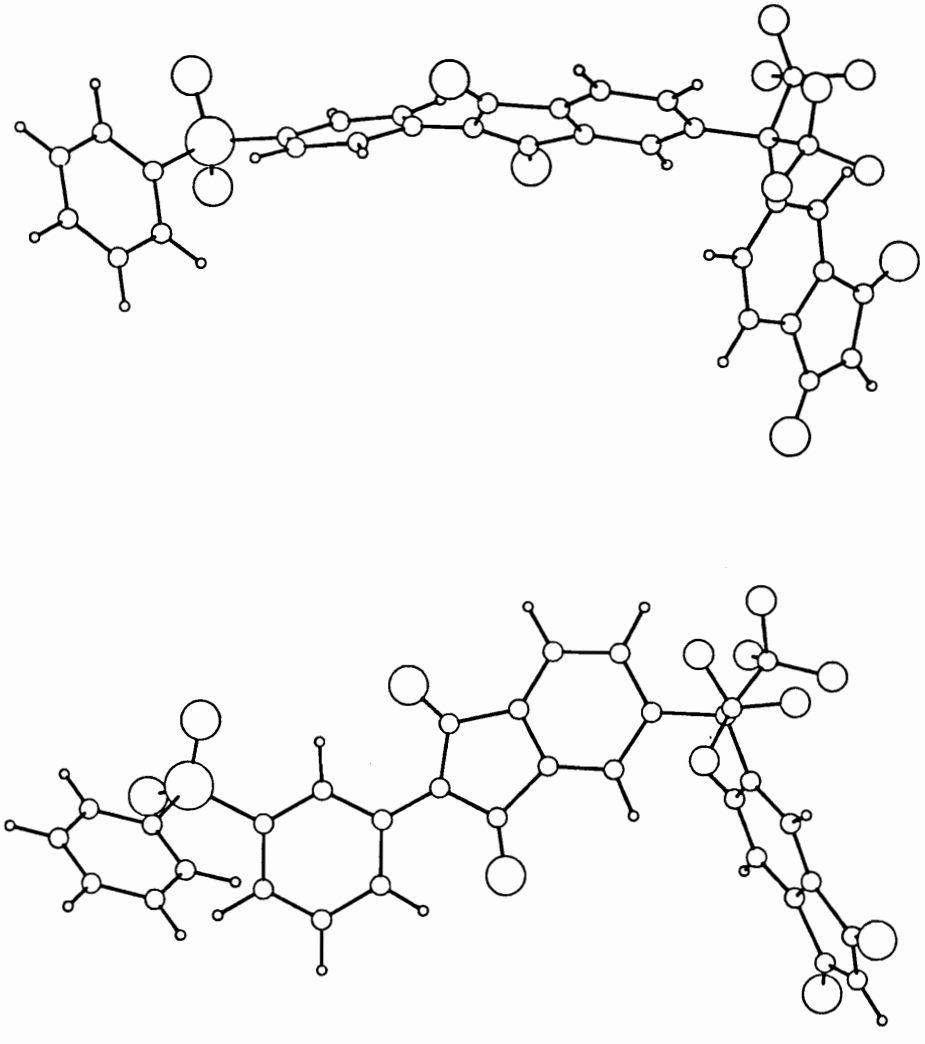

Figure 57, continued: Low energy conformers of 6F-p-DDS (upper) and 6F-m-DDS (lower) imide repeat units

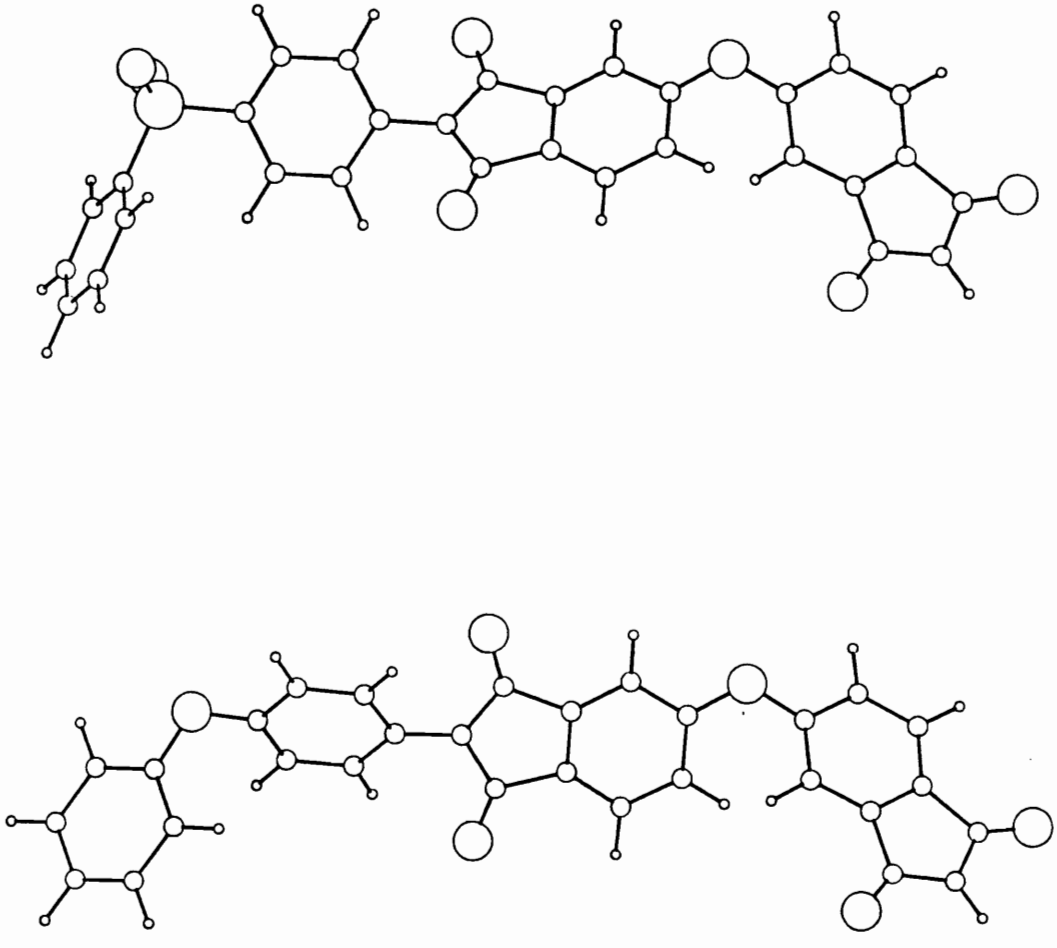

Figure 57, continued: Low energy conformers of ODPA-p-DDS (upper) and ODPA-p-ODA (lower) imide repeat units

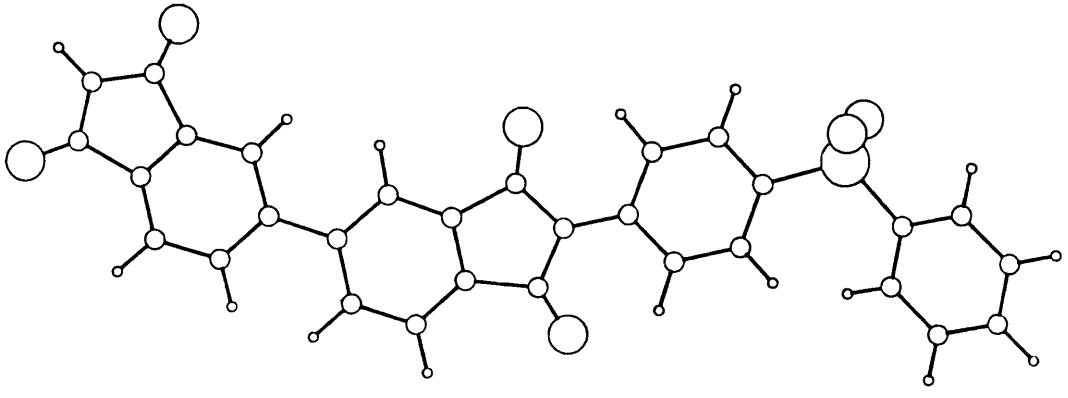

Figure 57, continued: Low energy conformer of BPDA-p-DDS imide repeat unit

CHAPTER 5

CONCLUSIONS----------

A variety of high molecular weight, soluble, processable polyimide homopolymers and copolymers have been synthesized which exhibit useful thermal, mechanical, adhesive, and dielectric properties for applications as structural matrix resins, structural adhesives, coatings, and dielectric materials. The synthesis of these materials was accomplished by an established poly(amic acid) intermediate route and solution imidization procedure. The solution imidization was conducted at ~ 15 percent solids concentration in an amide cosolvent system consisting of 80 percent N-methylpyrollidinone (NMP) and 20 percent cyclohexylpyrollidinone (CHP). Molecular weight control was achieved by the incorporation of phthalic anhydride or maleic anhydride, yielding nonreactive, or potentially reactive endgroups, respectively.

Variations of the dianhydride and diamine monomers produced significant changes in the solubility, processability, dielectric, and mechanical properties, although the glass transitions and thermal oxidative stability of the homopolyimides remained essentially constant for most of the monomer combinations employed in this study. For polyimides synthesized from monomers containing flexible ether connecting groups, glass transitions were approximately 220°C, solubility was improved, and stress-strain analysis indicated more yielding before failure. The bis (3-aminophenoxy-4'-phenyl) phosphine oxide diamine containing polyimides displayed an interesting two tiered thermogravimetric weight loss, indicative of their potential for flammability resistance. By incorporating a fluorinated dianhydride and relatively hydrophobic aromatic diamines into the polyimide backbone, significant reductions in the dielectric constant, and concomitant improvements in solubility

and processability were obtained. Ductility and toughness, as determined by stress-strain analysis, also improved, and water sorption decreased.

Variations of the imide component and molecular weight of the polydimethylsiloxane oligomer strongly influenced the morphology of poly(siloxane imide) segmented copolymers, as indirectly determined by thermal analysis. Incorporation of higher molecular weight siloxane oligomers favored microphase formation of a more homogeneous siloxane domain within an imide-dominated matrix, causing the upper glass transitions to approach those of the unmodified control. Lower glass transitions, in the range of -123 to -100°C, corresponding to the siloxane component, were also detectable. If the polarity of the imide component was decreased, compatibility of the imide with the siloxane was improved, leading to a more phase mixed morphology and depressed upper glass transition values. The mechanical properties of a series of poly(siloxane imide) segmented copolymers based upon benzophenone tetracarboxylic dianhydride (BTDA) and 3, 3'-diaminodiphenylsulfone (m-DDS) were highly dependent upon the amount of incorporated siloxane. At low levels of siloxane incorporation, the copolymers behaved essentially as modified polyimides, whereas at high levels of siloxane incorporation, thermoplastic elastomeric behavior was exhibited. The high temperature char yield by thermogravimetric analysis was proportional to the level of incorporated siloxane, indicative of the non-burning, flame resistant nature of the siloxane component.

The thermal properties of the poly(sulfone imide) segmented copolymers were also dependent on the imide composition. The ~6,000 g/mole number average molecular weight, amine terminated polysulfone oligomer was based upon bisphenol A and dichlorodiphenylsulfone. As the polarity of the imide component was increased, two glass

transitions corresponding to a two phase morphology developed. With a relatively nonpolar imide component, only one glass transition was observed.

To capitalize on the benefits of siloxane incorporation, miscible, compatible blends of poly(siloxane imide) segmented copolymers with other high performance engineering polymers were produced. Thus, poly(siloxane imide)s were solution blended with polybenzimidazole (PBI), yielding systems with reduced water sorption, high glass transition values in excess of 300°C, and significantly enhanced stability to a simulated low earth orbit (LEO) space environment as determined by weight loss data and scanning electron microscopy. The latter benefit was due to the transformation of the organic siloxane surface to an inorganic silicate in the presence of aggressive atomic oxygen, as determined by x-ray photoelectron spectroscopy. The miscibility of poly(siloxane imide) copolymers melt blended with semicrystalline poly(ether ether ketone) (PEEK) was found to improve with the incorporation of a less polar diamine (Bis P) than m-DDS. Indeed, miscibility was not obtained for polyimides based upon BTDA and m-DDS. Miscible, compatible blends of BTDA and Bis P based poly(siloxane imide) copolymers were obtained with PEEK, even with high siloxane contents, as determined by the existence of a single glass transition. These latter systems, however, were not transparent and their morphology is currently being explored.

CHAPTER 6

FUTURE SUGGESTED RESEARCH----------

During the course of this research, the relationship of polyimide structure to properties has been explored, however, certain aspects of this work merit further investigation. Primary areas of interest include the elucidation of morphology, the determination of molecular weights, and further rheological characterization. Also of interest are the analysis of the optical properties of atomic oxygen exposed samples, and an understanding of the basis of the miscibility of certain blends of polyimides with poly(ether ether ketone) (PEEK).

The first indication of the two phase morphology of the poly(siloxane imide) segmented copolymers was from thermal analysis. Specifically, the upper glass transition of the imide component was depressed to an extent dependent upon the degree of phase mixing of the imide and siloxane components. Thus, the upper glass transition was found to be a function of the siloxane molecular weight, the siloxane content in the copolymer, and the imide composition. Direct evidence of the degree of phase mixing and nature of the interphase region could be generated from small angle x-ray scattering. Additionally, the elevation of the low temperature transition of the siloxane phase could be determined by differential scanning calorimetry for the entire series of copolymers, although data have been generated for copolymers based upon benzophenone tetracarboxylic dianhydride and 3, 3'-diaminodiphenylsulfone. The breadth of both the upper and lower thermal transitions would also be indicative of the degree of phase mixing and the interphase region.

The great dependence of rheological properties on molecular weight necessitates the determination of number and weight average molecular weights, as well as

polydispersities, in order to accurately correlate these properties. Intrinsic viscosities are only indicative of molecular weight trends for similar compositions, therefore, more quantitative evaluation by gel permeation chromatography and light scattering techniques would be useful. The rheological properties of polyimides of greater structural diversity should be generated, and the influence of end group functionality should also be defined.

Solution gelation has been observed for some polyimides, particularly those of a more rigid structure. The gelation phenomena has also been found to be a function of time of solvation, solution concentration, thermal history, solvent, molecular weight and perhaps end groups. Data from dynamic light scattering may elucidate the nature of this phenomena, and quantify the effect of these variables. Molecular modeling may aid in predicting such phenomena, by providing details of the degree of backbone rigidity and free volume.

The homopolyimides, poly(siloxane imide) segmented copolymers, and copolymer blends with polybenzimidazole have been characterized for surface morphology (scanning electron microscopy), surface composition (x-ray photoelectron spectroscopy), and weight loss due to surface erosion. For applications as solar blankets, optical clarity after exposure to atomic oxygen is also necessary, and indeed, the siloxane containing samples do exhibit greater optical clarity after exposure than homopolymers. This observation, however, has only been qualitatively observed, and needs to be quantified, perhaps by ultraviolet absorption or refractive index determination. This technique must take into account the scatter due to surface roughness, particularly that caused by surface erosion. A sensitive profilometer may provide a measure of roughness which could be related to the degree of erosion in a high energy, high flux atomic oxygen environment.

The nature of the miscibility of the blends of PEEK and certain polyimides is not well understood, although by varying the polyimide composition, certain moieties (v. g., isopropylidene) have been defined which promote miscibility. Several groups of researchers are active in this field, and are currently attempting to determine specific interactions which give rise to the miscibility of these polymers. Techniques such as fourier transform infrared spectroscopy, solid state carbon-13 NMR, and neutron scattering may help characterize these interactions.

REFERENCES----------

1 W. M. Edwards and I. M. Robinson, U. S. Patent 2,710,853 (to DuPont) (1955).

2 W. M. Edwards and I. M. Robinson, U. S. Patent 2,867,609 (to DuPont) (1959).

3 C. E. Sroog, A. L. Endrey, S. V. Abramo, C. E. Berr, W. M. Edwards, K. L. Oliver, J. Polym. Sci., A, 3, 1373 (1965).

4 G. W. Bower and L. W. Frost, J. Polym. Sci, A 1, 3135 (1963).

5 L. W. Frost and I. Kesse, J. Appl. Polym. Sci., 8, 1039 (1964).

6 W. Wrasidlo, P. M. Hergenrother, and H. Levine, Polym. Prepr., 5, 141 (1964).

7 L. A. Laius, M. I. Bessonov, and F. S. Florinskii, Polym. Sci. U. S. S. R., 13, 2257 (1971).

8 A. K. St. Clair and T. L. St. Clair, Polym. Prepr., 27 (2), 406 (1986).

9 J. A. Kreuz, A. L. Endrey, F. P. Gay, and C. E. Sroog, J. Polym. Sci., A-1, 4, 2607 (1966).

10 S.-I. Numata, K. Fujisaki, and N. Kinjo, in "Polyimides: Synthesis, Characterization, and Applications", Vol. 1, K. L. Mittal, Ed., Plenum Press, New York, 259 (1984).

11 R. Ginsburg and J. R. Susko, in "Polyimides: Synthesis, Characterization, and Applications", Vol. 1, K. L. Mittal, Ed., Plenum Press, New York, 259 (1984).

12 A. I. Baise, J. Polym. Sci., 32(3), 4043 (1986).

13 P. R. Young and A. C. Chang, SAMPE J., 22, 70 (1986).

14 J. D. Summers, Ph. D. Dissertation, Virginia Polytechnic Institute and State University, Blacksburg, Virginia 24061 (1988).

15 M. Navarre, in "Polyimides: Synthesis, Characterization, and Applications", Vol. 1, K. L. Mittal, Ed., Plenum Press, New York, 429 (1984).

16 D. Day and S. Senturia, in "Polyimides: Synthesis, Characterization, and Applications", Vol. 1, K. L. Mittal, Ed., Plenum Press, New York, 249 (1984).

17 M. F. Hitchcock, SAMPE J. 19, 15 (1983).

18 J. I. Jones, F. W. Ochynski, and F. A. Rackley, Chem. Ind., 1686 (1962).

19 L. W. Frost and G. M. Bower, U. S. Patent 3,179,635 (1965).

20 P. Hermans and J. Streef, Die Makromol. Chemie, 74, 133 (1964).

21 G. S. Kolesnikov, O. Ya. Fedotova, E. I. Hofbauer, and V. G. Shelgayeva, Vysokomol. Soedin., A9, 612 (1967).

22 E. Sacher, J. Macromol. Sci., Phys., B25 (4), 405 (1986).

23 A. L. Endrey, U. S. Patent 3,179,630.

24 R. J. Angelo, U. S. Patent 3,282, 898 (1966).

25 M. M. Koton, T. K. Meleshko, V. V. Kudryavtsev, P. P. Nechayev, Y. V. Kamzolkina, and N. N. Bogorad, Polym. Sci. U. S. S. R., 24 (4), 791 (1982).

26 F. P. Gay and C. E. Berr, J. Polym. Sci., 6, 1935 (1968).

27 R. A. Dine-Hart, D. B. V. Parker, and W. W. Wright, Brit. Polym. J., 3, 222 (1971).

28 C. Arnold, Jr. and L. K. Burgmann, Ind. Chem. Prod. Res. Dev., 11(3), 322 (1972).

29 National Starch, Finderne Avenue, Bridgewater, NJ 08807.

30 D. Lewis, J. C. Hedrick, T. C. Ward, and J. E. McGrath, Polym. Prepr., 28(2), 330 (1987).

31 D. Lewis, T. C. Ward, J. D. Summers, and J. E. McGrath, Polym. Prepr., 29(1), 174 (1988).

32 B. J. Johnson, Ph. D. Dissertation, Virginia Polytechnic Institute and State University, Blacksburg, Virginia 24061 (1984).

33 R. O. Waldbauer and J. E. McGrath, Soc. Adv. Mat. Proc. Eng. Series, 35, in press (1990).

34 T. Takekoshi, J. E. Kochanowski, J. S. Manello, and M. J. Webber, J. Polym. Sci., Polym. Symp. 74, 93 (1986).

35 J. P. Critchley, G. J. Knight, and W. W. Wright, Heat-Resistant Polymers, Plenum Press, New York (1983).

36 P. E. Cassidy, "Thermally Stable Polymers: Synthesis and Properties", Marcel Dekker, Inc., New York (1980).

37 M. I. Bessonov, M. M. Koton, V. V. Kudryavtsev, and L. A. Laius, Ed., "Polyimides: Thermally Stable Polymers", Consultants Bureau, New York (1987).

38 K. L. Mittal, Ed., "Polyimides: Synthesis, Characterization, and Applications", Vol. 1, Plenum Press, New York (1984).

39 K. L. Mittal, Ed., "Polyimides: Synthesis, Characterization, and Applications", Vol. 2, Plenum Press, New York (1984).

40 C. Feger, M. Kojasteh, and J. E. McGrath, Eds., "Polyimides: Materials, Chemistry and Characterization", Elsevier, New York (1989).

41 H. D. Burks and T. L. St. Clair, in "Polyimides: Synthesis, Properties, and Applications", Vol 1, K. L. Mittal, Ed., Plenum, New York, 117 (1984).

42 P. R. Young and N. T. Wakelyn, in "Proceedings from the 2nd International Conference on Polyimides", Ellenville, New York, 414 (1985).

43 T. L. St. Clair, in "Proceedings from Recent Advances in Polyimides and Other High Performance Polymers", P. M. Hergenrother, Chairman, Reno, NV, July, 1987.

44 F. W. Harris, in "Proceedings from Recent Advances in Polyimides and Other High Performance Polymers", P. M. Hergenrother, Chairman, Reno, NV, July, 1987.

45 F. W. Harris, A. J. Karnavas, S. Das, C. N. Cucuras, and P. M. Hergenrother, Polym. Mat. Sci. Eng. Proc., 54, 89 (1986).

46 F. W. Harris and S. H. S. Lien, Polym. Mat. Sci. Eng., 60, 197 (1989).

47 F. W. Harris, M. W. Beltz, S. Das, and R. K. Gupta, Polym Prepr, 25 (1), 160 (1984).

48 W. A. Feld, F. W. Harris, and B. Ramalingam, Polym Prepr, 22(1), 215 (1981).

49 W. A. Feld, B. Ramalingam, and F. W. Harris, J Polym Sci, Polym Chem Ed, 21, 319 (1983).

50 F. W. Harris and S. L.-C. Hsu, Polym. Mat. Sci .Eng., 60, 206 (1989).

51 F. W. Harris and S. L.-C. Hsu, High Perf. Polym., 1 (1), 3 (1989).

52 K. Inoue, J. Polym. Sci., Polym. Chem. Ed., 14, 1509 (1976).

53 J. R. Evans, R. A. Orwoll, and S. S. Tang, J. Polym. Sci., Polym. Chem. Ed., 23, 971 (1985).

54 J. P. Critchley and M. A. White, J. Polym. Sci., A-1, 10, 1809 (1972); J. A. Webster, J. M. Butler, T. J. Morrow, Polym. Prepr., 13, 612 (1972).

55 J. P. Critchley, P. A. Grattan, M. A. White, and J. S. Pippett, J. Polym. Sci., A1, 10, 1789 (1972).

56 K. Kurita and R. L. Williams, J .Polym. Sci., Polym. Chem. Ed., 11, 3125 (1973).

57 K. Kurita and R. L. Williams, J. Polym. Sci., Polym. Chem. Ed., 12, 1809 (1974).

58 P. M. Hergenrother, N. T. Wakelyn, and S. J. Havens, J. Polym. Sci., Polym. Chem. Ed., 25, 1093 (1987).

59 P. M. Hergenrother and S. J. Havens, J. Polym. Sci., A, 27, 1161 (1989).

60 P. M. Hergenrother, N. T. Wakelyn, and S. J. Havens, Polym. Prepr., 28 (1), 92 (1987).

61 E. P. Woo, J. Polym. Sci., Polym. Chem. Ed., 24, 2823 (1986).

62 F. P. Darmory, M. D. DiBenedetto, U. S. Patent 3,705,869 (1972).

63 F. P. Darmory, M. D. DiBenedetto, U. S. Patent 3,748,338 (1973).

64 J. A. Kreuz, A. L. Endrey, F. P. Gray, and C. E. Sroog, J. Polym. Sci., A-1 2607 (1966).

65 V. V. Korshak, S. V. Vinogradova, Y. S. Vygod'skii, S. M. Pavlova, and L. V. Boyko, Izvest. Akad. Nauk., S. S. S. R., Ser. Khim., 10, 2267 (1967).

66 S. V. Vinogradova, G. L. Slonimskii, Y. S. Yygod'skii, A. Akadskii, A. I. Mzhel'skii, N. A. Churchina, and V. V. Korshak, Polym. Sci, U. S. S. R., A 11, 3098 (1969); ibid, Chem. Rev., 42, 551 (1973).

67 V. V. Korshak, "Heat-Resistant Polymers", Keter Press, Jerusalem (1971).

68 R. A. Dine-Hart, Makromol. Chem., 143, 189 (1971).

69 F. W. Harris, in "Proceedings from Recent Advances in Polyimides and Other High Performance Polymers", P. M. Hergenrother, chairman, San Diego, CA, Jan. 1990.

70 F. W. Harris, W. A. Feld, and L. H. Lanier, Appl Polym Symp, 26, N. Platzer, Ed., Wiley, NY, 149 (1984).

71 F. W. Harris, S. O. Norris, L. H. Lanier, B. A. Reinhardt, R. D. Case, S. Varaprath, S. M. Padaki, M. Torres, and W. A. Feld, in "Polyimides: Synthesis, Characterization, and Applications", Vol. 1, K. L. Mittal, Ed., Plenum, New York, 3 (1984).

72 F. W. Harris, M. W. Beltz, and P. M. Hergenrother, Soc. Adv. Mat. Proc. Eng. Technical Conference, 18, 209 (1986).

73 F. W. Harris and Y. Sakaguchi, Polym. Mat. Sci. Eng., 60, 187 (1989).

74 J. Malinge, J. Garapon, and B. Sillion, Brit Polym J, 20 (5), 431 (1988).

75 F. E. Rogers, U. S. Patent 3,356,648 (1967).

76 H. H. Gibbs and C. V. Breder, Polym. Prepr., 15, 775 (1974).

77 H. H. Gibbs, Soc. Adv. Mat. Proc. Eng. Series, 7, 244 (1962); Soc. Adv. Mat. Proc. Eng. Series, 21, 592 (1976).

78 Hoechst-Celanese, Specialty Products Groups, 500 Washington Street, Coventry, RI 02816.

79 W. H. Mueller and R. Vora, in "Proceedings from Chemistry and Properties of High Performance Composites", N. J. Johnston, chairman, Jackson, WY, (1988).

80 Ethyl Corporation, Baton Rouge, LA 70801.

81 R. J. Jones and E. M. Silverman, SAMPE J., 25 (2), 41 (1989).

82 R. J. Jones, M. O'Rell, and J. Hom, U. S. Pat. 4,203,922 (to TRW) (1980).

83 R. J. Jones, M. O'Rell, and J. Hom, U. S. Pat. 4,111,906 (to TRW) (1978).

84 Hysol Composites, 17960 Englewood Drive, Cleveland, OH 44130.

85 J. A. Cella and D. A. Haitko, U. S. Pat. 4,814,466 (to General Electric) (1989).

86 P. E. Cassidy, J. M. Farley, and M. Mores, Polym. Mat. Sci. Eng., 60, 299 (1989).

87 M. Arai, P. E. Cassidy, and J. M. Farley, Macromol., 22, 989 (1989).

88 P. E. Cassidy, M. Arai, J. M. Farley, and M. Mores, Polym. Mat. Sci. Eng., 60, 304 (1989).

89 V. L. Bell, B. L. Stump, and H. Gager, J. Polym. Sci., Poly. Chem. Ed., 14, 2275 (1976).

90 V. L. Bell, Org. Coat. Plast. Prepr., 33, 153 (1973).

91 J. K. Gillham and H. C. Gillham, Org. Coat. Plast. Prepr., 33, 201 (1973).

92 V. L. Bell, U. S. Patent 4,094,862 (to NASA) (1978).

93 F. W. Harris, A. J. Karnavas, C. N. Cucuras, and S. Das, Polym. Prepr., 287;

94 F. W. Harris, M. W. Beltz, S. Das, and R. H. Gupta, Polym. Prepr., 25 (1), 1984, 160.

95 A. K. St. Clair and T. L. St. Clair, in "Polymers for High Technology: Electronics and Photonics", M. J. Bowden and S. Richard Turner, Eds., Amer. Chem. Soc., 437 (1987)

96 The DuPont Company, Industrial Films Division, Wilmington, DE.

97 H. M. Relles, in "Contemporary Topics in Polymer Science", Vol. 5, E. J. Vandenberg, Ed., Plenum Press, New York, 261 (1977).

98 General Electric Company, Plastics Operations, Pittsfield, MA.

99 J. G. Wirth and D. R. Heath, U. S. Patent, 3,838,097 (to General Electric) (1974).

100 T. Takekoshi, J. E. Kochanowski, J. S. Manello and M. J. Webber, J. Polym. Sci., Polym. Symp. 74, 93 (1986).

101 D. M. White, T. Takekoshi, F. J. Williams, H. M. Relles, P. E. Donahue, H. J. Klopfer, G. R. Loucks, J. S. Manello and R. O. Matthews, J. Polym. Sci., Polym. Chem. Ed., 19, 1635 (1981).

102 I. W. Serfaty, in "Engineering Thermoplastics", J. M. Margolis, Ed., Marcel Dekker, New York, 283 (1983).

103 J. H. Bateman, W. Geresy, and A. D. Neiditch, Org. Coat. Plast. Prepr., 35 (2), 72 (1975).

104 U. S. Patent 3,708,458 (to Upjohn) (1973).

105 Upjohn Company, CPR Division, Torrance, CA.

106 T. P. Gannett, H. H. Gibbs, and R. J. Kassal, U. S. Patent 4,485,140 (to DuPont).

107 R. J. Boyce, T. P. Gannett, H. H. Gibbs, and A. R. Wedgewood, Soc. Adv. Mat. Proc. Eng. Series, 32, 169 (1987).

108 T. P. Gannett, H. H. Gibbs, and R. J. Kassal, U. S. Patent 4,485,140 (to DuPont) (1984).

109 Mitsui-Toatsu Chemicals, Inc., 140 E. 45th Street, New York, New York.

110 A. K. St. Clair and T. L. St. Clair, SAMPE Quart., 20, Oct (1981).

111 V. L. Bell, U. S. Patent 4,094,862 (to NASA) (1978).

112 H. D. Burks, T. Hou, T. L. St. Clair, SAMPE Quart., 18 (1), 1, Oct (1986).

113 T. Hou, J. Bai, and T. L. St. Clair, SAMPE Quart., 18 (4), 20, July (1987).

114 Rogers Corporation, One Technology Drive, Rogers, Rogers, CT 06263.

115 K. L. Oliver, U. S. Patent 3,234,181 (1966); A. J. Yerman, U. S. Patent 4,824,716, (to General Electric) (1989)..

116 F. W. Harris and H. J. Spinelli, "Reactive Oligomers", ACS Symp. Series 282, Amn. Chem. Soc., Washington, D. C. (1985).

117 A. Rudin, "The Elements of Polymer Science and Engineering", Academic Press, Orlando (1982).

118 F. W. Billmeyer, Jr., "Textbook of Polymer Science", 3rd Ed., Wiley-Interscience, New York (1984).

119 D. M. Stoakley and A. K. St. Clair, Polym. Prepr., 59(2) 33 (1988).

120 F. Grundschober and J. Sambeth, U. S. Patent 3,533,996 (to Societe Rhodiaceta, Paris, France) (1971).

121 M. Bargain, A. Combet, and P. Grosjean, U. S. Patent 3,562,223 (to Rhone Poulenc, S. A., Paris, France) (1971).

122 M. A. Mallet and R. P. Darmory, Org. Coat. Plast. Prepr., 34 (1), 174 (1973).

123 H. D. Stenzenberger, W. Romer, M. Herzog, and P. Konig, Soc. Adv. Mat. Proc. Eng. Series, 33, 1546 (1988) .

124 H. D. Stenzenberger, W. Romer, P. M. Hergenrother, and B. J. Jensen, Soc. Adv. Mat. Proc. Eng. Series, 34, 2054 (1989).

125 J. C. Hedrick, J. S. Senger, and J. E. McGrath, data to be published.

126 G. D. Lyle, D. K. Mohanty, J. A. Cecere, S. D. Wu, J. S. Senger, D. H. Chen, S. Kilic, and J. E. McGrath, Soc. Adv. Mat. Proc. Eng. Series, 33, 1080 (1988).

127 NARMCO Product Data Sheet on 5250-4, BASF NARMCO Materials, Inc., Anaheim, CA 92806.

128 A. L. Landis, N. Bilow, R. H. Boschan, R. E. Lawrence, and T. J. Aponyi, Polym. Prepr., 15 (2), 537 (1974).

129 N. Bilow, A. Landis, L. J. Miller, U. S. Patent 3,845,018, (to Hughes Aircraft Corp.) (1974).

130 Thermid Series, National Starch and Chemicals Corp., Bridgewater, NJ 08807.

131 H. R. Lubowitz, U. S. Patent 3,528,950 (1970); Polym. Prepr., 12 (1), 329 (1971).

132 T. T. Serafini, P. Delvigs, and G. R. Lightsey, J. Appl. Polym. Sci., 16, 905 (1972).

133 J. N. Hay, J. D. Boyle, P. G. James, and J. R. Walton, in "Proceedings from the International Conference on Polyimides", Ellenville, New York, 171 (1988).

134 S. D. Smith, Ph. D. Dissertation, Virginia Polytechnic Institute and State University, Blacksburg, Virginia 24061 (1987).

135 C. S. Elsbernd, Ph. D. Dissertation, Virginia Polytechnic Institute and State University, Blacksburg, VA 24061 (1989).

136 P. M. Sormani, R. Minton, and J. E. McGrath, in "Ring Opening Polymerization: Kinetics, Mechanisms, and Synthesis", J. E. McGrath, Ed., Amer. Chem. Soc. Symp. Series, 286, Amer. Chem. Soc., Washington, D. C., 147 (1985).

137 W. Noll, Chemistry and Technology of Silicones, Academic Press, NY, 1968.

138 M. G. Voronkov, V. P. Mileshkevich, and Y. A. Yuzhelevskii, "The Siloxane Bond", Plenum Press, New York (1978).

139 A. Berger, U. S. Patent 4,395,527 (to M&T Chemicals) (1983).

140 H. D. Burks and T. L. St. Clair, J. Appl. Polym. Sci., 34, 351 (1987).

141 N. Tsutsumi, A. Tsuji, C. Horie, and T. Kiyotsukuri, Eur. Polym. J., 24 (9), 837 (1988).

142 B. C. Johnson, I. Yilgor, and J. E. McGrath, Polym. Prepr., 25 (2), 54 (1984).

143 P. P. Policastro, J. H. Lupinski, and P. K. Hernandez, Polym. Mat. Sci. Eng. Prepr., 59, 209 (1988).

144 G. C. Tesoro, G. P. Rajendran, D. R. Uhlmann, and C.-E. Park, Ind. Eng. Chem., 26, 1672 (1987).

145 H. Kukertz, Makromol. Chem., 98, 101 (1966).

146 A. J. Yerman, U. S. Patent 4,017,340 (to General Electric) (1977).

147 V. G. Greber, Angew Makromol. Chem., 415, 212 (1968); V. G. Greber, J. Prakt. Chem., 313, 461 (1971).

148 J. T. Hoback and F. F. Holub, U. S. Patent 3,740,305 (to General Electric) (1973).

149 C. J. Lee, U. S. Patent 4,558,110 (to General Electric) (1985).

150 S. Maudgal and T. L. St. Clair, Int. J. Adh., 4(2), 87 (1984).

151 S. Maudgal and T. L. St. Clair, in "Proceedings from the Second International Conference on Polyimides", Ellenville, New York, 182 (1985).

152 B. Chowdhury, in "Polyimides: Synthesis, Characterization, and Applications", Vol. 1, K. L. Mittal, Ed., Plenum Press, New York, 401 (1984).

153 C. J. Lee, SAMPE J., 21(4), 34 (1985).

154 M. Rakoutz and M. Balme, Polymer J., 19(1), 173 (1987).

155 S. Maudgal and T. L. St. Clair, Soc. Adv. Mat. Proc. Eng. Series, 29, 437 (1984).

156 A. Berger and P. Juliano, U. S. Patent 4,011,279 (to General Electric) (1977).

157 S. Maudgal and T. L. St. Clair, SAMPE Quart., 16(1), 6 (1984).

158 C. W. Wilkins, E. Rechmanis, T. Wolf, B. C. Smith, J. Vac. Sci. Technol., 3, 306 (1985).

159 H. S. Ryang, U. S. Patent 4,381,396 (to General Electric) (1983).

160 J. D. Rich, P. P. Policastro, and P. K. Hernandez, U. S. Patent 4,795,680 (to General Electric) (1989).

161 R. J. Spontak and M. C. Williams, Polym. J., 20 (8), 649 (1988).

162 D. J. Meier, in Block Copolymers, J. Moacanin, G. Holden and N. W. Tschoegl, Ed., Interscience Publishers, 1969, 81.

163 Ph. Teyssie, R. Fayt, and R. Jerome, Makromol Chem, Macromol Symp, 1988, 16, 41.

164 I. Yilgor, J. S. Riffle, G. L. Wilkes, and J. E. McGrath, Polym. Bull., 8, 535 (1982).

165 M & T 3500 Siloxane Polyimide Data Sheet, M & T Chemicals, Rahway, NJ, (1983).

166 C. J. Lee, G. Fabianowski, R. J. Jaccodine, S. P. Murarka, and R. Sun, in "Proceedings of the ASM Electronic Materials and Processing Congress", April, (1989) Philadelphia, 359.

167 A. J. Yerman, U. S. Patent 4,824,716 (to General Electric) (1989).

168 T. Homma, Y. Numasawa, Y. Murao, and K. Hamano, JEE, 74, Nov (1988).

169 Chisso Corp., Patent Appl. 108055 (1986); "A Method of Manufacturing Soluble Polyimide Siloxane Precursor with Good Film Forming Ability and a Method of Manufacturing Hardened Product".

170 E. Moyer, D. K. Mohanty, J. Shaw, and J. E. McGrath, in "Proceedings from The 3rd International SAMPE Electronics Conference", Los Angeles, CA, 894 (1989).

171 E. Moyer, Ph. D. Dissertation, Virginia Polytechnic Institute and State University, Blacksburg, VA 24061 (1989).

172 G. C. Davis, in "Polymers in Electronics", Amer. Chem. Soc. Symp. Series, 242, 259 (1984).

173 E. Reichmanis, G. Smolinsky, and C. W. Wilkins, Jr., Solid State Tech., 8, 130 (1985).

174 E. Reichmanis, G. Smolinsky, in "Proceedings of the SPIE", 469, 38 (1984).

175 E. D. Roberts, J. Electrochem. Soc., 120, 1716 (1973).

176 M. Gazard, J. C. DuBois, C. Duchesne, Appl. Polym. Symp., 23, 107 (1974).

177 E. S. Moyer, D. K. Mohanty, C. A. Arnold, and J. E. McGrath, Polym. Mat. Sci. Eng., 60, 202 (1989).

178 F. G. Will, K. H. Janora, J. G. McMullen, A. J. Yerman, 25th Annual Proc. Rel. Phys., 34 (1987).

179 G. C. Davis, B. A. Heath, G. Gildenblatt, in "Proceedings of the Electrochem. Soc.", 82(2), 325 (1982).

180 G. C. Davis, B. A. Heath, and G. Gildenblat, in "Proceedings from the 1st International Conference on Polyimides", K. L. Mittal, Ed., 847 (1984).

181 R. H. Bott, Ph. D. Dissertation, Virginia Polytechnic Institute and State University, Blacksburg, Virginia 24061 (1988).

182 R. H. Bott, J. D. Summers, C. A. Arnold, L. T. Taylor, C. P. Blankenship, Jr., T. C. Ward, and J. E. McGrath, SAMPE J., 24(4), 7 (1988).

183 R. H. Bott, J. D. Summers, C. A. Arnold, L. T. Taylor, C. P. Blankenship, Jr., T. C. Ward, and J. E. McGrath, J. Adhesion, 23, 67 (1987).

184 A. Iwama, K. Tasaka, and Y. Kazuse, U. S. Patent 4,618,534 (1986).

185 W. S. Slemp, B. Santos-Mason, G. F. Sykes, Jr., and W. G. Witte, Jr., AIAA-85-0421, presented at AIAA 23rd Aerospace Sciences Meeting, January, 1985, Reno, NV.

186 L. Leger, J. Visentine, and B. Santos-Mason, SAMPE Quart., 1, 48 (1987).

187 Hitachi Chem. Co., Jpn. Kokai, Tokkyo Koho JP, 57/42733 A2 (CA 97(4): 24385b) (1982).

188 M. Spinu, C. A. Arnold, and J. E. McGrath, Polym. Prepr., 30 (2), 125 (1989).

189 M. Spinu, A. Brennan, G. L. Wilkes, and J. E. McGrath, in "Proceedings of the Materials Research Soc.", S3.5, 619 (1989).

190 N. A. Androva, M. J. Bessonov, L. A. Laius, and A. P. Rudakov, "Polyimides", English translation, Israel Program for Scientific Translations, Jerusalem (1969).

191 R. N. Johnson, A. G. Farnham, R. A. Clendinning, W. F. Hale, and C. N. Merriam, J. Polym. Sci., A-1, 5, 2375 (1967).

192 W. F. Hale, A. G. Farnham, R. N. Johnson, and R. A. Clendinning, J. Polym. Sci., A-1, 5, 2399 (1967).

193 G. L. Brode, in "The Chemistry of Sulfides", A. V. Tobolsky, Ed., Wiley, New York, 133 (1968).

194 J. E. Harris, in "Engineering Thermoplastics", J. M. Margolis, Ed., Marcel Dekker, Inc., New York, 177 (1985).

195 G. L. Brode, J. H. Kawakami, G. T. Kwiatkowski, and A. W. Bedwin, J. Polym. Sci., Polym. Chem. Ed., 12, 575 (1974).

196 C. E. Sroog, J. Poly. Sci., Macromol. Rev., 11, 161 (1976).

197 R. N. Johnson and A. G. Farnham, J. Polym. Sci., Polym. Chem. Ed., 5, 2375 (1962).

198 B. C. Johnson and J. E. McGrath, Polym Prepr, 25 (2), 1984, 49.

199 J. L. Hedrick, I. Yilgor, G. L. Wilkes, and J. E. McGrath, Polym. Bull., 13, 201 (1985).

200 J. L. Hedrick, Ph.D. Dissertation, Virginia Polytechnic Institute and State University, Blacksburg, VA 24061 (1985).

201 J. L. Hedrick, M. J. Jurek, I. Yilgor, and J. E. McGrath, Polym. Prepr., 26(2), 293 (1985).

202 B. J. Jensen and P. M. Hergenrother, Polym. Mat. Sci. Eng., 60, 294 (1989).

203 T. L. St. Clair and D. A. Yamaki, in "Polyimides: Synthesis, Characterization, and Applications", Vol. 1, K. L. Mittal, Ed., Plenum Press, New York, 99 (1984).

204 T. L. St. Clair and D. A. Yamaki, U. S. Patent 4,398,021 (1983) and U. S Patent 4,489,027 (1984) (to NASA).

205 T. Watanabe and K. Wada, Jpn. Kokai Tokkyo Koho JP 63 83,136 [88 83,136], (to Nippon Steel) (1988).

206 C. J. Billerbeck and S. J. Henke, in "Engineering Thermoplastics", J. M. Margolis, Ed., Marcel Dekker, New York, 373 (1985).

207 G. T. Kwiatkowski, G. L. Brode, and L. M. Robeson, U. S. Patent 3,658,938, (to Union Carbide Corporation) (1972).

208 J. Dezern, SAMPE J., March/April (1988) 27.

209 W. Wrasidlo and J. M. Augl, J. Polym. Sci., A-1, 7, 321 (1969).

210 D. F. Loncrini, J. Polym. Sci., A-1, 4, 1531 (1966).

211 H. R. Kricheldorf, R. Pakull, and S. Buchner, Macromol., 21, 1929 (1988).

212 H. R. Kricheldorf and R. Pakull, Polymer, 28, 1772 (1987).

213 N. Kokoski, S. Tohyama, S. Fujita, M. Kurihara, and N. Yoda, J. Polym. Sci, A-1, 8(8), 2197 (1970).

214 J. Preston, W. F. DeWinter, W. B. Black, J. Polym. Sci., A-1, 7, 282 (1969).

215 J. P. Preston, W. F. DeWinter, W. B. Black, and W. L. Hofferbert, Jr., J. Polym. Sci, A-1, 7(10), 3027 (1969).

216 J. L. Hedrick, J. G. Hilborn, and J. W. Labadie, Polym. Prepr., 30 (1), 265 (1989).

217 G. Mandric, G. Petrache, E. Patrahau, T. Popa, Rev. Roum. Chim., 29 (6), 521 (1984).

218 L. W. Frost, G. M. Bower, J. H. Freeman, H. A. Burgman, E. J. Traynor, and C. R. Ruffing, J. Polym. Sci., A-1, 6, 215 (1968).

219 V. V. Korshak, E. S. Krongauz, N. M. Belomoina, M. Bruna, I. Sava, C. I. Simionescu, Rev. Roum. Chim., 32 (4), 393 (1987).

220 S. S. Hirsch, J. Polym. Sci., A-1, 7(1), 15 (1969).

221 B. Sillion, in "Proceedings from the Third International Conference on Polyimides", Ellenville, New York, 60 (1988).

222 W. F. DeWinter and J. Preston, U. S. Patent 3,621,076 (1971).

223 F. Kobayahi, F. Sabata, T. Mizoguchi, and N. Suyama, Jpn. Kokai, 69 27, 674, (1969). (CA 72, 56598e)

224 W. L. Hergenrother and R. J. Ambrose, Polym. Letters, 12, 343 (1974).

225 W. L. Hergenrother and R. J. Ambrose, Polym. Letters, 10, 679 (1972).

226 S. A. Ezzel, A. K. St. Clair, and J. A. Hinkley, Polymer, 28, 1779 (1987).

227 M. M. Grade and J. W. Verbicky, Jr., J. Polym. Sci., A, 27, 1467 (1989).

228 D. R. Paul and S. Newman, Eds. "Polymer Blends", Vol. 1, Academic Press, New York (1978).

229 D. R. Paul and S. Newman, Eds., Polymer Blends, Vol 2, Academic Press, New York (1978).

230 O. Olabisi, L. M. Robeson, and M. T. Shaw, "Polymer-Polymer Miscibility", Academic Press, New York (1979).

231 D. R. Paul and J. W. Barlow, J. Macromol. Sci. Rev., Macromol. Chem., 18, 109 (1980).

232 R. Koningsveld, L. A. Kleintjens, and J. M. Schoffelers, Pure Appl. Chem., 39, 1 (1974).

233 O. Olabisi, in "Kirk-Othmer Encyclopedia of Chem. Technol.", 3rd Ed., Wiley-Interscience, New York (1982).

234 P. C. Painter, Y. Park, and M. M. Coleman, Macromol., 22, 570 (1989).

235 P. C. Painter, Y. Park, and M. M. Coleman, Macromol., 22, 580 (1989).

236 S. J. Krause, J. Macromol. Sci., Rev. Macromol. Chem., 7 (21), 251 (1972).

237 R. B. Seymour and G. S. Kirshenbaum, Ed., "High Performance Polymers: Their Origin and Development", Elsevier, NY, 1986; (a) A. S. Hay, p. 209, (b) J. M. Heuschen, p. 215.

238 J. E. Harris and L. M. Robeson, U. S. Patent 4,609,714 (to Union Carbide Corporation) (1986).

239 J. E. Harris and L. M. Robeson, U. S. Patent 4,624,997 (to Union Carbide Corporation) (1986).

240 J. E. Harris and L. M. Robeson, J. Appl. Polym. Sci., 35, 1877 (1988).

241 J. E. Harris and L. M. Robeson, Polym. Prepr., 28 (1), 56 (1987).

242 C. K. Sham, G. Guerra, F. E. Karasz, and W. J. MacKnight, Polymer, 29, 1016 (1988).

243 R. J. Karcha and R. S. Porter, J. Polym. Sci., Polym Physics, 27, 2153 (1989).

244 J. C. Hedrick, C. A. Arnold, M. Zumbrum, and J. E. McGrath, Soc. Adv. Mat. Proc. Eng. Series, 35, in press (1990).

245 P. Policastro, P. K. Hernandez, M. W. Davis, U. S. Patent 4,820,781 (to General Electric Corporation) (1989).

246 J. A. Rock, U. S. Patent 4,816,527 (to General Electric Corporation) (1989).

247 S. Stankovic, G. Guerra, D. J. Williams, F. E. Karasz, and W. J. MacKnight, Polym. Comm., 29, 14 (1988).

248 D. J. Williams, F. E. Karasz, and W. J. MacKnight, Polym. Prepr., 28 (1), 54 (1987).

249 P. N. Chen, Sr., T. S. Chung, P. J. Harget, and M. J. Jaffe, Polym. Mat. Sci. Eng., 59, 707 (1988).

250 G. Guerra, D. J. Williams, F. E. Karasz, and W. J. MacKnight, J. Polym. Sci., B, 26, 301 (1988).

251 G. Guerra, S. Choe, D. J. Williams, F. E. Karasz, and W. J. MacKnight, Macromol., 21, 231 (1988).

252 P. Musto, F. E. Karasz, and W. J. MacKnight, Polymer, 30, 1012 (1989).

253 M. Jaffe and M. Glick, 4th Quarter Technical Report, Polymer Blends, DARPA Order 6045, AFOSR Contract F9620-88-C-0014, July (1989).

254 L. Leung, D. J. Williams, F. E. Karasz, and W. J. MacKnight, Polym. Bull., 16, 457 (1986).

255 M. J. Jaffe, in "Proceedings from Recent Advances in Polyimides and Other High Performance Polymers", P. M. Hergenrother, chairman, San Diego, CA, Jan. 1990.

256 B. C. Ward and E. Alvarez, Polym. Mat. Sci. Eng., 59, 718 (1988).(PBI)

257 A. Buckley, D. E. Stuetz, G. A. Serad, in "Encyclopedia of Polym. Sci. Eng.", H. Mark and N. Bikales, Eds., 11, John Wiley and Sons, New York, 572 (1988).

258 M. Ree, D. Y. Yoon, and W. Volksen, Polym. Mat. Sci. Eng., 60, 179 (1989); C. Feger, in "Proceedings from Recent Advances in Polyimides and Other High Performance Polymers:, P. M. Hergenrother, chairman, San Diego, CA, Jan. 1990.

259 T. L. St. Clair, M. K. Gerber, and C. R. Gautreaux, Polym Mat Sci Eng, 60, 183 (1983).

260 N. J. Johnston, T. L. St. Clair, R. M. Baucom, and T. W. Towell, Soc. Adv. Mat. Proc. Eng., 34(1) 976 (1989).

261 S. Swaminathan and A. I. Isayev, Polym. Mat. Sci. Eng., 57, 330 (1987).

262 L. H. Sperling, "Interpenetrating Polymer Networks and Related Materials", Plenum Press, New York (1981).

263 T. Pascal, R. Mercier, and B. Sillion, Polymer, 30, 739 (1989).

264 A. O. Hanky and T. L. St. Clair, SAMPE J., 30, July/Aug (1985), 40.

265 A. H. Egli, L. L. King, and T. L. St. Clair, in "Proceedings from the 18th National SAMPE Technical Conference", 440 (1986).

266 Y. Yamamoto, S. Satoh, and S. Etoh, SAMPE J., July/Aug (1985) 6.

267 P. A. Steiner, J. M. Browne, M. T. Blain, and M. McKillen, SAMPE J., March/April , 8 (1987).

268 R. H. Pater and C. Morgan, in "Proceedings from the 1988 SPE ANTEC Technical Conference", Atlanta, GA, 1639 (1988).

269 J. Adduci, D. K. Dandge, and J. Kops, Polym. Prepr., 22 (2), 109 (1981).

270 S. Senturia, Polym. Mat. Sci. Eng., 55, 385 (1986).

271 J. Economy, in "Contemporary Topics in Polymer Science", E. J. Vandenburg, Ed., Plenum Press, New York, 351 (1985).

272 A. J. Beuhler, N. R. Nowicki, and J. M. Gaudette, Polym. Mat. Sci. Eng., 59, 339 (1988).

273 A. K. St. Clair, T. L. St. Clair, and W. P. Winfree, Polym. Mat. Sci. Eng., 59, 28 (1988).

274 S. Numata and N. Kinjo, Polym. Eng. Sci., 28(14) 906 (1988).

275 W. P. Johnson, SAMPE J., Oct (1986) 8.

276 P. M. Hergenrother, Polym. J., 19 (1), 73 (1987).

277 P. M. Hergenrother, Polym. Mat. Sci. Eng., 59, 697 (1988).

278 G. E. Caledonia and R. H. Krech, AIAA-87-0105, presented at AIAA 25th Aerospace Sciences Meeting, January, 1987, Reno, NV.

279 A. Garton, J. L. Henry, P. D. McLean, and W. J. K. Stevenson, Polym. Eng. Sci., 29(1), 23 (1989).

280 L. J. Leger, J. T. Visentine, J. A. Schliesing, AIAA-85-0476, presented at AIAA 23rd Aerospace Sciences Meeting, January, 1985, Reno, NV.

281 J. T. Visentine, L. J. Leger, J. F. Kuminecz, and I. K. Spiker, AIAA-85-0415, presented at AIAA 23st Aerospace Sciences Meeting, January, 1985, Reno, NV.

282 A. F. Whitaker, S. A. Little, R. J. Harwell, D. B. Griner, and R. F. DeHaye, AIAA-85-0416, presented at AIAA 23rd Aerospace Sciences Meeting, January, 1985, Reno, NV.

283 A. F. Whitaker, J. A. Burke, J. E. Coston, I. Dalins, S. A. Little, R. F. DeHaye, AIAA-85-7017, presented at AIAA 23rd Aerospace Sciences Meeting, January, 1985, Reno, NV.

284 D. G. Zimcik and C. R. Maag, AIAA-85-7020, presented at AIAA 23rd Aerospace Sciences Meeting, January, 1985, Reno, NV.

285 P. W. Knopf, R. J. Martin, R. E. Damman, and M. McCargo, AIAA-85-0415, presented at AIAA 23st Aerospace Sciences Meeting, January, 1985, Reno, NV.

286 P. J. Andolino-Brandt, Ph. D. Dissertation, Virginia Polytechnic Institute and State University, Blacksburg, Virginia 24061 (1985).

287 J. A. Barnes and F. N. Cogswell, SAMPE Quart., 4, 22 (1989).

288 R. H. Hansen, J. V. Pascale, T. DeBenedicts, and P. M. Rentzepis, J. Polym. Sci., A, 3, 2205 (1965).

289 G. N. Taylor and T. M. Wolf, Polym. Eng. Sci., 20, 1087 (1980).

290 G. N. Taylor, T. M. Wolf, and J. M. Moran, J. Vac. Sci. Technol., 19 (4), 872 (1981).

291 M. A. Golub, T. Wydeven, and R. D. Cormia, Polym. Comm., 29, 285 (1988).

292 M. Suzuki, K. Saigo, H. Gokan, Y. Ohnishi, J. Electrochem. Soc., 130, 1962 (1983).

293 J. F. Battey, Solid State Technol., 124, 1924 (1977)

294 R. L. Bersin, Solid State Technol., 13, 39 (1970).

295 L. F. Thompson, G. C. Willson, and M. J. Bowden, Eds., "Introduction to Microlithography", Amer. Chem. Soc. Series 219, Washington, D. C. (1983).

296 G. N. Taylor, T. M. Wolf, and J. M. Moran, J. Vacuum Sci. Technol., 19(4), 872 (1981).

297 J. M. DeSimone, G. A. York, F. R. Wilson, A. M. Hellstern, S. D. Smith, J. E. McGrath, A. S. Gozdz, and M. J. Bowden, in "Proceedings from the 3rd International SAMPE Electronics Conference", 872 (1989).

298 J. Shaw, E. Babich, M. Hatzakis, and J. Paraszczak, Solid State Technol. 6, 83 (1987).

299 A. Tanaka, Polym. Prepr., 25, 309 (1984).

300 C. W. Wilkins, E. Reichmanis, T. Wolf, B. C. Smith, J. Vacuum Sci. Technol., 3, 306 (1985).

301 E. Reichmanis, G. Smolinsky, Proc. SPIE, 469, 38 (1984).

302 F. Webster and J. P. Wightman, Final report to NASA, Langley Research Center, Grant NAG-1-521, May, 1989.

303 A. Garton, P. McLean, and W. T. K. Stevenson, Polym. Prepr., 29 (1), 104 (1988).

304 G. A. York, R. O. Waldbauer, C. A. Arnold, M. E. Rogers, and J. E. McGrath, Soc. Adv. Mat. Proc. Eng., 35, in press (1990).

305 A. P. Melissaris and J. A. Mikroyannidis, Eur Polym J, 25 (3), 1989, 275. (Ph)

306 M. Sato and M. Yokoyama, Eur Polym J, 15, 1979, 541.(Ph)

307 G. C. Tesoro and C. Meiser, Jr., Textile Res, 40, 1970, 430.(Ph-N)

308 P. Subramaniam and M. Srinivasan, J Polym Sci, A, 26, 1988, 1553.

309 C. D. Smith, D. K. Mohanty, R. L. Holzberlein, S. D. Wu, D. H. Chen, and J. E. McGrath, in "Proceedings of the 3rd International SAMPE Electronics Conference", Los Angeles, CA, 1989.

310 D. H. Chen, Y. P. Chen, C. A. Arnold, J. C. Hedrick, J. D. Graybeal, and J. E. McGrath, 34(1) 1247 (1989).

311 J. P. Puglia, C. A. Arnold, G. D. Lyle, C. D. Smith, J. C. Hedrick, and J. E. McGrath, in "Proceedings from Recent Advances in Polyimides and Other High Performance Polymers", P. M. Hergenrother, chairman, San Diego, CA, Jan. 1990.

APPENDIX ----------

Surface analysis via x-ray photoelectron spectroscopy of polyimide homopolymers, poly(siloxane imide) segmented copolymers, and blends with polybenzimidazole exposed to atomic oxygen

	ATOMIC CONCENTRATION							
Take-off angle	C1s	O1s	Si2p	S2p	N1s	F1s	$Fe2p^{3/2}$	Al2p
PBI before exposure to atomic oxygen								
15°	49	30	19	---	2	---	---	---
30°	51	28	18	---	3	---	---	---
90°	60	24	11	---	5	---	---	---
PBI after exposure to atomic oxygen								
15°	37	33	---	---	2.3	17	2.8	8.1
30°	41	31	---	---	3.4	15	2.3	6.9
90°	49	28	---	---	3.7	13	1.6	4.8
BTDA-m-DDS before exposure to atomic oxygen								
15°	49	26	25	<1	0	---	---	---
30°	50	27	22	<1	<1	---	---	---
90°	56	25	16	1.1	2.3	---	---	---
BTDA-m-DDS after exposure to atomic oxygen								
15°	56	33	---	4.8	---	4.4	1.5	---
30°	61	30	---	4.6	3.8	3.2	1.1	---
90°	66	26	---	3.9	---	3.2	1.1	---

Take-off angle	ATOMIC CONCENTRATION C1s	O1s	Si2p	S2p	N1s	F1s	$Fe2p^{3/2}$	Al2p
BTDA-M-DDS-10 PSX 950 before exposure to atomic oxygen								
15°	52	24	23	<1	<1	---	---	---
30°	55	24	18	1.0	1.7	---	---	---
90°	63	21	11	1.7	3.2	---	---	---
BTDA-M-DDS-10 PSX 950 after exposure to atomic oxygen								
15°	30	46	17	2.4	1.8	2.7	---	---
30°	30	45	18	2.0	1.9	2.8	---	---
90°	34	43	18	1.5	1.9	2.4	---	---
BTDA-M-DDS-40 PSX 950 before exposure to atomic oxygen								
15°	54	22	23	<1	1.0	---	---	---
30°	56	22	20	<1	1.8	---	---	---
90°	61	21	14	1.0	3.0	---	---	---
BTDA-M-DDS-40 PSX 950 after exposure to atomic oxygen								
15°	39	35	25	---	1.1	---	---	---
30°	39	38	22	<1	1.3	---	---	---
90°	44	36	17	<1	2.4	---	---	---

Take-off angle	ATOMIC CONCENTRATION C1s	O1s	Si2p	S2p	N1s	F1s	$Fe2p^{3/2}$	Al2p
PBI (25%) / BTDA-m-DDS-40 PSX 950 (75%) before exposure to atomic oxygen								
15°	51	23	17	<1	2.4	---	---	---
30°	59	22	15	<1	3.2	---	---	---
90°	61	22	13	<1	4.3	---	---	---
PBI (25%) / BTDA-m-DDS-40 PSX 950 (75%) after exposure to atomic oxygen								
15°	36	34	7.1	1.2	---	11	3.4	6.8
30°	34	35	8.3	1.3	---	11	3.2	6.3
90°	32	37	11	1.4	---	10	2.7	6.2
PBI (40%) / BTDA-m-DDS-40 PSX 950 (60%) before exposure to atomic oxygen								
15°	54	23	21	<1	1.9	---	---	---
30°	56	22	19	<1	2.3	---	---	---
90°	60	21	14	<1	3.9	---	---	---
PBI (40%) / BTDA-m-DDS-40 PSX 950 (60%) after exposure to atomic oxygen								
15°	33	42	1.1	1.1	---	12	5.1	6.0
30°	35	40	<1	<1	---	12	5.2	6.3
90°	36	39	1.4	1.2	---	12	4.5	6.2

Take-off angle	ATOMIC CONCENTRATION C1s	O1s	Si2p	S2p	N1s	F1s	$Fe2p^{3/2}$	Al2p
Kapton before exposure to atomic oxygen								
15°	55	22	22	---	1.0	---	---	---
30°	58	22	18	---	1.3	---	---	---
90°	65	20	12	---	3.3	---	---	---
Kapton after exposure to atomic oxygen								
15°	45	28	---	---	2.0	15	2.7	7.1
30°	49	27	---	---	2.2	13	2.7	6.3
90°	55	23	---	---	2.9	11	1.9	5.9
Kapton w/1500Å coating of BTDA-m-DDS-40 PSX 950 before exposure to atomic oxygen								
15°	58	21	19	<1	1.9	---	---	---
30°	60	21	16	<1	2.7	---	---	---
90°	64	19	12	1.4	3.5	---	---	---
Kapton w/1500Å coating of BTDA-m-DDS-40 PSX 950 after exposure to atomic oxygen								
15°	49	29	2.5	1.1	2.0	8.9	3.0	4.0
30°	48	29	3.2	1.3	2.1	8.5	3.3	4.1
90°	44	30	4.4	1.6	2.3	9.1	3.3	4.7

VITA----------
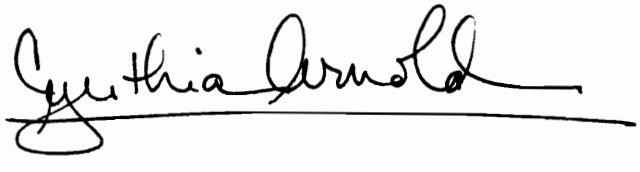
Cynthia A. Arnold was born in Peoria, Illinois on December 21, 1957. She attended elementary and high school at St. Andrew's parochial school in Detroit, Michigan, and graduated from Cabrini High School in Allen Park, Michigan, in 1975. After graduating from the University of California at Berkeley with a bachelors degree in chemical engineering in 1980, she joined Raychem Corporation in Menlo Park, California, as a process and product engineer. In 1982, she joined a small company in Berkeley, Thoratec Laboratories, which specialized in biomedical polymers. Here she worked on pilot scale polymer synthesis, and later in polymer manufacturing at a newly formed subsidiary of Thoratec, Mercor, Inc.. She attended evening classes at the University of California at Berkeley from 1982 through 1985, and received her masters degree in business administration in May, 1985. Swearing off the rigors of school, she drove cross country and joined Virginia Polytechnic Institute and State University in September, 1985. She received her doctorate degree in materials engineering science, specializing in polymer science, in October, 1989. In December, she joined Imperial Chemical Industry's Fiberite Composites Division in Tempe, Arizona. Her fiance, Herbert Rettke, has been her most appreciated companion throughout her graduate academic pursuits.